2006:65

DOCTORAL THESIS

Assessment of Fatigue Resistance and Strength in Existing Concrete Structures

Håkan Thun

Luleå University of Technology
Department of Civil and Environmental Engineering
Division of Structural Engineering

ISBN: 978-91-85685-03-5 | 2006:65 | ISSN: 1402-1544 | ISRN: LTU-DT -- 06/65 -- SE

LULEÅ
UNIVERSITY
OF TECHNOLOGY

Doctoral thesis 2006:65

Assessment of Fatigue Resistance and Strength in Existing Concrete Structures

Håkan Thun

Division of Structural Engineering
Department of Civil & Environmental Engineering
Luleå University of Technology
SE-971 87 Luleå
Sweden
Phone (+) 46 920 49 10 00
Fax (+) 46 920 49 19 13
http://www.ltu.se

Assessment of Fatigue Resistance and Strength in Existing Concrete Structures

HÅKAN THUN
Avdelningen för byggkonstruktion
Institutionen för samhällsbyggnad
Luleå tekniska universitet

Akademisk avhandling

som med vederbörligt tillstånd av Tekniska fakultetsnämnden vid Luleå tekniska universitet för avläggande av teknologie doktorsexamen, kommer att offentligt försvaras i

universitetssal F1031, torsdagen den 21 december 2006, klockan 10.00

Fakultetsopponent: Professor Kent Gylltoft, Betongbyggnad, Chalmers Tekniska Högskola, Göteborg

Betygsnämnd: *Biträdande professor emeritus Ralejs Tepfers, Betongbyggnad, Chalmers Tekniska Högskola, Göteborg*

Professor Sven Thelandersson, Konstruktionsteknik, Lunds Universitet, Lund

Adjungerad professor Bo Westerberg, Byggvetenskap, Kungliga Tekniska Högskolan samt Tyréns AB, Stockholm

ISBN 978-91-85685-03-5
Doctoral Thesis 2006:65
ISSN 1402-1544
ISRN LTU-DT—06/65—SE

Preface

This thesis presents work that has been carried out at the Division of Structural Engineering, Department of Civil and Environmental Engineering at Luleå University of Technology (LTU). The work has mainly been funded by Banverket (the Swedish National Rail Administration). Additional funding has been provided by Sustainable Bridges – an Integrated Research Project within the European Community 6th Framework Program, the European Rail Research Institute (ERRI), The Development Fund of the Swedish Construction Industry (SBUF) and LTU.

First of all I would like to thank my supervisors Professor Lennart Elfgren, Dr. Tech. Ulf Ohlsson and Professor Thomas Olofsson for all their help and advice during the years.

My thanks are also due to the staff at TESTLAB, the laboratory at LTU. All of you have been involved in my work, but I would especially like to thank Mr. Georg Daneielsson, Mr. Håkan Johansson and Mr. Lars Åström. They have performed, helped and advised me during all the tests/experiments during the past few years.

Additionally, I am very thankful to the colleagues and friends at the Division of Structural Engineering for making the environment creative and joyful, especially Dr. Tech. Anders Carolin, Dr. Tech. Martin Nilsson, Lic. Tech. Håkan Nordin and Lic. Tech. Sofia Utsi who have been with me from the beginning of this journey.

Finally, writing a thesis is not possible without an extremely understanding family, thanks mother and father for helping us out during this period. I cannot express in words how grateful I am to Anna, my wife, for her support and patience during my work with the thesis. My kids, Cecilia and Alexander – your smiles kept me going! Love you all!

Luleå in November 2005

Håkan

The first draft of the text above was written on November 12, 2005, about 8 pm. An accident about one hour later, resulting in a bilateral hypoglossal nerve injury, postponed the completion of this preface until now. I am extremely thankful to my family – Anna, Cecilia, Alexander, my parents and my brother Magnus – and all of you, who have helped and supported me since the accident and made it possible for me to return to work and finish this thesis. Thank you all!

Luleå in December 2006

Håkan

Abstract

During the last few decades, it has become more and more important to assess, maintain and strengthen structures like bridges, dams and buildings. This is mainly due to the fact that: (a) many structures are getting old and many have started to deteriorate, (b) there is sometimes a need to increase the load carrying capacity of an existing structure due to e.g. a demand for higher loads or (c) the cost to build new infrastructure is often higher than to repair/strengthen existing structures. Therefore it is of great interest to find methods to evaluate existing concrete structures in an efficient way. In this thesis parameters influencing the evaluation process have been investigated and analysed and the results are presented in the appended papers. Below, findings from the main areas are presented.

The development and variation of compressive and tensile strength of concrete are presented for old concrete bridges in Sweden. The mean increase in concrete compressive strength was about 70% for twenty bridges built during 1931–1962 (a rather high dispersion must be taken into consideration). The increase is related to the original 28-day concrete compressive strength which varied between 18 and 51 MPa. The compressive strength within a typical reinforced railway concrete trough bridge was approximately 15% higher in the longitudinal beams than in the bottom slab (measured on drilled cores).

A pullout test method, the Capo-test, has been examined as an alternative to drilled cores to determine the in-place concrete compressive strength. A strength relationship is proposed between the compressive strength of a drilled core with the diameter and the height of about 100 mm, f_{core}, and the pullout force, F, from the Capo-test.

A probabilistic approach has been proposed for the evaluation of the shear force fatigue capacity of a concrete bridge slab. In the reliability analysis three different combinations of shear and fatigue models have been compared. The models have been used to determine the safety index β (and the probability of failure) after another 5 or 25 years of traffic with higher axle loads (300 kN) than the bridge already has been exposed to. The most interesting combination seems to be the shear model of Hedman & Losberg (1975)/BBK04 (2004) and the fatigue model of Tepfers (1979).

Results and analyses are presented from cyclic uniaxial tensile tests performed on new and old concrete. The results from the tests indicate that the deformation criterion proposed by Balázs (1991) for bond slip may also be applied to plain concrete exposed to cyclic tensile load. A

method is proposed for how the deformation criterion may be used also for assessment of existing structures.

The load carrying capacity of damaged prestressed concrete railway sleepers has been investigated. The sleepers had an age of five to ten years and the damage, in form of more or less severe cracking, is believed to be caused by delayed ettringite formation. The following tests have been performed: (a) bending capacity of the midsection and the rail section, (b) horizontal load capacity of the fastener, (c) control of the concrete properties and (d) fatigue capacity in bending of the rail section. A visual inspection and classification of the damages are also presented. The test results show that railway sleepers are quite robust. Small cracks do not seem to influence the load carrying capacity and it is first when the cracking is very severe that the load carrying capacity is reduced significantly.

Keywords: concrete, bridges, strength development, Capo-test, reliability analysis, tensile fatigue, deformation criterion, sleepers, delayed ettringite formation.

Sammanfattning

Under de senaste årtiondena har det blivit allt viktigare att tillståndsbedöma, underhålla och förstärka konstruktioner såsom broar, dammar och byggnader. Huvudorsakerna till detta är: a) många konstruktioner är gamla och nedbrytning har påbörjats, b) ett behov av att öka kapaciteten t.ex. höja axellasterna för en järnvägsbro samt c) kostnaden att bygga ny infrastruktur ofta är mycket högre än att reparera eller förstärka en existerande konstruktion. Allt detta medför att det är av största intresse att finna metoder att tillståndsbedöma en konstruktion på ett så effektivt sätt som möjligt. I denna avhandling har delar av tillståndsbedömningsprocessen studerats och analyserats och resultatet finns presenterat i bifogade artiklar. Nedan följer en kort beskrivning av de områden som studerats.

Hållfasthetens variation i en konstruktion och dess utveckling över tiden har studerats för gamla betongbroar. För de studerade broarna, byggda mellan 1931-1962, har tryckhållfastheten i genomsnitt ökat med 70%. Denna ökning är relaterad till 28-dygnshållfastheten då respektive bro byggdes och varierar mellan 18 och 51 MPa. Undersökningar har visat att för en standard trågbro är tryckhållfastheten ca 15% högre i de längsgående huvudbalkarna än i den bottenplatta de bär.

En testmetod för att kontrollera hållfastheten i en befintlig konstruktion, det s.k. Capo-testet, har studerats. Ett hållfasthetssamband presenteras mellan den utdragskraft som erhålls vid ett försök med Capo-testet, F, och tryckhållfastheten, f_{core}, för utborrade cylindrar med diametern och höjden ca 100 mm.

En sannolikhetsbaserad metod har använts för att bedöma tvärkraftskapaciteten vid utmattning av en bros betongplatta. Tre olika kombinationer av modeller för utmattning och tvärkraft har undersökts. Modellerna har använts för att bestämma ett s.k. säkerhetsindex, β-index, för 5 eller 25 år av ytterligare trafik med förhöjd axellast, 30 ton. Av de kombinationer av modeller som studerats har tvärkraftsmodellen av Hedman & Losberg (1975)/BBK04 (2004) och utmattningsmodellen av Tepfers (1979) visat sig vara en intressant kombination.

Vidare redovisas resultat och analyser från cykliska enaxiella dragförsök för ny respektive gammal betong. Resultaten indikerar att det deformationskriterium som föreslagits av Balázs (1991) för förankring även är möjligt att använda för oarmerad betong utsatt för cyklisk dragbelastning. En metod är föreslagen för hur detta kan tillämpas vid tillståndsbedömning av konstruktioner.

Slutligen har bärförmågan för skadade spännbetongsliprar undersökts. Sliprarna har haft en ålder av 5 till 10 år och skadorna de uppvisat är sprickbildning av varierande grad. Denna är troligtvis orakad av s.k. försenad ettringitbildning. Följande försök har utförts: a) böjkapacitet i mitt-

sektion och i rälläge, (b) horisontell dragkapacitet av befästningar, (c) kontroll av betonghållfastheten och (d) utmattningskapacitet i rälläge. En visuell inspektion och klassificering av de skadade sliprarna är också redovisad. Resultaten visar att sliprarna är relativt robusta, små sprickor verkar inte påverka bärförmågan nämnvärt utan det är först vid kraftig uppsprickning som bärförmågan reduceras avsevärt.

Nyckelord: betong, broar, hållfasthetsutveckling, Capo-test, sannolikhetsbaserad analys, utmattning vid dragbelastning, deformationskriterium, sliprar, försenad ettringitbildning.

Table of Contents

1 Introduction

1.1 Background - Assessment of Concrete Structures

During the last few decades, it has become more and more important to assess, maintain and strengthen structures like bridges, dams and buildings. This is mainly due to the fact that (a) many structures are getting old and many have started to deteriorate, (b) there is sometimes a need to increase the load carrying capacity of an existing structure due to e.g. a demand for higher loads or (c) the cost to build new infrastructure is often higher than to repair/strengthen existing structures. Therefore it is of great interest to find methods to evaluate existing concrete structures in an efficient way.

Research regarding condition evaluation of concrete structures has literally exploded lately. This is not only due to the reasons mentioned above but also due to the possibilities new technique has brought. The procedure of inspection of e.g. a bridge, using new types of sensors and the fast development in data communications have made it possible to monitor structures continuously, so-called Structural Health Monitoring, see e.g. Utsi et al. (2001), Olofsson et al. (2002), Hejll (2004) or Hejll & Täljsten (2005).

How can then an evaluation of e.g. a bridge be performed? What shall be checked? The questions are many and in most cases not easy to answer. In Figure 1.1 an idea is presented of how such an evaluation could be performed. The procedure is suggested by the partners in the European-project "Sustainable Bridges - Assessment for Future Traffic Demands and Longer Lives". The aims of the project are to increase the transport capacity, the residual lifetime, allow higher traffic speeds for passenger traffic and enhance strengthening and repair systems of existing railway bridges. The consortium consists of 32 partners and it started in 2004 and will end in 2007, see Sustainable Bridges (2006).

The proposed procedure consists of three phases. The first, initial, phase is the simplest of them: an inspection at site, study of documents and simple calculations. The second, intermediate, phase is a more refined check and might be more costly and time-consuming. It consists of e.g. strength tests and measuring at site of some parameters like strain or deflection or it can be monitoring for a longer period etc. With this information new and more detailed calculations could be performed. The third and last, enhanced, phase is an even more refined check. The question that must be answered after each phase is if the structure is safe and what action must be taken. In the end one of the following actions must be considered:

- Unchanged use of the structure?
- Supervise the structure e.g. measurement of the strain development over a longer time?
- Strengthen the structure with e.g. carbon fibre reinforced polymers, see e.g. Carolin (2003), Täljsten & Carolin (1999) or the Swedish guidelines for FRP-strengthening in Täljsten (2004)?
- Demolish the structure and build a new one?

As can be seen in the figure there are several influencing factors that could be considered. If the point "material investigations", see phase 2, is used as an example some of the factors that could be checked are: in-place concrete strength, cover of the reinforcement, amount and quality of the reinforcement, degree of degradation etc. If every point in Figure 1.1 is broken down like this it is easy to see that condition evaluation of a bridge is a difficult and in many cases a time-consuming task.

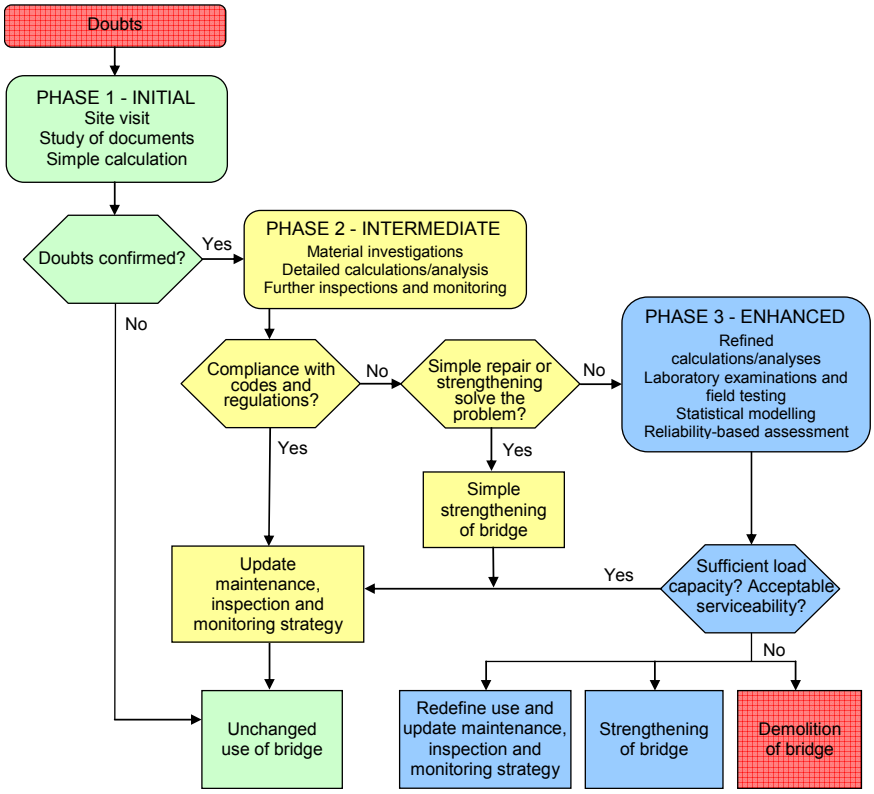

Figure 1.1 Suggested flow-chart for reassessment of existing bridges proposed by the EU-project Sustainable Bridges (2006).

Some of the checks in Figure 1.1 are not easy to perform, but if they are made, they often give very valuable information. Field testing for example, see phase 3 in Figure 1.1, has in earlier research projects at LTU shown to be a very valuable instrument when evaluating the condition of a bridge, see Paulsson et al. (1996,1997).

Regarding the analysis methods, statistical modelling and reliability-based methods are perhaps the most suitable methods when evaluating e.g. a concrete bridge. These types of analysis methods have been used in an assessment project of a bridge in northern Sweden, the Luossajokk

Bridge, see Enochsson et al. (2002, 2005). Instead of strengthening the bridge, the result from the reliability analysis showed that the bridge could be kept as it was but with continuous monitoring – in this case measuring of the strain development in the reinforcement bars.

1.2 Aims

The aim is to study some of the factors that are of importance in the assessment process of an existing concrete structure, see Figure 1.1.

Firstly, to investigate the in-place concrete strength in an existing bridge. What variation of concrete strength can be expected? Can an increase of concrete compressive strength be expected for old concrete structures and what methods to investigate the strength are available.

Secondly, to present a method that can be used for shear fatigue evaluation of concrete bridge slabs and to study the influence of different factors on this method.

Thirdly, to investigate a deformation criterion and to verify it for plain concrete exposed to cyclic loading in tension. Furthermore to investigate if it can be used on an entire structure.

Fourthly, the thesis aims to investigate methods to evaluate damaged railway sleepers and determine their remaining load carrying capacity.

1.3 Limitations

When evaluating an existing structure there are several factors that influence the load carrying capacity. In this thesis the study has been limited to investigate some of the aspects of in-place concrete strength. The fatigue phenomenon has only been investigated with respect to plain concrete exposed to cyclic load in tension.

1.4 Contents

This thesis consists of five papers. Background material, theories etc. to every subject that is investigated are presented in the following chapters:

In Chapter 2 a brief introduction is presented to in-place concrete strength, i.e. the development, variation and testing of tensile and compressive strength for old reinforced concrete bridges. This subject is further presented in paper A and B where analyses and test results can be found of concrete trough bridges.

Chapter 3 contains a brief introduction to reliability analysis of structures. The method has been used in the study presented in paper C to determine a safety index for a typical railway bridge exposed to fatigue load in tension.

In Chapter 4 fatigue of concrete structures in general is described and in Chapter 5 concrete fatigue in tension is described. The intentions with these parts are to present research that is of special interest to the theme of this thesis. Background to the fatigue behaviour of concrete is presented. A deformation criterion for fatigue failure in concrete is also described. Some of the models that are presented are used in papers C, D and E.

In Chapter 6 an investigation of prestressed concrete sleepers is presented.

Chapter 7 includes a short summary of each appended paper and an outlook.

Appendix A includes results from the fatigue tests presented in paper D "Concrete Fatigue Capacity in Tension- a Study of Deformations".

Appended papers:

Paper A – is titled "Concrete Strength in Old Swedish Concrete Bridges" by Håkan Thun, Ulf Ohlsson and Lennart Elfgren.

Paper B – is titled "Determination of Concrete Compressive Strength with Pullout Test" by Håkan Thun, Ulf Ohlsson and Lennart Elfgren.

Paper C – is titled "Probabilistic Modelling of the Shear Fatigue Capacity" by Håkan Thun, Ulf Ohlsson and Lennart Elfgren.

Paper D – is titled "Concrete Fatigue Capacity in Tension – a Study of Deformations" by Håkan Thun, Ulf Ohlsson and Lennart Elfgren.

Håkan Thun´s contribution to the papers A, B, C and D is planning a large part of the tests, participating in most of them, evaluating the data, performing the analyses and finally writing the papers including drawing some of the figures. Guidance and comments have been given by the co-authors Dr. Tech. Ulf Ohlsson and Professor Lennart Elfgren throughout the project.

Paper E – is titled "Load Carrying Capacity of Cracked Concrete Railway Sleepers" by Håkan Thun, Sofia Utsi and Lennart Elfgren, and is submitted to Structural Concrete, Journal of the *fib*. The laboratory tests of the bending capacity of the midsection and the rail section have been performed by Sofia Utsi while the tests of the horizontal load carrying capacity of the fastener (except for one of the tests) and the fatigue tests have been performed by Håkan Thun. Håkan Thun and Sofia Utsi have written the paper and drawing the figures with guidance and comments by Professor Lennart Elfgren.

2 In-place Concrete Strength

Different aspects of the subjects presented in this chapter have been used/investigated in paper A and B where the in-place concrete strength variation and concrete strength development with time have been investigated together with a comparison between different methods to determine the in-place concrete strength. An introduction to different aspects of in-place concrete testing can be found in e.g. Bungey & Millard (1996), Carino (2004) or Thelandersson (2007) and is in this chapter described briefly.

2.1 Strength Development with Time

When assessing e.g. a bridge, several factors are examined and one of them which is important is the concrete strength. Studies found in the literature show that the compressive strength of concrete could increase with age for old structures. This is in turn a huge bonus since "nature's own strengthening" is less expensive, actually free of charge, than strengthening with e.g. carbon fibre would be. The phenomenon has been investigated for Swedish bridges and the findings are presented in paper A.

Why the increase then? Several reasons are possible. According to Johansson (2005), the most likely has to do with the properties of the Portland cements used during the 1930s and 1940s. During this period the Portland cements had a different ratio of dicalcium silicate (C_2S) to tricalcium silicate (C_3S) and were more coarsely ground (i.e. the fineness was lower) compared to the Portland cements of today, see e.g. Lea (1970), Taylor (2002) or Neville (1995). The two silicates are primarily responsible for the strength of the hydrated cement paste: where the tricalcium silicate (C_3S) influences the early strength and the dicalcium silicate (C_2S) the later increase in strength. The trend during the last few decades has been that, due to improved manufacturing methods, the amount of tricalcium silicate has increased which results in higher early compressive strength (in combination with a higher fineness) and a lower increase in long-term strength. In this context it must also be mentioned that the concrete compressive strength of course can decrease with time due to e.g. environmentally caused degradation.

An example is given in Wood (1991) where long-term data are compiled from four different studies initiated between 1940 and 1956 by the Portland Cement Association. In the investigation data on the variation of concrete compressive strength, flexural stiffness and modulus of elasticity with time are presented. The cement, Type I according to ASTM, used in one of the studies was produced in 1947 and the potential compound composition of C_2S and C_3S was about 16-30% and 43-58 % respectively. The cement was also coarser compared to modern

cements. After 20 years the mean concrete compressive strength was approximately 40 % higher than the 28-day strengths (the percentage level is derived manually from graphs in Wood (1991)). The difference between the concrete compressive strength development of specimens cured in a moist room and specimens stored outside were slight. From the results Wood could also conclude that the compressive strength of concrete increased with a decrease in the water to cement ratio. Other examples are given in Washa & Wendt (1975), Walz (1976) or Washa et al. (1989).

No literature regarding a similar increase of the tensile strength of concrete with time has been found.

2.2 Strength Variation

It is a well-known fact that there is a variation of concrete properties within a member of a structure. This variation may be due to differences in concrete compaction and curing and/or differences in the quality of the concrete delivered. In the literature one can find that the bottom parts are usually better compacted with higher density than the top parts, where the percentage of ballast may be smaller. This is due to the influence of the gravity force and the stability of the concrete mixture. Strength variation has been investigated for Swedish bridges and the findings are presented in paper A.

The variation of in-place concrete strength in a structure could, according to Bartlett & MacGregor (1999), be due to:

- Within-batch variation (e.g. the randomness of the strength of different parts included in a single batch of concrete)
- Batch-to-batch variation (factors that could vary between batches e.g. difference in amounts, properties of the components, mixing procedures)
- Systematic within-member variation (if the consolidation, water content or curing conditions vary in a consistent manner)
- Systematic between-member strength variation (could be due to different curing conditions, e.g. different ambient temperature for a column on different floors)
- Strength variation between different types of members

If the concrete strength property is considered, the strength variations that can be found in a member of a structure are different depending on if it is e.g. a wall or a slab. According to Bungey & Millard (1996) the variation between the top and the bottom for a beam can be up to 40% and for a slab up to 20% (here the loss in strength is concentrated to the top 50 mm), see Figure 2.1. Bungey & Millard point out that the curves in Figure 2.1 are based on numerous reports of non-destructive testing and can only be regarded as indicating general trends which may be expected. A variation of strength in a member, i.e. higher in the bottom than in the top, could also be found in e.g. Bartlett & MacGregor (1999).

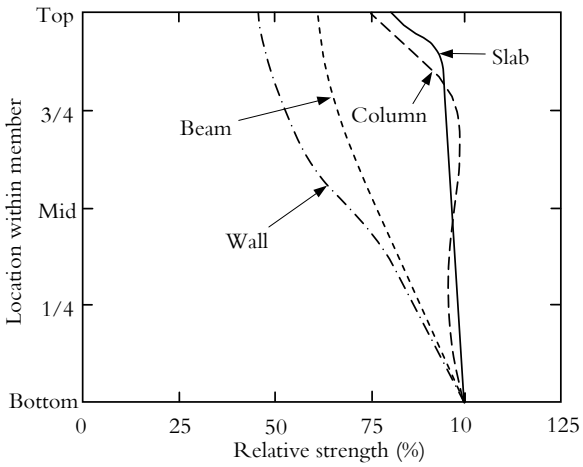

Figure 2.1 Typical within-member variations of relative strength for normal concretes according to member type, from Bungey & Millard (1996).

2.3 Methods to Determine the in-place Concrete Strength

There are several methods to test the in-place concrete strength of a structure. The methods can be divided into three basic categories, depending on the type of damage they cause on the structure:

- non-destructive testing (causes no damage on the test object)
- semi-destructive testing (causes minor local surface damage on the test object)
- destructive testing (causes major damage on the test object)

However, the boundaries between the first two named above, are slightly indistinct. According to The American Society for Non-destructive Testing (ASNT) the definition of non-destructive testing is "Nondestructive testing (NDT) has been defined as comprising those test methods used to examine an object, material or system without impairing its future usefulness". What makes the boundaries vague, according to ASNT, is the words "future usefulness". Some methods involve taking samples from the test object and would then make the methods destructive but since the samples are often taken in parts that do not reduce future usefulness of the object - it could be argued that the method is non-destructive.

In this investigation two methods have been used to determine the in-place concrete strength of reinforced concrete railway trough bridges; drilled cores and the so-called Capo-test. They both belong to the category semi-destructive testing – at least the Capo-test which is a so-called pullout method.

To drill out and test cores is a common method to estimate the in-place strength of a concrete structure. Most countries have adopted standard procedures for how a core should be prepared, stored, etc. before testing.

The Capo-test (from "**c**ut **a**nd **p**ull **o**ut"-test) is a method to determine the concrete strength of the cover-layer for an existing structure. It was developed in Denmark by C German Petersen and E Poulsen in the middle of the 1970s, see e.g. German Petersen & Poulsen (1993). The test procedure of the Capo-test consists of drilling a 65 mm deep hole with a diameter of 18 mm using a water-cooled diamond bit, see Figure 2.2a. Then a 25 mm recess is made at a depth of

25 mm using a portable router. An expandable split steel ring is inserted through the hole in the recess and expanded by means of a special tool. Finally the ring is pulled through a 55 mm counter pressure placed concentrically on the surface. The pullout force, F, is measured by the pull machine and can be converted into concrete compressive strength, f_c, by means of calibration charts provided by German Petersen & Poulsen (1993). A description of the method can also be found in e.g. Bungey & Millard (1996). An example of the cone that is extracted after a performed test is shown in Figure 2.2b.

If the two methods are compared in general, the Capo-test is a simpler and less expensive test to perform compared to drilled cores on the bridges. The Capo-test has the advantage that the equipment is lighter and easier to transport to the bridge compared with the equipment used for drilling cores. This was one of the key-advantages since many of the bridges in this investigation could only be reached by train or on foot. Important in this case was also the less damage the Capo-test inflicts on the bridges.

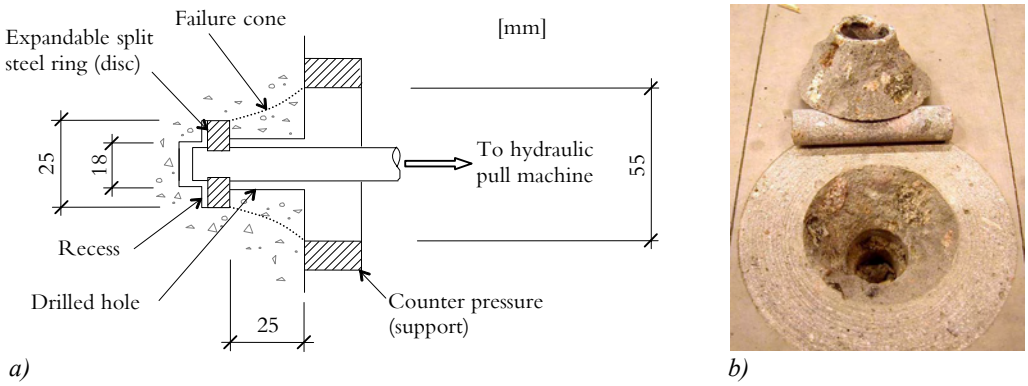

Figure 2.2 a) Schematic drawing of the Capo-test, based on German Petersen & Poulsen (1993), Bungey & Millard (1996) and Carino (2004) and b) Picture showing the extracted cone after a performed Capo-test. Photo from Johansson (2000).

The Capo-test correlation charts for concrete compressive strength and the pullout force are based on several laboratory and field studies made by the manufacturer as well as by other researchers. In most cases it is the results from the Lok-test (see below) that are the basis of the correlations charts, but in some cases also the Capo-test. The suggested general correlation for standard 150 mm cubes is shown in Eqs. (1) and (2) in Figure 2.3, from German Petersen (1997).

Rockström & Molin (1989) have shown that the relation suggested by German Petersen (1997), see Figure 2.3, can be improved when the test object is an old structure, i.e. an old road bridge. They got higher concrete strengths according to Eq. (1) in Figure 2.3, when they performed tests with both the Capo-test and drilled cores on six road bridges that had ages up to 54 years.

The studies in this thesis of the Capo-test confirm the findings by Rockström & Molin, i.e. a need for an improved strength relation between the pullout force from the Capo-test and the compressive strength of a drilled core with the diameter and height of 100 mm. The proposal could be found in paper B.

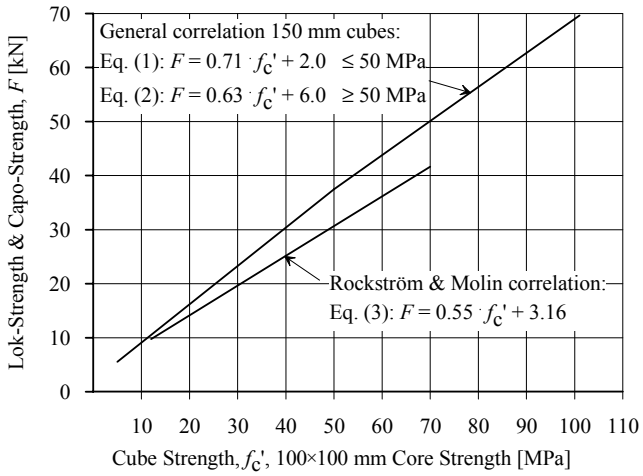

Figure 2.3 Correlation between Capo-test and drilled cores with the height and the diameter of 100 mm, trimmed and air-cured 3 days before testing, made by Rockström & Molin (1989) based on 5 old Swedish bridges. The correlation is compared with the general correlation for 150 mm standard cubes suggested by the manufacturer. From German Petersen (1997).

The Capo-test is a further development of the so-called Lok-test where the pullout bolt is embedded in fresh concrete. Carino (2004) reports that the first time a description of the pullout test method was presented in the literature, was in 1938 in a paper by Skramtajew (1938) where different test methods to measure the in-place concrete strength were reviewed. Later on in 1944 Tremper (1944) published research results of pullout tests with a design similar to the design described by Skramtajew. In 1962 Kierkegaard-Hansen (1975) initiated a research programme and the result of the work led to the test-system known as the Lok-test. Kierkegaard-Hansen improved the original design by introducing the support ring (also called the bearing ring or reaction ring) - this support ring was not used in the tests reported by Skramtajew and Tremper. For more detailed information regarding the history of the pullout test method see e.g. Carino (2004).

From the end of the 1970s until the beginning of the 1990s the Lok-test and similar methods were subject to discussions in the concrete society, particularly regarding what property that is actually measured in a pullout test. In the literature different theories have been presented over the years. One of them is a non-linear finite element analysis presented in Ottosen (1981). His analysis of the Lok-test showed that large compressive forces run from the disc in a rather narrow band towards the support and this constitutes the load carrying mechanism. Ottosen concluded further, that the failure in a Lok-Test is caused by the crushing of the concrete and not by cracking. Therefore, the force that is needed in a Lok-test to extract the embedded disc directly depends on the compressive strength of the concrete.

Stone & Carino (1983) raised doubts regarding the thesis with narrow bands proposed by Ottosen (1981). The reasons for this were that the model assumed a perfect bond between the pullout disc and the surrounding concrete which they believed to be unlikely since the pullout insert is often coated with oil prior to casting and that no evidence of narrow bands had been detected in physical tests. In their own study they carried out large-scale pullout tests and they identified three distinct phases in a failure sequence of a pullout test.

- Phase 1: initiation of circumferential cracking near the upper edge of the disc at approximately 1/3 of ultimate load.

- Phase 2: completion of circumferential cracking from disc edge to support ring at approximately 2/3 of the ultimate load.
- Phase 3: shear failure of matrix and degradation of aggregate interlock beginning at about 80% of ultimate load.

They proposed that ultimate failure was probably due to pullout from the matrix of the bridging aggregate particles.

The idea by Stone & Carino (1983), that aggregate-interlock across the failure surface is the reason for the load capacity above the 64% mentioned in Ottosen (1981), was rejected in Yener (1994), since aggregate interlocking would be very sensitive to different types of aggregate. This would in turn had led to reports of high within-test variations in performed tests. The large scale test by Stone & Carino was also commented by Krenchel & Shah (1985). They pointed out that the results in Stone & Carino do not necessarily correspond to the conventional pullout test since they did not scale up the maximum aggregate size, only the dimensions of the test specimens.

In 1984 Stone & Carino (1984) presented an axisymmetric linear elastic finite element analysis and compared it with their experimental results presented in Stone & Carino (1983). They concluded that because the complex three-dimensional stress states produced during the test (there are no regions where the stresses are simple unidirectional tensile or compressive stresses), it was unlikely that the pullout strength was directly related to the compressive strength and that an alternative explanation was needed for the observed correlation between the two strengths. They proposed that the correlation between the calculated principal tensile stress trajectories and the measured failure surface geometry from experiments suggested that formation of the complete failure surface is governed primarily by the tensile strength of the mortar. They proposed that this is the explanation of the correlation between the pullout strength and the compressive strength of concrete, i.e. both are governed primarily by the tensile strength of he mortar.

The method used by Stone & Carino (1984) was questioned by Yener (1994), since the cracking in concrete in a pullout test initiates at a load which is only a small fraction of the failure load, an interpretation drawn from a linear elastic analysis does not provide sufficient information regarding the progressive failure of the concrete medium. Further, Yener states that, it does not provide a clear insight into the interesting phenomenon that, although at 65 percent of the ultimate load and the failure surface is already formed, concrete still possesses additional strength.

Yener (1994) described the progressive failure of concrete subjected to pullout tests based on a plastic-fracture finite element analysis. Based on numerical results, Yener's examination of the stress distribution in the uncracked and cracked concrete, indicated that the behaviour of concrete subjected to a pullout force in a Lok-Test is primarily controlled by combined compression and bending actions, where the bending actions are pronounced in the latter stages of the loading. Yener also pointed out that it may not be appropriate to describe the complex state of stress in a pullout test by a uniaxial mode of failure. Based on his study, Yener concluded that the reasonable and consistent experimental correlation between the pullout force and the compressive strength of concrete is explained by indicating that the residual strength in pullout tests is a consequence of crushing of the concrete close to the support.

If the results from the different theories described above are compared there are, however, some similarities. In all investigations a complex stress state during the pullout test has been confirmed. The cracking initiates at a small fraction of the ultimate load and two major cracks are present: a circumferential crack that starts to develop at approximately 25-30% of the ultimate load, see Figure 2.4 and moves toward the support ring and a secondary circumferential crack

that forms the completed failure surface (which is reached at approximately 60-70% of ultimate load). A thing common for all studies of the Capo-test, is that a fairly good correlation has been found to exist between the pullout force and the concrete compressive strength.

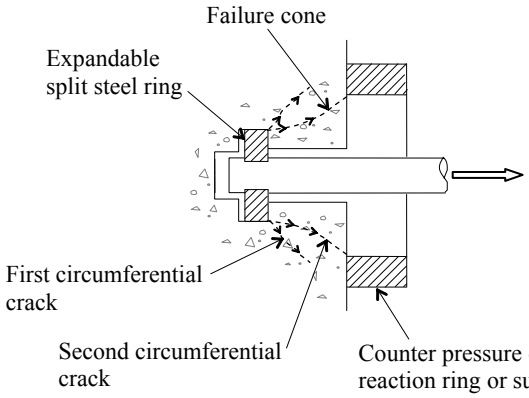

Figure 2.4 Schematic drawing of the circumferential cracks from Lok-test/Capo-test. Based on Carino (2004).

All investigations mentioned above have studied the Lok-test where the pullout bolt is inserted before casting. The Capo-test, which has been used in this investigation, has not been a subject for as many studies. The main difference between the two test methods, regarding the failure process, is that no bond exists between the steel disc and the surrounding concrete in the Capo-test and that the geometry is a bit different. Otherwise, the failure process should be similar.

If the failure surface of the extracted failure cones from the Capo-tests performed in this thesis is studied and compared to the failure theories in the literature, there are some similarities as well as discrepancies. The failure has in most cases not been only due to "pullout from the matrix of the bridging aggregate particles", as formulated by Stone & Carino (1983). Instead the failure has in many cases been due to failure of the ballast which indicates a good bond between the ballast and the cement paste in these cases, i.e. high strength of the mortar (the compressive strength of concrete has been high in most cases). It also indicates that the failure in this case supports the theories that the ultimate failure could be due to e.g. crushing of the concrete rather than aggregate interlocking – at least when the compressive strength of the tested concrete is high. The tensile strength of the concrete does seem to have an impact on the failure mechanism. This is indicated if the general shape of the proposed modified correlation curve between the compressive strength of drilled cores and the pullout strength from the Capo-test is studied, see paper B. The shape agrees with the general form of the correlation between the compressive strength of concrete and the tensile strength of concrete that could be found in the literature. Perhaps the failure type changes, depending on the strength of the concrete, during the test, compare with Figure 2.3. However, these ideas are just speculations since the failure itself has not been investigated in this thesis.

As mentioned earlier, the Capo-test is intended to determine the strength of the cover-layer, but in this thesis efforts have been made to use it as an alternative to drilled cores to determine the in-place concrete compressive strength.

3 Reliability Analysis

In this chapter reliability analysis is described briefly and in paper C the method has been used on a railway concrete bridge in order to determine the remaining shear fatigue capacity. An introduction to reliability analysis can be found in Schneider (1997) and Diamantides (2001). General textbooks of reliability analysis have been written by e.g. Thoft-Christensen & Baker (1982) and Ditlevsen & Madsen (1996). Swedish examples where a reliability analysis has been applied in practice in structural analysis are given in Fahleson (1995), Enochsson (2002), Jeppsson (2003) and Nilsson (2003).

In Figure 3.1 an illustration proposed by Schneider (1997) is shown that in general describes the process of safety evaluation of an existing structure. The need to assess the reliability of an existing structure can be due to many reasons, but as mentioned in Schneider (1997), the reasons can be traced back to doubts about the safety or the reliability of the structure. The aim of the reliability assessment of an existing structure is to produce proof that it will function safely over a specified residual service life, see Diamantides (2001).

What are the definitions of the terms safety and reliability? The term reliability can, according to Schneider (1997), be defined as "the probability that an item or facility will perform its intended function for a specified period of time, under defined conditions". The term safety is defined with respect to safety for people. Schneider (1997) exemplifies with the Swiss Standard, where safety is defined as "The term safety in the SIA Building Code is primarily related to the safety for people affected by structural failures". Schneider further emphasizes that in the definition of safety, it is not the structure as such that is designated safe, but rather the people in its area of influence.

In Figure 3.1 an illustration of the engineer's situation in the assessment of a structure's safety is shown, Schneider (1997). The question that must be answered is if the structure is safe enough and depending on what answer is given, different actions have to be taken, see Figure 3.1 (compare with Figure 1.1).

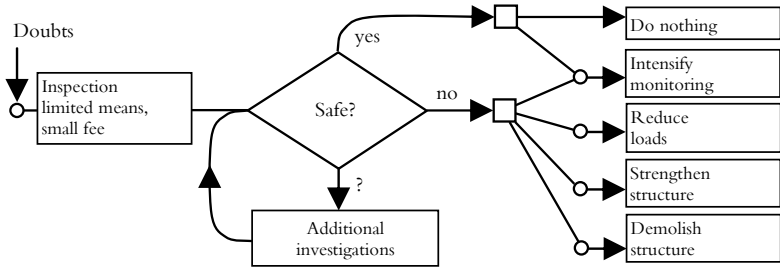

Figure 3.1 Illustration of the engineer's situation in the assessment of a structure's safety, from Schneider (1997).

Schneider further writes that the assessment of structural reliability of an existing structure is a difficult task since statements about its possible behaviour under conditions of extreme loading must be made. Such conditions normally lie outside the range of experience gained from observing the behaviour under service loads. Another important factor when assessing existing structures is that it is essential to know for how long the structure is intended to serve its purpose, the so-called residual service life.

According to Schneider (1997) experience has shown that the assessment procedure is gained by subdividing the scheme given in Figure 3.1 into three phases where each phase should be completed before the next starts. The subdivided scheme presented by Schneider is very similar to the one shown in Figure 1.1, but with a few significant differences. Schneider is of the opinion that each phase should begin with a precisely formulated contract, usually in written form, which has been made by the consulting engineer and the client together. Each phase should end with a report leaving the owner with his responsibility and freedom of decision, where this freedom is restricted by the recommendations of the engineer and the requirements of the law. Schneider also suggests, which is interesting, that phase 2 and 3 are carried out by a team of engineers (experts) in contrast to the first phase, a preliminary assessment, which could be done by one engineer alone. For more details about the procedures see Schneider (1997) or Diamantides (2001).

3.1 Structural Reliability Analysis

What methods can be used to determine the safety of an existing structure? Is it perhaps appropriate to use the same methods as when the structure was built? An answer to these two questions can be given if the difference between the two situations is studied. As pointed out by Melchers (1999) a reason for not using design codes in an assessment situation is that a design code needs to allow for uncertainties in the design and construction process and these uncertainties will have been realised in the finished structure. Another difference between design of a new structure and assessment of an existing structure is that the information available at the two situations is different. A critical aspect, as Schneider (1997) points out, when assessing the structural safety is the rather poor information about the condition of certain structural elements, e.g. with respect to corrosion or fatigue. However, this can be true for the examples given by Schneider, but on the other hand, other information is known e.g. some of the design loads can perhaps be excluded, the material strength can be investigated, dimensions could be measured etc.

Another question that can be discussed is: if reliability methods are chosen for evaluation of a bridge - what analytical models shall then be used e.g. to calculate the fatigue capacity of the concrete? The problem that arises if the analytical models in the codes are used could be exemplified with the study performed by Johansson (2004), where an investigation was performed to

see if present concrete codes were underestimating the fatigue capacity. Fatigue tests were performed on beams with the length of 2.5 m (and 2 m), width of 0.8 m and the thickness of 0.2 m and the results were compared to calculations according to BBK94 (1994,1996), CEB-FIP (1993) and EC2-2 (1996). Among other things the result was compared to the predictions according to the above-mentioned concrete design codes. It was then found that CEB-FIP (1993) was extremely conservative regarding fatigue capacity in shear and that BBK (1994, 1996) resulted in very conservative fatigue life predictions of fatigue of concrete in compression. This shows that if the analytical models presented in the codes are used in a reliability analysis, they can give an unnecessary conservative result – as in the case with fatigue capacity where big safety factors are included.

What procedure is used when a structure is designed? In many areas the so-called allowable stress format is still used. This design criterion limits the maximum stress to be less or equal to allowable values prescribed in standards or codes. In Schneider (1997) the safety condition is written as:

$$\sigma_{\text{allowed}} \geq \sigma_{\max} \tag{1}$$

In Sweden, and other countries as well, the so-called partial factor format is primarily used and it applies factors to all relevant design parameters. The partial factor format could according to Fahleson (1995) be described as a semi-probabilistic method since the partial coefficients are calibrated, in contrast to e.g. the allowable stress format, against probabilistic methods so that the method will give a reliability close to a predetermined reliability. In the Swedish Building Code, BKR03 (2003), it is written in the following way:

$$S\left(F_{\text{d}}, f_{\text{d}}, a_{\text{d}}, \gamma_{\text{S}}\right) \leq R\left(f_{\text{d}}, a_{\text{d}}, C, \gamma_{\text{R}}\right) \tag{2}$$

where *d* indicates design value, *S* is effect of action, *R* is resistance. *F* is action, *f* is the material property, *a* is geometrical parameters, γ_{S} is partial factor for the analytical model for the effect of action, γ_{R} is partial factor for the analytical model for resistance and finally *C* is a limiting value e.g. the greatest deformation for which the performance requirement is satisfied.

A method that can also be used for design of new structures is a probabilistic method where the probability of failure is calculated. This method is perhaps even more suitable to use in assessment of existing structures since the method uses available information regarding a specific structure. The factors that influence the problem are introduced as random variables with their distribution types and their respective parameters.

In Melchers (1999) the methods to calculate the probability of failure are divided into the following techniques: direct integration (possible only in some special cases), numerical integration (such as the Monte-Carlo simulation) or second-moment and transformation methods. In this paper a brief description of structural reliability analysis will be presented and a full description of the mathematical backgrounds and theories of structural reliability analysis can be found in e.g. Thoft-Christensen & Baker (1982), Schneider (1997), Ditlevsen & Madsen (1996) or Melchers (1999).

In Melchers (1999) structural reliability analysis is explained with the basic structural reliability problem consisting of one load function, *S,* and one resistance function, *R*. They are both described by a known probability density function $f_{\text{S}}()$ and $f_{\text{R}}()$ respectively. The probability of failure, p_{f}, is given by:

$$p_{\text{f}} = P\left(R - S \leq 0\right) \tag{3}$$

The principle is often described with an example where it is possible to solve the reliability problem analytically. This can be performed when *R* and *S* are two normally distributed random variables with means μ_R and μ_S and variances σ_R^2 and σ_S^2 respectively, see Figure 3.2. The safety margin $M = R - S$ then has a mean and a variance according to:

$$\mu_M = \mu_R - \mu_S \tag{4}$$

$$\sigma_Z^2 = \sigma_R^2 + \sigma_S^2 \tag{5}$$

Eq. (3) could then be written as:

$$p_f = P(R - S \le 0) = P(M \le 0) = \Phi\left(\frac{0 - \mu_M}{\sigma_M}\right) = \Phi\left[\frac{-(\mu_R - \mu_S)}{\left(\sigma_S^2 + \sigma_R^2\right)^{1/2}}\right] = \Phi(-\beta) \tag{6}$$

here $\Phi(\,)$ is the standard normal distribution function with zero mean and unit variance and is given in normal distribution tables. The higher β is, the higher is the safety of the structure. $\beta = \mu_M/\sigma_M$ is defined as the so-called safety index. β can also be expressed in words as the measure, see Figure 3.2, in standard deviation σ_M units, from the mean value, μ_M, to the failure limit $M = 0$. The random variable $M = R - S$ is also shown in Figure 3.2, in which the failure region $M \le 0$ is equal to the shaded area.

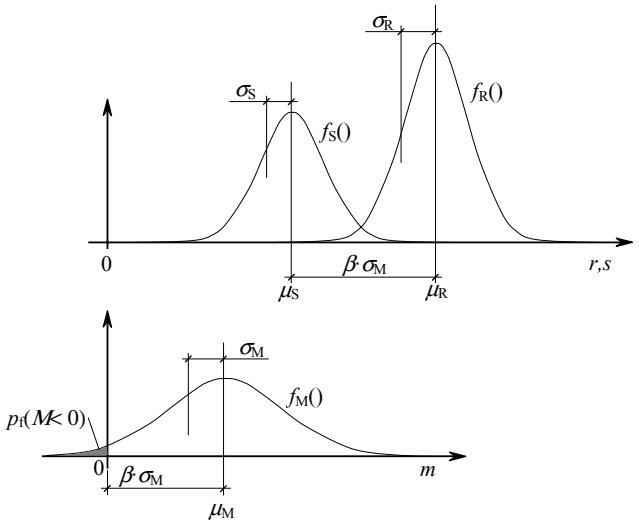

Figure 3.2 Probability density functions for the parameters, R, S and M i.e. $f_R()$, $f_S()$ and $f_M()$. Based on Schneider (1997).

The so-called weighting factors (or sensitivity factors), α_i, are of special interest, since they show what importance the corresponding variable has in the value of the probability of failure. For the example above these can be calculated from, Schneider (1997):

$$\alpha_R = \frac{\sigma_R}{\sqrt{\sigma_R^2 + \sigma_S^2}} \;;\; \alpha_S = \frac{\sigma_S}{\sqrt{\sigma_R^2 + \sigma_S^2}} \tag{7}$$

where $\alpha_R^2 + \alpha_S^2 = 1$. The values of these sensitivity factors are between 1 and -1. They are positive for favourable parameters (resistance) and negative for unfavourable (loads).

One method, which belongs to the numerical integration methods, of solving the expression for the probability of failure, p_f, is to use so-called Monte-Carlo simulation. The method uses random sampling to simulate a large number of experiments and register the result. Random sampling is performed for all involved stochastic variables to obtain random sample values of the stochastic variables which are then used to check *R-S*. This is repeated many times and the number of times *R-S* is less or equal to zero, i.e. when the structure has failed, are registered and the probability of failure, p_f, is given as:

$$p_f = \frac{n_{fail}}{N_{total}} \tag{8}$$

where N_{total} is the total number of trials and n_{fail} is the number of trials where $R\text{-}S \leq 0$.

In JCSS (2001) it is stated that there are mainly two different fatigue models that are used in a reliability analysis, i.e. S-N models based on experiments or fracture mechanic models. If e.g. the S-N model is used, Melchers (1999) points out that e.g. constants used in the models must be introduced as random variables (combined with estimates of the uncertainties of the parameters) and the model itself must give a realistic estimation of the fatigue life. This compared to e.g. the design codes where constants could be found in tables and the model often gives conservative result. If this is commented, i.e. the introduction of the constants as random variables and as realistic models as possible, it seems to be something that is not something specific only to fatigue analyses, but something that is a must for all reliability analyses.

In this thesis the computer programme Variable Processor, VaP, developed by Petschascher (1993) and Schneider (1997), has been used to determine the probability of failure, p_f, or the so-called safety index β. The program uses, among others, the First Order Reliability Method (FORM) and the Monte Carlo method in the analysis.

3.2 Target Reliability Index

One way to determine if a structure is safe enough is to compare the calculated reliability index, β, to a so-called target reliability index, β_0, that represents the safety level of the existing codes, see Schneider (1997).

Values of this target reliability index, β_0, are given in e.g. the Probabilistic Model Code issued by the Joint Committee on Structural Safety, JCSS (2001). In the Swedish Design Regulation, BKR03 (2003), the following target reliability index, β_0, is given for a reference period of 1 year:

$\beta_0 > 3.7$ for Safety Class 1 (corresponds to the probability of failure, $p_f = 1 \cdot 10^{-4}$)
$\beta_0 > 4.3$ for Safety Class 2 (corresponds to the probability of failure, $p_f = 8 \cdot 10^{-6}$)
$\beta_0 > 4.8$ for Safety Class 3 (corresponds to the probability of failure, $p_f = 8 \cdot 10^{-7}$)

The safety classes above are in turn connected to the possible injury to persons:

- Safety Class 1 (low), little risk of serious injury to persons
- Safety Class 2 (normal), some risk of serious injury to persons
- Safety Class 3 (high), great risk of serious injury to persons

4 Fatigue

In this chapter fatigue in general is described. The parts that have been chosen are ones that are common and they show some of the different factors that have been studied over the years. Fatigue analysis has been described in several textbooks for different materials over the years, see e.g. Frost et al. (1974), Mallet (1991), Gylltoft (1994), Suresh (1998) or Dahlberg & Ekberg (2002).

Fatigue of materials was first observed and documented for iron. Suresh (1998) states that the first study of metal fatigue is believed to have been conducted around 1829 by the German engineer Albert (1838). He performed repeated load proof tests on mine-hoist chains made of iron. The interest in the study of fatigue expanded later on due to the increasing use of iron particularly in wheel axis and in bridges in railway systems, see e.g. general text books by Suresh (1998) and Frost et al. (1974). For concrete on the other hand, the fatigue phenomenon was observed rather late. According to Mallet (1991) the first fatigue curve for concrete cubes in compression was published by Van Ornum (1903). Van Ornum found no endurance limit for concrete similar to that which had been assumed for steel but he concluded that concrete had a fatigue strength about 55% of its static ultimate strength for a life of 7000 cycles. Hsu (1981) states that later on the development of highway systems in the 1920s led to further interest in the fatigue of concrete, since the concrete pavements used for the highways are subjected to millions of load cycles from axle loads of cars and trucks.

The concrete fatigue research was later on intensified especially in Scandinavia during the 1970s. According to Gylltoft (1994) this was related to the oil industry and their many offshore structures that were exposed to forces from the sea.

During the last few years the concrete fatigue phenomenon has once again gained interest, especially for railway bridges due to more slender structures, higher traffic speeds and higher axle loads. In Sweden for example, the increased axle loads on the existing railway lines have caused problems with the bridges since it has led to a change of the conditions for the bridges compared to the ones when they were built. One of the problems is that the bridges often are predicted to fail in the fatigue analysis when they are evaluated with the present concrete codes.

Over the years some Swedish fatigue tests have been performed. In Tepfers (1973) fatigue strength of overlap splices was studied, in Westerberg (1973) fatigue capacity of reinforced beams designed to fail in shear was tested (cited from Johansson (2004)), in Emborg et al. (1982) fatigue of cable couplings in prestressed beams was studied and in Ohlsson et al. (1990) fatigue strength

for unreinforced beams was tested for temperatures down to -35°C. The latest tests seem to have been presented in Johansson (2004), where bridge deck fatigue tests were conducted in order to compare the results with predictions according to concrete codes.

4.1 Fatigue in General

What is then a fatigue failure? Fatigue failure can be defined as a failure that occurs below the stress limit of a material when it has been exposed to repeated loading. Some materials have a fatigue limit, which implies that below this load no fatigue failure will occur. Steel is such a material but for concrete no such limit has been detected (reports of a limit could be found though, see Hordijk (1991)). The reason for this difference is that steel is a strain-hardening material (the strength increases at large strains) and concrete is a strain-softening material (the strength decreases at large strains).

Fatigue tests are often very expensive and time-consuming to perform due to the many factors that influence the fatigue capacity. The many factors lead in turn often to great variation in the results. A few of the influencing factors are: material composition, load frequency, maximum load level, moisture content etc.

If a fatigue test only lasts a few load cycles it is named low-cycle fatigue (LCF). The limit that is used is approximate up to 10^3 (-10^4) load cycles. If the test lasts longer than this limit it is called high-cycle fatigue (HCF). There is also a third limit for a fatigue test, approximately 10^7 load cycles, called super-high cycle fatigue (SHCF) which is not so common. Many structures are subjected to fatigue loads. Some of them are bridges, roads, railway sleepers, offshore structures etc. The limits that have been mentioned here are not absolute ones, you can find other ones in the literature. In Figure 4.1 Hsu (1981) has given some examples of some structures and to which fatigue category they belong.

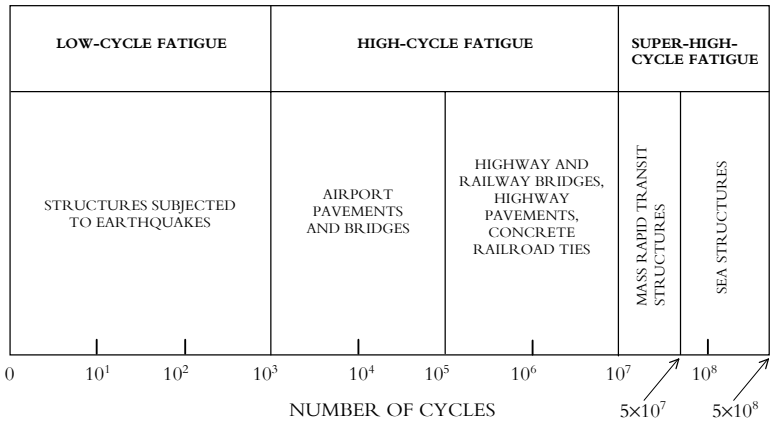

Figure 4.1 Fatigue load spectrum according to Hsu (1981).

Hsu (1981) points out that it is important to look at the fatigue problem with a broad view and have in mind that rules and equations derived in research projects regarding high-cycle fatigue cannot be used in a study regarding low-cycle fatigue since the two ranges are different. Two reasons for this difference are the rate of loading and the effect of time in a fatigue test. Some researchers have claimed that the rate of loading is of no importance in a fatigue test but others have shown that it is of great importance regarding low-cycle fatigue. The same could be said regarding the effect of time in a fatigue test.

4.2 Steel

The fatigue behaviour of steel has been described in several textbooks, e.g. Suresh (1998), Dahlberg & Ekberg (2002) or Gylltoft (1994). In Dahlberg & Ekberg (2002) the fatigue failure is described with three phases; crack initiation, crack growth and finally a brittle failure. The process starts with crack initiation and if the test continues these cracks will grow in size and a dominant crack will form with failure as consequence. If the failure surface is studied it is often possible to identify two regions; a fairly smooth surface where the dominant crack has formed and the failure surface that is rougher.

Fatigue capacity is normally described by so-called Wöhler curves. They are named after the German engineer August Wöhler who conducted studies of the fatigue capacity of railway axles in the late nineteenth century, Wöhler (1858-1870). In Figure 4.2 results from fatigue tests are presented. If the loading of the material has a constant mean value and a constant amplitude then the fatigue life can be estimated directly from the Wöhler diagram of the material. The figure shows the number of load cycles for different applied amplitudes of stresses and as one can see the fatigue life decreases with increasing number of cycles. The curve is also sometimes called an *S-N*-curve (Stress-Number-curve). If the number of load cycles at failure, *N*, is presented on a logarithmic axle the curve becomes linear.

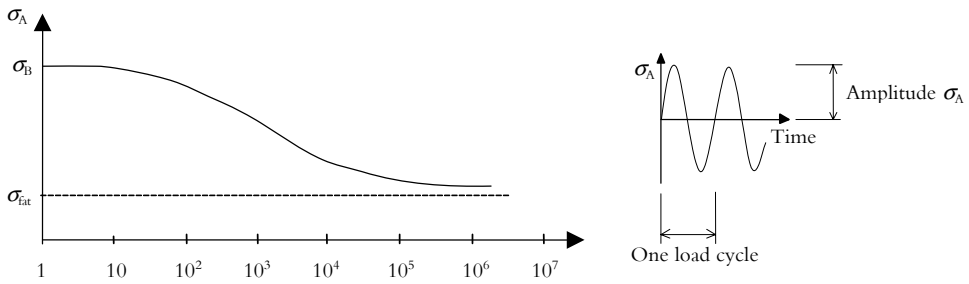

Figure 4.2 Number of load cycles N for different applied amplitudes of stresses, σ_A. σ_B is the static failure load. For e.g. steel, σ_{fat} is the fatigue limit, if the loading does not exceed this limit no fatigue failure occurs, Elfgren & Gylltoft (1997).

The most well-known relationship when analysing steel fatigue is perhaps Paris' law, Paris et al. (1961). In Shah et al. (1995) the equation is written as follows:

$$\frac{da}{dN} = C_F \left(\Delta K\right)^{m_F} \tag{9}$$

where the parameters C_F and m_F in Eq. (9) are experimental constants, da/dN is the crack propagation rate and K is the stress intensity factor. It could also be written in logarithmic form:

$$\log\frac{da}{dN} = m_F \log\Delta K + \log C_F \tag{10}$$

4.3 Concrete Fatigue

Unlike steel, concrete is not a homogeneous material. Already during the hardening process micro cracks and air bubbles are formed. Mallet (1991) writes that fatigue of concrete is a progressive process of micro-crack initiation and propagation leading to macro-cracks which can grow and determine the remaining fatigue life by causing stress to increase until failure occurs.

4.3.1 Influencing Factors

There are several factors that influence a fatigue test. Some of them are; the maximum stress level (often the live load), the lower stress level (often the dead load), the load amplitude, loading frequency (lower frequency gives lower number of cycles to failure) etc., see e.g Holmen (1979), Cornelissen (1986a), Mallet (1991), Sørensen (1993) or Gylltoft (1994).

The load can also be varied in many ways in a fatigue test, see Figure 4.3. You can have pulsating sinusoidal load (which implies that the mean stress, σ_m, is equal to zero, see Figure 4.3a and the amplitude is σ_a, the load can be the same as in example a) in Figure 4.3 but with a mean stress equal to the amplitude and $\sigma_{min} = 0$. A more general case is shown in Figure 4.3c where $\sigma_m \neq 0$ and $\sigma_m \neq \sigma_{min}$. There is also a type of loading called irregular loading which perhaps is the most "correct" type of loading a structure is exposed to, see Figure 4.3d. In this case it is a bit more difficult to decide loading cycle, mean value or the amplitude. There are several methods that can be used to determine these parameters for example the peak count method, range pair count or the rain flow count method. A description of the methods could be found in e.g. Mallet (1991) or Dahlberg & Ekberg (2002).

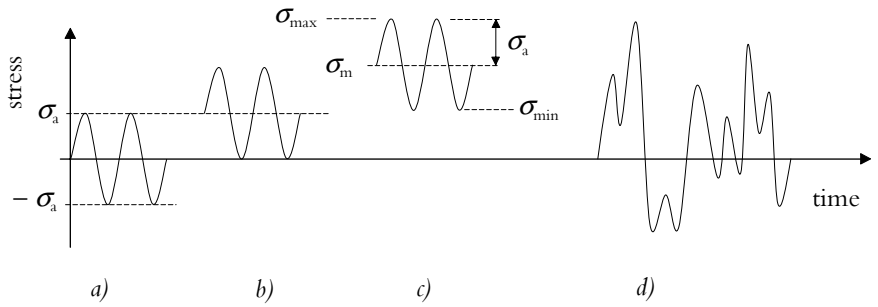

Figure 4.3 Different types of loading that can be used in a fatigue test. Definitions: $\sigma_m = 0.5(\sigma_{max}+\sigma_{min})$, $\sigma_a = 0.5(\sigma_{max}-\sigma_{min})$. Based on figures in Dahlberg & Ekberg (2002) and Gylltoft & Elfgren (1977).

4.3.2 Refined Wöhler Curves

In order to improve the Wöhler curve Aas-Jakobsen (1970) examined the influence of the minimum stress, f_{min}, on the fatigue strength. He showed that the relationship between f_{max}/f' and f_{min}/f' is linear for fatigue failure at $N = 2 \cdot 10^6$ load cycles. If R is defined as the ratio between the maximum and minimum stress, f_{max}/f_{min}, then the relationship between f_{max}/f' and R should also be linear (f' equal to the static strength). Combining these linear relationships he derived the following expression:

$$\frac{f_{max}}{f'} = 1 - 0.064(1-R)\log N \tag{11}$$

where $\beta = 0.064$ (β is the slope of the S-N curve when $R = 0$). Eq. (11) is valid for $0 \leq R \leq 1$, but not for stresses which alternate between compression and tension.

Tepfers & Kutti (1979) made an extensive study of Eq. (11) for ordinary concrete and lightweight concrete with the intention of proposing a fatigue relationship common for both types of concrete. They used experimental data from the literature (corresponding to $\log(N) = 6$) and their own studies and proposed the following equation (see also the plot in Figure 4.4):

$$\frac{f_c^{max}}{f_c^{'}} = 1 - 0.0685(1 - R)\log N \tag{12}$$

where N is the number of loading cycles at fatigue failure, R is the ratio between the maximum and minimum stress (f_c^{min} / f_c^{max}), f_c^{max} is the highest compressive stress under pulsating load, f_c^{min} is the lowest compressive stress under pulsating load and, finally, $f_c^{'}$ is the static cylinder strength.

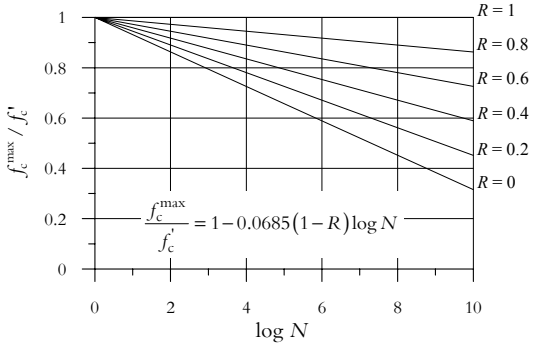

Figure 4.4 Graphical representation of Eq. (12). From Tepfers & Kutti (1979).

Tepfers & Kutti (1979) also pointed out that it is of great importance that if Eq. (11) is valid, Wöhler curves shall not be based on measurements where the amplitude or the lower stress f_c^{max} is kept constant, but on a constant $R = f_c^{min} / f_c^{max}$.

Hsu (1981) studied the work done by Aas-Jakobsen (1970) and Tepfers & Kutti (1979) and even though he considered Eq. (12) being a big step forward in the development of the S-N-curve, it had in his opinion two essential weaknesses. The first one is when R = 1, Eq. (12) becomes $f_c^{min} / f_c^{max} = 1$ and f_{max} equals to a constant. He points out that this is theoretically incorrect because when R approaches unity a repeated load becomes a sustained load. It has by other researchers been established that sustained strength of concrete is time-dependent. Therefore time must be included in the relationship. The second weakness is that it does not include the rate of loading as a variable and this must be considered at least in low-cycle fatigue.

In order to eliminate these two weaknesses Hsu (1981) introduced the element of time into the relationship by introducing the third dimension of T, where T is the period of the repetitive loads expressed in seconds per cycle. By doing this, a three-dimensional space is created consisting of nondimensionalized f as the vertical axis with log N and log T as the two mutual perpendicular horizontal axes, see Figure 4.5a ($f = f_{st}^{'} / f_{sus}^{'}$, where $f_{sus}^{'}$ is the sustained strength, or discontinuity strength at 10 years, and $f_{st}^{'}$ is the static strength at a period of 1 sec/cycle). Hsu then drew a 45° diagonal straight line connecting these two axes and expressed the line by the equation (log N+log T) = *constant*, which leads to NT=*constant* where NT expressed the duration of time of the repetitive loading. He could now draw a series of straight lines representing increasing duration of loading time.

Using the S-N-T space Hsu (1981) added the influence of time on the strength of concrete by using stress-time relationships found in the literature. Hsu (1981) plotted the curve FC_1 in the f-N plane and the curve FB in the f-T plane with the help of stress-time relationships for sustained load strength found in the literature which corresponds to the case of cyclic loading when R=1, see Figure 4.5a. He then joined the points C_1 and B and thereby created the surface FBC_1. Fur-

thermore, again with the help of relationships found in the literature, the interaction surface ABC could be created for R=0 where the curve AB shows that the strength of concrete increases with increasing rate of stressing. In addition, the f-N curve AC was shown to have a steeper slope in the low-cycle region than in the high-cycle region which was consistent with observations that fatigue strength in low-cycle fatigue region is sensitive to the load duration and the rate of loading.

The two interaction surfaces ABC and FBC_1 in Figure 4.5a then defined the cases of R=0 and R=1. A family of interaction surfaces could then be constructed between these two boundary cases by linear interpolation using R as the parameter.

Since these spaces that were created between the boundary conditions R=0 and R=1 were complex to describe, he simplified them into planes, see Figure 4.5b. The FBC_1 surface in Figure 4.5a can be substituted with the FBC_1 plane in Figure 4.5b, but the ABC surface for R=0 in Figure 4.5a should be approximated by the planes ABD (low-cycle region) and BDC (high-cycle region) in Figure 4.5b.

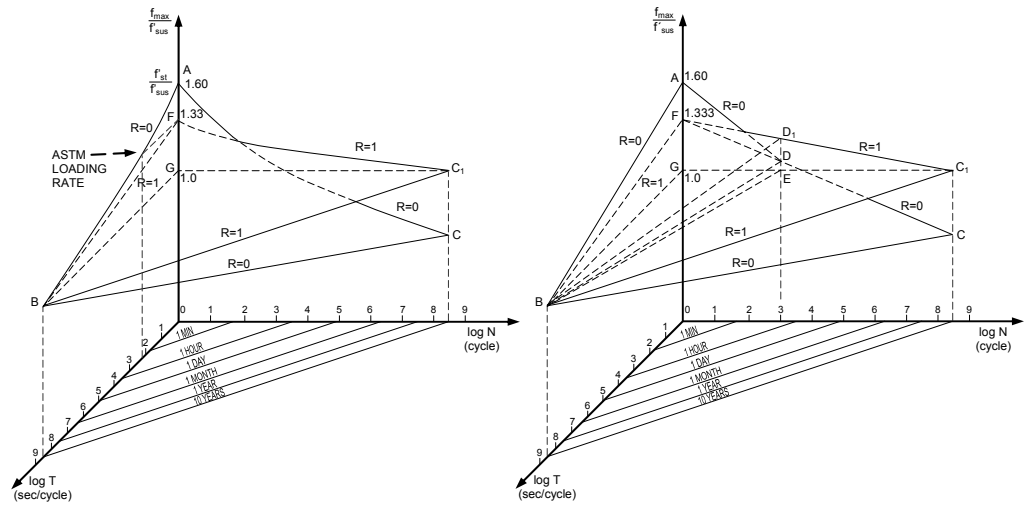

Figure 4.5 a) Graphical representation of S-N-T-R relationship. b) Simplification of S-N-T-R relationship. From Hsu (1981).

Assuming that the transition from R=0 to R=1 was linear Hsu established two equations, one for high-cycle fatigue and one for low-cycle fatigue (Hsu also introduced an equation for the boundary between high-cycle fatigue and low-cycle fatigue). By introducing some assumptions and using data from the literature the following equations were established (see Hsu (1981)):

High-cycle fatigue:

$$\frac{f_{\max}}{f_c'} = 1 - 0.0662\left(1 - 0.556R\right)\log N - 0.0294\log T \tag{13}$$

Low-cycle fatigue:

$$\frac{f_{max}}{f_c'} = 1.20 - 0.20R - 0.133(1 - 0.779R)\log N - 0.053(1 - 0.445R)\log T \quad (14)$$

where N is the number of loading cycles up to fatigue failure, $R = f_{min}/f_{max}$, f_{max} is the maximum stress in repetitive loading, f_{min} is the minimum stress in repetitive loading, f_c' is the static compression strength of concrete tested at ASTM loading rate and T is the period of the repetitive loads expressed in sec per cycle. Hsu (1981) mentions that it is generally accepted that if the maximum fatigue stress, σ_{max}, is nondimensionalized by the static strength σ' of an identical specimen, this nondimensionalized S-N curve (σ_{max}/σ' versus log N) is independent of specimen shape, the concrete strength, the curing conditions etc.

Hsu compared the equations with experimental data from the literature and the equations fitted the data rather well in some cases. Hsu has also examined the effect of T (the rate of loading) and found out that it had an influence but due to scatter of test results it could not be clearly established unless the difference in T was of two orders of magnitude. More thorough information can be found in Hsu (1981).

The model presented by Hsu (1981) was compared to three similar models by Sørensen (1993), among them the model presented by Tepfers & Kutti (1979), see Eq. (12). Sørensen (1993) was unable to decide which model that was most appropriate to predict the fatigue life for plain concrete. One observation that Sørensen (1993) made, was that the proposal by Hsu (1981) predicts smaller slopes in the high-cycle region than in the low-cycle region, which is a phenomenon observed in the literature.

A model proposed by Stemland et al. (1990) was developed to predict the relation between S_{max}, S_{min} and N. The main intention with the constant amplitude tests performed on non-reinforced concrete by Stemland et al. (1990) was to evaluate the effect of the change in minimum stress level on the fatigue life. Their design proposal for fatigue in compression has the following formula:

$$\log N = \left(12 + 16 \cdot S_{min} + 8 \cdot S_{min}^2\right) \cdot \left(1 - S_{max}\right) \quad (15)$$

where, N is the number of load cycles, S_{min} is the minimum level of loading in one cycle (= relative stress, reference stress is the static strength) and S_{max} is the maximum level of loading in one cycle(= relative stress, reference stress is the static strength).

As can be seen in Figure 4.6 the slope of the curves changes at log N = 6. They found that this is approximately where the experimental results started to deflect towards longer lives than indicated by the equation. They therefore proposed that log N greater than log N = 6 should be multiplied by the factor (based on Norwegian Code), X:

$$X = 1 - 0.2 \cdot (\log N - 6) \quad (16)$$

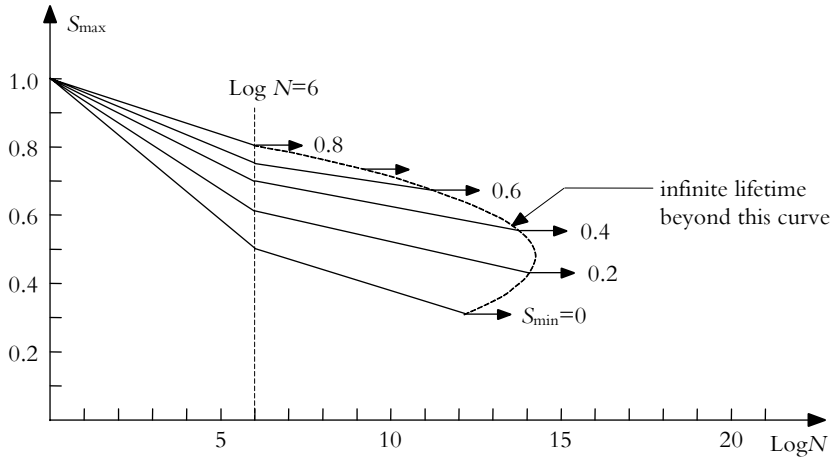

Figure 4.6 S-N diagram for fatigue of concrete in compression according to Stemland et al. (1990).

According to Sørensen (1993) some positive features in this model are the distinction between the inclination in the low- and high-cycle region and the simplicity in practical use. One problem with the model was that the time effects are omitted in case of low-cycle fatigue. For further information, see Stemland et al. (1990) or Sørensen (1993). The model proposed in CEB-FIP (1993) is based on the model suggested by Stemland et al. (1990).

4.4 Accumulated Fatigue Damage, Palmgren-Miner

A relation called the Palmgren–Miner rule can be used when estimating the accumulated fatigue damage. The rule was first proposed by Palmgren (1924) and independently by Miner (1945), see also Mindess et al. (2002). It is convenient to use the rule as an approximation for high cycle fatigue and the rule suggests that failure occurs when:

$$\sum_{i=1}^{I} \frac{n_i}{N_i} = 1 \tag{17}$$

Here n_i is the number of load cycles at some stress condition and N_i is the number of load cycles required to cause failure at that condition. The rule assumes that there will be a linear accumulation of damage due to each loading cycle and that the hypothesis is not always conservative, i.e. it must be used with care.

5 Concrete Fatigue in Tension

In this chapter the tensile behaviour of concrete is described briefly and in papers C, D and E the described methods/models have been used. More information can be found in e.g. Cornelissen (1986a), Hordijk (1989), Hordijk (1991), Pinto (1996) or Noghabai (1998).

For concrete subjected to static compression load several studies have been performed over the years, but when it comes to tensile loading far fewer studies have been carried out. According to Hordijk (1989) the first publication demonstrating a post-peak behaviour of concrete under tensile loading is believed to be the one by Rüsch & Hilsdorf (1963). One reason for the increased interest in the tensile behaviour of concrete was that fracture mechanics began to be used for concrete structures in order to understand and describe the mechanisms of cracking.

Even though nowadays the tensile strength of concrete is neglected in many design codes, it is of importance. Because, as pointed out by Cornelissen (1986a), the tensile strength governs the cracking behaviour and therefore also, e.g. the stiffness, the damping action, the bond to embedded steel and the durability of concrete. The tensile properties are also of importance when it comes to shear capacity of concrete.

5.1 Tensile Behaviour of Concrete and Fracture Mechanics

In order to describe the phenomenon of cracking of concrete in tension researchers started to use fracture mechanics, methods that had been used since the 1940s for metals and glass. Fracture mechanics methods study the conditions in the area in front of and around a crack tip. There are several text books on the subject of fracture mechanics of concrete, e.g. Elfgren (1989) or Bažant & Planas (1998).

In Pinto (1996) the tensile behaviour of concrete is very well explained with the help of Figure 5.1: In Figure 5.1 a deformation controlled centric tension test is performed on a specimen, where the specimen is loaded with the force P and the total deformation is measured over the length l. At the left side of Figure 5.1 the specimen is plotted for the load steps A, B and C. The load steps are also marked in the load-deformation curve at the right side. Load step A is before peak load, load step B at peak load and load step C after the peak load in the descending branch of the load-deformation curve. Already before the peak load is reached, some microcracking occurs see Figure 5.1a. As the microcracking is uniformly distributed at the macrolevel, a uniform strain over the length of the specimen may be assumed. The strain ε is plotted over the length of the specimen in Figure 5.1 right next to the specimen. Immediately before the

peak load, an accumulation of micro cracks occurs at the weakest part of the specimen. At the macrolevel this leads to an additional strain over the length h of this weak part. A crack band (also called process zone or softening zone) of width h develops, see Figure 5.1b. Having passed the peak load, the crack band localizes more and more. The crack band width diminishes, and the deformation within the crack band increases. The final failure occurs due to one single crack.

Pinto (1996) states that the total deformation of the specimen may be split up in the bulk deformation - which is almost linearly elastic up to the peak load – and the deformation of the crack band. Just before the peak load is reached, between point A and B in Figure 5.1, the σ–ε relationship bends off from the linear behaviour. Where the non-linear behaviour starts to deviate varies between the studies performed in the literature. According to Pinto (1996) these differences in the experimental results are caused by different boundary conditions. Any source of non-uniformity, like internal bending due to non-uniform cracking, eigenstresses due to differential shrinkage and temperature, notch effects etc. causes nonlinearities.

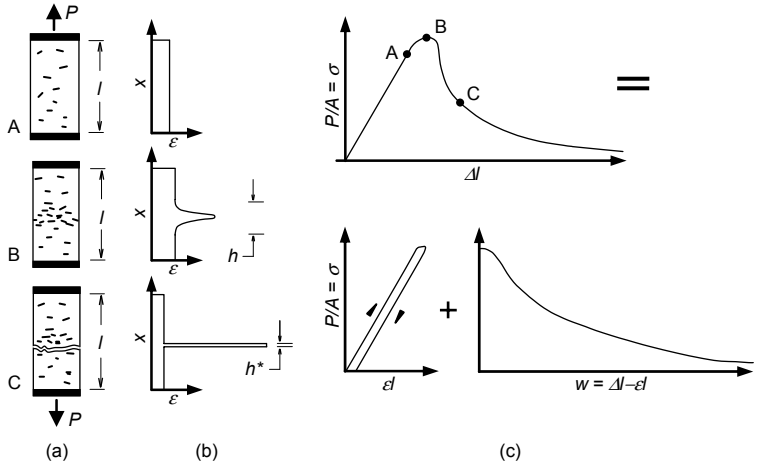

Figure 5.1 The tensile behaviour of concrete. Based on figure in Pinto (1996).

In Pinto (1996) some suggestions are presented for the σ-w relation in the case of monotonic loading, see Figure 5.2.

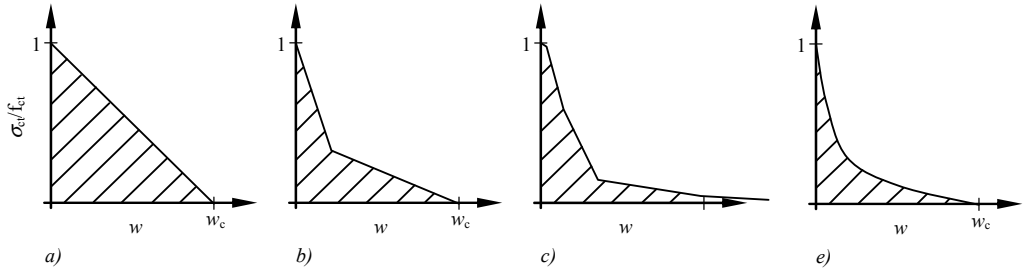

Figure 5.2 Suggestions for the σ-w relation: (a) linear, (b) bilinear – Petersson (1981), (c) multilinear – Gustafsson (1985) and (d) Cornelissen et al. (1986). Based on Pinto (1996).

5.2 Fictitious Crack Model

The classical concept of fracture mechanics was not appropriate for concrete because, as formulated by Mihashi & Rokugo (1998), concrete is a kind of composite and a very heterogeneous material (compared to glass and metals). Therefore, cracks are arrested when they encounter aggregates and a large fracture process zone is developed in front of the main crack. The breakthrough was done by A Hillerborg, who proposed a model that became well-known as the "fictitious-crack-model", which represents a relation between transmitted stress over a narrow crack and the crack width, see Hillerborg et al. (1976).

In Hordijk (1991) the model proposed by Hillerborg et al. is described with Figure 5.3. Briefly, the model assumes the existence of a "fictitious" crack ahead of a visible crack see Figure 5.3. The visible crack is a crack that cannot transfer tensile stress, while in the fictitious crack (also called the process zone) so-called crack-closing stresses are active. The stress depends on the crack opening in the fictitious crack. The relation between crack opening and stress can be obtained from a deformation controlled uniaxial tensile test.

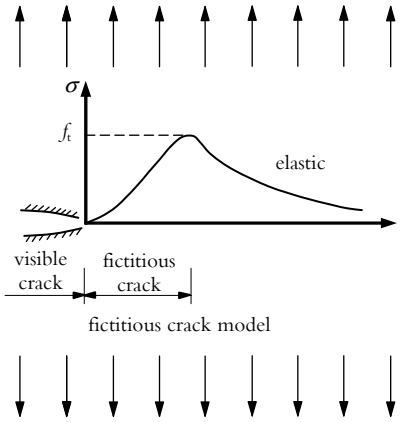

Figure 5.3 Assumed stress distribution ahead of visible crack according to a model for a softening material like concrete, from Hordijk (1991).

5.3 Fatigue Capacity of Concrete in Tension

Tensile fatigue tests have been performed in different ways during the years. At the beginning e.g. tests on specimens loaded in bending and on specimens exposed to splitting load were used due to the fact that they were fairly simple to perform. During the last few decades direct deformation-controlled uniaxial tensile tests have become a more common method. The reason for this is that special grips are not needed, as in the early days, instead the development in the adhesive trade has made it easier to fix the specimens together with more advanced test apparatus.

One of the first tensile fatigue strength tests of plain concrete was performed by Tepfers (1979), who made a study to see if the equation for concrete fatigue subjected to compression load, see section 4.3.2, was also possible to use for concrete fatigue in tension. The fatigue tests were performed on cube splitting test specimens. Tepfers tested two different concrete strengths (with R = 0.2, 0.3 and 0.4) and found that the sensitivity to fatigue due to tensile stresses was independent of the level of strength. The main object of the investigation was to determine Wöhler curves for ordinary plain concrete subjected to pulsating tensile stresses, and to compare

these Wöhler curves with the relationship determined for compressive stresses. The relationship is as follows for $0 \le R \le 1$:

$$\frac{f_r^{max}}{f_r^{'}} = 1 - \beta(1-R)\log N \tag{18}$$

,where N is the number of loading cycles up to fatigue failure, $R = f_r^{min} / f_r^{max}$, f_r^{max} is the upper limit of fluctuating splitting stress in tension, f_r^{min} is the lower limit of fluctuating splitting stress in tension and $f_r^{'}$ is the static splitting strength in tension

Tepfers received $\beta = 0.0597$ (standard deviation $s = 0.0206$) for all his tests where 71 of 83 test specimens had $f_r^{max} / f_r^{'} \ge 0.80$. Since uncertainties in the fatigue result can appear due to difficulties to determine exactly the static tensile strength of the individual test specimen at such high values of $f_r^{max} / f_r^{'}$ he then excluded the values of $f_r^{max} / f_r^{'} \ge 0.80$ and obtained $\beta = 0.0675$ (standard deviation $s = 0.0133$) for these 12 remaining tests. Since this β-value differed so little from the original value $\beta = 0.0685$ he concluded that this value could be used and with that, Eq. (18) could also be applied for concrete subjected to pulsating tensile stresses. Worth mentioning is that when values of $f_r^{max} / f_r^{'} = 0.80$ were included in the evaluation the value of β increased to 0.0704 (standard deviation $s = 0.0238$).

5.3.1 Material Models for Concrete Fatigue in Tension

During the 1980s and 1990s several material models for the fatigue behaviour of concrete in tension were developed which could be implemented in FE-analysis. Some of them are presented and can be seen as a description of how this research field has developed over the years. Models have been proposed by e.g. Gylltoft (1983), Rots et al. (1985), Reinhardt et al. (1986), Yankelevsky & Reinhardt (1989), Hordijk (1991) and Duda & König (1991) and some of them are here described briefly. In Pinto (1996) these models, except the last one, are described as "phenomenological" i.e. the material behaviour is determined by test and then described by curve fitting, where the curve fitting only describes the material behaviour but does not describe the physical background. The model proposed by Duda & König (1991) is described as a semi-physical model since it uses mechanical elements such as blocks and springs.

In Gylltoft (1983) a fracture mechanics model for direct tensile cyclic loading is presented. The model is based on an energy criterion. Path OABC in Figure 5.4 represents a uniaxial static tensile test and the micro cracking is considered to start when point A is reached. If unloading is performed, e.g. at point E, path EFG represents unloading and when zero stress is reached the remaining strain is denoted ε_f. When changing over to compressive stresses it is proposed that the microcracks will not close completely resulting in a strain gap, GF (e.g. due to particles within the microcracks which have come loose etc.). When reloading, path GF'E', only a partial re-opening of the cracks occurs, path GF', and this is due to irreversible deformations near the tips of the microcracks. The gradient of path EF and F'E' is assumed to be equal to the "linear elastic gradient", path OA.

The model could also be explained as if unloading is performed in the area to the left of the unloading path EF and corresponds to that part of the fracture energy already used in creating partial cracking, microcracking. The energy corresponding to the area to the right of path EF remains, i.e. the area below path FEBC. If reloading is performed along path F'E' the remaining stress-strain path EBC must be lowered to path E'B'C' in order to keep the remaining energy constant. It can also be explained as if the energy supplied to the fracture zone in an unloading-reloading cycle, corresponding to the "hysteresis loop" surrounding the area A_1, is used for mi-

crocracking, corresponding to the area A_2. Therefore, in every load cycle a certain amount of energy is consumed by the material. When the sum of all amounts of energy consumed in the fracture zone equals the fracture energy G_f, the fracture process is finished, Gylltoft (1983) summarized in Elfgren (1989).

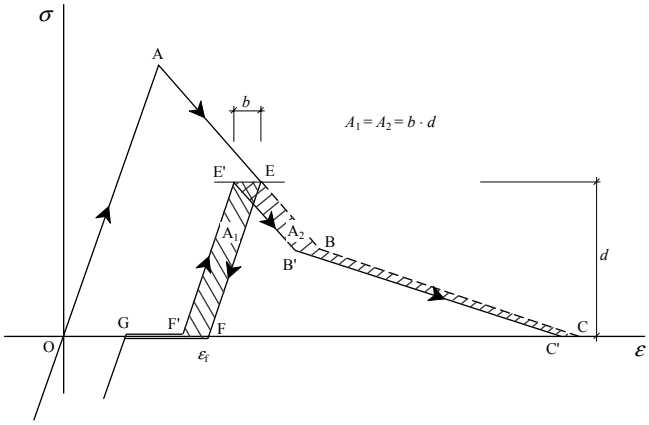

Figure 5.4 An energy criterion implying lowering of the remaining stress-strain curve after an unloading-reloading cycle. Based on Gylltoft (1983).

In 1991 Hordijk (1991) presented a model for the cyclic behaviour of concrete called the continuous-function model and it is presented visually in Figure 5.5. The model is similar to a model presented by Yankelevsky & Reinhardt (1989) and according to Hordijk their model probably gives the best approach to the real cyclic behaviour. The model uses a set of geometrical loci (so-called "focal points") to compute the piecewise linear branches of the unloading reloading cycles. This model was also suitable for implementation in FE codes. Why then develop a new model Hordijk asked? The reason for this was that the model demanded many operations in the FE analysis (the model was also, according to Hordijk, found to give incorrect results for very small crack openings).

The model by Hordijk (1991) uses, in contrast to the model by Yankelevsky & Reinhardt, analytical expressions for the unloading and reloading curve. The model consists of three expressions, based on close inspection of the experimental results: expression for the unloading curve (I), the gap in the envelope curve (II) and the reloading curve (III), see Figure 5.5. Starting from point (w_{eu}, σ_{eu}) at the envelope curve, the unloading curve is determined by:

$$\frac{\sigma}{f_t} = \frac{\sigma_{eu}}{f_t} + \left\{ \frac{1}{3\left(\frac{w_{eu}}{w_c}\right) + 0.4} \right\} \left[0.014 \left\{ \ln\left(\frac{w}{w_{eu}}\right) \right\}^5 - 0.57 \left(1 - \frac{w}{w_{eu}} \right)^{0.5} \right] \tag{19}$$

For the description of the gap in the envelope curve the description of w_{inc} was preferred. The expression for w_{inc} as a function of the coordinates at the point of leaving the envelope curve and the lower stress is:

$$\frac{w_{inc}}{w_c} = 0.1 \frac{w_{eu}}{w_c} \left\{ \ln\left(1 + 3 \frac{\sigma_{eu} - \sigma_L}{f_t} \right) \right\} \tag{20}$$

The coordinates of the returning point on the envelope curve (w_{er}, σ_{er}) could now be found with:

$$w_{er} = w_{eu} + w_{inc} \tag{21}$$

Starting from the point at the lower stress level (w_L, σ_L) up to point (w_{er}, σ_{er}) at the envelope curve the reloading curve is determined by:

$$\frac{\sigma}{\sigma_L} = 1 + \left[\frac{1}{c_3} \left\{ \frac{(w - w_L)}{(w_{er} - w_L)} \right\}^{0.2c_3} + \left\{ 1 - \left(1 - \frac{(w - w_L)}{(w_{er} - w_L)} \right)^2 \right\}^{c_4} \right] \left(\frac{c_3}{c_3 + 1} \right) \left(\frac{\sigma_{er}}{\sigma_L} - 1 \right) \tag{22}$$

where the coefficients c_3 and c_4 are:

$$c_3 = 3 \left(3 \frac{f_t - \sigma_L}{f_t} \right)^{\left(-1 - 0.5 \frac{w_{eu}}{w_c} \right)} \cdot \left\{ 1 - \left(\frac{w_{eu}}{w_c} \right)^{\left(\frac{0.71 f_t}{f_t - \sigma_L} \right)} \right\} \tag{23}$$

$$c_4 = \left[2 \left(3 \frac{f_t - \sigma_L}{f_t} \right)^{-3} + 0.5 \right]^{-1} \tag{24}$$

When the model was compared with experimental results Hordijk found that the model appeared to predict the cyclic behaviour well. The model by Hordijk (1991) could also describe the procedure for reversals of crack opening within a loop. For further details regarding the complex expressions, see Hordijk (1991).

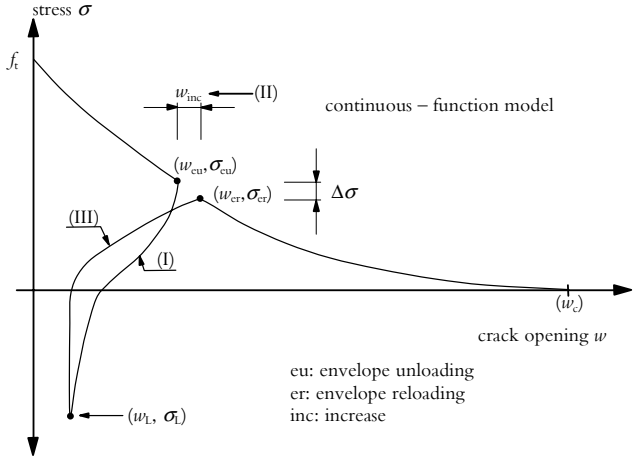

Figure 5.5 Set-up for the description of crack cyclic behaviour with the continuous-function model, from Hordijk (1991).

The model by Duda & König (1991) consists of simple rheological elements (springs and friction blocks) and describes the σ-w relation for monotonic loading as well as cyclic loading, using physical parameters. The background to the model is that transfer of stresses over a crack is possible due to the friction forces acting between grains and matrix. Considering every single grain

as a friction block a concrete cross section in which a crack is developing can be described as a parallel arrangement of many friction blocks (Duda & König (1991)). Duda & König concluded that their model, compared with other formulations known to that time in the literature, had several advantages e.g. the model is based on mechanically clear and reproducible conception, the relation between stress and crack width is described by simple analytical relations etc. Duda & König achieved, after implementation in a finite element program, good correlation with experimental results.

An investigation of bridge deck slab was presented by Schläfli (1999) and a model based on fracture mechanics and dowel action of the longitudinal reinforcement was presented. The most recent fatigue model seems to be a rheological-statistical model consisting of dashpots, springs and friction blocks proposed by Kessler-Kramer (2002) in a PhD-thesis written in German. The model is based on an earlier model proposed by Duda, see Duda & König (1991). In the experimental part of the investigation, Kessler-Kramer also found that the difference between the static deformation-stress curve and the envelope of the deformation-stress curve in a fatigue test, increased with increasing number of load cycles for notched prisms. However, in the tensile fatigue tests this phenomenon was not as evident.

5.4 Fatigue Failure Criterion Based on Deformation

A fatigue failure criterion based on deformation was proposed in 1991 by Balázs (1991). The model was successfully used to describe bond failure between re-bars and the concrete. The growth in deformation during a fatigue test could according to the model be divided into three phases, see Figure 5.6. At the beginning of the first phase the deformation rate is high but stagnates after a while. The second phase is characterised by a constant deformation rate. These two phases can be described as stable. During the third phase, the failure phase, the deformation rate increases rapidly leading to failure within a short time.

The strain criterion for fatigue failure is that the strain at peak load during a static test corresponds to the strain at the changeover between phases two and three during a fatigue failure, see Figure 5.6. When $\varepsilon(\sigma_u)$ has been reached only a limited number of cycles are needed until failure occurs. Since there is a difference between the number of cycles at failure and at initiation of phase three one can consider the criterion as safe, Balázs (1991).

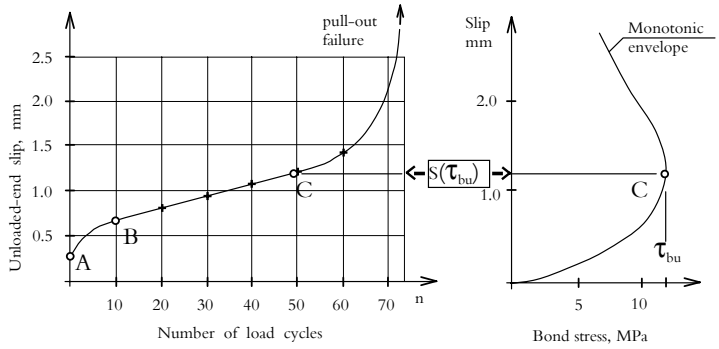

Figure 5.6 Strain criterion for fatigue failure according to Balázs (1991).

This criterion, among other things, was examined by Hordijk (1991). When Hordijk studied the result from his tests, see Figure 5.7, he found that point C, indicating the ending of the secondary branch in the cyclic creep curve, does not give a decisive answer to the question of

whether this point coincides with the deformation at peak load in a static test, as assumed by Balázs (1991) in his tests. According to Hordijk there are several reasons why such a relation is not possible in these experiments. The main reason is that the deformation at peak load depends on the measuring length; elastic deformation, while the deformation at point B is partly due to elastic deformation and partly due to the opening of the crack or process zone, which is independent of the measuring length. Therefore, Hordijk concluded, if there is a criterion based on a deformation marking the end of the secondary branch in the cyclic creep curve, it will be related to crack opening.

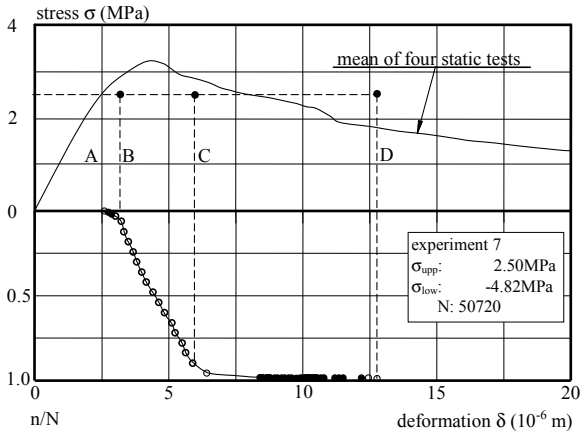

Figure 5.7 Average stress-deformation relation of the static tests and cycle ratio versus deformation in a fatigue test, from Hordijk (1991).

Kessler-Kramer (2002) also compared the static deformation-stress curve with the deformation-load cycle curve but did not find any obvious common points.

Daerga & Pöntinen (1993) applied the deformation criterion proposed by Balázs (1991) when they performed three-point bending fatigue tests on notched beams cast with plain high performance concrete (dimensions of the beams: 0.8×0.1×0.1m). They performed deformation controlled monotonic tests and fatigue tests with a constant lower load level of 10% of the maximum average static flexural strength and varied the higher load level (70%, 80% and 90%). Their idea was that by using the criterion it should in principal be possible to predict the fatigue failure for a structure, if the development of deformation in a fatigue test was monitored and then relate it to the deformation capacity of an identical structure exposed to static load.

From their results they concluded that the deformation corresponding to the monotonic maximum load, point C in Figure 5.6, could be applied as a fatigue failure criterion (at least for repeated loading in flexural tension). The deformation at the end of the linear section of the fatigue creep curve, point C in Figure 5.6, was on average found to be lower than the monotonic (static) deformation capacity at point C in Figure 5.6. The highest difference between these two deformations was when the higher load level was 70%, but when the higher load level was 90% the difference was rather low – 0.17 compared to 0.16 mm (static and fatigue deformation, respectively). It was also pointed out by Daerga & Pöntinen (1993) that it could be advantageous that the deformation at point C in Figure 5.6 for the fatigue test was somewhat smaller since it in turn increases the safety margin to ultimate failure. They also mentioned that the hypothesis could still be used for a structure even though the deformation at point C in Figure 5.6 in a static test is missing, since by studying the slope of the fatigue creep curve, the rate of deformation tells the status of the structure.

6 Assessment of a Railway Element – Prestressed Sleepers

6.1 Background

This thesis also contains a study of a concrete railway element presented in paper E and some aspects discovered during the project are discussed in this chapter. This element is a railway sleeper made of prestressed concrete. The tested sleepers have been damaged in form of more or less severe cracking, which thereby could potentially reduce its function as e.g. being an elastic foundation for the rails, keeping the right distance between the rails etc. Normally a concrete sleeper sustains its properties for more than 50 years but these sleepers had an age of only five to ten years. The cracking is believed to be caused by so-called delayed ettringite formation (DEF), which leads to an internal expansion and, gradually, cracks. In combination with moisture and/or cyclic frost action the deterioration may accelerate.

DEF is not a new phenomenon, it has been reported from many countries over the years and it is often sleepers that have started to deteriorate, see e.g. Tepponen & Eriksson (1987), Collepardi (1999), Hime (1996) or Metha (2000). A summary of recent work in the research field of DEF could be found in CBI (2000) and Scrivener & Skalny (2005). Due to the many problems connected to DEF, recommendations have now been established in many countries, in particular regarding the use of heat curing which seems to be an important factor, e.g. in the German recommendations regarding heat curing, see DAfStb (1989), the rules were revised due to the reported damages.

When Banverket (the Swedish National Rail Administration) in the late 1990s became aware of the problem with the cracked sleepers, several investigations were initiated. These showed, among other things, that the damaged sleepers could be found all over Sweden. The visual inspections were performed with two inspectors walking on opposite sides along a railway track, which is a difficult and a time-consuming work. The area on the sleeper where the first visible cracks appear when they lie in the track, seems to be on the upper side at the end, near the edge, see Figure 6.1. The first inspections led to a categorisation of the sleepers depending on the cracking. They were divided into three classes and the typical damages for each class are, briefly:

- Class Green / OK: No visible cracks.
- Class Yellow / Initial degradation: Some cracks. The cracking is of the kind that the load carrying capacity is almost intact.
- Class Red / Acute: The cracking is so severe that there is a considerable reduction of the load carrying capacity.

6.2 Results

6.2.1 Load-carrying Capacity

The remaining load carrying capacity of the damaged sleepers has been investigated and test results are presented in paper E. The following tests have been performed:

a) bending capacity of the midsection
b) bending capacity of the rail section
c) horizontal load capacity of the fastener
d) control of the concrete properties
e) fatigue capacity in bending of the rail section.

The purpose of the tests has been to get an idea of how the cracking influences the load carrying capacity and to determine how many and at what rate the damaged sleepers must be replaced from the track due to safety reasons. In turn this also decides how much it will cost to replace the damaged sleepers. The test results show that railway sleepers are quite robust. Small cracks do not seem to influence the load carrying capacity and it is first when the cracking is very severe that the load carrying capacity is reduced significantly.

The sleepers were made of prestressed concrete with the concrete class K60 (the Swedish concrete class K60 corresponds approximately to the concrete strength class C45/55 in Eurocode 2).The sleepers are prestressed with 8 strands (each strand consists of 4 wires with the diameter of 3 mm), see Figure 6.1

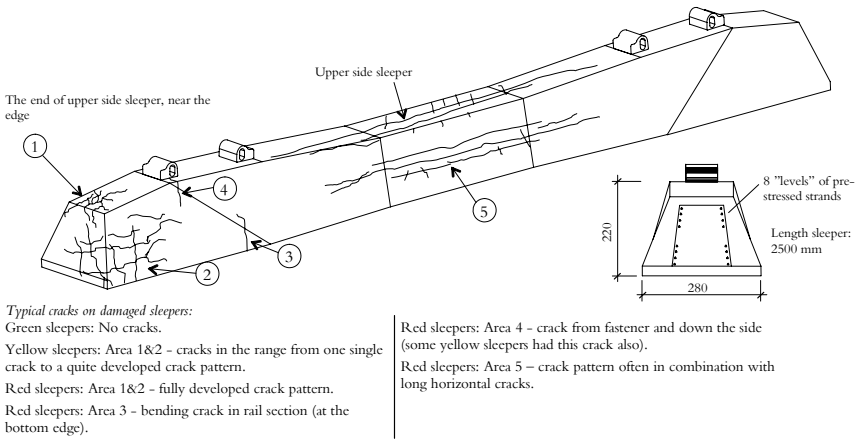

Figure 6.1 Drawing of a typical damaged concrete sleeper with characteristic crack pattern classified as green (no cracks), yellow or red.

The load carrying capacity of sleepers has earlier been studied in Sweden, see Gylltoft & Elfgren (1977), Gylltoft (1978) and Gustavson (2002). Background material can be found in reports by Elfgren (2001) and Thun et al. (2001, 2003).

6.2.2 A Follow-up of Damaged Sleepers

A preliminary study has been performed with twenty-eight sleepers, manufactured in 1992 and delivered to LTU in November 2000. Thirteen of them were tested in 2000 and fifteen were stored and visually inspected in the summer of 2003. The remaining load carrying capacity for these fifteen were estimated, i.e. compared with the result from the thirteen in 2000.

The yellow sleepers had been stored next to a wall of a house, stacked on each other during November 2000 to June 2003, which corresponds to about 2.5 years, see Figure 6.2. The sleepers had during this period been moved a number of times, which means that the sleepers lying in the bottom in Figure 6.2 also could have been on top for some period. This also means that they for some time could have been lying in water and some time lying relatively protected. The sleepers could also have been exposed to water coming from the roof of the nearby house. Despite this it is believed that this environment is more favourable than what sleepers are exposed to when lying in the track. A comparison between the two environments is hard to perform since e.g. the sleepers in the track are also exposed to loads from the trains which could result in crack propagation.

Figure 6.2 Picture showing how the sleepers have been stored during the period November 2000 – June 2003, Thun & Elfgren (2003).

Based on this assessment it was concluded that the degradation rate was still high and showing tendencies to increase, Thun & Elfgren (2003).

6.2.3 Wheel Load Distribution

During the tests of the bending capacity in the rail section, one important aspect was discovered regarding the load a railway sleeper is exposed to. In BVH (2005) it is suggested how the wheel load can be distributed along the sleepers and which load a sleeper is exposed to, see Figure 6.3. If continuous-welded rails are assumed along the railway track, the maximum load will be $0.5Q_{axle}$ on one sleeper (the rest of Q_{axle} is taken by adjacent sleepers), see Figure 6.3.

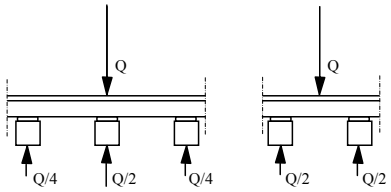

Figure 6.3 Wheel load distributions along sleepers, from BVH (2005).

Other values of this load distribution factor, i.e. the percentage of how much of the wheel load a single sleeper is exposed to, can be found in the literature. In Profillidis (2000) a distribution of the wheel load along the sleepers is presented that is based on measurements and Finite-element analysis, see Figure 6.4. In this case the maximum load is 40% of the axle load, i.e. lower than suggested by BVH (2005) for the sleeper that is beneath the wheel. Unfortunately

there is no information of the distribution when the wheel is between two sleepers. If this distribution is compared to the one in BVH (2005) the difference is that the wheel load is distributed to 5 sleepers instead of 3 as in BVH (2005).

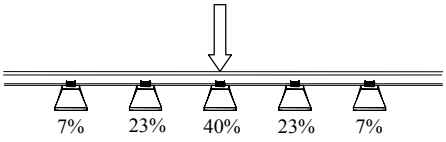

Figure 6.4 Wheel load distribution along sleepers, from Profillidis (2000).

In Holm et al. (2002) a measured wheel load distribution similar to the distribution in Figure 6.4 is given, see Figure 6.5. Measurements also indicated that for high axle loads, the sleeper just beneath the wheel is exposed to a higher percentage of the axle load than for lower axle loads. For the axle load of 30 tons the percentage could be up to 60%. Unfortunately no information regarding the adjacent sleepers and their load percentage was mentioned in this case.

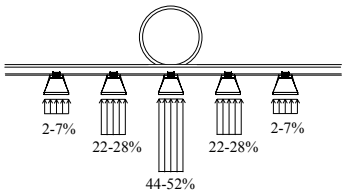

Figure 6.5 Wheel load distribution along sleepers, from Holm et al. (2002).

If the different distributions of the wheel load along the sleepers are compared one could conclude that the work by Holm et al. (2002) suggests that BVH (2005) is un-conservative for the axle load of 30 tons. If this is connected to the measured axle loads presented in paper C, which is higher than the allowed axle load 30 tons, it is realised that this is something that would be interesting to study. If measurements of the distribution is performed this variation shows that to obtain a correct distribution several tests must be performed since the distribution is very sensitive to e.g. the stiffness of the embankment and if one sleeper is "hanging".

7 Summary of Appended Papers and Outlook

Paper A - Concrete Strength in Old Swedish Concrete Bridges

In this paper the development and variation of compressive and tensile strength of concrete are presented for old reinforced concrete bridges in Sweden. A mean increase of about 70% in concrete compressive strength has been verified for twenty bridges built during 1931-1962 (a rather high dispersion must be taken into consideration). The increase is related to the original 28-day concrete compressive strength which varied between 18 and 51 MPa.

The compressive strength within a typical reinforced railway concrete trough bridge was approximately 15% higher in the longitudinal beams than in the bottom slab (measured on drilled cores). The tensile strength showed a similar variation as the compressive strength, but the difference could not be statistically verified.

Different equations to convert compressive strength into tensile strength have also been studied. The investigation shows that it is important which conversion equation that is used in an assessment situation, especially when low compressive strengths are converted into tensile strengths (in this case lower than 50 MPa). There is a need to study these relationships further, since it has become common to substitute the tensile strength with an expression for the compressive strength. Still better would be to develop methods which can measure the actual tensile and shear capacity of the concrete in existing structures.

Paper B – Determination of Concrete Compressive Strength with Pullout Test

A pullout test method, the Capo-test, has been examined as an alternative to drilled cores to determine the in-place concrete compressive strength. Tests have been carried out on eight railway bridges from 1965 to 1980 and on a one year old slab. An interesting next step regarding the Capo-test can be to analyse the failure, compare it with different FEM-models and test results.

A strength relationship is proposed between the compressive strength of a drilled core with the diameter and the height of 100 mm, f_{core}, and the pullout force, F, from the Capo-test. It is a power function and has the form, $f_{core} = 0.98F^{1.14}$. The relation is valid for concrete compressive strengths up to 105 MPa. It gives higher concrete strengths than earlier proposed functions. A way to improve the relationship further would be to increase the background data by performing more field tests.

Paper C – Probabilistic Modelling of the Shear Fatigue Capacity in a Concrete Bridge Slab

A probabilistic approach is used for the evaluation of the shear fatigue capacity of a concrete railway bridge slab. In the reliability analysis three different combinations of shear and fatigue models have been compared. The models have been used to determine the safety index β (and the probability of failure) after another 5 or 25 years of traffic with higher axle loads 300 kN instead of 250 kN.

Results are given for the shear model used in the Eurocode, EC2 (2004), and for a traditional shear model, Hedman & Losberg (1975), which is used in the Swedish concrete recommendations, BBK04 (2004). The results are combined with fatigue models by Aas-Jakobsen (1970), Tepfers (1979) and Eurocode 2, EC2 (2004). The bridge slab obtains β-values which indicates that it may carry increased axle loads for 5 years or more with kept safety, depending on which model is chosen. The most interesting combination seems to be the shear model of Hedman & Losberg (1975)/BBK04 (2004) and the fatigue model of Tepfers (1979).

To improve this method further studies should be made of the influencing factors in a reliability analysis of a bridge, e.g. the model uncertainties and the dynamic amplification factor. Another option would be to find other models for shear and fatigue which are more suitable for this kind of analysis.

Paper D – Concrete Fatigue Capacity in Tension – a Study of Deformations

In this paper results and analyses are presented from cyclic uniaxial tensile tests performed on new and old concrete. The results from the tests indicate that the deformation criterion proposed by Balázs (1991) for bond slip might also be applied to plain concrete exposed to cyclic tensile load. A method is proposed for how the deformation criterion may be used also for assessment of existing structures. A Wöhler curve for cyclic loads in tension is derived from the tests.

It would be interesting to develop the use of the deformation criterion further by performing tests on small elements, like reinforced beams, in order to form a better basis for a design and assessment procedure for concrete structures.

Paper E – Load Carrying Capacity of Cracked Concrete Railway Sleepers

The load carrying capacity of damaged prestressed concrete railway sleepers has been investigated. The sleepers had an age of five to ten years and the damage, in form of more or less severe cracking, is believed to be caused by delayed ettringite formation. The following tests have been performed: (a) bending capacity of the midsection and the rail section, (b) horizontal load capacity of the fastener, (c) control of the concrete properties and (d) fatigue capacity in bending of the rail section. A visual inspection and classification of the damages are also presented.

The purpose of the tests has been to get information about how the cracking influences the remaining load carrying capacity compared to an un-cracked sleeper. The test results show that railway sleepers are quite robust. Small cracks do not seem to influence the load carrying capacity and it is first when the cracking is very severe that the load carrying capacity is reduced significantly.

An interesting extension would be to study the influence of environmental conditions on the development of the cracks. i.e. follow up the cracked sleepers to see how the degradation proceeds (one small study has been performed). Another topic would be to check how the wheel load is distributed between adjacent sleepers for various ballast conditions and train speeds.

References

Aas-Jakobsen K. (1970). Fatigue of Concrete Beams and Columns. Trondheim: The Norwegian Institute of Technology. Bulletin No 70-1, September 1970. pp. 148.

Albert W. A. J. (1838). Über Treibseile am Harz. Archive für Mineralogie, Geognosie, Bergbau und Hüttenkunde 10, 215-34.

Balázs G. L. (1991). Fatigue of Bond. ACI Material Journal Vol. 88, No. 6. pp. 620-629.

Bartlett M. F. and MacGregor J. G. (1999). Variation of In-place Concrete Strength in Structures. ACI Materials Journal, V.96, No.2, March-April. pp. 261-270.

Bažant Z. and Planas J. (1998). Fracture and Size Effect in Concrete and Other Quasibrittle Materials. CRC press LLC. pp. 616. ISBN 0-8493-8284-X

BBK 94 (1994, 1996). Swedish Recommendations for Concrete Structures. Volume 1 – Design, Volume 2 – Materials, Construction, Control. Svensk Byggtjänst, Stockholm 1994, 185 + 116 pp. ISBN 91-7332-686-0, 91-7332-687-9. Supplement 1996. pp. 57. ISBN 91-7147-274-6. In Swedish.

BBK04 (2004). Swedish Code for Concrete Structures. (Boverkets handbok om betongkonstruktioner, BBK 04. In Swedish). Boverket, Karlskrona 2004. pp. 271.

BKR03 (2003). Regelsamling för konstruktion – Boverkets konstruktionsregler, BKR, byggnadsverkslagen och byggnadsverksförordningen. Boverket, Karlskrona. Upplaga: 1. Elanders Gotab, Vällingby. ISBN 91-7147-740-3. pp. 256.

Bungey J.H. and Millard S.G. (1996). Testing of Concrete in Structures. Blackie Academic & Professional, an imprint of Chapman & Hall, London 1996. pp. 286. ISBN 0 7514 0241 9

BVH (2005). Evaluation of Concrete Railway Bridges. (Bärighetsberäkning av järnvägsbroar. In Swedish). Handbok BVH 583.11. Banverket, CB, Borlänge 2005-06-01, s 108 + 9 bilagor.

Carino, N. J. (2004). Pullout Test. Chapter 3 in "Handbook on Nondestructive Testing of Concrete", edited by V. M. Malhotra and N. J. Carniro, 2 Ed, Boca Raton, FL: CRC Press, pp. 3-1 to 3-40. ISBN0-8031-2099-0

Carolin A. (2003). Carbon Fibre Reinforced Polymers for Strengthening of Structural Elements. Doctoral Thesis 2003:18. Luleå University of Technology, Department of Civil and Mining Engineering, Division of Structural Engineering. pp. 178. ISBN 89580-04-4

CBI (2000). Uppdragsrapport nr 2000-91. Mikrostruktur och kemisk analys av värmehär-dade betongslipers med inre sprickbildning och massiv ettringitbildning. (Research report No. 2000-91. Micro structure and chemical analysis of heat cured concrete sleepers with inner cracks and massive ettringite formation. In Swedish). The Swedish Cement and Concrete Research Institute, CBI, Stockholm, pp. 61.

CEB-FIP (1993). CEB-FIP Model code 1990. Design Code. Comité Euro-International du Béton Fédération Internationale de la Précontrainte, Thomas Telford Ltd. pp. 437. ISBN 0-7277-1696-4

Collepardi Mario (1999). Damage by Delayed Ettringite Formation. Concrete International, American Concrete Institute, Farmington Hills, MI, USA, V.21, No. 1, 1999. pp. 69-74.

Cornelissen H. A. W, Hordijk D.A. and Reinhardt H.W. (1986). Experiments and Theory for the Application of Fracture Mechanics to Normal and Lightweight Concrete. Fracture Toughness and Fracture Energy of Concrete. F. H. Wittman (Ed.). Proceedings of the International Conference on Fracture Mechanics of Concrete, Lausanne, Switzerland, 1-3 October 1985. pp. 565-575.

Cornelissen H. A. W. (1986a). State-of-the-art Report on Fatigue of Plain Concrete. Delft, The Netherlands: Delft University of Technology. Report 5-86-3. pp. 62

Daerga P.-A. and Pöntinen D. (1993). A Fatigue Failure Criterion for Concrete based on Deformation. Nordic Concrete Research, No. 2/1993. pp. 6-20.

DAfStb (1989). Richtlinie zur Nachbehandlung von Beton. (Rules for curing of concrete. In German) Deutscher Ausschuss fur Stahlbeton, Beuth Verlag GmbH, Vertriebsnummer 65013, Berlin, September 1989. pp. 6.

Dahlberg T. and Ekberg A. (2002). Failure, Fracture, Fatigue. Lund, Studentlitteratur. pp. 356. ISBN 1-44-02096-1

Diamantides D., Editor (2001). Probabilistic Assessment of Existing Structures. A Publication of the Joint Committee on Structural Safety (JCSS). RILEM Publications Sarl, Cachan Cedex, France, pp. 162. ISBN 2-912143-24-1.

Ditlevsen O. and Madsen H.O. (1996). Structural Reliability Methods. Chichester: Wiley, cop. 1996. pp. 372. ISBN 0-471-96086-1

Duda H. and König G. (1991). Rheological Material Model for the Stress-Crack-Width Relation of Concrete Under Monotonic and Cyclic Tension. ACI Materials Journal, V 88, Issue:3. pp. 278-287.

EC2-2 (1996). Eurocode 2: Design of Concrete Structures, Part 2: Concrete Bridges. ENV 1992-2. CEN, Comité Européen de Normalisation, Central Secretariat: rue de Stassart 36, B-1050 Brussels.

Elfgren L. (2001). Värmehärdning av betong (Heat-curing of Concrete. In Swedish). Division of Structural Engineering , Luleå University of Technology. Skrift, Luleå 2001, sid. 9.

Elfgren L. and Gylltoft K. (1997). Fatigue of Concrete Structures. Division of Structural Engineering, Luleå University of Technology, Report 90:10, Revised version, Luleå 1997. pp. 50. In Swedish

Elfgren L., Ed. (1989). Fracture Mechanics of Concrete Structures. From Theory to Applications. Rilem Report, Technical Committee 90 FMA. Chapman and Hall, London. pp. 407. ISBN 0-412-30680-8

Emborg Mats, Cederwall Krister and Elfgren Lennart (1982). Cable Couplers, Nordic Concrete Research, Oslo, 1982, pp. 5.1-5.14.

Enochsson O., Hejll A., Nilsson M., Thun H., Olofsson T. and Elfgren L. (2002). Bro över Luossajokk: beräkning med säkerhetsindexmetod, böjdragkapacitet i överkant i mittsnittet i korta spannet. Luleå University of Technology, Division of Structural Engineering. Teknisk Rapport 2002:06. pp. 93.

Enochsson O., Puurula A., Stenlund A., Thun H., Nilsson M., Täljsten B., Olofsson T. and Elfgren L. (2005). Condition Assessment of Concrete Bridges in Sweden. In ICCRRR 2005 – International Conference on Concrete Repair, Rehabilitation and Retrofitting, Cape Town, South Africa, 21-23 November 2005, Leiden: Taylor & Francis/Balkema, pp. 257-259 (extended abstract; full length paper, pp. 677-682, on enclosed CD). ISBN 0-415-39656-5

Fahleson C. (1995). Ice and Wind Loads on Guyed Masts. Doctoral Thesis 1995:174. Luleå University of Technology, Department of Civil & Mining Engineering, Division of Steel Structures. pp. 224

Frost N. E., Marsh K. J. and Pook L. P. (1974). Metal Fatigue. Clarendon Press, Oxford. Oxford University Presss, Ely House, London W.I. pp. 499. ISBN 0-19-856114-8

German Petersen C. (1997). LOK-test and CAPO-test Pullout Testing, Twenty Years Experience. NDT-CE ´97, The British Institute of Non-Destructive Testing. pp. 18.

German Petersen C. and Poulsen E. (1993). Pull-out Testing by LOK-test and CAPO-test, with Particular Reference to the Iin-place Concrete of the Great Belt Link. Revised edition November 1993. Danish Concrete Institute A/S, Datavej 36, DK-3460 Birkerød, Denmark. pp. 140.

Gustafsson P. J. (1985). Fracture Mechanics Studies of Non-yielding Materials like Concrete: modelling of tensile fracture and applied strength analyses. Doctoral Thesis. Report ISSN 0348-7911 ; 1007. Division of Building Materials, Lund Institute of Technology. pp. 430.

Gustavson R. (2002). Structural Behaviour of Concrete Railway Sleepers. PhD thesis No 1909, Publication 2002:06, Department of Structural Engineering, Chalmers University of Technology. Gothenburg. pp. 51+102. ISBN 91-7291-227-8

Gylltoft K. (1978). Utmattningsprov av betongsliprar - Utveckling av provnings- och mätmetodik vid experimentell utmattningsforskning (Fatigue of concrete sleepers. Test methods. In Swedish). Byggforskningen, Rapport R103:1978, Stockholm 1978. pp. 92. ISBN 91-540-2939-2

Gylltoft K. (1983). Fracture Mechanics Models for Fatigue in Concrete Structures. Doctoral Thesis 1983:25D. Luleå University of Technology. Division of Structural Engineering. pp. 210.

Gylltoft K. (1994). Utmattning (Fatigue. In Swedish). Betonghandboken - Material. Utgåva 2. (Concrete Handbook - Materials. Second edition, Ed. by C. Ljungkrantz et al.) Stockholm, Svensk Byggtjänst och Cementa AB. pp. 1127.

Gylltoft K. and Elfgren L. (1977). Utmattningshållfasthet för anläggningskon-struktioner (Fatigue of Civil Engineering Structures. In Swedish). Byggforskningen, Rapport R68:1977, Stockholm 1987. pp.160. ISBN 91-540-2750-0

Hedman O. and Losberg A. (1975). Dimensionering av betongkonstruktioner med hänsyn till tvärkrafter (Shear Design of Concrete Structures, in Swedish). Stockholm. Nordisk Betong. 5-1975. pp. 19-29.

Hejll A. (2004). Structural Health of Bridges: monitor, assess and retrofit. Licentiate thesis 2004:46. Luleå University of Technology, Division of Structural Engineering. pp. 155.

Hejll A. and Täljsten B. (2005). Civil Structural Health Monitoring (CSHM). tillstånds-bedömning genom mätning anpassad för anläggningskonstruktioner. Teknisk rapport 2005:33. Division of Structural Engineering, Luleå University of Technology, Luleå, 2005. pp. 71. In Swedish.

Hillerborg A., Modeer M. and Petersson P. E. (1976). Analysis of Crack Formation and Crack Growth in Concrete by Means of Fracture Mechanics and Finite Elements. Cement and Concrete Research 6. pp. 773-782.

Hime W. (1996). Delayed Ettringite Formation - A Concern for Precast Concrete? PCI Journal, Precast/Prestressed Concrete Institute, Chicago, IL, USA, V.41, No. 4. 1996, pp. 26-30.

Holm G, Bengtsson P-E, Carlsten P, Johansson L O and Larsson R. (2002). Befintliga bankar vid ökad tåglast och högre tåghastighet. Statusbestämning av befintliga bankar. Förbättrings- och förstärkningsåtgärder under driftsförhållanden. "State of the art" (Upgrading of existing railway lines for increased axle loads and speed. Diagnosis and improvement methods. State of the art) Swedish Geotechnical Institute, SGI. Linköping. Varia 520. pp. 102.

Holmen J. O. (1979). Fatigue of Concrete by Constant and VariableAmplitude Loading. Bulletin No. 79-1 November 1979. The University of Trondheim, Norway. pp. 218.

Hordijk D. A. (1989). Deformation-controlledUniaxial Tensile Tests on Concrete. Report 25.5-89-15/VFA. Delft University of Technology. pp. 118.

Hordijk D. A. (1991). Local Approch to Fatigue of Concrete. Delft University of Technology. The Netherlands. PhD thesis. pp. 210. ISBN 90-9004519-8

Hsu T. T. C. (1981). Fatigue of Plain Concrete. ACI Journal, Journal Proceedings Vol 78, No. 4. pp. 292-304.

JCSS (2001). Probabilistic Model Code, Issued by the Joint Committee on Struc-tural Safety, JCSS, 12th Draft, March 2001. 1. Basis of Design, 62 pp; 2. Load Models, 73 pp; 3. Material properties. pp. 43.

Jeppsson J. (2003). Reliability-based Assessment Procedures for Existing Concrete Structures. Doctoral thesis. Report: TVBK-1026. Lunds University, Structural Engineering, Division of Structural Engineering. pp. 184.

Johansson A. (2000). Hållfasthetsvariationer inom betongkonstruktioner. Jämförelse mellan CAPO-test och utborrade cylindrar. (Strength variations within concrete structures. Comparision between the Capo-test and drilled cores). Master Thesis 2000:337. Luleå University of Technology, Division of Structural Engineering. pp. 82. In Swedish.

Johansson S-E. (2005). Personal communications. Heidelberg Group, Lund, Sweden.

Johansson U. (2004). Fatigue Tests and Analysis of Reinforced Concrete Bridge Deck Models. Civil and Architectural Engineering. Royal Institute of Technology. Licentiate thesis. Trita-BKN. Bulletin, ISSN 1103-4270 ; 76. pp. 198.

Kessler-Kramer C. (2002). Zugtragverhalten von Beton unter Ermüdungs-beanspruchung. Institut für Massivbau und Baustofftechnologie. Universität Karlsruhe. Dissertation. Karlsruhe 2002. pp. 286.

Kierkegaard-Hansen P. (1975). Lok-Strength, Nordisk Betong (Journal of the Nordic Concrete Federation). No.3, Stockholm, Sweden. pp. 19-28.

Krenchel H. & Shah S.P. (1985). Fracture Analysis of the Pullout Test. Materials and Structure, Vol. 18, No.108. pp. 439-446.

Lea F. M. (1970). The Chemistry of Cement and Concrete. 3 ed. London: Edward Arnold, 1970, pr. 1983. pp 727. ISBN 0-7131-2277-3

Mallet G. (1991). Fatigue of Reinforced Concrete. State of the Art Review / 2., HMSO, London, U.K. pp. 165. ISBN 0-11-550979-8

Mehta P. K. (2000). Sulphate Attack on Concrete: Separating Myths From Reality. Concrete International, Farmington Hills, MI, Vol 22, No. 8, August 2000, pp. 57-61. Discussion by William G. Hime, Gunnar M. Idorn, and author in Vol 23, No. 2, February 2001. pp. 10-13.

Melchers R. E. (1999). Strutural Reliability Analysis and Prediction, 2nd Ed, John Wiley & Sons, Chichester, UK, 1999. pp. 437. ISBN 0 471 98771 9

Mihashi H. and Rokugo K., Eds. (1998). Fracture Properties and Parameters. Fracture Mechanics of Concrete Structures. Volume 1. Aedificatio Publishers. pp. 824. ISBN 3-931681-22-X

Mindess S., Young F. J. and Darwin D. (2002). Concrete, 2nd Edition. Prentice Hall. Aug 20, 2002. pp. 644. ISBN 0-13-064632-6

Miner M. A. (1945). Cumulative Damage in Fatigue. Transactions of the American Society of Mechanical Engineers (ASME), Journal of Applied Mechanics 67: A. pp. 159-164.

Neville A. M. (1995). Properties of Concrete. 4 ed. Harlow: Longman Group. pp. 844. ISBN 0-582-23070-5

Nilsson M. (2003). Restraint Factors and Partial Coefficients in Crack Risk Analyses of Early Age Concrete Structures. Doctoral Thesis 2003:19. Luleå University of Technology, Department of Civil and Mining Engineering, Division of Structural Engineering. pp. 170. ISBN 91-89580-05-02

Noghabai K. (1998). Effect of Tension Softening on the Performance of Concrete Structures. Doctoral Thesis 1998:21. Luleå University of Technology, Division of Structural Engineering. pp. 150.

Ohlsson U., Daerga P-A. and Elfgren L. (1990). Fracture Energy and Fatigue Strength of Unreinforced Concrete Beams at Normal and Low Temperatures. Engineering Fracture Mechanics, Vol 35, No. 1/2/3. pp. 195-203, 1990.

Olofsson T., Hejll A. and Enochsson O. (2002). Health Monitoring and Assessment of Railway Bridges, Proceedings of International Conference on Structural Health Monitoring, Paris France 10-12 July. pp. 256-264.

Ottosen N.S. (1981). Nonlinear Finite Element Analysis of Pullout Test. Journal of the Structural Division, ASCE, V. 107,Apr. 1981. pp. 591-603.

Palmgren A. (1924). Die Lebensdauer von Kugellagern. Zeitschrift des Vereins Deutcher Ingenieure. Vol 68. 14. pp. 339-341.

Paris P. C., Gomez M. P. and Anderson W. E. (1961). A Rational Analytical Theory of Fatigue. The trend in Engineering Vol 13 (University of Washington, Seattle, WA). pp. 9-14.

Paulsson B., Töyrä B., Elfgren L., Ohlsson U. and Danielsson G. (1996). Load Bearing Capacity of Concrete Bridges. Research and development project. (Forsknings- och

utvecklingsprojekt avseende betongbroars bärighet. "30 ton på Malmbanan"). Rapport 3.3 Infrastruktur, Banverket, Borlänge 1996. pp. 51 + appendix. In Swedish.

Paulsson B., Töyrä B., Elfgren L., Ohlsson U. and Danielsson G. (1997). Increased Loads on Railway Bridges of Concrete. "Advanced Design of Concrete Structures" (Ed. by K Gylltoft et al.), Cimne, Barcelona, 1997. pp. 201-206. ISBN 84-87867-94-4

Petersson P.-E. (1981). Crack Growth and Development of Fracture Zones in Plain Concrete and Similar Materials. Doctoral Thesis. Report TVBM, ISSN 0348-7911; 1006. Lund: Division of Building Materials, Lund Institute of Technology. pp. 174.

Petschacher M (1993). Zuverlässigjkeit technisher Systeme – Computor-unterstützte Verarbeitung von stochastichen Grössen mit dem Programm *VaP*. Bericht Nr 199, Institut für Baustatik und Konstruktion, ETH, Zürich 1993. pp. 136. ISBN 3-7643-2967-X.

Pinto P., Ed. (1996). RC Elements under Cyclic Loading. Comité Euro-International du Béton Fédération Internationale de la Précontrainte, Thomas Telford Ltd. pp. 190. ISBN 0-7277-2086-4

Profillidis, V. A. (2000). Railway Engineering, 2. ed. Aldershot: Ashgate, cop. 2000. pp 291. ISBN 0-7546-1279-1.

Reinhardt H.-W., Cornelissen H. A. W. and Hordijk D. A. (1986). Tensile Tests and Failure Analysis of Concrete. ASCE Journal of Structural Engineering, Vol. 112, No. 11. pp. 2462-2477.

Rockström J. and Molin C. (1989). Limited Study of Relationship between Strength Measured by Rebound Hammer, Capo-Test and Drilled-out Cores. (Begränsad studie av sambandet mellan hållfasthet mätt med studshammare, capo-test resp. utborrade betongcylindrar). Statens Provningsanstalt. Byggteknik. Stockholm. Arbetsrapport SP-AR 1989:17. pp. 34. In Swedish.

Rots J. G., Nauta P., Kusters G. M. A. and Blaauwendraad J. (1985). Smeared Crack Approach and Fracture Localization in Concrete. Heron, Vol. 30, No. 1, 1985.

Rüsch H. and Hilsdorf H. (1963). Verformungseigenschaften von Beton unter Zentrischen Zugspannungen. Berict Nr. 44. Materialprüfungsamt für das Bauwesen der Technischen Hochschule München.

Schläfli M. (1999). Ermüdung von Brückenfahrbahnplatten aus Stahlbeton. Thèse N° 1998, Ecole Poly-technique Fédérale de Lausanne, Switzerland. 1999. pp. 113.

Schneider J. (1997). Introduction to Safety and Reliability of Structures. International Association for Bridges and Structural Engineering, IABSE, Structural Engineering. Documents No 5, Zürich, August 1997. pp. 138. ISBN 3-85748-093-6.

Scrivener K. and Skalny J. P. (2005). Conclusions of the International RILEM TC 186-ISA Workshop on Internal Sulphate Attack and Delayed Ettringite Formation. 4-6 September 2002, Villars, Switzerland. Rilem, Materials and Structures, Issue: Volume 38, N° 280. pp. 659 – 663.

Shah S.P., Swartz S.E. and Ouyang C. (1995). Fracture Mechanics of Concrete. Applications of Fracture Mechanics to Concrete, Rock and Other Quasi-Brittle Materails. Joh Wiley & Sons, Inc. pp. 552. ISBN 0-471-30311-9

Skramtajew B.G. (1938). Determinining Concrete Strength for Control of Concrete in Structures, J. Am. Concr. Inst., 34, 285, 1938.

Stemland H., Petkovic G., Rosseland S. and Lenschow R. (1990). Fatigue of High Strength Concrete. Nordic Concrete Research. Publication No. 90. pp. 172-196.

Stone W.C. and Carino N.J. (1983). Deformation and Failure in Large-Scale Pullout Tests. ACI Journal, Proceedings V.80, No.6, Nov-Dec. 1983. pp. 501-513.

Stone W.C. and Carino N.J. (1984). Comparison of Analytical with Experimental Internal Strain distributuion for the Pullout Test. ACI Journal, Proceedings V.81, No.1, Jan-Feb. 1984. pp. 3-12.

Suresh S. (1998). Fatigue of Materials. Second Edition. Cambridge University Press. U.K. pp. 677. ISBN 0-521-57046-8

Sustainable Bridges (2006). Assessement for Future Traffic Demands and Longer Lives of Railway Bridges. An Integrated Research Project in the 6th Framework Program of the European Union, Contract TIP3-CT-2003-001653. Information available at: www.sustainablebridges.net [cited 21 November 2006]

Sørensen N. B. (1993). The Damaged Viscoelastic Material Model For Concrete Under Cycllic Load, Rapport 6.8. High Performance Concretes in the 90'es. AALBBORG Universitetscenter. pp. 163.

Taylor G.D. (2002). Materials in Construction: Principles, Practice and Performance. 2 ed. Pearson Higher Edsucation. pp. 597. ISBN 0582369347

Tepfers R. (1973). A Theory of Bond applied to Overlapped Tensile Reinforcement Splices for Deformed Bars. Doctoral Thesis, Publication 73:2, Division of Concrete Structrures. Chalmers University of Technology, Gothenburg, Sweden. pp. 328.

Tepfers R. (1979). Tensile Fatigue Strength of Plain Concrete. ACI Journal Vol 76, No 8. pp. 919-933.

Tepfers R. and Kutti T. (1979). Fatigue Strength of Plain and Ordinary and Lightweight Concrete. ACI Journal Vol. 76, No. 5. pp. 635-652.

Tepponen Pirjo and Eriksson Bo.-Erik. (1987). Damages in Concrete Railway Sleepers in Finland. Nordic Concrete Research, Oslo, V.6. 1987. pp. 199-209.

Thelandersson S. (2007). Evaluation of Material Properties. Chapter 4 in "Non-Linear Analysis and Remaining Fatigue Life of Reinforced Concrete Bridges". Background document D4.5 to Guideline for Load and Resistance Assessment of Railway Bridges. Prepared by Sustainable Bridges – a project within EU FP6. Available from: www.sustainablebridges.net. [cited 21 November 2006]

Thoft-Christensen P. and Baker M. J. (1982). Structural Reliability Theory and Its Applications. Springer Verlag, Berlin 1982. pp. 267. ISBN 3-540-11731-8

Thun H. and Elfgren L. (2003). Uppföljning av skadade betongsliprar under tiden 2000-2003. (Follow-up of damaged railway sleepers during the period 2000-2003). Division of Structural Engineering, Luleå University of Technology. Skrift 03:03. pp.10.

Thun Håkan, Utsi Sofia and Elfgren Lennart (2001). Spruckna betongsliprars bärförmåga: provning av böjmomentkapacitet, dragkapacitet hos befästningar samt betonghållfasthet. (Bearing Capacity of Cracked Concrete Railway Sleepers. In Swedish). Division of Structural Engineering, Luleå University of Technology. Technical Report 2001:11. pp. 63.

Thun Håkan, Utsi Sofia and Elfgren Lennart (2003). Spruckna betongsliprars bärförmåga vid utmattande last. (Fatigue Capacity of Cracked Concrete Railway Sleepers. In Swedish).

Division of Structural Engineering, Luleå University of Technology. Technical Report 2003:04. pp. 23.

Tremper B. (1944). The Measurement of Concrete Strength by Embedded Pull-out Bars. Proc. Am. Soc. Testing Mater., 44, 880, 1944.

Täljsten B. (2004). FRP Strengthening of Existing Concrete Structures - Design Guidelines. Third Edition. Division of Structural Engineering, Luleå University of Technology. pp. 228. ISBN 91-89580-6.

Täljsten B. and Carolin A. (1999). Strengthening of a Concrete Railway Bridge in Luleå with Carbon Fibre Reinforced Polymers - CFRP. Load bearing capacity before and after strengthening. Technical Report 1999:18, December 1998. pp. 61.

Utsi S., Olofsson T. and Täljsten B. (2001). Health Monitoring of a CFRP Strengthened Bridge. Composites in Constructions. Proc. of the Int. Conf. Composites in Construction - CCC 2001, Porto, Portugal, 10-12 October 2001 (Edited by J. Figueiras, L. Juvandes and R. Faria). Balkema, Lisse 2001. pp. 745-749. ISBN 90 2651 858 7.

Walz K. (1976). Festigheitsentwicklung von Beton bis zum Alter von 30 and 50 Jahren. Betontechnische Berichte, 3, 1976. pp. 57-78.

Van Ornum J. L. (1903). Fatigue of Cement Products. Transaction, ASCE, V. 51. pp. 443.

Washa G. W., Saemann J. C. and Cramer S. M. (1989). Fifty-Year Properties of Concrete made in 1937. ACI Materials Journal, V.86, No.4, July 1989. pp. 367-371.

Washa, G. W. and Wendt, K. F. (1975). Fifty Year Properties of Concrete, ACI Journal, January 1975. pp. 20-28.

Westerberg B. (1973). Utmattningsförsök på armerade betongbalkar. KTH, Brobyggnad, Publikation 1/73. pp. 192. In Swedish.

Wood S. L. (1991). Evaluation of the Long-Term Properties of Concrete. ACI Material Journal Vol. 88, No. 6. pp. 630-643.

Wöhler A. (1858-1870). Tests to determine forces and deformations of railway carrige axles (In German). Zeitschrift fur bauwesen Vol 8, 1858, p 641-652; Vol. 10, 1860, p 583-616, Vol. 13, 1863, p 233-258; Vol. 16, 1866, p 67-84; Vol. 20, 1870. pp. 73-106.

Yankelevsky D. Z. and Reinhardt H. W. (1989). Uniaxial Behavior of Concrete in Cyclic Tension. Journal of Structural Engineering, ASCE, Vol. 115, No. 1, January 1989, pp. 166-182.

Yener M. (1994). Overview and Progressive Finite Element Analysis of Pullout Tests. ACI Structural Journal, V.91, No.1, Jan.-Feb. 1991. pp. 49-58.

Paper A

Concrete Strength in Old Swedish Concrete Bridges

by Håkan Thun, Ulf Ohlsson and Lennart Elfgren

Concrete Strength in Old Swedish Concrete Bridges

by Håkan Thun, Ulf Ohlsson and Lennart Elfgren

ABSTRACT

In this paper the development and variation of compressive and tensile strength of concrete are presented for old reinforced concrete bridges in Sweden.

The mean increase in concrete compressive strength was about 70% for twenty bridges built during 1931-1962 (a rather high dispersion must be taken into consideration). The increase is related to the original 28-day concrete compressive strength which varied between 18 and 51 MPa.

The compressive strength within a typical reinforced railway concrete trough bridge was approximately 15% higher in the longitudinal beams than in the bottom slab (measured on drilled cores). The tensile strength showed a similar variation as the compressive strength, but the difference could not be statistically verified.

Different equations to convert compressive strength into tensile strength have also been studied. The investigation shows that it is important which conversion equation that is used in an assessment situation, especially when low compressive strengths are converted into tensile strengths (in this case lower than 50 MPa).

Keywords: strength variation; strength development; drilled cores; concrete; bridges

1 INTRODUCTION

When a bridge is evaluated regarding its load carrying capacity there are several influencing factors that have to be considered. Some of these factors are: in-place concrete strength, concrete cover of the reinforcement, amount and quality of the reinforcement, degree of degradation etc. Of the factors mentioned, the main focus in this paper has been on studying the in-place concrete strength, since e.g. an increase of the concrete strength with time can be a valuable asset when assessing a bridge several years after it was constructed. The subject has in turn been divided into the following areas:

- Development of concrete strength with time: Is the concrete compressive strength of old bridges increasing with time? Efforts have been made to establish the phenomenon for old Swedish road bridges.
- The variation of concrete strength within a structure: Can a concrete strength variation be expected between different structural members in a reinforced railway trough bridge (i.e. the slab versus the longitudinal beams)?

- How to determine the tensile strength when only the compressive strength of concrete is examined?

The origin of the results presented in this paper is a project that was initiated when an increase of the axle load from 25 tons to 30 tons was planned on the railway line between Luleå in Sweden and Narvik in Norway. The railway line, with a total length of 473 km, was built between 1884 and 1902 for the transportation of iron ore and is now used for both iron ore and passenger transport.

2 METHODS

Drilled cores have been used in this investigation to determine the in-place concrete strength of old reinforced concrete railway trough bridges.

To drill out and test cores is a common method to estimate the in-place strength of a structure. Most countries have adopted standard procedures for how a core should be prepared, stored, etc. before testing. In this study the preparation, the storage etc. have been made according to the Swedish concrete recommendations, BBK94[1]. A water-cooled drill with diamond edges has been used. The cores have been air-cured for at least three days before testing. The ratio between the length and the diameter has been 1.0 (a diameter of approximately 100 mm). The cores have been marked with a drill hole number and a serial number. The cores have been used for uniaxial tensile tests, splitting tensile tests and compressive tests.

The uniaxial tensile tests have been performed with a closed-loop servo-hydraulic test machine (Dartec) under displacement control. Prior to testing, a notch has been milled on each specimen and after cleaning the specimen has been glued to the steel plates and then attached to the test machine. The data have been collected using four Crack Opening Displacement gauges (COD-gauges) with 90 degrees between the gauges.

3 STRENGTH DEVELOPMENT WITH TIME FOR OLD BRIDGES

3.1 Test results from 20 bridges built during 1931-1946

Data from Vägverket, the Swedish Road Administration, have been examined and evaluated for nineteen bridges built during 1931-1946 and one bridge built in 1962. This investigation is a further study of the work presented in Rådman[2]. The focus has been on comparing the concrete cube compressive strength at 28 days with the concrete compressive strength from drilled cores that have been tested during the years 1990-1994 (i.e comparison between 150 mm standard cubes and cylinders with the diameter and length of 100 mm). These two different concrete compressive strengths have been compared and the result is presented in Figure 1.

To be able to compare the two concrete compressive strengths the original concrete cube compressive strength at 28 days, $f_{c,200}$, has been increased with a factor of 1.053 (= 1/0.95, according to Swedish standard, Betongprovning[3]) to correspond to standard cubes, $f_{c,150}$, with the dimension of 150 mm (the original cube size was 200 mm), $f_{c,150} = 1.053\, f_{c,200}$.

The drilled core dimensions had an approximate length/diameter-ratio of 1.0 (the diameter was approximately 100 mm). In Figure 1 the x-axis shows the year of construction for each bridge with the oldest to the left. On the y-axis the concrete compressive strength at 28 days is given together with the concrete compressive strength from drilled cores, $f_{c,100}^{core}$. The 28 days' compressive strength values represent the strength in the bridge deck or the main girders, from where it is assumed that the drilled cores are obtained.

The bridge records that have been used in this investigation are not complete. This leads to the fact that e.g. the cement content and the water to cement ratio have not been found for all bridges. For the bridges where this information has been found the water-cement-ratio varies between 0.49-0.65 and the cement content varies between 300-400 kg/m^3. Regarding the cement type that has been used, the investigation shows that it varies between the bridges - at least seven different brands have been used. Unfortunately no information regarding the properties of the cement types used has been obtained. A reasonable assumption is that these cement types had similar properties as cement types used in other countries during the same period.

In Figure 1 all bridges show an increase in concrete compressive strength. Of the 20 bridges, 5 bridges show a moderate increase: 0-10 MPa, 10 bridges: 10-30 MPa and 5 bridges more than 30 MPa (up to 52 MPa). For the bridge that shows the highest increase, i.e. 52 MPa, the high increase is probably due to the fact that the cubes were not stored according to the regulations the first few days - the temperature was lower, which can be seen from the bridge records. This gives a misleading concrete compressive strength at 28 days and if it had been stored according to the concrete recommendations it would probably have been higher.

If this bridge is excluded, the average increase in concrete compressive strength for the remaining 19 bridges is approximately 20.7 MPa (corresponds roughly to an increase of 70%) compared to the 28-day strength. The standard deviation is 13.7 MPa (if the bridge mentioned above is included the average increase is 22.2 MPa with a standard deviation of 15 MPa). One way to confirm the time-dependent differences statistically is to perform a paired sample comparison between the mean value of the cube compressive strength at 28 days and the mean value of the compressive strength from drilled cores for each bridge. A so-called statistical hypothesis test, using a method called *t*-test where the means are compared (see Montgomery[4] or Coladarci[5]), confirms the difference. This kind of analysis presumes that the observations are independent random variables, both samples are drawn from independent populations that can be described by a normal distribution and that the standard deviation or variances of both populations are equal. Since there are not so many tests it is not certain that all three conditions are satisfied. However, if it is assumed that the conditions above are fulfilled, the null-hypothesis (H_0) would be that the mean values are equal (i.e. there is no statistical difference between the cube compressive strength at 28 days and the compressive strength from drilled cores) and the alternative hypothesis (H_1) that the mean values are not equal. If the level of significance is chosen to 0.05 (α) an analysis with the software Statgraphics (by Statistical Graphics Corp.) leads to rejection of the null-hypothesis at the 95% confidence level since the *p*-value is less than 0.05, i.e. 0.000003. Thus, the growth of concrete strength is confirmed.

3.2 Discussion and comparison with other tests

Bungey & Millard[6] state that measured in-situ values expressed as equivalent cube strengths, are usually lower than the strengths of cubes made of concrete from the same mix compacted and cured in a "standard" way. This is probably due to the fact that in-situ compaction and curing vary widely. This variation is confirmed in Möller et al.[7] where work by Bellander[8] is presented which shows that this difference between concrete compressive strength of cores and cubes increases with increased concrete compressive strength. With this in mind, the core compressive strengths, $f_{c,100}^{core}$, ought to be lower than the cube compressive strengths, $f_{c,150}$.

Why the increase then? Several reasons are possible. According to Johansson[9], the most likely has to do with the properties of the Portland cements used during the 1930s and 1940s. During this period the Portland cements had a different ratio of dicalcium silicate (C_2S) to tricalcium silicate (C_3S) and were more coarsely ground (i.e. the fineness was lower) compared to

the Portland cements of today, see e.g. Lea[10], Taylor[11] or Neville[12]. The two silicates are primarily responsible for the strength of the hydrated cement paste: where the tricalcium silicate (C_3S) influences the early strength and the dicalcium silicate (C_2S) the later increase in strength. The trend during the last few decades has been that, due to improved manufacturing methods, the amount of tricalcium silicate has increased which results in higher early compressive strength (in combination with a higher fineness) and a lower increase in long-term strength. If the content of C_3S and C_2S is compared for an "old" cement and a "modern" cement, one can in an example presented by Lea[10] find that the average content of C_2S was 45% and for C_3S 25% (the cements in this example were from 1900-1910). For a "modern" cement the average content of C_2S is between 15-20% and for C_3S between 50-70%.

In tests performed by Washa & Wendt[13], in which concrete cylinders from 1910 and 1923 were tested, cylinders *stored indoors* exhibit a little change in compressive strength from 2 to 10 years but thereafter showed large strength increases, in the order of 30 to 70% at 50 years. For concrete cylinders *stored outdoors* the increase was in the order of 10 to 40% during the 10 to 50 year period. The 50 year strength was on average 2.35 times the average 1 month strength for the cylinders from 1910 and 1.5 for the cylinders from 1923.

The specimens used in the study from 1910 were made with relatively coarse cement with the highest C_2S content (i.e. 44%, a C_3S content of 28.9% and with a specific surface of 104.5 m^2/kg, average values) and the concrete cylinders from 1923 were made with cements having intermediate specific surface and C_2S content (i.e. 33.7%, a C_3S content of 38.3% and with a specific surface of 123 m^2/kg, average values). Later on, in Washa et al.[14], results from concrete cylinders made in 1937 and stored outdoor for 50 years were presented (from the same test programme as in Washa & Wendt[13]). For these concrete cylinders it was shown that the increase in compressive strength was on average 65% from 1 month to 10 years, but after 10 years the compressive strength decreased or remained essentially the same up to 50 years. The cylinders were made with cement with relatively low C_2S content (i.e. 23.2% and with a C_3S content of 50%, average values) and a higher specific surface (on average 179.5 m^2/kg) compared to the cylinders made in 1910 and 1923.

In a German study by Walz[15] it is reported that concrete specimens stored outside and made with German Portland cement after 30 years had a compressive strength 2.3 times the 28-day compressive strength tested on drilled cores. The average content of C_2S was 13% and for C_3S 62%, the water-to-cement ratio varied between 0.5-1.29 and the cement had a specific surface of 230 kg/m^3.

The mean increase in our tests, 70% during 30 to 60 years, is thus somewhat lower than the corresponding American and German results.

How can this phenomenon with strength development with time be used in practice? In the Danish Road Report 291[16], a guideline for reliability-based classification of existing bridges, a conservative increase in the compressive strength of concrete is proposed when evaluating the load carrying capacity of existing bridges. A deterministic increase in the compressive strength can be assumed for intact concrete structures in the absence of contradictory information. For bridges built in 1945 or earlier a compressive strength 50% higher than the original 28-day strength may be assumed (with references to Walz[15] and Washa & Wendt[13]). However, for concretes containing silica fume or accelerators no increase above the 28-day strength should be assumed.

In this context it must also be mentioned that the concrete compressive strength of course can decrease with time due to e.g. environmental degradation.

As mentioned earlier all but one bridge in this study are built during the 1930s and 1940s and the phenomenon with increased concrete compressive strength could in other words be expected for bridges built during the same period. If this increase can also be expected for bridges built during the 1950s and 1960s has not been verified in this study, but the bridge built in 1962 that is included, indicates that an increase could be expected but probably not as high as for the older bridges. The reason for this is the above-mentioned change in composition of the cements that has taken place over the years.

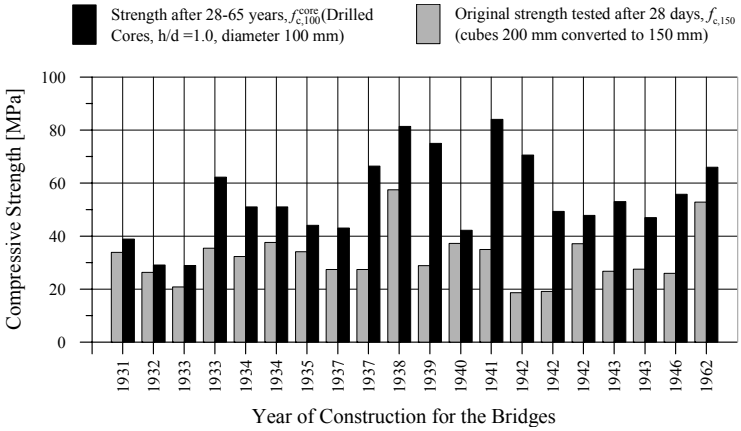

Figure 1 Concrete compressive strength for 20 Swedish road bridges built during 1931-1962. The concrete cube compressive strength at 28-days at the time the bridges were built has been converted into concrete compressive strength of 150 mm standard cubes (from 200 mm standard cubes). The cores have been obtained and tested during the period 1990-1994 with the approximate length/diameter-ratio of 1.0, (diameter about 100 mm). Based on work by Rådman[2].

3.3 Test results for eight bridges built between 1965-1990

An increase in the compressive strength can also be seen for another series of bridges built between 1965 and 1980, see Table 1, where the results from compressive and tensile strength tests are presented from an investigation of eight railway bridges (road underpasses), Thun et al.[24]. The concrete compressive strength was examined during the late 1990s. Unfortunately there is no possibility to compare these mean values in Table 1 with the 28-day compressive strength from the time the bridges were built, since no information regarding this has been available. However, since the bridges are built with the Swedish concrete class K400 and K45, the concrete delivered to the construction sites should probably have a mean concrete compressive strength of approximately 45-47 MPa tested on 150 mm cubes after 28 days (maximum aggregate size of 32 mm). This should at least be a qualified guess.

The mean concrete core compressive strength varies between 61.3 and 85.3 MPa which is an increase with some 30 to 90%. Table 1 also shows the tensile strength. The mean uniaxial tensile strength varies between 2.6 and 3.8 MPa. To some extent the concrete compressive strength "follows" the tensile strength, i.e. a bridge with high tensile strength has also a high compressive strength.

Table 1 - Concrete compressive and tensile strengths for eight concrete bridges determined with drilled cores with the diameter and height of 100 mm. The cores are obtained from the longitudinal beams if nothing else is said.

Bridge No. [a]	Type of Strength/Force		Individual Values								*m*	*s*	*CoV*
1	Compressive strength drilled cores, [MPa]	$f_c' =$	--	--	--	--	--	68.4	78.7	71.9	**73.0**	**4.3**	**0.06**
	Uniaxial tensile strength, [MPa]	$f_{t,uni}' =$	--	--	--	--	--	2.3	3.2	2.3	**2.6**	**0.4**	**0.16**
2	Compressive strength drilled cores, [MPa]	$f_c' =$	--	--	--	--	--	88.3	77.3	84.5	**83.4**	**4.6**	**0.05**
	Uniaxial tensile strength, [MPa]	$f_{t,uni}' =$	--	--	--	--	--	4.1	3.6	3.8	**3.8**	**0.2**	**0.05**
3	Compressive strength drilled cores, [MPa]	$f_c' =$	--	--	--	--	--	74.0	77.0	69.7	**73.6**	**3.0**	**0.04**
	Uniaxial tensile strength, [MPa]	$f_{t,uni}' =$	--	--	--	--	--	2.77	3.76	3.30	**3.3**	**0.4**	**0.01**
4	Compressive strength drilled cores, [MPa]	$f_c' =$	--	65.7	71.1	64.2	58.7	54.7	65.0	60.4	**62.8**	**5.0**	**0.08**
	Uniaxial tensile strength, [MPa]	$f_{t,uni}' =$	--	--	--	--	--	--	2.33	2.98	**2.7**	**0.3**	**0.12**
5	Compressive strength drilled cores, [MPa]	$f_c' =$	--	--	--	--	--	77.0	86.0	75.4	**79.5**	**4.7**	**0.06**
	Uniaxial tensile strength, [MPa]	$f_{t,uni}' =$	--	--	--	--	--	3.89	3.49	3.09	**3.5**	**0.3**	**0.09**
6	Compressive strength drilled cores, [MPa]	$f_c' =$	--	--	--	71.7	61.5	63.8	53.9	55.6	**61.3**	**6.4**	**0.10**
	Uniaxial tensile strength, [MPa]	$f_{t,uni}' =$	--	--	--	--	--	2.72	3.26	2.97	**3.0**	**0.2**	**0.07**
7	Compressive strength drilled cores, [MPa]	$f_c' =$	--	--	--	--	--	71.2	65.5	59.1	**65.3**	**4.9**	**0.08**
	Uniaxial tensile strength, [MPa]	$f_{t,uni}' =$	--	--	--	--	--	2.72	2.53	4.07	**3.1**	**0.7**	**0.22**
8	1 Specimen No.:		S1:2	S3:2	S5:2	S6:2	S2:1	S2:2	S4:1	S4:2			
	Compressive strength drilled cores, [MPa]	$f_c' =$	69.9	70.8	78.2	66.5	69.3	74.1	74.0	77.8	**72.6**	**4.2**	**0.06**
	1 Specimen No.:		--	--	S13 [b]	S14 [b]	S10	S8:2	S11:2	S12:2			
	Uniaxial tensile strength, [MPa]	$f_{t,uni}' =$	--	--	2.90	2.91	3.12	3.17	2.49	2.71	**2.9**	**0.3**	**0.09**
	1 Specimen No.:		--	--	S1:1	S3:1	S5:1	S6:1	S8:1	S9:1			
	Splitting strength, [MPa]	$f_{t,sp}' =$	--	--	3.93	4.67	5.19	3.89	5.1	5.2	**4.7**	**0.6**	**0.14**
	2 Specimen No.:		--	--	B1:2	B1:1	B7-1:3	B8-2:2	B9:2	B10:2			
	Compressive strength drilled cores, [MPa]	$f_c' =$	--	--	80.3	83.4	86.4	83.9	88.3	89.2	**85.3**	**3.4**	**0.04**
	2 Specimen No.:		--	--	B2:2	B4:2	B5:2	B7-1:2	B8-1:2	B9-3:2			
	Uniaxial tensile strength, [MPa]	$f_{t,uni}' =$	--	--	3.64	2.25	2.62	3.63	3.25	3.47	**3.2**	**0.6**	**0.21**
	2 Specimen No.:		--	--	B5:1	B6:1	B6-2:1	B7-1:1	B8-1:1	B9:1			
	Splitting strength, [MPa]	$f_{t,sp}' =$	--	--	4.4	4.8	5	4.9	4.8	5.2	**4.9**	**0.3**	**0.06**

m = mean value, *s* = standard deviation, *CoV* = coefficient of variation.

[a] Bridge No. 1 = Boden C (year of construction 1971), 2 = Garnisonsgatan (1970), 3 = Gammelstad (1970), 4 = Luossajokk (1965), 5 = Haparandavägen (1980), 6 = Kallkällevägen (1966), 7= Bensbyvägen (1965) and 8= Lautajokki (1967, 2= long. beam and 1 = slab).

[b] No record left of exact location in the longitudinal beams for the core.

4 STRENGTH VARIATION WITHIN A TROUGH BRIDGE

An extensive study was carried out on a typical reinforced concrete railway trough bridge in order to check the concrete strength variation within this type of structure, see Figure 2. The bridge was situated at Lautajokki close to the Artic Circle and had a span length of 6.1 m and a width of 4.1 m and was built in 1967. It was exposed to railway traffic until 1988 when it was taken out of traffic when a part of the railway line was rebuilt. The reinforced concrete trough bridge consists of a slab, filled with ballast, connected to and carried by two longitudinal beams. This type of concrete trough bridge was very common between 1950 and 1980.

Before the concrete strength was examined, the bridge was exposed to a full-scale fatigue test performed in the laboratory at Luleå University of Technology during 1996, Paulsson et al.[17, 18]. The Swedish Concrete Recommendations, BBK94[1] indicated that it would only last for 500 load cycles with an axle load of 360 kN, but the bridge managed 6 million load cycles and it showed no signs of being close to failure.

In the strength investigation after the fatigue test a total of 12 cores were taken from the slab and 10 from the longitudinal beams. For every strength test, see Table 1, efforts have been

made to test cores from the same level, but in some cases this has not been possible to achieve due to heavy reinforcement. The purpose has also been to receive 3 test specimens from each drilled core, but for drill holes B6, B7, B8 and B9 it has not been possible, which has led to the need of drilling a new hole very close to the first one, see Figure 2. The cement used in the bridge has been Swedish Standard Portland Cement with a fineness of approximately 360 m^2/kg (Blaine). The results from the tensile and compressive strength tests are presented as bridge no. 8 in Table 1. The mean concrete core compressive strength is 72.6 MPa for the slab and 85.3 MPa for the beam. For the slab the mean uniaxial tensile strength is 2.9 MPa and the splitting strength is 4.7 MPa. For the beam the mean uniaxial tensile strength is 3.2 MPa and the mean splitting strength is 4.9 MPa.

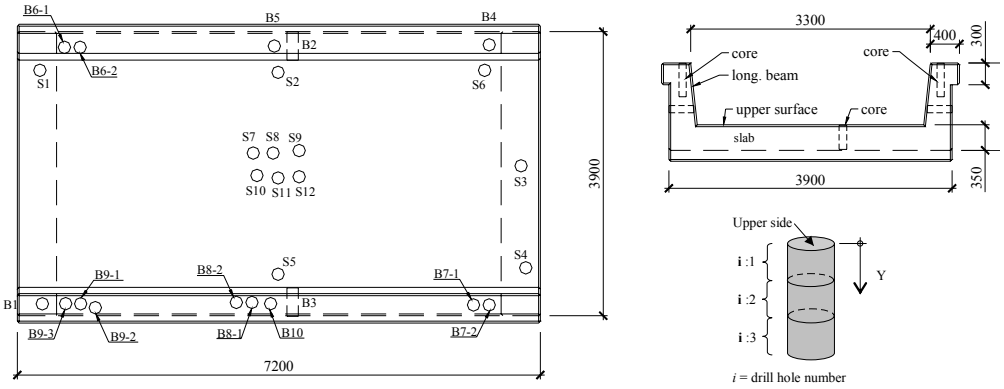

Figure 2 Dimensions and cross-section of the Lautajokki Bridge – a typical Swedish railway reinforced concrete trough bridge. The illustration also shows, in principle, where the cores have been obtained.

It is a well-known fact that there is a variation of concrete properties within a member of a structure. This variation may be due to differences in concrete compaction and curing and/or differences in the quality of the concrete delivered. The bottom parts are usually better compacted with higher density than the top parts, where the percentage of ballast may be smaller. This is due to the influence of the gravity force and the stability of the concrete mixture. If the concrete strength property is considered, the strength variations that can be found in a member of a structure are different depending on if it is eg. a wall or a slab. According to Bungey & Millard[6] the variation between the top and the bottom for a beam can be up to 40% and for a slab 20% (here the loss in strength is concentrated to the top 50 mm). This variation of strength in a member, i.e. higher in the bottom than in the top, has also been found by e.g. Bartlett & MacGregor[19].

If the result presented in Table 1 is compared for the structural parts, i.e. the slab and the longitudinal beams, it appears that the mean compressive strength is 12.7 MPa (approximately 15%) higher in the longitudinal beam than in the slab for the Lautajokki Bridge. This indicates that there is a difference in concrete compressive strength between the side beams and the slab (this difference can be introduced as a partial coefficient for strength, see Nilsson et al.[20]).

The tensile strength for the Lautajokki Bridge shows a similar variation as the compressive strength, but the difference is lower. The mean uniaxial tensile strength is 0.3 MPa (8.5%) higher in the beam than in the slab and for the splitting strength the same relationship is 0.2 MPa (4%). If the two test methods and the result they give are compared the difference is a bit high. The mean uniaxial tensile strength for the slab is 2.9 MPa and the mean splitting strength

is 4.7 MPa. In e.g. Eurocode[21] and CEB-FIP[22] an approximate value of the axial tensile strength is set to 90% of the splitting strength and in the Swedish concrete recommendations, BBK94[1], it is set to 80% of the splitting strength. In this case the approximate value of the axial tensile strength becomes only 62% of the value from the direct tensile test.

In order to clarify if there is a statistical difference between the structural parts regarding the compressive strength and the tensile strength, a similar hypothesis test that was mentioned earlier can be performed. However, if it is assumed that the conditions mentioned earlier are satisfied, the null-hypothesis (H_0) would be that the mean values are equal (i.e. there is no statistical difference between the two structural parts) and the alternative hypothesis (H_1) that the mean values are not equal. If the level of significance is chosen to 0.05 (α) an analysis with the software Statgraphics (by Statistical Graphics Corp.) for the case of compressive strength leads to rejection of the null-hypothesis at the 95% confidence level since the *p*-value is less than 0.05, i.e. 0.00005. The confidence interval for the difference between the means extends from 8.1 to 17.2. Since the interval does not contain the value 0.0, there is a statistically significant difference between the means of the two samples at the 95% confidence level.

If the same analysis is performed for the mean value of the uniaxial tensile strength and the splitting strength, it is shown, contrary to the case for compressive strength, that there is no statistically significant difference between the means of the two structural parts at the 95% confidence level for neither the uniaxial tensile strength nor the splitting strength.

5 TENSILE STRENGTH AS A FUNCTION OF THE COMPRESSIVE STRENGTH

In this paper the concrete tensile strength has been presented along with the compressive strength for the tested bridges. The reason for this is that the tensile strength is a fundamental property. However, as the tensile strength is difficult to test, it has become common to use equations where the tensile strength is expressed as a function of the compressive strength. This can e.g. be found in Eurocode[21] when calculating the concrete shear force capacity. Here, the tensile strength is set to the cubic root of the compressive strength. In the equation for the shear capacity there is probably also a coefficient, A, included that has to do with the correlation between the tensile strength and the concrete strength, but it is not given.

$$f_t = A \cdot f_c^{1/3} \tag{1}$$

What other correlations between the two strengths can be found in the literature? In Möller et al.[7] the following equation is proposed for the correlation between the compressive strength, f_c, and the uniaxial tensile strength, f_t:

$$f_t = B \cdot f_c^{2/3} \tag{2}$$

where the coefficient $B = 0.21$ or 0.24 (in HPCS[23] a similar relation as Eq. (2) is suggested between the compressive strength and the tensile splitting strength, i.e. $f_{t,sp} = 0.25 f_c^{0.7}$).

In HPCS[23] the following relationship between the compressive strength and uniaxial tensile strength is given (Note, that it is similar to the equation used in Eurocode since it is raised to approximately 1/3):

$$f_t = 0.87 \cdot f_c^{0.37} \tag{3}$$

In Figure 3 Eqs. (1) to (3) are shown. For Eq. (1) A is assumed to be 1.0 and 0.21 respectively in Figure 3a. If the different curves in the figure are compared the general difference between the compressive strength being raised to 2/3 or 1/3 is obvious. Eqs. (1) and (2), with $A = 1$ and

B = 0.21, have approximately the same tensile strength at 110 MPa but the form of the curves are very different for the lower strengths. If the compressive strength is e.g. 40 MPa, Eq. (1) gives a tensile strength of approximately 3.5 MPa and Eq. (2) a tensile strength of approximately 2.5 MPa. This indicates the magnitude of the difference that could be obtained if the relationship used in an analysis does not represent the examined concrete well.

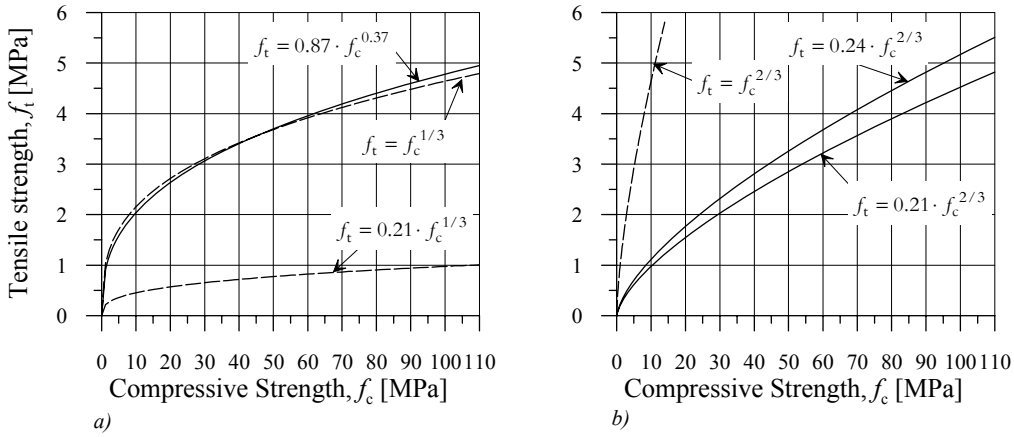

Figure 3 Variation obtained when different correlations between compressive and tensile strength are used.

In Figure 4 the mean compressive and the mean uniaxial tensile strength for the eight bridges are plotted together with two fitted equations that are based on Eqs. (1) and (2). As can be expected both fitted equations can be plausible for this strength region, but Eq. (1) is perhaps slightly more likely than Eq. (2) since it does not give as low tensile strengths for let us say 25 MPa as Eq. (2) does. Eq. (2) is more conservative and would probably underestimate the tensile strengths in this region too much when e.g. assessing the tensile strength of a bridge. Note, the two fitted equations are only intended to show the principal behaviour and nothing else.

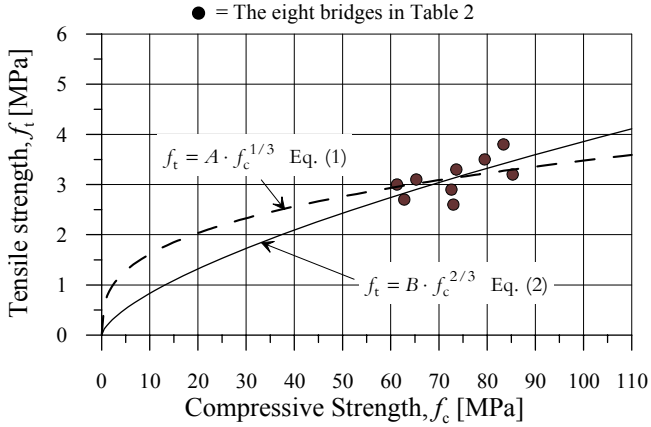

Figure 4 Compressive and tensile strength for eight railway concrete bridges together with two fitted equations. (A=0.75 and B=0.18 where the coefficients of determination, R-squared is 0.30 and 0.39, respectively, i.e. poor fits - the fitted equations are only used to show the principal behaviour of the two equations).

If the tensile strength is investigated for an existing structure another interesting problem arises. Should the uniaxial tensile test or the splitting test be used. If the uniaxial tensile strength for the slab in Table 1 is compared to the splitting tensile strength (i.e. the splitting strength reduced to 80 % according to the Swedish regulations, BBK94[1]) the difference is about 30 % (2.9 MPa compared to 3.7 MPa). For this bridge it is most favourable to use the splitting test, but it is the national regulations that decide the choice between the methods.

6 SUMMARY AND CONCLUSIONS

In a study of the concrete compressive strengths for twenty Swedish bridges built during 1931-1962, the mean increase in compressive strength is about 70% compared to the 28-day concrete strength (corresponding to a mean increase of 21 MPa with a high standard variation of 14 MPa). This increase could be expected for bridges built during the 1940s and 1950s. An increase in concrete compressive strength can also be expected for bridges built during the 1960s but probably not as high.

The study of a typical reinforced railway concrete trough bridge, the Lautajokki Bridge, showed that the concrete compressive strength was approximately 15% higher in the longitudinal beam (85.3 MPa) than in the slab (72.6 MPa which is a statistically significant difference at the 95% confidence level).

The tensile strength for the Lautajokki Bridge showed a similar variation as the compressive strength, but the difference was lower (and not statistically verified). The mean uniaxial tensile strength was approximately 8.5% higher in the beam (3.2 MPa) than in the slab (2.9 MPa) and for the splitting test the same relationship was 4%. The ratio between the uniaxial and the splitting tensile strength was approximately 0.6 which is lower than what could be found in e.g. Eurocode[21], where the axial tensile strength is 90% of the splitting tensile strength.

When conversion equations are used to determine the tensile strength with the help of the compressive strength, caution should be used. The Eurocode[21] relation $f_t = A f_c^{1/3}$ with A = 0.75-0.9 gave a good correlation for high concrete strengths (60 to 85 MPa) while the relation in Möller et al.[7] $f_t = B f_c^{2/3}$ with B = 0.21-0.24 gave conservative values for strengths below 50 MPa.

Background material to the presented investigation can be found in Thun et al.[24].

ACKNOWLEDGEMENTS

The investigation was carried out on behalf of Banverket, the Swedish National Rail Administration. Mr. Björn Töyrä and Mr. Anders Kronborg together with their staff at Banverket Northern Region, have provided much information and help. TESTLAB (the test laboratory at Luleå University of Technology) has performed the tests.

REFERENCES

1. BBK94 (1994, 1996). Swedish Recommendations for Concrete Structures. Volume 1 – Design, Volume 2 – Materials, Construction, Control. Svensk Byggtjänst, Stockholm 1994, 185 + 116 pp. ISBN 91-7332-686-0, 91-7332-687-9. Supplement 1996. pp. 57. ISBN 91-7147-274-6. In Swedish.

2. Rådman J. (1998). Development of Concrete Compressive Strength. A study of Swedish Bridges constructed During the 20th Century. Division of Structural Engineering. Luleå University of Technology. Master's Thesis, 1998:258 CIV. pp. 55.

3. Betongprovning (2002). Betongprovning med svensk standard. 1 utg. Stockholm: SIS förl., 2002. (SIS handbok, 0347-2019; 5). pp. 283. ISBN 91-7162-553-4

4. Montgomery, D. C. (2001). Design and Analysis of Experiments, 5th Edition. John Wiley & Sons Inc. pp. 696. ISBN 0471316490

5. Coladarci T, Cobb C. D., Minium E. W., Clarke R. C. (2003). Fundamentals of Statistical Reasoning in Education. John Wiley 6 Sons Inc. October 2003. pp. 480. ISBN 0-471-06972-8

6. Bungey J.H. and Millard S.G. (1996). Testing of Concrete in Structures. Blackie Academic & Professional, an imprint of Chapman & Hall, London 1996. pp. 286. ISBN 0-7514-0241-9.

7. Möller G., Petersons N. and Elfgren L. (1994). Asessement of In-Place Concrete Strength in Structures. (Bedömning av hållfasthet i färdig konstruktion). Betonghandbok – Material utgåva 2. Avsnitt 11. Stockholm: Svensk Byggtjänst. pp. 373. ISBN 91-7332-709-3. In Swedish.

8. Bellander U. (1976). Concrete Strength in Finished Structure. Part 1, Destructive Testing Methods. (Hållfasthet i färdig konstruktion Del 1, Förstörande metoder. Rimliga kravnivåer). Cement och Betonginstitut Forskning 13:76, Stockholm 1976. In Swedish.

9. Johansson S-E. (2005). Personal Communication. Cementa (Heidelberg Cement Group), Malmö, Sweden.

10. Lea F. M. (1970). The Chemistry of Cement and Concrete. 3 ed. London: Edward Arnold, 1970, pr. 1983. pp. 727. ISBN 0-7131-2277-3

11. Taylor G.D. (2002). Materials in Construction: Principles, Practice and Performance. 2 ed. Pearson Higher Edsucation. pp. 597. ISBN 0582369347

12. Neville, A. M. (1995). Properties of Concrete. 4 ed. Harlow: Longman Group. pp. 844. ISBN 0-582-23070-5

13. Washa, G. W. and Wendt, K. F. (1975). Fifty Year Properties of Concrete, ACI Journal, January 1975. pp. 20-28.

14. Washa, G. W., Saemann J. C., and Cramer S. M. (1989). Fifty-Year Properties of Concrete made in 1937. ACI Materials Journal, V.86, No.4, July 1989, pp. 367-371.

15. Walz K. (1976). Festigheitsentwicklung von Beton bis zum Alter von 30 and 50 Jahren. Betontechnische Berichte, 3, 1976. pp. 57-78.

16. Report 291 (2004). Reliability-Based Classification of the Load Carrying Capacity of Existing Bridges. Guideline Document. Report 291. October 2004. Road Directorate, Ministry of Transport, Denmark. pp. 48.

17. Paulsson B., Töyrä B., Elfgren L., Ohlsson U. and Danielsson G. (1996). Load Bearing Capacity of Concrete Bridges. Research and Development Project. (Forsknings- och utvecklingsprojekt avseende betongbroars bärighet. "30 ton på Malmbanan"). Rapport 3.3 Infrastruktur, Banverket, Borlänge 1996. pp. 51 + appendix. In Swedish.

18. Paulsson B., Töyrä B., Elfgren L., Ohlsson U. and Danielsson G. (1997). Increased Loads on Railway Bridges of Concrete. “Advanced Design of Concrete Structures“ (Ed. by K. Gylltoft et al.), Cimne, Barcelona, 1997. pp. 201-206. ISBN 84-87867-94-4.

19. Bartlett M. F. and MacGregor J. G. (1999). Variation of In-place Concrete Strength in Structures. ACI Materials Journal, V.96, No.2, March-April. 1999. pp. 261-270.

20. Nilsson M., Ohlsson U. and Elfgren L. (1999). Partial Coefficients for Concrete Strength for Railway Bridges along the railway line ”Malmbanan”. (Partialkoefficienter för hållfasthet i betongbroar längs Malmbanan). Division of Structural Engineering, Luleå University of Technology. Technical Report 1999:03. pp. 67. In Swedish.

21. Eurocode (2004). Eurocode 2: Design of Concrete Structures - Part 1-1: General Rules and Rules for Buildings. European Committee for Standardization, CEN. April 2004. EN 1992-1-1. pp. 225.

22. CEB-FIP (1993). Model Code 1990. Design Code, Comité Euro-International du Béton, Bulletin d’Information No 213/214, Thomas Telford, London 1993. pp. 437. ISBN 0-2777-1696-4.

23. HPCS (2000). High Performance Concrete Structures - Design Examples. AB Svensk byggtjänst, Stockholm. 2000. pp. 157. ISBN 91-7332-930-4

24. Thun H., Ohlsson U. and Elfgren L. (1999). Concrete Strength in Railway Bridges along Malmbanan. Characteristic Compression and Tensile Strength for 20 bridges between Luleå and Gällivare. (Betonghållfasthet i järnvägsbroar på Malmbanan. Karakteristisk tryck- och draghållfasthet för 20 broar mellan Luleå och Gällivare). Technical Report 1999:02. pp.34. In Swedish.

Paper B

Determination of Concrete Compressive Strength with Pullout Test

by Håkan Thun, Ulf Ohlsson and Lennart Elfgren

Determination of Concrete Compressive Strength with Pullout Test

by Håkan Thun, Ulf Ohlsson and Lennart Elfgren

ABSTRACT

A pullout test method, the Capo-test, has been examined as an alternative to drilled cores to determine the in-place concrete compressive strength. Tests have been carried out on eight railway bridges from 1965 to 1980 and on a one year old slab.

A strength relationship is proposed between the compressive strength of a drilled core with the diameter and the height of 100 mm, f_{core}, and the pullout force, F, from the Capo-test. It is a power function and has the form, $f_{core} = 0.98F^{1.14}$. The relation is valid for concrete compressive strengths up to 105 MPa. It gives higher concrete strengths than earlier proposed functions.

Keywords: Capo-test; pullout test; drilled cores; concrete; bridges; compressive strength

RESEARCH SIGNIFICANCE

During the last few decades, it has become more and more important to assess, maintain and strengthen structures like bridges, dams and buildings due to a combination of increased loads, time-dependent deterioration, increasing age of many structures and the high costs to build new infrastructure. Therefore it is of great interest to find methods to evaluate existing concrete structures in an efficient way. In this paper the focus is concentrated on examining a test method to determine the in-place concrete compressive strength – the so-called Capo-test.

INTRODUCTION

A pullout test method, the Capo-test, is examined for its ability to determine the in-place concrete compressive strength in old bridges. The method has primarily been intended for estimating the strength of the cover-layer of new structures, see German Petersen & Poulsen[1] or Carino[2]. Here the ability to predict the concrete compressive strength in old concrete structures is also studied.

The project was initiated in 1995 when an increase of the axle load was planned for a railway line and its bridges in northern Sweden, see Paulson et al [3,4]. The object of the axle load increase, from 25 tons to 30 tons, was to reduce transportation costs for carrying iron ore from the mine fields in the mountains to the harbours in Luleå on the Gulf of Bothnia and in Narvik on the Norwegian Sea. The railway line has a length of 473 km and was built between 1884 and 1902. There are 112 bridges on the line, most of them rebuilt between 1950 and 1980. In order to check the present concrete strength in the bridges a study was carried out by Thun et al. [5,6].

METHODS

The methods that have been used in this investigation to determine the in-place concrete compressive strength of the reinforced concrete railway trough bridges are drilled cores and Capo-tests.

To drill out and test cores is a common method to estimate the in-place strength of a structure. Most countries have adopted standard procedures for how a core should be prepared, stored, etc. before testing. In this study the preparation, the storage etc. have been made according to the Swedish concrete recommendations, BBK94[7]. A water-cooled drill with diamond edges has been used. The cores have then been air-cured for at least three days before testing, see Möller et al.[8] or prEN 13791[23]. The reason for this is that the cores are moistened by water during the drilling and cutting process and this inflicts a reduction of the strength (about 10-15%) that needs to be considered, see Möller et al. [8]. The ratio between the length and the diameter has been 1.0 (approximately a diameter of 100 mm). The cores have been marked with a drill hole number and a serial number. The cores have been used for uniaxial tensile tests, splitting tensile tests and compressive tests.

The Capo-test (from "**c**ut **a**nd **p**ull **o**ut"-test) is a method to determine the concrete strength of the cover-layer for an existing structure. It was developed in Denmark by German Petersen & Poulsen[1] in the middle of the 1970s. The test procedure consists of drilling a 65 mm deep hole with a diameter of 18 mm using a water-cooled diamond bit, see Fig. 1. Then a 25 mm recess is made at a depth of 25 mm using a portable router. An expandable split steel ring is inserted through the hole in the recess and expanded by means of a special tool. Finally the ring is pulled through a 55 mm counter pressure placed concentrically on the surface. A description of the method can also be found in e.g. Bungey & Millard[10]. The pullout force, F, is measured by the pull machine and can be converted into concrete compressive strength, f_c, by means of calibration charts provided by German Petersen & Poulsen[1]. In Fig. 2 the suggested general correlation for standard 150 mm cubes is presented and the equations are:

$$F = 0.71 \cdot f_c^{'} + 2 \quad \leq 50 \text{ kN} \tag{1}$$

$$F = 0.63 \cdot f_c^{'} + 6 \quad \geq 50 \text{ kN} \tag{2}$$

The background to the correlation charts is several laboratory and field studies made by the manufacturer as well as by other researchers. The Capo-test is a further development of an earlier developed test method, the Lok-test (from Danish for "punch-out test"). In this method a

bolt is embedded in fresh concrete and then pulled out when the concrete has hardened, see German Petersen[9].

If the two methods are compared in general, the Capo-test is a simpler and less expensive test to perform compared to drilled cores on the bridges. The Capo-test has the advantage that the equipment is lighter and easier to transport to the bridge compared with the equipment used for drilling cores. This was one of the key-advantages since many of the bridges in this investigation could only be reached by train or on foot. Important in this case was also the less damage the Capo-test inflicts on the bridges.

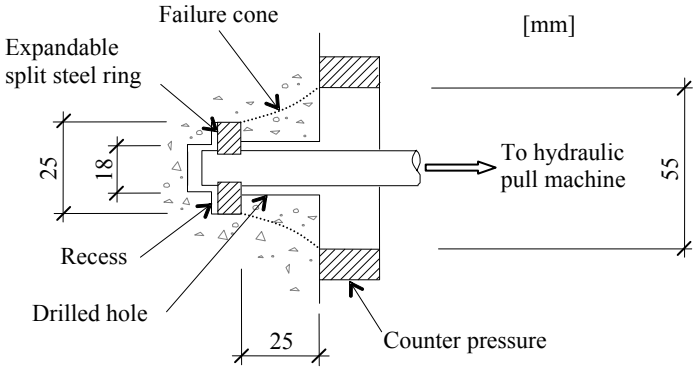

Fig. 1 - Schematic drawing of the Capo-test, based on German Petersen & Poulsen[1], Bungey & Millard[10] and Carino[2].

Rockström & Molin[22] have shown that the relation suggested by German Petersen[9], Eqs.(1) and (2), can be improved when the test object is an old structure, i.e. an old road bridge. They got higher concrete strengths according to Eq. (3) in Fig. 2, when they performed tests with both the Capo-test and drilled cores on six road bridges that had ages up to 54 years. The equation proposed by Rockström & Molin is:

$$F = 0.55 \cdot f_c' + 3.16 \tag{3}$$

The reasons for this discrepancy for old structures could according to Rockström & Molin be due to: *(a)* Difference in concrete strength of the cover-layer and concrete further into the structure, *(b)* For older structures the aggregate size may vary greatly and *(c)* Risk for irregular and insufficient concrete compaction. These three reasons are probably valid also for newly cast concrete – at least reasons *(a)* and *(b)*. Worth mentioning is that the study in Rockström & Molin[22] was based on five objects where the Capo-test and cores were taken from the same test spot. Rockström & Molin rejected the results from one bridge because of the great difference between the Capo-test and the drilled cores due to low strength of the cover-layer (high porosity). The result by Rockström & Molin was commented by German Petersen[9] who suggested that the difference between the Capo-Test measured at the 25 mm surface layer and the core strength 75-100 mm deep found by Rockström & Molin may be explained partly by the 3-day air-curing of the cores prior to crushing, and partly by actual different concrete qualities at the two depth levels.

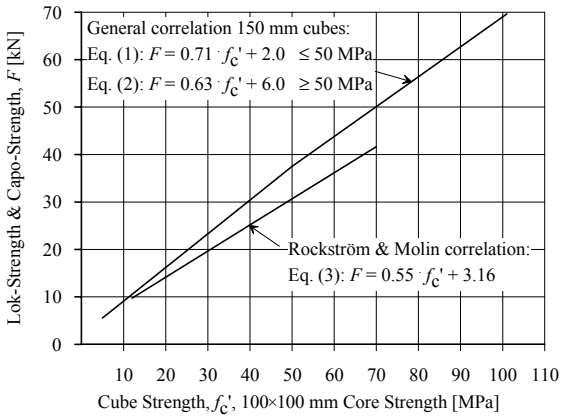

Fig. 2 - Correlation between Capo-test and drilled cores with the height and the diameter of 100 mm, trimmed and air-cured 3 days before testing, made by Rockström & Molin[22] based on 5 old Swedish bridges. The correlation is compared with the general correlation for 150 mm standard cubes suggested by the manufacturer. From German Petersen[9].

The failure mechanism when an anchor bolt is pulled out has been investigated extensively both with experimental and analytical studies and an overview could be found in e.g. Eligehausen et al.[12]. Results from fracture mechanics analyses and a Round-Robin study of plane stress and axi-symmetric tests are presented by Elfgren et al.[13-16], see Fig. 3 and an example of a specific study could be found in Ohlsson & Olofsson[21]. In these it is shown that the geometry, the boundary conditions and the material properties are very important for the outcome of the results. For the pullout-test method an overview is presented in e.g. Carino[2] or Bungey & Millard[10] and specific studies could be found in e.g. Yener[17], Ottoson[18] or Stone & Carino[19,20]. The pullout test subjects the concrete to a nonuniform three-dimensional state of stress. A primary stable crack system is initiated from the insert at an early stage and propagates into the concrete at a large apex angle. Then, governed by the distance to the supports, which gives a counter pressure to the pull-out force, a second system arises. This second system develops to form the shape of the extracted cone, see Fig. 1. In the literature, different hypotheses for the failure mechanism at the ultimate load have been suggested. Some researchers argue that compression failure is the main reason for failure, some say aggregate interlocking and others shear/tensile failure of concrete, see surveys in e.g. Carino[2] or Yener[17].

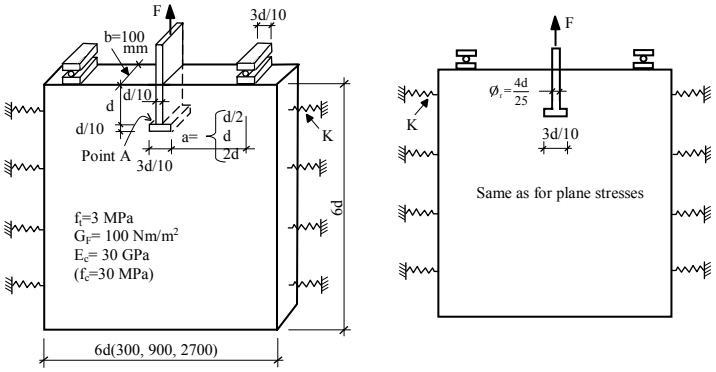

Fig. 3 – Round Robin Analyses and Tests of Anchor Bolts for Plane Stresses (left) and Axi-symmetric Stresses (right) for varying embedment depths d = 50 mm, 150 mm and 450 mm. Elfgren et al.[13,14].

Initially in this study, the general correlation for the pullout force and standard 150 mm cubes suggested by the manufacturer of the Capo-test-system, was used to calculate the compressive strength. This strength was then compared with the compressive strength of tested cores with the height and diameter of 100 mm taken from old bridges. This choice of comparison by the authors of this paper was based on the established relationship between the compressive strength of a horizontally drilled core with the height and diameter of 100 mm and the compressive strength of a 150 mm cube, see Möller et al.[8] or prEN 13791[23]. Furthermore, the compressive strength determined from drilled cores has in this study been regarded to represent the "true compressive strength" since it constitutes the reference method in the new standard for assessment of in-situ compressive strength in structures and precast concrete components (see e.g. prEN 13791[23]).

A thing common for all studies of the Capo-test, is that a fairly good correlation has been found to exist between the pullout force and the concrete compressive strength. In this paper this correlation between the pullout force and the concrete compressive strength has been accepted and utilized to determine the in-place concrete compressive strength.

INVESTIGATION OF CONCRETE STRENGTH

Two series of tests have been performed. The first series is a field study of eight concrete trough bridges. Here the Capo-tests are compared to drilled core tests. In the second series, a laboratory study is conducted.

Field survey of eight railway bridges

In order to get reference material regarding the relationship between the concrete compressive strength of drilled cores and the pullout forces from the Capo-test, the concrete compressive strength was examined for eight railway bridges (road underpasses) during the late 1990s. The bridges were built between 1965 and 1980 with the Swedish concrete class K400 (in most cases), with a mean concrete compressive strength of approximately 45-47 MPa tested on 150 mm cubes after 28 days (maximum aggregate size of 32 mm).

In Table 1 a summary is presented of the results from the tests. Eq. (1) and (2), see Fig. 2, are used to calculate the compressive strength obtained with the Capo-test. The mean concrete core compressive strength varies between 61.3 and 85.3 MPa and the mean compressive strength calculated from the pullout strength varies between 51.6 and 76.9 MPa. These values are substantially lower than the ones from the concrete cores and indicate that the relationship between the pullout load, F, and the concrete compressive strength, f_c, ought to be improved for old concrete. In order to check this a laboratory study was initiated.

Table 1 - Concrete compressive and tensile strengths for eight trough bridges determined with drilled cores and Capo-tests. The cores are obtained from the longitudinal beams if nothing else is said (drilled vertically from above in most cases). The Capo-test compressive strength is evaluated with Eq. (1) and (2), see Fig. 2.

Bridge No. [a]	Type of Strength/Force		Individual Values								*m*	*s*	*CoV*
1	Pull-out force from Capo-Test, [kN]	F =	--	--	--	--	34.9	45.6	46.5	33.4	**40.1**	**5.4**	**0.13**
	Compressive strength Capo-test [b], [MPa]	f_c' =	--	--	--	--	46.3	61.5	62.6	44.2	**53.6**	**8.4**	**0.16**
	Compressive strength drilled cores, [MPa]	f_{cc} =	--	--	--	--	--	68.4	78.7	71.9	**73.0**	**4.3**	**0.06**
2	Pull-out force from Capo-Test, [kN]	F =	--	--	--	--	48.8	46.7	50.3	54.3	**50.0**	**2.5**	**0.05**
	Compressive strength Capo-test [b], [MPa]	f_c' =	--	--	--	--	65.9	62.9	70.3	76.6	**68.9**	**5.2**	**0.07**
	Compressive strength drilled cores, [MPa]	f_{cc} =	--	--	--	--	--	88.3	77.3	84.5	**83.4**	**4.6**	**0.05**
3	Pull-out force from Capo-Test, [kN]	F =	--	--	--	--	42.7	41.2	41.7	46.4	**43.0**	**2.0**	**0.05**
	Compressive strength Capo-test [b], [MPa]	f_c' =	--	--	--	--	57.3	55.2	55.9	62.5	**57.7**	**2.8**	**0.05**
	Compressive strength drilled cores, [MPa]	f_{cc} =	--	--	--	--	--	74.0	77.0	69.7	**73.6**	**3.0**	**0.04**
4	Pull-out force from Capo-Test, [kN]	F =	48.7	45.0	36.6	33.8	42.1	31.2	32.3	39.5	**38.7**	**5.9**	**0.15**
	Compressive strength Capo-test [b], [MPa]	f_c' =	65.8	60.6	48.7	44.7	56.5	41.2	42.7	52.7	**51.6**	**8.3**	**0.16**
	Compressive strength drilled cores, [MPa]	f_{cc} =	--	65.7	71.1	64.2	58.7	54.7	65.0	60.4	**62.8**	**5.0**	**0.08**
5	Pull-out force from Capo-Test, [kN]	F =	--	--	--	--	49.1	52.4	52.9	38.5	**48.3**	**5.2**	**0.11**
	Compressive strength Capo-test [b], [MPa]	f_c' =	--	--	--	--	66.3	73.7	74.5	51.5	**66.5**	**9.3**	**0.14**
	Compressive strength drilled cores, [MPa]	f_{cc} =	--	--	--	--	--	77.0	86.0	75.4	**79.5**	**4.7**	**0.06**
6	Pull-out force from Capo-Test, [kN]	F =	--	--	--	--	--	58.3	46.5	45.1	**50.0**	**5.1**	**0.10**
	Compressive strength Capo-test [b], [MPa]	f_c' =	--	--	--	--	--	83.1	62.6	60.8	**68.8**	**10.1**	**0.15**
	Compressive strength drilled cores, [MPa]	f_{cc} =	--	--	--	71.7	61.5	63.8	53.9	55.6	**61.3**	**6.4**	**0.10**
7	Pull-out force from Capo-Test, [kN]	F =	--	--	--	--	42.6	49.2	35.6	45.5	**43.2**	**4.5**	**0.10**
	Compressive strength Capo-test [b], [MPa]	f_c' =	--	--	--	--	57.2	66.5	47.3	61.3	**58.1**	**7.0**	**0.12**
	Compressive strength drilled cores, [MPa]	f_{cc} =	--	--	--	--	--	71.2	65.5	59.1	**65.3**	**4.9**	**0.08**
8	1:Pull-out force from Capo-Test, [kN]	F =	--	--	--	54.6	54.3	52.4	51.8	59.0	**54.4**	**2.3**	**0.04**
	1:Compressive strength Capo-test [b], [MPa]	f_c' =	--	--	--	77.1	76.6	73.7	72.7	84.2	**76.9**	**4.0**	**0.05**
	1:Compressive strength drilled cores, [MPa]	f_{cc} =	--	--	80.3	83.4	86.4	83.9	88.3	89.2	**85.3**	**3.4**	**0.04**
	2:Pull-out force from Capo-Test, [kN]	F =	--	--	--	--	--	--	53.8	50.7	**52.2**	**1.2**	**0.02**
	2:Compressive strength Capo-test [b], [MPa]	f_c' =	--	--	--	--	--	--	75.8	71.0	**73.4**	**2.4**	**0.03**
	2:Compressive strength drilled cores, [MPa]	f_{cc} =	69.9	70.8	78.2	66.5	69.3	74.1	74.0	77.8	**72.6**	**4.2**	**0.06**

m = mean value, *s* = standard deviation, *CoV* = coefficient of variation.
a) Bridge No. 1 = Boden C (year of construction 1971), 2 = Garnisonsgatan (1970), 3 = Gammelstad (1970), 4 = Luossajokk (1965), 5 = Haparandavägen (1980), 6 = Kallkällevägen (1966), 7= Bensbyvägen (1965) and 8= Lautajokki (1967, 2= long. beam and 1 = slab).
b) Compression strength according to Eqs. (1) or (2).

Laboratory study

In order to check the difference obtained in the filed study of eight bridges, a simple laboratory test was performed. In it we would like to check the sensitivity to what kind of surface the Capo-test was performed on. First, a reinforced slab with the dimensions 0.35×0.70×1.4 m was cast and vibrated with a handheld stick vibrator in the laboratory, see Fig. 4. The idea was then to cut the slab into two beams, dimensions 0.35×0.35×1.4 m, by using a water-cooled hydraulic saw with a diamond blade and perform the Capo-test on both the cut surface and the mould surface. Between these two surfaces cores were to be drilled so a comparison could be made between the Capo-test and the drilled cores. The slab was cast on the ground as shown in Fig. 4. The following concrete mixture was used (1m^3): Cem I 42.5 BV/SR/LA: 432 kg/m^3, Fine aggregate 0-8 mm: 910 kg/m^3, Coarse aggregate 8-16 mm: 945 kg/m^3, Silica fume: 39 kg/m^3, Super-plasticizer: 1.1%, Water reducing agent: 0.5%, Water-to-cement ratio: 0.29, Water-to-

binder content: 0.27. The mixture was tested in connection with casting and the slump was 120 mm and the air content was 1.7%.

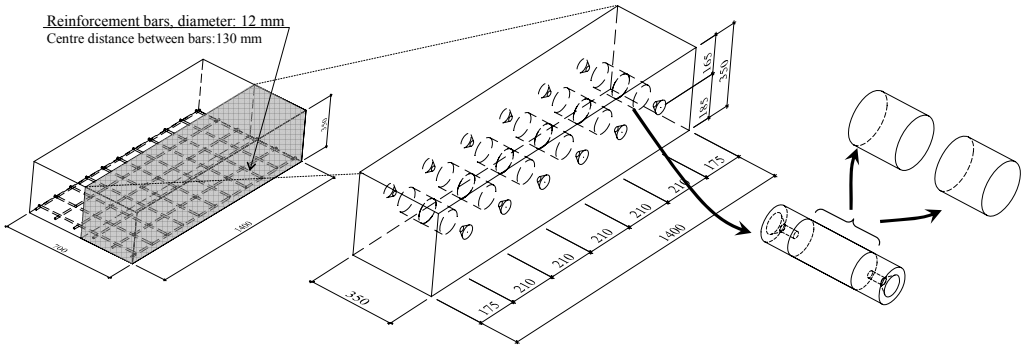

Fig. 4 - Dimensions of slab cast in the laboratory.

After the slab was cast it was stored for three days in the laboratory at room temperature. After these 3 days it was placed in a water tank with a water temperature of approximately +20°C. 36 days after casting it was cut and the two "beams" were again placed in the water tank, where they remained until the day the tests were performed, i.e. 398 days after casting. The Capo-test was performed according to the manufacturer's directions, which recommended corner/end distance of minimum 100 mm and 200-300 mm between each Capo-test on the same horizontal level (the tests were performed during a period of about 2 weeks due to problems with the equipment). A total of twelve Capo-tests on each type of surface could be performed and twelve cores, containing 24 specimens, could be extracted (diameter of about 100 mm, height and diameter ratio of 1.0). In Fig. 5 the results from the Capo-test and the drilled cores are presented visually.

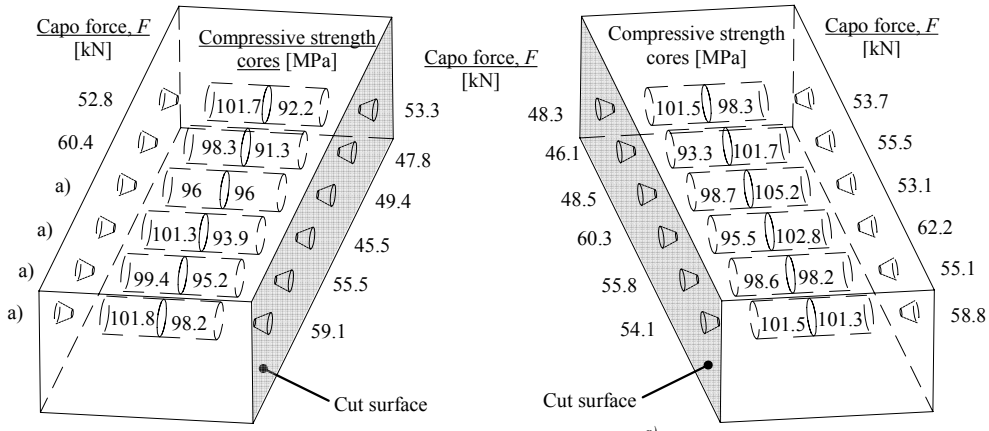

Fig. 5 – Figure showing results from performed tests. [a)] For four locations no result from the Capo-test could be presented due to human errors.

At the same time as the drilled cores were tested, six 150 mm standard cubes were also tested for compressive strength together with three 150 mm standard cubes that were exposed to tensile splitting test. The mean concrete compressive strength was 97.4 MPa (the standard deviation is 2.7 MPa and the coefficient of variation is 0.03) for these six specimens and the mean splitting tensile strength was 5.7 MPa (the standard deviation is 0.3 MPa and the coefficient of variation is 0.05). The 28-day 150 mm standard cube compressive strength was 81.4 MPa (cube compressive strength, mean values of three cubes, for 1-day = 20 MPa, 7-days = 52.9 MPa, 14-days = 65.2 MPa).

DISCUSSION AND ANALYSIS

Field survey of eight railway bridges

In Table 1 it can be seen for bridge 8 that the compressive strength is higher in the slab (Test 1) than in the longitudinal beams (Test 2). The Capo-test gives in fact a higher value of the concrete compressive strength for the slab than the drilled cores from the slab. One explanation could be that the slab contains micro cracks in the tension zone (as the bridge has earlier been exposed to a fatigue test, see Paulsson et al.[3,4]) which are reflected in the cores partly taken from this zone, but not in the Capo-test since it has been performed on the top surface – the compression zone. Another explanation might be that too few Capo-tests are performed on the slab, they are also performed vertically. According to German Petersen & Poulsen[1] testing the upper side of a slab gives a higher standard deviation than testing on a vertical surface.

In Table 1 only two bridges (bridges no. 6 and no. 8) have higher Capo-test concrete compressive strength values than the core strength values. One reason for this could be that only three tests have been performed on these bridges, i.e too few in comparison with the recommended four. For bridges no. 7 and 8 there is a difference between the Capo-test and the core strength of about 8 MPa, but for the other bridges Eqs. (1) and (2) give very low concrete compressive strengths compared with the drilled core compressive strength. It is almost a difference of 20 MPa.

Laboratory study

When the values of the Capo-force presented in Fig. 5 are studied it can be seen that the Capo-forces for the cut surface is lower than the Capo-forces for the mould surface. The mean pullout force for the cut surface is 52 kN (the standard deviation is 5 MPa and the coefficient of variation is 0.1). The mean pullout force for the mould surface is 56 MPa (the standard deviation is 3.5 MPa and the coefficient of variation is 0.06).

Statistical hypothesis test - A way to confirm or deny the difference statistically is to compare the mean values obtained on the two different surfaces. One approach to evaluating this is to perform a so-called statistical hypothesis test which could be found in e.g. Montgomery[25] or Coladarci et al.[26]. In this case a method called two-sample *t*-test can be performed where the mean values of two groups are analysed if they are statistically different from each other. But, to be able to perform this test the following conditions must be fulfilled, firstly: both samples are drawn from independent populations that can be described by a normal distribution, secondly: the observations are independent random variables and thirdly: the standard deviation or variances of both populations are equal. In the laboratory study there are too few tests that have been conducted on each type of surface, so it is difficult to decide if all three conditions are fulfilled.

But, if it is assumed that the conditions above are fulfilled a two-sample *t*-test could be performed with the null-hypothesis (H_0) that the mean values are equal (i.e the Capo-test is not sensitive to what surface it is performed on) and with the alternative hypothesis (H_1) that the mean values are not equal. If the level of significance is chosen to 0.05 (α) a calculation analysis with the software Statgraphics (by Statistical Graphics Corp.) leads to rejection of the null-hypothesis at the 95% confidence level since the *p*-value is less than 0.05, i.e. 0.044. The confidence interval for the difference between the means extends from 0.13 to 8.81. Since the interval does not contain the value 0.0, there is a statistically significant difference between the means of the two samples at the 95% confidence level.

Thus, we can reject the null-hypothesis in favour of the alternative, i.e. the Capo-test gives different results for the two types of tested surfaces. But, as mentioned earlier, if any of the

assumptions made is not correct, the result is uncertain and in this case more studies should be made since the *p*-value is very close to the level of significance which indicates that the result could be discussed (a bit more explicit result would have been wanted).

Now an interesting question arises; why does the Capo-test give higher values when performed on the mould surface? The spontaneous guess is that it would be higher on a cut surface since there is probably more ballast involved in the test volume. One reason for the lower values on the cut surface could be that micro cracks have formed when the surface was cut with the diamond blade, but this is something for future studies. Another explanation could be that there is a difference of moisture content between the two surfaces. As mentioned earlier a reduction of the strength for the cut surface occurs during the cutting process since the cut surface is moistened by water, see Möller et al.[8]. However, since the two cut halves are placed in a water tank for more than a year before the test was performed, this difference in moisture content between the mould surface and the cut surface has most likely been levelled out. Nevertheless, a difference in moisture content between the different capo-test spots arise though during the actual testing period since it takes some time between the first and last test. Efforts have been made to reduce this by keeping the specimens wet and as sealed as possible until all the tests were done.

If the conclusion above is accepted, i.e. the Capo-test is sensitive to the surface, how does it influence the pullout force from an old concrete surface, e.g. an old concrete bridge? We have seen that Eqs. (1) and (2) give lower strengths than the tested cores. If the reason for this difference is only because the Capo-test is performed on an old surface, it seems realistic that a lower pullout force is obtained when the Capo-test is performed on an old surface (even though the concrete compressive strength is high a bit further in the structure e.g. at the level where a core is obtained which is often a few centimetres inwards). Since the surface of an old concrete bridge has often been exposed to environmental degradation over the years e.g. carbonation (i.e. the reaction between the hydrated cement and carbon dioxide) which could reduce the concrete strength. Maybe more grinding is needed of the surface in the preparation phase of a Capo-test when the Capo-test is performed on an old concrete surface.

There could of course also be an actual variation of concrete compressive strength between the cover-layer and the interior mass. In Fig. 5 it could be seen that the concrete core compressive strength varies even if the cores are lying next to each other and as pointed out by Stone & Carino[19] or German Petersen[9] the Capo-test only measures the concrete compressive strength of the cover-layer and not the interior of the concrete structure.

Revised strength relationship for cores with the diameter and the height of about 100 mm

In order to establish a strength relationship between the pullout force from the Capo-test and the compressive strength of a drilled core with the diameter and the height of about 100 mm, the following has been done:

- Field survey of eight bridges - The result from the tests on the eight railway bridges is used, i.e. the mean pullout forces are plotted versus the mean compressive strengths from Table 2 – see the crosses in Fig. 6. Unfortunately it is not possible to use all the data obtained in this study. Thus it is not possible to connect the pullout force from a Capo-test to a certain core. This is due to the fact that several companies have performed the tests and there is no record of core numbers (the cores were taken prior to this study). So it is only possible to connect the pullout force from the Capo-tests to the concrete core compressive strength for a whole bridge. In Fig. 6 two values for very old bridges are also presented, the ones with a circle. As the cores from these bridges showed that the concrete used in the bridges was composed of a

few very big aggregates (approximately 70 mm) and the rest were small ones (approximately 8 mm) combined with mortar, they are not included in the regression analysis. As one can see in Fig. 6 these two bridges give somewhat different values compared with the others. In Fig. 6 it could be seen that this investigation has one so-called outliner (bridge no. 6 in Table 1, where F = 50 kN and f_c' = 61.3 MPa). Note that the mean pullout force for this bridge is also only based on 3 values).

- Laboratory study - If only the tests performed on the mould surface are used from the laboratory study and each pullout force is connected to the "nearest" core compressive strength, e.g. 52.8 kN to 101.7 MPa in Fig. 5, eight "connected" values are obtained. If the "connected" values are studied - the dots in Fig. 6 - they show that lower pullout forces are obtained also for fairly newly cast concrete compared to the suggested general equation for 150 mm standard cubes (the slab was about 1 year old at the time of the tests). This indicates that the main reason for discrepancy is not that the concrete is old (with reduced concrete strength) for the eight railway bridges - at least when the concrete compressive strength is high i.e. between 61 and 105 MPa. This is in contradiction to the previous analysis which said that the Capo-test was sensitive to what surface it is performed on (however, remember that it was not an explicit result).
- A way to complete the set of data is to use the data from Rockström & Molin[22] – see the triangles in Fig. 6. The data come from six road bridges that had ages up to 54 years.

Based on these data a regression analysis can be performed. The relationship between the pullout force, F, and the compressive strength of a drilled core with the diameter and the height of 100 mm, f_{core}, can be modelled with a power function instead of the linear functions used in Fig.2, see Carino[2]. This gives a possibility to model the nonlinearities of concrete behaviour in a better way. Germann Petersen[11] suggests that the following equation could be used as an alternative to Eqs. (1) and (2):

$$f_{cube} = 0.76 \cdot F^{1.16} \tag{4}$$

With the data used in this study we arrive at the following equation:

$$f_{core} = 0.98 \cdot F^{1.14} \tag{5}$$

The regression analysis is based on a power function, $y = ax^b$. The correlation coefficient is 0.97, indicating a relatively strong relationship between the variables. The equation is valid in the interval 11 to 105 MPa.

If the two strength relationships are compared it could be seen that Eq. (5) gives higher compressive strengths than Eq. (4) for the same pullout force. A possible explanation of the deviation between the two equations when the compressive strength becomes high can be due to a change of failure type for the pullout test when the concrete strength is high compared to when it is low and this is due to e.g. higher brittleness of the concrete.

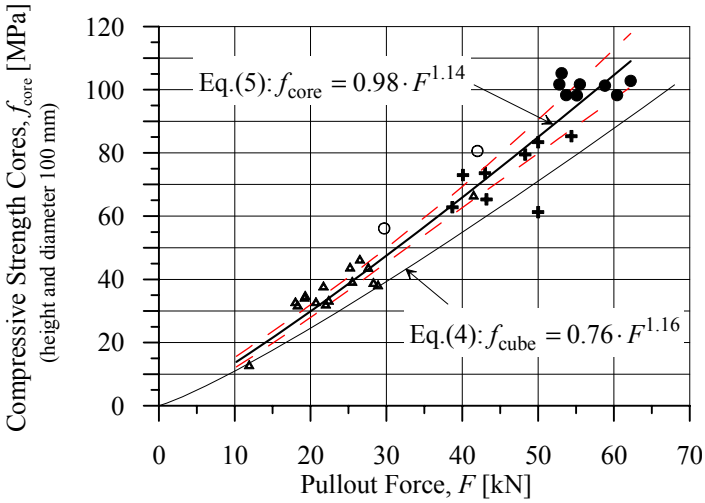

Fig. 6 – Proposed strength relationship, Eq. (5), between the pullout force from the Capo-test and drilled cores with the height and diameter ratio of 1.0 (diameter of about 100 mm). The dashed lines are confidence limits at 95% confidence level. The equation is valid in the interval 11 to 105 MPa. Eq. (4) is the general correlation for 150 mm cubes suggested by the manufacturer, from German Petersen[11].

Illustration of the proposed strength relationship

In an extensive field study involving 37 reinforced concrete trough bridges, a mean pullout force was established for every bridge. Based on these mean values the concrete compressive strength has been calculated for every bridge, using Eq. (3) proposed by Rockström & Molin[22], Eq. (4) and the new proposed Eq.(5). The difference between the equations is shown in Fig. 7.

The bridges are located along the northern railway line in Sweden and a total of four Capo-tests have been performed on each bridge during the summer of 2000 (two tests on the outer surface on each side of the longitudinal beams). The bridges in Fig. 7 are sorted after increasing compressive strength. The bridges were built between 1953 and 1980 with the Swedish concrete class K400 (in most cases), with a mean concrete compressive strength of approximately 45-47 MPa tested on 150 mm cubes after 28 days (maximum aggregate size of 32 mm). The maximum aggregate size is 32 mm for the bridges built in the eighties. It is probably also 32 mm for the bridges built during the fifties and sixties due to the heavy reinforcement in the bridges but it can be as high as 128 mm (128 mm was the maximum aggregate size allowed in sections thicker than 150 mm according to the Swedish concrete code at that time). For bridges no. 1 and 12, from the left in Fig. 7, a high variance in aggregate size has been confirmed by drilled cores. For bridge no. 1 the Capo-test resulted in the compressive strength of 29 MPa, but when cores were obtained later on they gave the concrete compressive strength of 56 MPa. For bridge no.12 the cores gave a mean concrete compressive strength of 80.6 MPa. The difference between the methods in these two cases was probably due to the big difference in aggregate size. Perhaps there is a need to perform more tests than the suggested four when such a difference in aggregate size can be expected.

An idea is then that these calculated mean values of the concrete compressive strength, with their origin in the pullout force from the Capo-test method, could be used e.g. to determine the characteristic in-situ compressive strength and then in turn establish a strength class for each bridge (according to e.g. prEN 13791[23]). An alternative could be to use the calculated mean value, with its dispersion, in a reliability analysis.

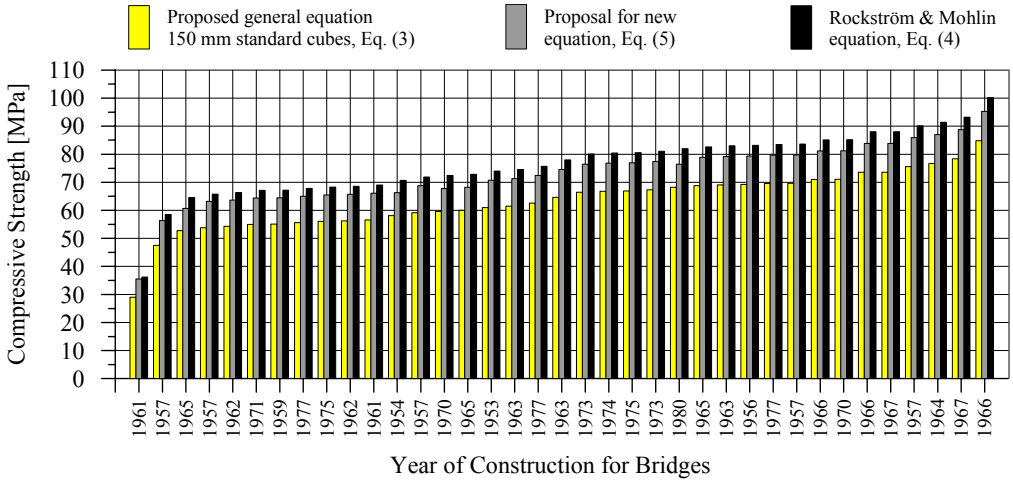

Fig. 7 - Graph showing the concrete compressive strength obtained with the Capo-test on 37 trough bridges, evaluated with three different equations – the general equation for 150 mm standard cubes suggested by the manufacturer Eq. (4), the new proposed equation Eq. (5) and the equation proposed by Rockström & Molin[22] Eq. (3).

SUMMARY AND CONCLUSIONS

The studies in this paper indicate that a pullout method, the Capo-test for concrete strength assessment in new structures, can also be used to estimate the in-place concrete strength in old structures such as bridges.

We have found that the power function relating the compressive strength f_c [MPa] and the pullout force F [kN] given by the manufacturer, $f_c = 0.76\ F^{1.16}$, give conservative values of the compressive strength f_c. For that reason we propose an improved function, $f_{core} = 0.98\ F^{1.14}$ for the interval 11 to 105 MPa. The proposal is based on tests on 8 bridges built between 1965 and 1980, on laboratory tests on one year old concrete and data from Rockström & Molin[22] from six road bridges that had ages up to 54 years. The results are also used to analyse the strength of 37 bridges built between 1953 and 1980.

When the Capo-test is performed on an old concrete surface, e.g. an old bridge, caution must be used since there is a risk of a big difference in aggregate size which could affect the result. In this case more tests should be performed in order to obtain a reliable result.

ACKNOWLEDGEMENTS

The investigation was carried out on behalf of Banverket, the Swedish National Rail Administration. Mr. Björn Töyrä and Mr. Anders Kronborg together with their staff at Banverket Northern Region, have provided much information and help. TESTLAB (the test laboratory at Luleå University of Technology) has performed the tests.

NOTATIONS

f_c' Concrete compressive strength of 150 mm standard cube [MPa].

F Pullout force from the Capo-test, [kN].

f_{cc} Tested core compressive strength. Compressive strength for a drilled core with the

height and the diameter of 100 mm that has been tested in a test apparatus.

f_{core} Calculated compressive strength using a strength relationship between the pullout force and the concrete compressive strength of a core with the diameter and the height of 100 mm, [MPa].

REFERENCES

1. German Petersen C. and Poulsen E. (1993). Pull-out testing by LOK-test and CAPO-test, with particular reference to the in-place concrete of the Great Belt Link. Revised edition November 1993. Danish Concrete Institute A/S, Datavej 36, DK-3460 Birkerød, Denmark. pp. 140.
2. Carino, N. J. (2004). Pullout Test. Chapter 3 in "Handbook on nondestructive testing of concrete", edited by V. M. Malhotra and N. J. Carniro, 2 Ed, Boca Raton, FL: CRC Press. pp. 3-1 to 3-40. ISBN0-8031-2099-0
3. Paulsson B., Töyrä B., Elfgren L., Ohlsson U. and Danielsson G. (1996). Load Bearing Capacity of Concrete Bridges. Research and development project. (Forsknings- och utvecklingsprojekt avseende betongbroars bärighet. "30 ton på Malmbanan"). Rapport 3.3 Infrastruktur, Banverket, Borlänge 1996. pp. 51 + appendix. In Swedish.
4. Paulsson B., Töyrä B., Elfgren L., Ohlsson U. and Danielsson G. (1997). Increased Loads on Railway Bridges of Concrete. "Advanced Design of Concrete Structures" (Ed. by K. Gylltoft et al.), Cimne, Barcelona, 1997. pp. 201-206. ISBN 84-87867-94-4.
5. Thun H., Ohlsson U. and Elfgren L. (1999). Concrete Strength in Railway Bridges along Malmbanan. Characteristic Compression and Tensile Strength for 20 bridges between Luleå and Gällivare. (Betonghållfasthet i järnvägsbroar på Malmbanan. Karakteristisk tryck- och draghållfasthet för 20 broar mellan Luleå och Gällivare). Technical Report 1999:02. pp. 34. In Swedish.
6. Thun H. (2001). Evaluation of concrete structures. Strength development and fatigue capacity. Licentiate thesis 2001:25. Division of Structural Engineering, Luleå University of Technology, Luleå, Sweden, June 2001. pp. 164. ISBN 91-89580-08-2
7. BBK94 (1994, 1996). Swedish Recommendations for Concrete Structures. Volume 1 – Design, Volume 2 – Materials, Construction, Control. Svensk Byggtjänst, Stockholm 1994, 185 + 116 pp. ISBN 91-7332-686-0, 91-7332-687-9. Supplement 1996. pp. 57. ISBN 91-7147-274-6. In Swedish.
8. Möller G., Petersons N. and Elfgren L. (1994). Asessement of In-Place Concrete Strength in Structures. (Bedömning av hållfasthet i färdig konstruktion). Betonghandbok – Material utgåva 2. Avsnitt 11. Stockholm: Svensk Byggtjänst. pp. 132. ISBN 91-7332-709-3. In Swedish.
9. German Petersen C. (1997). LOK-test and CAPO-test pullout testing, twenty years experience. NDT-CE ´97, The British Institute of Non-Destructive Testing. pp. 18.
10. Bungey J.H. and Millard S.G. (1996). Testing of Concrete in Structures. Blackie Academic & Professional, an imprint of Chapman & Hall, London 1996. pp. 286. ISBN 0-7514-0241-9.
11. German Petersen C. (2006). Personal communication, October 2006. (germann @post6.tele.dk)
12. Eligehausen R., Mallée R. and Silva J. F (2006). Anchorage in Concrete Construction. Berlin: Ernst und Sohn. pp. 378. ISBN 978-3-433-01143-5.

13. Elfgren L., Eligehausen R. and Rots J. G. (2001). Anchor bolts in concrete structures: summary of Round Robin tests and analysis arranged by RILEM TC 90-FMA Fracture Mechanics of Concrete - Applications. Materials and Structures, Vol 34, No 242, October 2001. pp. 451-457.

14. Elfgren L., Editor (1998). Round Robin Analyses and Tests of Anchor Bolts in Concrete Structures. RILEM Technical Committee 90-FMA, Fracture Mechanics to Concrete - Applications. With a summary by L. Elfgren, R. Eligehausen, and J. Rots. Research Report 1998:14, Division of Structural Engineering, Luleå Univ. of Technology. pp. 60 + 370.

15. Elfgren L., Editor (1989). Fracture Mechanics of Concrete Structures. From theory to applications. A RILEM Report. Chapman and Hall, London 1989. pp. 407. ISBN 0 412-30680-8

16. Elfgren L. and Shah S. P., Editors (1991). Analysis of Concrete Structures by Fracture Mechanics. Proceedings of the International RILEM Workshop dedicated to Professor Arne Hillerborg. Chapman and Hall, London 1991. pp. 305. ISBN 0-412-369870-x

17. Yener M. (1994). Overview and Progressive Finite Element Analysis of Pullout Tests. ACI Structural Journal, V.91, No.1, Jan.-Feb. 1991. pp. 49-58.

18. Ottosen N.S. (1981). Nonlinear Finite Element Analysis of Pullout Test. Journal of the Structural Division, ASCE, V. 107,Apr. 1981. pp. 591-603.

19. Stone W.C. and Carino N.J. (1983). Deformation and failure in large-scale pullout tests. ACI Journal, Proceedings V.80, No.6, Nov-Dec. 1983. pp. 501-513.

20. Stone W.C. and Carino N.J. (1984). Comparison of Analytical with ExperimentalInternal Strain distributuion for the Pullout Test. ACI Journal, Proceedings V.81, No.1, Jan-Feb. 1984. pp. 3-12.

21. Ohlsson U. and Olofsson T. (1997). Mixed-Mode Fracture and Anchor Bolts in Concrete Analysis with Inner Softening Bands. Journal of Engineering Mechanics, Vol 123, No. 10, October, 1997.

22. Rockström J. and Molin C. (1989). Limited study of relationship between strength measured by rebound hammer, Capo-Test and drilled-out cores. (Begränsad studie av sambandet mellan hållfasthet mätt med studshammare, capo-test resp. utborrade betongcylindrar). Statens Provningsanstalt. Byggteknik. Stockholm. Arbetsrapport SP-AR 1989:17. pp. 34. In Swedish.

23. prEN 13971 (2006). Assessment of in-situ compressive strength in structures and precast concrete components. Final draft. prEN 13791:2006:E. European Committee for Standardization, June 2006. pp. 28. *Note that this is a draft version of the standard.*

24. ASTM C900-01. Standard Test Method for Pullout Strength of Hardened Concrete. Book of Standards Volume: 04.02. ASTM International.

25. Montgomery, D. C. (2001). Design and Analysis of Experiments, 5th Edition. John Wiley & Sons Inc. pp. 696 . ISBN 0-471-31649-0

26. Coladarci T., Cobb C. D., Minium E. W. and Clarke R. C. (2003). Fundamentals of Statistical Reasoning in Education. John Wiley 6 Sons Inc. October 2003. pp. 480. ISBN 0-471-06972-8

Paper C

Probabilistic Modelling of the Shear Fatigue Capacity in a Concrete Bridge Slab

by Håkan Thun, Ulf Ohlsson and Lennart Elfgren

Probabilistic Modelling of the Shear Fatigue Capacity in a Concrete Bridge Slab

Håkan Thun, Ulf Ohlsson and Lennart Elfgren

Luleå University of Technology, SE-97187 Luleå, Sweden

In this paper a probabilistic approach is used for the evaluation of the shear fatigue capacity of a concrete railway bridge slab. In the reliability analysis three different combinations of shear and fatigue models have been compared. The models have been used to determine the safety index β (and the probability of failure) after another 5 or 25 years of traffic with higher axle loads (300 kN) than the bridge has already been exposed to.

Results are given for the shear model used in the Eurocode, EC2 (2004), and for a traditional shear model, Hedman & Losberg (1975), which is used in the Swedish concrete recommendations, BBK04 (2004). The results are combined with fatigue models by Aas-Jakobsen (1970), Tepfers (1979) and Eurocode 2, EC2 (2004). The bridge slab obtains β-values which indicate that it may carry increased axle loads for 5 to 25 years with kept safety, depending on which model is chosen. The most interesting combination seems to be the shear model of Hedman & Losberg (1975)/BBK04 (2004) and the fatigue model of Tepfers (1979).

Keywords: Concrete; Tension; Shear; Fatigue; Safety index; Reliability analysis

1. Introduction

How do you perform a shear force fatigue evaluation of a concrete railway bridge? One solution would be to perform an assessment based on a standard method in a handbook for evaluation of concrete railway bridges. Another solution is to use the methods in a present concrete code for design of new structures. But, are any of the two methods an optimal solution? For instance, a lot more information is now known about the structure in the present situation compared to the design situation, e.g. the actual dimensions of the bridge could be measured with high accuracy; the concrete strength could be determined from tests and so on. It is also possible that some load combinations can be eliminated due to e.g. a change in the use of the railway line. The classification calculation according to the Swedish handbook for evaluation of concrete railway bridges, BVH (2005), mostly refers to the Swedish concrete recommendation,

BBK04 (2004), where large safety factors can be found in most cases. Furthermore, it is also possible that it is sufficient that the bridge is intact for only another five to ten years and not a hundred years as in the case for a newly built bridge.

In this paper a probabilistic analysis has been performed on a bridge slab and the result has been compared to an evaluation performed earlier according to the Swedish concrete code (a deterministic solution). In the analysis different models for the fatigue capacity and the shear force capacity have been studied in the hope of finding a combination that gives a less rigid result than the standard code methods. The probabilistic assessment has been designed to answer the following question: What is the probability that a typical reinforced concrete bridge slab has sufficient shear fatigue capacity for another 5 or 25 years of traffic with kept safety (i.e. safety class 3)? To be able to answer this question a so-called safety index, the β-index, has been calculated.

The study has been limited to calculating and comparing the shear force fatigue capacity of the bridge slab (i.e. the connection between the slab and the longitudinal beams). A standard reinforced concrete railway trough bridge has been used. Different shear/fatigue models are studied and the geometry and the material properties have been obtained from the object that has been used as an example, i.e. the Lautajokki Bridge. The values will be introduced when they appear in the paper with a brief description.

2. Used Methods and Studied Bridge

2.1. Probabilistic assessment

The computer software Variables Processor, VaP (1999) and Schneider (1997), has been used in this paper to determine the probability of failure, p_f, and the so-called safety index β. The program uses, among others, the First Order Reliability Method (FORM) and the Monte Carlo method in the analysis.

To determine if the bridge slab is safe enough the calculated reliability index, β, has been compared to the so-called target reliability index, β_0, that represents the safety level of the existing codes. The values of this target reliability index, β_0, that have been used here are given in the Swedish design regulation, BKR03 (2003), for a reference period of 1 year:

$\beta_0 > 3.7$ for Safety Class 1 (corresponds to the probability of failure, $p_f = 1 \cdot 10^{-4}$)
$\beta_0 > 4.3$ for Safety Class 2 (corresponds to the probability of failure, $p_f = 8 \cdot 10^{-6}$)
$\beta_0 > 4.8$ for Safety Class 3 (corresponds to the probability of failure, $p_f = 8 \cdot 10^{-7}$)

The safety classes above are connected to the risk of injury to persons: Safety Class 1 (low) little risk of serious injury to persons, Safety Class 2 (normal) some risk of serious injury to persons and Safety Class 3 (high) great risk of serious injury to persons.

2.2. The studied bridge - a typical reinforced concrete railway trough bridge

The bridge analysed in this study is a reinforced concrete trough railway bridge – the Lautajokki Bridge - from Lautajokki close to the Artic Circle in northern Sweden. It is a standard railway bridge of a type which was built between 1950 and 1980 and the bridge consist of a slab, connected to and carried by two longitudinal beams, see Figure 1.

In Figure 1 a presentation of the design dimensions of the Lautajokki bridge can be found and in Table 1 some interesting parameters for the bridge are presented. Note that the tensile split-

ting strength has been converted into tensile strength by multiplying the splitting strength by 0.8 according to the Swedish concrete recommendations.

Table 1 Parameters used in the calculations. m is the mean value, s is the standard deviation, CoV (= s/m) is the coefficient of variation. Parameters are taken from a standard drawing of the bridge type if nothing else is stipulated.

Parameter	*m*	*s*	*CoV*	*Distr*	Comments
Amount of bending reinforcement, A_{s0} and A_{sl} [mm^2]:	2010	-	-	Det	10 rebars ϕ16 mm, which is the amount according to drawing (assumed deterministic).
Effective depth, d [mm]:	295	10	0.07	N	s = 10 mm[a)]. Normal distribution assumed.
Compressive strength, f_{cc} [MPa]:	72.6	4.2	0.06	LN	m and s are based on tests performed on the bridge. Log-normal distribution, JCSS (2001).
Uniaxial tensile strength, f_{ct} [MPa]:	2.9	0.3	0.09	LN	m and s are based on tests performed on the bridge. Log-normal distribution, JCSS (2001).
Tensile strength based on splitting test, f_{ct} [MPa]:	3.7	0.45	0.1	LN	m and s are based on tests performed on the bridge. Log-normal distribution, JCSS (2001).

[a)] *The tolerance for the effective depth according to B6 (1969) for this effective depth, i.e. 295 mm, is 20 mm. However, this tolerance could be considered as a maximum allowed value and therefore half this value has been assumed for the calculations since the focus in this study is on the comparison between the models.*

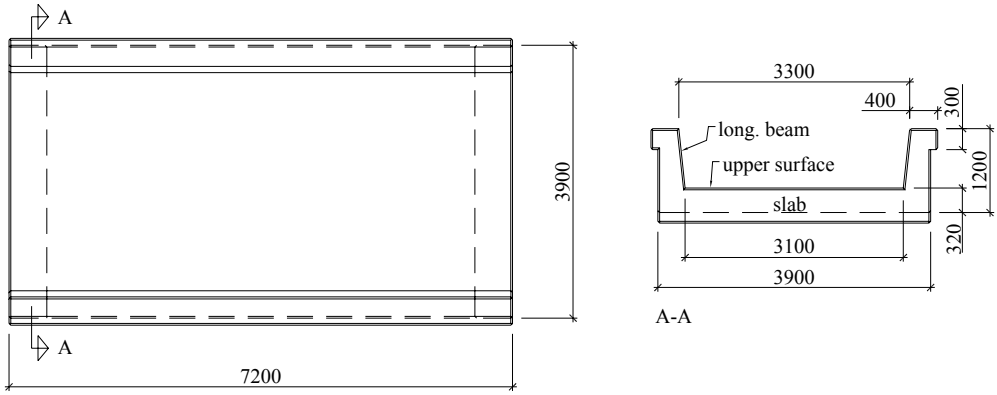

Figure 1 Dimensions and cross-section of the Lautajokki Bridge– a typical Swedish reinforced concrete railway trough bridge. The bridge had a length of 7.2 m and a width of 4.1 m and was built in 1967.

In order to get an idea of how many load cycles the Lautajokki Bridge has already been exposed to during its service life, the following estimation was performed: According to Banverket (the Swedish National Rail Administration) the railway line between Boden and Luleå in the north of Sweden has been exposed to 128.036 Mtons of traffic between 1968 and 1976. This

corresponds to 128.036 / 9 = 14.2 million tons/year. About 81% of these tons/year are iron ore trains with the axle load of 22.5 tons while the rest are trains with lower axle loads. From measurements it could be seen that a load cycle consists of four axles (two axles on one wagon plus two axles on the next wagon) which gives the following number of load cycles during the 21 years (1967-1988) the Lautajokki Bridge was in traffic, N_{old} = 0.81·21·14.2/(4·22.5) = 2.7 million load cycles with the axle load of 22.5 tons.

If the past traffic volume is compared to the planned future traffic volume the traffic will be changed in the way that fewer sets of trains are going between Luleå and Gällivare but the transported volume of iron ore will be increased. This is possible with longer train sets and a higher volume of iron ore on each wagon. An approximation of the coming number of load cycles for a similar bridge as the Lautajokki Bridge can be: 4 train sets/day · (68 wagons/train set + 4 bogies of the IORE-locomotive)·365 days/year = 105120 load cycles/year. This corresponds to, N_{new} = 0.53 million cycles after 5 years and N_{new} = 2.6 million cycles after 25 years. This is an approximation since no consideration has been taken to the other traffic along the railway line. However, other traffic does not influence the fatigue endurance notably.

3. Analysis of Resistance Models

3.1. Shear force capacity

Two expressions to determine the resistance, i.e. the shear force capacity, are discussed and compared in this section. They are: (1) the equation in the Swedish concrete recommendations, BBK04 (2004), based on an expression proposed by Hedman & Losberg (1975) and (2) the expression in the EC2 (2004).

(1) Hedman & Losberg/BBK: The Swedish equation for the shear force capacity, according to equation 3.7.3.2a in BBK04 (2004), is as follows:

$$V_c = b_w \cdot d \cdot f_v \tag{1}$$

where b_w is the smallest width of the beam width within the effective depth in the actual section and d is the effective depth in the actual section. The formal shear strength, f_v, is defined by equation 3.7.3.2b in BBK04 (2004) as follows:

$$f_v = 0.3 \cdot \xi \left(1 + 50 \cdot \frac{A_{s0}}{b_w \cdot d} \right) \cdot f_{ct} \tag{2}$$

where, ξ, is a "height factor" that varies depending on the effective depth, d. ξ is equal to (1.6 – d) when the effective depth is in the range of 0.2 m< $d \leq$ 0.5 m, as in the example. A_{s0}, is the smallest amount of reinforcement due to bending in the tension zone, in the actual beam section, between the zero-point of the bending moment and its maximum point. As an alternative the amount of reinforcement that has a length of (d+l_b) and that passes the actual section can be used. l_b is the length that is required to anchor the design tension force.

Eqs. (1) and (2) are based on Hedman & Losberg (1975) and the so-called addition principle where the shear force capacity is divided into one concrete part and one shear reinforcement part. Hedman & Losberg proposed their expressions after a statistical analysis of their own test results and of test results found in the literature. They derived the following expressions for the concrete part of the shear force capacity:

$$V_c = b_w \cdot d \cdot f_v \cdot \xi \tag{3}$$

where $\xi = 1.6\text{-}d$ is a factor that considers the size effect and f_v, the nominal shear strength, is expressed as:

$$f_v = k_c \left(1 + 50 \cdot \rho\right) \sqrt{f_{cc}} \tag{4}$$

Here ρ is the amount of reinforcement due to bending in the tension zone, (A_s/bd), f_{cc} is the concrete compressive strength and k_c is a factor, determined from regression analysis, with a mean value of 0.09 and a coefficient of variation of 0.15. This factor, k_c, sums up, in some sense, all the uncertainties for Eq. (4), e.g. the correlation between the concrete compressive strength and the tensile strength etc. The expression for the shear force capacity by Hedman & Losberg has also been used earlier in a probabilistic structural analysis by Jeppsson (2003).

(2) EC2: The second expression is the equation given in EC2 (2004) where the design value for the shear resistance, $V_{Rd,c}$, is given in section 6.2.2 "Members not requiring design shear reinforcement" (equation 6.2.a, the compressive stress in the concrete from axial load or prestressing is excluded) and is as follows:

$$V_{Rd,\,c} = b_w \cdot d \cdot \frac{0.18}{\gamma_c} \cdot \left(1 + \sqrt{\frac{200}{d}}\right) \left(100 \cdot \frac{A_{sl}}{b_w \cdot d} \cdot f_{ck}\right)^{1/3} \tag{5}$$

where f_{ck} characteristic compressive cylinder strength of concrete at 28 days [MPa], A_{sl} is the area of the tensile reinforcement, which extends $\geq (l_{bd} + d)$ beyond the section considered (see figure 6.3 in EC2 (2004)), b_w is the smallest width of the cross-section in the tensile area [mm] and γ_c partial safety factor for concrete, i.e. 1.5.

3.2. Fatigue capacity

The fatigue capacity (or the number of load cycles before failure) can be calculated using different models. Common for almost all of them is that the static capacity and the maximum and the minimum load levels must be established. The fatigue requirements will be met, if under cyclic loading the required life (number of cycles n) is less than or equal to the numbers of cycles to failure:

$$n \leq N \tag{6}$$

(1) Aas-Jakobsen/BBK: In the Swedish concrete recommendations, BBK04 (2004) a Wöhler curve proposed by, among others, Aas-Jakobsen (1970), is used:

$$\frac{\sigma_{c,max}}{f_c} = 1 - \chi_1 \left(1 - \frac{\sigma_{c,min}}{\sigma_{c,max}}\right) \log N \quad \text{or} \quad S_{c,max} = 1 - \chi_1 \left(1 - R\right) \log N \tag{7}$$

Here $\sigma_{c,min}$ is the minimum stress, $\sigma_{c,max}$ is the maximum stress, f_c is the static strength, $S_{c,max} = \sigma_{c,max} / f_c$, $R = \sigma_{c,min}/ \sigma_{c,max}$ and N is the number of load cycles. $\chi_1 = 1/C = 1/14 \approx 0.0714$ (in BBK04 (2004) the constant C is 14), see Figure 2.

(2) EC2: In Eurocode 2, EC2 (2004) section 6.8.7, a model similar to the one proposed by Aas-Jakobsen (1970) is used for concrete in compression or shear. The difference between the two equations is that in the EC2 (2004) the term $1\text{-}R$ is replaced by $\sqrt{1-R}$, which makes it somewhat more conservative than the Swedish one. The origin of this expression is work by, among others, Cornelissen (1986). $\chi_2 = 1/C = 1/14 \approx 0.0714$ (in EC2 (2004) the constant C is 14), see Figure 2.

$$\frac{\sigma_{c,max}}{f_c} = 1 - \chi_2 \left(\sqrt{1 - \frac{\sigma_{c,min}}{\sigma_{c,max}}} \right) \log N \Leftrightarrow S_{c,max} = 1 - \chi_2 \left(\sqrt{1-R} \right) \log N \tag{8}$$

Worth mentioning is that f_c in EC2 (2004) is not the design strength, but the design fatigue strength. This is a strength reduced due to e.g. concrete strength at first load application and the time of the start of the cyclic loading on concrete. This reduction makes the expression even more conservative than the more basic Eq. (8).

(3) Tepfers: A Wöhler curve for cyclic load in tension has been proposed by Tepfers (1979), see Figure 2. This curve is interesting since the fatigue models presented in concrete design codes are rather conservative and Tepfers' model is directly based on test results. The Wöhler curve Tepfers proposed has its origin in a Wöhler curve for concrete in compression, see Tepfers & Kutti (1979). The Wöhler curve proposed for tension is:

$$\frac{f_r^{max}}{f_r^{'}} = 1 - \chi_3 (1-R) \log N \quad \text{for } 0 \le R \le \frac{f_{r,min}}{f_{r,max}} \le 1 \tag{9}$$

Here N is the number of load cycles up to fatigue failure, f_r^{max} is the upper limit of fluctuating splitting stress in tension, f_r^{min} is the lower limit of fluctuating splitting stress in tension and $f_r^{'}$ is the static splitting strength in tension.

Tepfers found that since uncertainties in the fatigue result could appear due to difficulties to determine exactly the static tensile strength of the individual test specimen at so high values of $f_r^{max} / f_r^{'}$ as equal to and above 0.8, he excluded the values of $f_r^{max} / f_r^{'} \ge 0.80$ and obtained $\chi_3 = 0.0675$ (12 tests). Since this χ-value differed so little from the original value $\chi_3 = 0.0685$, used in the expression for compression, he concluded that this value could be used. But, when all tests, i.e. all 83, were included in the analysis he received $\chi_3 = 0.0597$ (standard deviation s = 0.0206) and a normal distribution. It corresponds to $C = 1/\chi_3 = 16.7$, see Figure 2.

(4) CEB-FIP: In CEB-FIP (1993) models for compression, tension and shear design are proposed, see Figure 2. The model for compression is based on work by Stemland et.al. (1990) and others but the origin of the tension and shear model is not known to the authors of this paper. For members without shear reinforcement N should be calculated from the fatigue strength functions given below (equation 6.7-9 in CEB-FIP (1993)):

$$\frac{V_{max}}{V_{ref}} = 1 - \frac{1}{C} \cdot \log N = 1 - \frac{1}{10} \cdot \log N = 1 - 0.1 \cdot \log N \tag{10}$$

where V_{max} is the maximum shear force under the relevant representative values of permanent loads including prestress and maximum cyclic loading. V_{ref} is equal to V_{Rd1}, i.e. the design shear force capacity, and this expression is the same as the expression in EC2 (2004), see Eq. (5). The only difference is that the safety factor for concrete, i.e. 1.5, seems to be included in the factor 0.12 (0.18/1.5 = 0.12) in the equation in CEB-FIP (1993). The fatigue model for tension is the same as the one shown in Eq. (10) for shear except that the constant C = 10 is replaced by the constant C = 12.

In Figure 2 the presented fatigue models are shown, for R = 0, together with the model for compression given in CEB-FIP (1993). If the models are compared it is shown that the shear model from CEB-FIP (1993) is the most conservative one, closely followed by the model for tension, also proposed in CEB-FIP (1993). The models for tension and compression in CEB-FIP are the same up to *log N* equal to 6, where the model for compression starts to move to-

wards longer fatigue lives. Since the models are shown for $R = 0$, the model in EC2 (2004) gives the same values as the model by Aas-Jakobsen (1970).

The three least conservative models in Figure 2 have been used in the analysis, i.e. Aas-Jakobsen (1970), Tepfers (1979) and EC2 (2004).

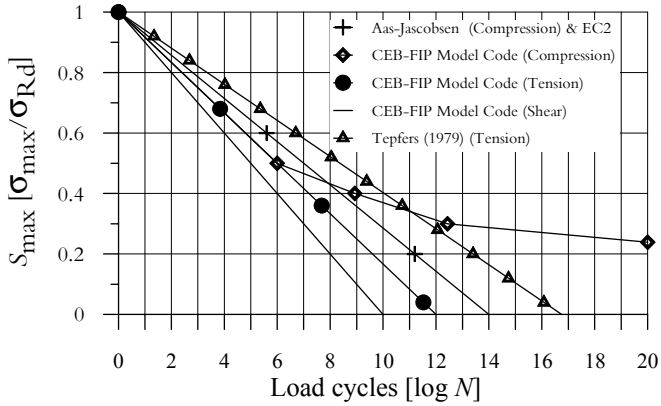

Figure 2 Wöhler-curves for $R = \sigma_{c,min}/\sigma_{c,max} = 0$ according to Aas-Jacobsen (1970), EC2 (2004),Tepfers (1979) and CEB-FIP (1993).

3.3. Model uncertainties

Model uncertainties are used to describe how close the used model comes to the reality (or as a basic random variable describing the ratio "actual value/predicted value"). For the two *shear models* in the codes, see Eqs. (1) and (5), no model uncertainties are given. Therefore the results from Hedman & Losberg will be used. In their model, the factor k_c (with a coefficient of variation of 15%) that could be found in Eq. (4), is believed to, in some sense, describe the model uncertainties. Since the model in BBK04 (2004) is based on Hedman & Losberg their coefficient of variation (15%) would thereby give a reasonable dispersion also for the model in BBK04 (2004). The model uncertainty for the shear model in BBK04 (2004) will be called δ_1, see Eq. (11). It will be assumed that the mean value is 1.0 and in JCSS (2003) it is recommended that the model uncertainty for concrete shear has a lognormal distribution.

The model uncertainty in the expression for the shear force capacity in EC2 (2004) is as mentioned not given. Therefore the same coefficient of variation as for the Swedish equation will be used, i.e. 15% and applied on the coefficient called δ_2 in Eq. (12). It will be assumed that the mean value is 1.0 and in JCSS (2003) it is recommended that the model uncertainty for concrete shear has a lognormal distribution.

Regarding the model uncertainty for the *fatigue models*, no model uncertainties are given except for Tepfers' model where the factor χ_3, see Eq. (9), could be considered to be one. Therefore, the coefficient of variation of 34.5% for the factor χ_3 will be applied on a factor denoted δ_3 which will represent the model uncertainty for all the fatigue models. Since there is no reason to believe that any of the three models are considerably better than the others, the same coefficient of variation as for Tepfers' model (normally distributed) has been assumed for the model of Aas-Jaakobsen/BBK and the EC2 (2004).

4. Results

4.1. Analysis – deterministic assessment of the bridge

The background to this investigation is an assessment project that was initiated to check the condition of reinforced railway concrete trough bridges in Sweden. The aim was to increase the axle load from 25 tons to 30 tons. One of the first actions was to recalculate the bridges with the new axle load according to the present concrete design code. Many of the studied bridges showed that they would not manage the increase in axle load from 25 tons to 30 tons. One critical issue was the concrete shear fatigue capacity (particularly at the connection between the longitudinal beams and the slab). To check whether this was correct one typical reinforced concrete trough bridge – the Lautajokki Bridge - was exposed to a full-scale fatigue test in the laboratory at Luleå University of Technology (LTU) in 1996, Paulsson et al. (1996, 1997). The Swedish concrete recommendations, BBK04 (2004) and its predecessor BBK94 (1994,1996), indicated that it would only last for about 500 load cycles (with safety class 3) with an axle load of 360 kN, but the bridge managed 6 million load cycles in the laboratory without any signs of a reduction of its capacity.

4.2. Analysis – reliability assessment

The reliability analysis of the bridge has been performed for three different cases where two cases are based on two different tensile strength test methods.

(1) Hedman & Losberg/BBK and Aas-Jakobsen/BBK: In the first case the shear force model in BBK04 (2004) is combined with a model proposed by Aas-Jakobsen (1979), which is partly the base for the fatigue model in BBK04 (2004). Note that the model by Aas-Jakobsen is proposed for fatigue in compression.

(2) EC2: The second case is where the shear force model by EC2 (2004) is combined with the fatigue model from EC2 (2004). This combination is probably the most conservative of the ones that are studied.

(3) Hedman & Losberg/BBK and Tepfers: The third case seems to be suitable for a reliability analysis of shear fatigue since most of the coefficients could be tracked down with their dispersions. Here, the shear model proposed in BBK04 (2004), which is based on a model by Hedman & Losberg derived from experiments, is combined with the fatigue model proposed by Tepfers (1979) for tension, which is also based on tests.

4.2.1. Resistance – V_c – static shear force capacity

If the expression for the shear force capacity, i.e. the resistance, is summarised it becomes for the equation in Hedman & Losberg/BBK04, see Eqs. (1) and (2):

$$V_{\mathrm{c}}^{\mathrm{BBK}} = \delta_1 \cdot 0.3 \cdot b_{\mathrm{w}} \cdot d \cdot \xi\left(1+50\cdot\rho\right)\cdot f_{\mathrm{ct}} = \delta_1 \cdot 0.3 \cdot b_{\mathrm{w}} \cdot d \cdot \left(1.6-d\right)\left(1+50\cdot\frac{A_{\mathrm{s0}}}{b_{\mathrm{w}}\cdot d}\right)\cdot f_{\mathrm{ct}} \qquad (11)$$

where b_{w} and A_{s0} are assumed to be deterministic. The other parameters could be found in Table 1.

For the expression in EC2 (2004) the shear force capacity becomes, see Eq. (5):

$$V_{\mathrm{c}}^{\mathrm{EC2}} = \delta_2 \cdot 0.18 \cdot b_{\mathrm{w}} \cdot d \cdot \left(1+\sqrt{\frac{200}{d}}\right)\cdot\left(100\cdot\left(\frac{A_{\mathrm{sl}}}{b_{\mathrm{w}}\cdot d}\right)\cdot f_{\mathrm{cc}}\right)^{1/3} \qquad (12)$$

where the parameters with their mean, standard deviation and distribution are given in Table 1. The width of the studied slab is 1000 mm. The model uncertainties for the model in BBK04 and EC2, δ_1 and δ_2, are both assumed to have a mean value of 1.0 and a coefficient of variation of 0.15 (the same as in Hedman & Losberg (1975)), leading to a standard deviation of 0.15. The distribution type is assumed to be lognormal in accordance with JCSS (2003).

By using the mean values and values for the standard deviations that are presented above the shear force capacity has been calculated with the computer program VaP (1999). The results from a Monte-Carlo simulation of the shear force capacity for the slab after 100 000 runs for three different cases are presented in Table 2.

Table 2 Results from Monte-Carlo simulation of the shear force capacity, V_c. m_R =mean value, s_R = standard deviation, CoV = coefficient of variation where CoV = s_R / m_R,

Shear force capacity based on….		m_R [kN]	s_R [kN]	*CoV*
Model…	**Strength…**			
Hedman & Losberg /BBK04	uniaxial tensile strength	449	82.8	0.18
	splitting tensile strength	572.6	111.4	0.2
EC2	compressive strength	355.6	54.2	0.15

4.2.2. Resistance – V_{res} – fatigue capacity

In order to obtain an estimation if a typical bridge manages another 5 or 25 years of traffic – with kept safety i.e class 3 - in addition to the traffic it has already been exposed to, Eqs.(7), (8) and (9) must be rearranged. The equations have been rewritten with respect to shear force and the following is then obtained:

1) Aas-Jakobsen/BBK: Eq.(7) can be rewritten with respect to shear with $V_{res}^{Aas} / V_{res}^{BBK}$ instead of $\sigma_{c,max}/f_c$ in the following way:

$$V_{res}^{Aas} = V_c^{BBK}\left(1-\chi_1\left(1-\frac{V_{min}^{load}}{V_{max}^{load}}\right)\log N\right)\cdot\delta_3 \tag{13}$$

Here V_{res}^{Aas} is the residual fatigue shear capacity according to the Aas-Jakobsen/BBK model after being exposed to N load cycles. In the term *log N* the old number of load cycles for the bridge, N_{old}, and the new number of load cycles, N_{new}, for e.g. 5 years of more traffic are included. χ_1 is the constant, $\chi_1 = 1/C = 1/14 \approx 0.0714$. V_c^{BBK} is the shear capacity according to BBK04 and V_{min}^{load} and V_{max}^{load} are the minimum and maximum applied shear force respectively.

(2) EC2: If Eq. (8) is rewritten in the same way as Eq. (7) the following is obtained:

$$V_{res}^{EC2} = V_c^{EC2}\left(1-\chi_2\left(\sqrt{1-\frac{V_{min}^{load}}{V_{max}^{load}}}\right)\log N\right)\cdot\delta_3 \tag{14}$$

with similar notation as in Eq. (13) except that χ_2 is the constant, $\chi_2 = 0.0714$.

(3) Tepfers: If Eq. (9) is rewritten in the same way as Eq. (7) the following is obtained:

$$V_{res}^{Tepfers} = V_c^{BBK}\left(1-\chi_3\cdot\left(1-\frac{V_{min}^{load}}{V_{max}^{load}}\right)\cdot\log N\right)\cdot\delta_3 \tag{15}$$

with similar notation as in Eq. (13) except that χ_3 is the constant, $\chi_3 = 0.0597$.

Eqs. (13)-(15) are complemented with the model uncertainty for the fatigue models, δ_2, which is assumed to have a mean value of 1.0 and a coefficient of variation of 0.15 (lognormal distribution).

4.2.3. Load effect - V^{load}

The minimum and the maximum load effect, i.e. shear force, is given by $V_i = q_i L/2$. The minimum shear force, V_{min}^{load}, is given when only the self-weight is acting on the bridge (the calculations are performed on 1 m of the slab):

$$V_{min}^{load} = \frac{q_{self\text{-}weight} \cdot L}{2} = \frac{20.4 \cdot 3.1}{2} = 31.5 \text{ kN}$$

The maximum shear force, V_{max}^{load}, including the dynamic coefficient γ_d, occurs when the traffic load is added to the minimum load (the calculations are performed on 1 m of the slab):

$$V_{max}^{load} = V_{min}^{load} + \frac{L}{2} \cdot q_{traffic} = 31.5 + \frac{3.1}{2} \cdot \left(0.18 \cdot Q_{axle} \cdot \gamma_d\right) = \left(31.5 + 0.279 \cdot Q_{axle} \cdot \gamma_d\right) \text{ kN} \quad (16)$$

The loads are presented in more detail in appendix I.

4.2.4. Safety, *G*: Determination of *β*-index for a typical bridge after another 5 or 25 years of traffic

(1) BBK and Aas-Jakobsen: The expression for the safety is given by the function *G(=R-S)*. For the fatigue model proposed by Aas-Jakobsen, Eq. (13), and the shear model according to Hedman & Losberg/BBK04, Eq. (11), *G* becomes:

$$G = R - S = V_{res}^{Aas} - V_{max}^{load} = \delta_3 \cdot V_c^{BBK} \cdot \left(1 - \chi_1 \cdot \left(1 - \frac{V_{min}^{load}}{V_{max}^{load}}\right) \cdot \log N\right) - V_{max}^{load} \quad (17)$$

(2) EC2-draft and EC2-draft: The expression for the safety is given by the function *G.* For the fatigue model, Eq. (14), and shear model proposed in EC2 (2004), Eq. (12), *G* becomes:

$$G = R - S = V_{res}^{EC2} - V_{max}^{load} = \delta_3 \cdot V_c^{EC2} \left(1 - \chi_2 \left(\sqrt{1 - \frac{V_{min}^{load}}{V_{max}^{load}}}\right) \log N\right) - V_{max}^{load} \quad (18)$$

(3) BBK and Tepfers: For the fatigue model proposed by Tepfers, Eq.(15), and the shear model according to Hedman & Losberg/BBK04, Eq. (11), *G* becomes:

$$G = R - S = V_{res}^{Tepfers} - V_{max}^{load} = \delta_3 \cdot V_c^{BBK} \cdot \left(1 - \chi_3 \cdot \left(1 - \frac{V_{min}^{load}}{V_{max}^{load}}\right) \cdot \log N\right) - V_{max}^{load} \quad (19)$$

The parameters with their mean, standard deviation and distribution are given in Table 1 and Table 3 except for $\chi_1 = \chi_2 = 0.0714$ and $\chi_3 = 0.0597$.

Table 3 Parameters used in the calculations of the resistance, i.e. the shear force capacity. m is the mean value, s is the standard deviation and CoV (= s/m) is the coefficient of variation.

Parameter	*m*	*s*	*CoV*	*Distr*[a)]	Comments
Minimum shear force, V_{min}^{load} [kN]:	31.5	-	-	Det	Assumed deterministic
Traffic load, iron ore, Q_{axle} [kN]:	296.3	6.1	0.02	N	Normal distribution
Dynamic amplification factor, γ_d:	1.13	0.11	0.1	N	*m* see appendix I. *CoV* is assumed
Model uncertainty for fatigue, for all models, δ_3:	1	0.345	0.345	N	*CoV* from Tepfers (1979).
Number of load cycles [million cycles], *N*:	3.23 or 5.3	-	-	Det	$N = N_{old}+N_{new}$, where N_{old} = 2.7 Mc 5 years: N_{new} = 0.53; 25 years: N_{new} =2.6

[a)] *Det* is deterministic and *N* is normal distribution which is chosen in accordance with JCSS (2003).

In Table 4 and Table 5 the results from the calculation are presented for the different fatigue and shear models and for two different tensile strengths, i.e. the uniaxial tensile strength and the splitting tensile strength.

Table 4 Probability of failure from analysis with VaP (1999) for different cases. m is the mean value and s is the standard deviation.

Fatigue and shear force model	No. of years of more traffic	Strength based on…	β-index (HL-index)	Probability of failure P(G<0)	Monte Carlo analysis of G [kN]	
					m	*s*
Aas-Jakobsen/BBK04 and Hedman & Losberg/BBK04	5	Uniaxial tensile	5.03	$2.4\cdot10^{-7}$	247.2	74.4
	25	Uniaxial tensile	3.52	$2.1\cdot10^{-4}$	197.1	75
	5	Tensile splitting	5.9	$1.8\cdot10^{-9}$	350	99.5
	25	Tensile splitting	4.2	$1.3\cdot10^{-5}$	286.3	99.7
EC2	5	Compressive	4.18	$1.5\cdot10^{-5}$	159.2	50.9
	25	Compressive	2.39	$8.4\cdot10^{-3}$	114.5	55.7
Tepfers and Hedman & Losberg/BBK04	5	Uniaxial tensile	5.35	$4.4\cdot10^{-8}$	359.4	75
	25	Uniaxial tensile	4.19	$1.4\cdot10^{-5}$	218	74.1
	5	Tensile splitting	6.23	$2.4\cdot10^{-10}$	365.7	100.7
	25	Tensile splitting	4.97	$3.3\cdot10^{-7}$	312.4	98.3

In Table 5 so-called sensitivity factors, α-values, are presented. The α-values vary between 1 and -1 and give indications of which parameters that influence the calculations most (values close to 1 or -1 mean that the parameter has a high influence on the result).

Table 5 Sensitivity factors, α-values, for studied cases.

Fatigue and shear force model	No. of years of more traffic	Strength based on	α-values					
			d	δ_i	f_{ct} or f_{cc}	γ_d	χ_i	Q_{axle}
Aas-Jakobsen/BBK04 and Hedman & Losberg/BBK04	5	Uniaxial	0.08	0.69	0.48	0.34	0.41	0.08
	25	Uniaxial	0.06	0.49	0.34	0.31	0.73	0.07
	5	Splitting	0.08	0.66	0.53	0.32	0.41	0.08
	25	Splitting	0.07	0.59	0.41	0.33	0.61	0.08
EC2-draft	5	Comp.	0.08	0.74	0.10	0.36	0.55	0.09
	25	Comp.	0.05	0.48	0.06	0.27	0.83	0.06
Tepfers and Hedman & Losberg/BBK04	5	Uniaxial	0.09	0.72	0.50	0.34	0.33	0.08
	25	Uniaxial	0.05	0.44	0.36	0.29	0.77	0.07
	5	Splitting	0.08	0.69	0.56	32	0.32	0.08
	25	Splitting	0.07	0.55	0.44	0.31	0.63	0.08

In Figure 3 the β-index is summarised for the studied cases. In the figure it is shown that the highest safety index β is obtained if the shear model of Hedman & Losberg/BBK04 is used together with the fatigue model by Tepfers and if the tensile strength is derived from splitting strength (which has been converted into uniaxial tensile strength). This combination gives that the bridge manages more than 25 years of further traffic, before the bridge is no longer in safety class 3.

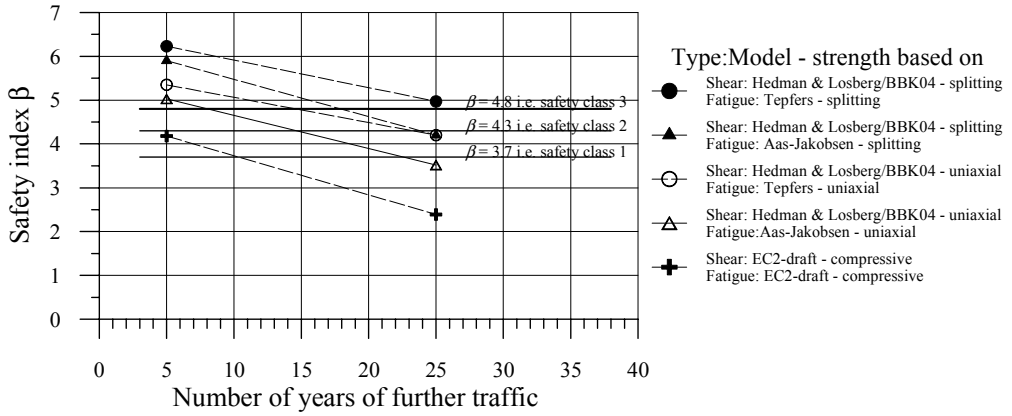

Figure 3 Safety index β shown on the y-axis and the corresponding number of years of further traffic on the x-axis. The horizontal lines represent the β -index for the three different safety classes, 1, 2 and 3 (safety class 3 is the line that is on top). The dashed lines between the two calculated values of β for the different cases are only visual aids (it is not certain that it is a linear relationship).

5. Discussion

The purpose of the evaluation in this paper is to find a more accurate method to estimate the remaining shear force fatigue capacity of a concrete bridge slab than what is given in e.g. national regulations. A structural reliability approach has been used and when the two different

approaches to carry out an evaluation are compared it is evident that a reliability analysis gives a more nuanced result.

The main advantage, generally speaking, with a reliability analysis of a bridge compared to a deterministic analysis is that the answer is not simply a yes or a no to the question if the bridge manages e.g. the higher load, but it gives the engineer a possibility to consider special aspects just for this particular bridge.

The other standard method, an evaluation according to the Swedish regulations that were performed on the bridge used in the example, showed that the bridge would only last for approximately 500 load cycles with the design concrete strength. This result showed to be conservative since the bridge had already managed about 2.7 million load cycles and managed another 6 million load cycles with the axle load of 360 kN. The reliability method presented shows that a bridge similar to the one used in the example, manages up to 25 years of more traffic depending on what combination of shear/fatigue models that is used. One advantage with the method presented is that the history of the bridge, i.e. the number of load cycles it has already been exposed to, is incorporated in the method.

5.1. Shear force capacity

Of the two models that have been used in this study, the model in Hedman & Losberg/BBK04 gives a higher shear force capacity than the model in EC2 (or CEB-FIP). The main reason for the difference is how the concrete strength is used in the different equations. In EC2 (or CEB-FIP) the tensile strength is based on the compressive strength and is raised to 1/3, which gives a lower value than BBK04 where the model is based on the tensile strength. No information is given in EC2 what correlation equation that has been used when the tensile strength is derived from the compressive strength. The model in Hedman & Losberg/BBK04 could in some sense be considered as a mean value model, partly because it is based on the mean model derived from test results by Hedman & Losberg with few changes and partly because the transformation to, most likely, a code model is done by reducing the tensile strength from a mean value via a characteristic value into a design value. On the other hand, the model in Hedman & Losberg/BBK04 contains the coefficient 0.3 and it would be interesting to know what this "factor" includes.

A qualified assumption is that the model in BBK04 is a fairly suitable model to use for concrete shear in a reliability analysis since the background material is known by the work of Hedman & Losberg – there are relatively few "hidden" factors.

A disadvantage with the model in EC2 is due to the fact that the equation is based on the compressive strength and therefore a high tensile strength is not utilized. The tensile strength is not always proportional to the cubic root of the compressive strength and the full potential of the tensile strength is therefore not taken into account.

It is also interesting to see the difference in the result depending on which tensile strength that has been used in the model in Hedman & Losberg/BBK04. In this model a high tensile strength is used at its full potential (whether this is correct or not). In this case it is much more favourable to use the tensile strength derived from the splitting test than the uniaxial tensile test, since the shear force capacity becomes almost twice the result from the uniaxial strength.

5.2. Probabilistic analysis – three different cases

The following could be summarised when the three different combinations of models are used to determine if a bridge manages another 5 or 25 years of more traffic:

- Since Hedman & Losberg/BBK04 gives the highest shear force capacities and that the fatigue model by Tepfers is less conservative than the others, it is not surprising that they also give the highest safety index, (β-index), i.e. 5.03 and 5.9 traffic.

- If the curves in Figure 3 are compared it is shown that the combination of the shear model in Hedman & Losberg/BBK04 and the fatigue model in Aas-Jokobsen/BBK04 give higher β-values than when EC2 (2004) is used. Since the shear model in EC2 (2004) gives the lowest shear force capacity this result is not surprising.

Of the models that have been compared, the combination of Hedman & Losberg/BBK04 and Tepfers seems to be a suitable combination to use in a reliability analysis of a concrete railway bridge, since e.g. many of the dispersions of included factors are known.

5.3. Influencing factors

The sensitivity factors, the α-values, are given in Table 4 (they show the importance the corresponding variable has in the value of the probability of failure). The model uncertainty factor, δ_i, has the highest influence on the β-index, followed by the tensile strength, f_{ct}, and the dynamic coefficient, γ_d. This shows how important it is that these factors are described as good as possible. Note that the compressive strength (in the expression used in EC2) has less influence on the β-index compared to the influence of the tensile strength (the reason for this is how the strength of concrete is used, see below).

The effective depth, d, and the axle load, Q_{axle}, have no major influence on the β-index in the compared cases. These factors could in fact be approximated as deterministic factors in this case. On the other hand a project at LTU has shown that it is important to check as many parameters as possible, see Enochsson et al. (2002). In this particular case measurements of the effective depth, d, of the reinforcement bars, showed that the effective depth was 50 mm less than according to the drawings of the bridge. This, together with the fact that one of 12 reinforcement bars with the diameter of 25 mm was cut off about every 2 meters when cores were drilled to test the concrete strength, reduced the bearing capacity of that bridge significantly. This shows the importance of being careful when performing a test on a bridge and that a factor that was not important on one bridge could be very important on another.

5.4. Need of further studies

There are several parts of this study that could be investigated further. Some of them are:

- What correlation exists between the tensile strength and the compressive strength of concrete? Different correlation equations are used in different models and these equations vary a lot. If the tensile strength is used which method should be used to determine the concrete tensile strength – uniaxial test or splitting test? According to the Swedish regulations the tensile splitting test should be used (if the tensile strength is tested), but on the other hand the tensile strength is in the newer versions of the concrete codes replaced in favour of the compressive strength.
- The dynamic coefficient. For short span bridges studies found in the literature show that the dynamic coefficient could be lower than what the codes stipulate.
- What parameters are interesting to investigate further in an assessment situation and which could be kept as deterministic parameters?

6. Conclusions

Based on the analysis performed in this paper the following conclusions can be drawn:

- The fatigue model by Tepfers and the shear force model in Hedman & Losberg/BBK04 provide a reasonable method for prediction of the shear fatigue capacity of a slab. The reasons for this are:
  - the history of the bridge can be incorporated, i.e. the number of load cycles it already has been exposed to is included.
  - model uncertainties for both the fatigue model and the shear model are known and can be introduced with their dispersions.
- The shear model in Hedman & Losberg/BBK04, has shown that it is more accurate to test the tensile strength and not only rely on the compressive strength since the full potential of the concrete is then not utilised. When only the compressive strength is used higher model uncertainties must be introduced, which reduce the capacity.

Acknowledgement

The study has been financially supported by Banverket (the Swedish National Rail Administration). Thanks are also due to Tech. Dr. Claes Fahleson for valuable comments.

References

Aas-Jakobsen K. (1970). Fatigue of Concrete Beams and Columns. Trondheim: The Norwegian Institute of Technology. Bulletin No 70-1, September 1970. pp. 148.

B6 (1969). Swedish Code for Concrete Structures. Materials and Construction. Reinforcement. (Bestämmelser för Betongkonstruktioner. Material och utförande. Armering. . In Swedish). Statens Betongkommitté 1969, Svensk Byggtjänst, Stockholm. pp. 77.

BBK04 (2004). Swedish Code for Concrete Structures. (Boverkets handbok om betongkonstruktioner, BBK 04. In Swedish). Boverket, Karlskrona 2004. pp. 271.

BBK94 (1994, 1996). Swedish Code for Concrete Structures. Volume1 - Design, Volume 2 - Materials, Construction, Control (Boverkets handbok om betongkonstruktioner, BBK 94, Band 1, Konstruktion, och Band 2, Material, Utförande, Kontroll. In Swedish), Svensk Byggtjänst, Stockholm 1994. pp.185 + 116. ISBN 91-7332-686-0, 91-7332-687-9. Supplement 1996. pp. 57. ISBN 91-7147-274-6

BKR03 (2003). Swedish Code for Design of Structures (Regelsamling för konstruktion – Boverkets konstruktionsregler, BKR, byggnadsverkslagen och byggnadsverksförordningen. In Swedish). Boverket, Karlskrona. Upplaga: 1. Elanders Gotab, Vällingby. ISBN 91-7147-740-3. pp. 256.

BVH (2005). Evaluation of Concrete Railway Bridges. (Bärighetsberäkning av järnvägsbroar. In Swedish). Handbok BVH 583.11. Banverket, CB, Borlänge 2005-06-01. pp. 108 + 9 bilagor.

CEB-FIP (1993). CEB-FIP Model Code 1990. Design Code. Comité Euro-International du Béton Fédération Internationale de la Précontrainte, Thomas Telford Ltd. pp. 437. ISBN 0-7277-1696-4

Cornelissen H. A. W. (1986). State-of-the-art Report on Fatigue of Plain Concrete. Delft, The Netherlands: Delft University of Technology. Report 5-86-3. pp. 62.

EC1 (2003). Eurocode 1: Actions on Structures - Part 2: Traffic Loads on Bridges. European Committee for Standardization, CEN. EN 1991-2. September 2003. pp. 165.

EC2 (2004). Eurocode 2: Design of Concrete Structures. Part 2: Concrete Bridges. Design and Detailing Rules. Stage 49. European Committee for Standardization, CEN. November 2004. prEN 1992-2:2004 (E). pp. 93.

Hedman O and Losberg A. (1975). Dimensionering av betongkonstruktioner med hänsyn till tvärkrafter (Shear design of concrete structures, in Swedish). Stockholm. Nordisk Betong. 5-1975. pp.19-29.

James G (2003). Infrastruktur för effektivare godstransporter på järnväg. Effektiva tågsystem för godstransporter, Underlagsrapport. Rapport 0506F. Järnvägsgruppen KTH, Avd för brobyggnad, Stockholm, 2003. pp. 23. In Swedish.

JCSS (2001). Probabilistic Model Code, Issued by the Joint Committee on Structural Safety, JCSS, 12th Draft, March 2001. 1. Basis of Design, 62 pp; 2. Load Models, 73 pp; 3. Material properties. pp. 43.

Jeppsson J. (2003). Reliability-based Assessment Procedures for Existing Concrete Structures. Lunds University, Structural Engineering, Division of Structural Engineering. Doctoral thesis. Report: TVBK-1026. pp. 184.

Nilsson M., Ohlsson U and Elfgren L. (1999). Partial Coefficients for Material Strength in Reinforced Concrete Bridges at the Iron Ore Line. (Partialkoefficienter för hållfasthet i betongbroar längs Malmbanan. In Swedish). Teknisk rapport 1999:03. Luleå University of Technology, Division of Structural Engineering. pp. 38.

Paulsson B., Töyrä B., Elfgren L., Ohlsson U. and Danielsson G. (1996). Load Bearing Capacity of Concrete Bridges. Research and development project. (Forsknings- och utvecklingsprojekt avseende betongbroars bärighet. “30 ton på Malmbanan“. In Swedish). Rapport 3.3 Infrastruktur, Banverket, Borlänge 1996. pp. 51 + appendix.

Paulsson B., Töyrä B., Elfgren L., Ohlsson U. and Danielsson G. (1997). Increased Loads on Railway Bridges of Concrete. “Advanced Design of Concrete Structures“ (Ed. by K Gylltoft et al.), Cimne, Barcelona, 1997. pp. 201-206. ISBN 84-87867-94-4

Schneider J. (1997). Introduction to Safety and Reliability of Structures. International Association for Bridges and Structural Engineering, IABSE, Structural Engineering. Documents No 5, Zürich, August 1997. pp. 138. ISBN 3-85748-093-6

Simonsson A (2002). Assessment of Railway Bridges. The Influence of the Dynamic Factor on Reinforced Concrete Trough Bridges. (Tillståndsbedömning av järnvägsbroar: inverkan av dynamisk last på trågbroar av betong. In Swedish9. Avdelningen för konstruktionsteknik, Luleå tekniska universitet. Examensarbete 2002:357. pp. 88.

Stemland, H., Petkovic, G., Rosseland, S. and Lenschow, R. (1990). Fatigue of High Strength Concrete. Nordic Concrete Research. Publication No. 90: pp. 172-196.

Tepfers R. (1979). Tensile Fatigue Strength of Plain Concrete. ACI Journal Vol 76, No 8: pp. 919-933.

Tepfers R. and Kutti T. (1979). Fatigue Strength of Plain and Ordinary and Lightweight Concrete. ACI Journal Vol. 76, No. 5: pp. 635-652.

VaP (1999). VaP 1.6. Variables Processor. Computer software created by Dr. Markus Petschacher. Institute of Structural Engineering, ETH, Zurich. Switzerland.

Appendix I - Load Effect

Real Loads on Bridge - V^{load}

The heaviest traffic load a bridge can be exposed to in Sweden is an iron ore train set, i.e. an engine and fully loaded iron ore wagons. This traffic load must in turn be multiplied by a dynamic coefficient, γ_d.

The load combination that is most critical for this type of trough bridge with a span length of about 6 m, is presented in Figure Ia. It consists of the bogies from two coupled iron ore wagons. In BVH (2005) the four point load, i.e. the axle loads, can be substituted with a uniformly distributed load of 188 kN/m and this load is obtained by distributing the four axle loads on the distance of 6.4 m. If this is applied in the example the full length and width of the bridge will be used, i.e. 7.2 m and 3.1 m respectively. The uniformly distributed load, $q_{traffic}$, will then be:

$$q_{traffic} = \frac{4 \cdot Q_{axle}}{7.2 \cdot 3.1} = 0.18 \cdot Q_{axle} \text{ kN/m}^2 \qquad \text{I.1}$$

The weight of all iron ore wagons is measured after they are loaded with iron ore and before the departure from Gällivare to Luleå. In Simonsson (2002) measured weights of two iron ore train sets are presented. Each boogie of the wagons has been measured and if these loads are rearranged according to the load case in Figure Ia the mean bogie load case is 118.6 tons with a standard deviation of 1.5 tons (maximum load is 124.1 tons and minimum load is 114.8 tons), see Figure Ib. The analysis also shows that the load distribution could be approximated with a normal distribution. The load from the critical load case has been converted into axle loads, Q_{axle}, with a mean axle load of 29.6 tons (296.3 kN) and a standard deviation of 0.61 tons (6.1 kN).

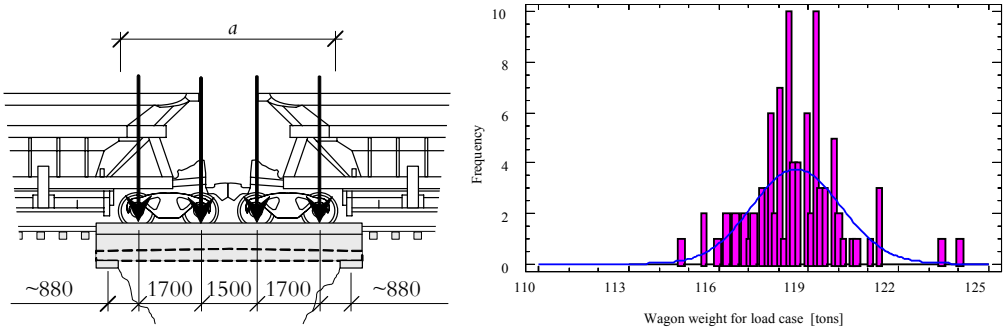

a) *b)*

Figure I a) Critical load combination, with four axle loads of 300 kN occurring when the bogies from two wagons are placed on the bridge, from Nilsson et al. (1999). b) Histogram of measured weights of loaded iron ore wagons. The measured weights have been rearranged according to the critical load case in Figure 3a.

Together with the traffic load, the following permanent loads are considered in the calculations: self-weight of the concrete of the slab, weight of the ballast (the ballast depth must be measured), weight of the sleepers and weight of the reels. These loads give the following expression for the total load effect:

$$q_{total} = \left(q_{concrete} + q_{ballast} + q_{sleepers} + q_{reel}\right) + q_{traffic} \cdot \gamma_d \text{ kN/m} \qquad \text{I.2}$$

If the permanent loads are calculated, with the assumptions made above, the following is obtained (assuming: the density of reinforced concrete is 24 kN/m^3 and the density of the ballast 20 kN/m^3 according to BVH (2005)):

Self-weight of concrete (only the slab):
Q_{concrete} = 24 kN/m^3 · (0.295·5.92 + 0.275·1.28) m ·7.2 m · 3.1 m = 150.12 kN

Self-weight ballast:
Q_{ballast} = 20 kN/m^3 · 0.6m · 7.2 m · 3.05 m = 267.84 kN

Self-weight sleepers (the spacing 0.65 m):
Q_{sleepers} = 12 · 250 kg · 10 = 30 kN

Self-weight reel ([a] measured weight of reel):
Q_{sleepers} = ca (1000/33 ·1.44·10)[a] N/m· 7.2 m · 2 reels = 6.3 kN

Total self-weight: 454.24 kN

This load is distributed on the whole slab area = 7.2·3.1 = 22.32 m^2 which gives:
$q_{\text{self-weight}}$ = 454.24 /22.32 = 20.4 kN/m^2

Dynamic amplification factor

The dynamic effects are summarised in a so-called dynamic amplification factor, γ_d, that increases the static load. This factor considers e.g. the eigenfrequencies of the bridge and irregularities from e.g. the track, the wheels, the loads etc. In James (2003a) the historical background, among other things, to the different expressions to estimate the dynamic amplification factor found in Eurocode, CEN (1995), has been studied. James writes that the origin of the expressions in CEN (1995) to estimate the dynamic amplification factor, are both field measurements and theoretical studies, where the former were performed during the 50's and 60's on bridges of varying types and materials using different types of locomotives.

The equations to determine the dynamic amplification factor in EC1 (2003) or the Swedish code BVH (2005) seem to be the same as in CEN (1995). There are three different methods of estimating the dynamic amplifications factor with increasing degree of complexity. The first and simplest method (which can be used for bridges with iron ore load in Sweden) is as follows:

$$\gamma_d = 1 + \frac{4}{(8+L)} \qquad \text{I.3}$$

where L is the determinant length which in this example is equal to the width of the bridge slab, i.e. 3.1 m, and if L is inserted in Eq. I.3 the amplification factor becomes 1.36.

The second method can be used for fatigue evaluation with "real trains". The dynamic amplification factor, γ_d, can then be calculated according to Appendix 3 in BVH (2005) or Annex D in EC1 (2003):

$$\gamma_d = 1 + \frac{1}{2}\left(\varphi' + \frac{1}{2}\varphi''\right) \qquad \text{I.4}$$

where φ' represents the dynamic effect due to the vibration of a beam traversed by forces travelling at speed on a perfect track and φ'' represents the dynamic effect due to the influence of track irregularities, James (2003a). These two parameters are calculated as follows:

$$\varphi' = \frac{K}{1 - K + K^4} \qquad \text{I.5}$$

$$\varphi'' = 0.56 \cdot e^{-\frac{L^2}{100}} \qquad \text{I.6}$$

$$K = \frac{v}{160} \text{ for } L \le 20 \text{ m} \qquad \text{I.7}$$

where v is the speed in m/s and L is the determinant length of the bridge, in this case the width of the bridge slab. The dynamic amplification factor for the bridge in the example will be 1.20 for a slab width of 3.1 m and a speed of 70 km/h.

The third method and the most complex one is written as follows:

$$\gamma_d = 1 + \varphi' + \frac{1}{2}\varphi'' \qquad \text{I.8}$$

here φ' is the same as in Eq. I.5 but where φ'' is calculated as follows:

$$\varphi'' = \frac{\alpha}{100}\left(56 \cdot e^{-\left(\frac{L}{10}\right)^2} + 50 \cdot \left(\frac{n_0 \cdot L}{80} - 1 \right) \cdot e^{-\left(\frac{L}{20}\right)^2} \right) \qquad \text{I.9}$$

where α and n_0 can be found in EC1 (2003) Annex C.

Which method to estimate the dynamic amplification factor should then be used in the reliability analysis performed in this paper? In the investigation presented in James (2003a) the second method was chosen, i.e. Eq. I.4. The reasons for this were that Eq. I.8 seemed to represent approximately the 95% quantile and that James assumed that it would be reasonable that Eq. I.4 would give a mean value since it was intended for fatigue evaluation. This assumption seems likely if the formulation in EC1 (2003), Annex D, is considered: "To take account of the *average* effect over the assumed 100 years life of the structure, …". This is stated in conjunction with where the equation is presented.

It is easily understood that this coefficient can be subject for discussion. There are also some indications that even if a mean model (if Eq. I.4 is assumed to be one) is used to calculate the dynamic amplification factor it could give a result that is most likely too high in some cases. In a full-scale test performed at LTU the dynamic amplification factor was determined to 1.12 for a two-span bridge, while calculations indicated 1.24 for the same bridge, see Enochsson et al. (2002) and Simonsson (2002). Measurements of the strain and deflections on another bridge showed that the difference between the strain and deflections for a train standing still and a moving train was small, see Täljsten & Carolin (1999). In James (2003b) it is written that for bridges with short spans, where the track irregularities are a major part of the dynamic amplification factor, the development of new bogies etc. which results in lower vertical dynamic effects compared to old systems, should be favourable and contribute to lower dynamic factors.

These findings indicate that the calculated dynamic amplification factor could be reduced. The main problem with this factor is probably that the equations to estimate the factor is based on old tests with very different equipment than what is used today (there is a big difference between a modern train and an old locomotive). This is perhaps the reason why the contribution from φ'' is about 3.5 times bigger ($\varphi'' = 0.51$ compared to $\varphi' = 0.14$) than the contribution from φ' for the bridge in this example.

If the contribution from the track irregularities is removed for the bridge in this study the dynamic amplification factor, γ_d, would be $\gamma_d = 1.0 + 0.14 \times 0.5 = 1.07$, but on the other hand if φ' is removed the dynamic amplification factor, γ_d, would be $\gamma_d = 1.0 + 0.51 \times 0.25 = 1.13$. Since the measurements by Täljsten & Carolin (1999) show little difference between a train standing still and a moving train the dynamic effect, φ', will be removed from the dynamic amplification factor, i.e. a dynamic amplification factor of 1.13 could be used.

The next questions are what dispersion and distribution type that should be used? Since not so many field measurements have been found by the authors of this paper a log normal distribution and a coefficient of variation, *CoV*, of 10% have been assumed. The reason for the estimation of *CoV* and the log normal distribution, is that it is more common that an intact train set is passing the bridge, or one that has fewer defects, than a train with high irregularities which implies high values of the dynamic amplification factor.

As a comparison, the dynamic amplification factor was assumed to be normally distributed with a coefficient of variation of 0.5 in Nilsson et al. (1999) for a two-span bridge. In the studies made by James (2003a) *CoV* was assumed to vary between 0.2-0.5 and a normal distribution type was also assumed. It is clear that there is a need for studies regarding this parameter in order to clarify how big this factor actually is, the dispersion of it, what dynamic effects that contribute to it and so on.

Paper D

Concrete Fatigue Capacity in Tension - a Study of Deformations

by Håkan Thun, Ulf Ohlsson and Lennart Elfgren

Concrete Fatigue Capacity
- a Study of Deformations at Tensile Forces

by Håkan Thun, Ulf Ohlsson and Lennart Elfgren

ABSTRACT

In this paper results and analyses are presented from cyclic uniaxial tensile tests performed on new and old concrete. The results from the tests indicate that the deformation criterion proposed by Balázs[1] for bond slip might also be applied to plain concrete exposed to cyclic tensile load. A method is proposed for how the deformation criterion may be used also for assessment of existing structures. A Wöhler curve for cyclic loads in tension is derived from the tests.

Keywords: concrete, fatigue, tensile strength, strain criterion, uniaxial tensile test.

RESEARCH SIGNIFICANCE

Even though not many failures of concrete structures due to fatigue - if any at all – have been reported in recent years, the trend in new concrete codes is to increase the safety against fatigue failure. This trend is even more pronounced when shear fatigue failure is considered. In that case the shear/tensile strength of concrete is often replaced by the compressive strength of concrete and additional safety factors are introduced when the shear force capacity is calculated. This makes it difficult for existing bridges to fulfil the new requirements in assessment procedures. Therefore, the investigation in this paper is focused on a deformation criterion proposed in the literature that can hopefully be used to determine the number of load cycles to fatigue failure in a more accurate way.

1 INTRODUCTION

The main intention with this paper is to examine a fatigue failure criterion based on deformation proposed by Balázs[1]. The criterion has successfully been used to describe bond failure between re-bars and concrete. The criterion is that the deformation at peak load during a static test corresponds to the deformation where the failure process in a fatigue test begins, see Fig. 1.

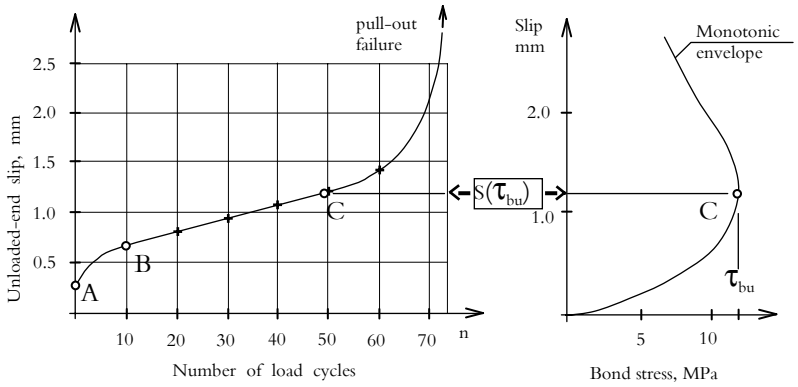

Fig. 1 - Bond fatigue process under repeated loading: a) slip-versus-number of load cycles diagram and b) monotonic bond stress-slip diagram. From Balázs[1].

Daerga & Pöntinen[2] applied the deformation criterion when they performed three-point bending fatigue tests on notched beams cast with plain high performance concrete. Their idea was to predict the fatigue failure for a structure, using monitored deformations and compare them to the deformation capacity of an identical structure exposed to static load.

If this objective should be possible to achieve, i.e to use the failure criterion for a whole structure, some conditions must be met. One of them is to verify the criterion for new as well as for old concrete exposed to cyclic load in tension.

The fatigue tests performed in this paper are a continuation of pilot tests presented in Andersson[3] and Thun[4]. The background to the presented investigation is that the fatigue capacity was too small for a common type of trough bridge, along the railway line "Malmbanan" that transports iron ore in northern Sweden. The capacity had been shown to be too low according to the Swedish concrete code when the axle load was to be increased from 25 to 30 tons. A concrete trough bridge consists of a slab, filled with ballast, connected to and carried by two longitudinal beams, see Fig. 3. A critical section was the connection between the longitudinal beams and the slab and these old bridges were designed without any special shear reinforcement. The bridges of this standard type were usually built between 1950 and 1980. There are some 70 bridges of this trough type along "Malmbanan" and approximately 650 in the rest of Sweden.

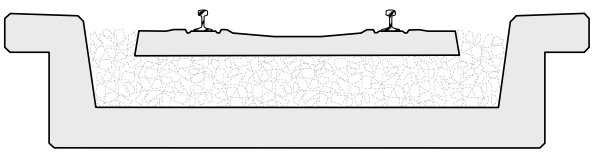

Fig. 2 – Typical section for a Swedish concrete railway trough bridge. The trough, filled with ballast, consists of a slab connected to two longitudinal beams, Nilsson[5].

1.1 Fatigue of concrete in tension

For concrete subjected to static compression loads many studies have been performed over the years, but when it comes to tensile loading far fewer studies have been carried out. According to Hordijk[6] the first publication demonstrating a post-peak behaviour of concrete under tensile loading is believed to be the one by Rüsch & Hilsdorf[7]. One reason for the increased interest in the tensile behaviour of concrete was that fracture mechanics began to be used for concrete structures in order to understand and describe the mechanisms of cracking.

Even though nowadays the tensile strength of concrete is neglected in many design codes, it is of importance. Because, as pointed out by Cornelissen[8], the tensile strength governs the cracking behaviour and therefore also, e.g. the stiffness, the bond to embedded steel and therefore in turn the durability of concrete. Last but not least – compressive failure and shear failure – both failures start with local tensile stresses.

Tensile fatigue tests have been performed in different ways during the years. At the beginning tests on e.g. specimens loaded in bending and on specimens exposed to splitting load were used due to the fact that they were fairly simple to perform. During the last few decades direct deformation-controlled uniaxial tensile tests have become a more common method. The reason for this is that no special grips are needed, as in the early days. Instead the development in the adhesive trade has made it easier to fasten the specimens directly in an advanced test apparatus.

One of the first tests on tensile fatigue was performed by Tepfers[9] using cube splitting test specimens. Later on, especially during the 1980s and 1990s several material models for the fatigue behaviour of concrete in tension were developed which could be implemented in FE-analysis. Models have been proposed by e.g. Gylltoft[10], Rots et al.[11], Reinhardt et al.[12], Yankelevsky & Reinhardt[13], Hordijk[14] and Duda & König[15]. The most recent one seems to be the one proposed by Kessler-Kramer[16].

The fatigue tests in this paper are, as mentioned above, compared to a deformation criterion proposed by Balázs[1]. The criterion has been studied by other researchers, e.g. Hordijk[14], Daerga & Pöntinen[2] and Kessler-Kramer[16]. The model has successfully been used to describe bond failure between reinforcing bars and the concrete. The growth in deformation during a fatigue test can according to the model be divided into three phases, see Fig. 1. At the beginning of the first phase the deformation rate is high but stagnates after a while. The second phase is characterised by a constant deformation rate. These two phases can be described as stable. During the third phase, the failure phase, the deformation rate increases rapidly leading to failure within a short time. The deformation criterion for fatigue failure is that the deformation at peak load, $\delta(\sigma_u)$, during a static test corresponds to the strain at the changeover between phases two and three during a fatigue failure, see Fig. 1. When $\delta(\sigma_u)$ has been reached, only a limited number of cycles are needed until failure occurs. Since there is a difference between the number of cycles at failure and at initiation of phase three the criterion could be considered as safe, Balázs[1].

2 EXPERIMENTAL PROGRAM

2.1 Experimental Design

The fatigue experiments performed in this paper could have been performed without any special strategy and the main objective would even then have been obtained, i.e. an investigation of the above-mentioned deformation criterion. However, since there are two different factors, the mean load level and the amplitude, that are going to be varied at two different levels, additional information can be obtained as a bonus if an experimental strategy was used. The strategy chosen is called factorial design and with this method it could be possible to investigate which one of the chosen factors that has the biggest influence on the number of load cycles to failure, see Appendix 1 in Thun[17].

In this study two different factors that influence the fatigue capacity have been compared, i.e. the load amplitude and the mean load level, hopefully to see which of them is the most important parameter. In Fig. 3 the experimental design is shown. Two different mean load levels (40% and 60% of F_{peak}) have been tested with two different load amplitudes (40% and 60% of

F_{peak}). The limit of maximum load, F_{max} (or f_{max} if the stress is used) for the tests have been set to 90 % of the mean peak load, F_{peak} (or f_{peak} if the stress is used) from the static uniaxial tests.

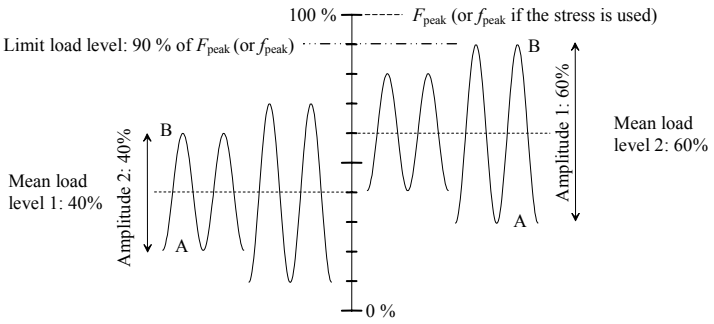

Fig. 3 - Visualisation of the experimental design used in the fatigue tests.

2.2 Test Specimens and Concrete

The tensile fatigue tests have been performed on drilled cores with a height and a diameter of approximately 100 mm. The cores were drilled from both newly cast concrete and old concrete slabs.

The "new" cores have been taken from small slabs cast in March 2004. The concrete used was a normal strength concrete (NSC). The concrete was designed to have a characteristic compressive strength of 45 MPa, tested on 150 mm cubes after 28 days (according to the Swedish concrete recommendation, BBK94[18]). The concrete had the following mixture ($1m^3$): Cem I 42.5 BV/SR/LA: 413.9 kg/m^3, Fine aggregate 0-8 mm: 928.3 kg/m^3, Coarse aggregate 8-16 mm: 856.5 kg/m^3, Silica fume: 15.2kg/m^3, Super-plasticizer: 2 kg/m^3, Water reducing agent: 1.3 kg/m^3, Water-to-cement ratio: 0.4. The mixture was tested in connection with casting and the slump was 64 mm and the air content was 5.4%. After casting the small slabs were stored in a water tank (cores were drilled before the tests and stored together with the small slabs). Three days before testing the drilled cores were cut into a suitable length, a notch was milled and they were then air-cured in the laboratory at room temperature until the testing day. For dimensions see Fig. 4.

The "old" cores have been taken from a small slab that has been cut out in 1996 from the slab of an old bridge that was built in 1968. Little information is available regarding the aggregate size, the composition of the concrete mixture etc. The small slab has been stored indoors as well as outdoors since 1996 until cores were drilled in 2004 and these cores were then stored in room temperature until the tests began.

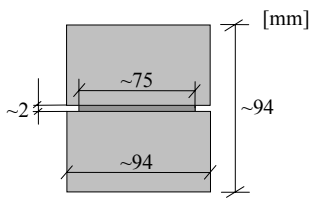

Fig. 4 - Above left: Dimensions of specimen used in the tensile fatigue test, Andersson[3]. Below left: Photo of a specimen, from Andersson[3]. Right: Servo hydraulic machine and other equipment used in the tests.

2.3 Uniaxial tensile tests

In order to determine the strength of the concrete (so that the load levels in the fatigue test could be set) uniaxial tensile tests were performed. Due to limited amount of specimens with old concrete, only three tests were performed on the "old" concrete, while eight tests were performed with the "new" concrete.

Today there is still no international standard on how to perform such a test. There is an influence of the shape and the dimension, which has been studied by several researchers, e.g. Hordijk[14], Daerga[19] and Noghabai[20].

If the uniaxial tensile test is performed under displacement control instead of load control it is possible to obtain the tension-softening branch of the material. At LTU several researchers have performed uniaxial tensile tests using a closed-loop servo-hydraulic test machine. This has led to a local "standard" for this kind of tests, see e.g. Noghabai[20], Hedlund[21] and Groth[22].

Every specimen was ground and cleaned with acetone before it was attached to two steel plates with an adhesive. The adhesive was a two-component adhesive manufactured by Hottinger Baldwin Messtechnik (HBM) called "Schnellklebstoff X-60". The adhesive was first put on the lower steel plate (see Fig. 5) under a small compressive load. When it had hardened the test specimen and the lower steel plate were mounted in the test machine. Adhesive was then put on the upper side of the test specimen. Finally a compressive load was applied to facilitate the hardening process.

Steel rings with holders for COD-gauges were attached to the specimen at each side of the notch with a centre distance of 42 mm. When the steel ring is in place a total of four Crack Opening Displacement gauges (COD-gauges) can be mounted with 90 degrees between each of them. The feed-back signal to the machine was the mean value of all four COD-gauges. Fig. 5 shows a photo of the test set-up.

A Dartec servo-hydraulic test machine has been used and all the data were collected with a Spider8 (multi-channel electronic PC measurement unit) with the help of the computer software Catman (HBM).

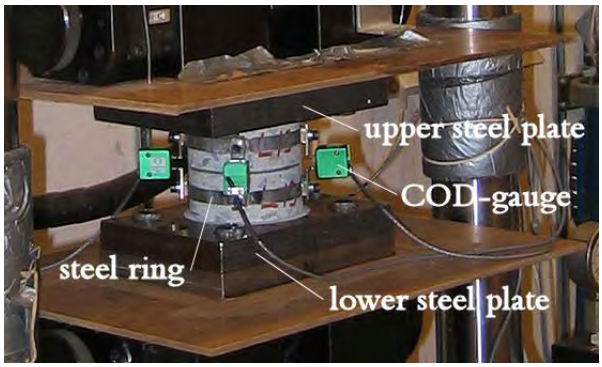

Fig. 5 - Test set-up used in the uniaxial tensile tests and fatigue tensile tests.

2.4 Fatigue tests

All fatigue tests have been performed under load control with sinusoidal load cycles. The load frequency has been 2.0 Hz.

The intention was to sample the data from the COD-gauges in the fatigue tests continuously with a frequency of 60 Hz. However, this leads to very large data files which are difficult to handle. This problem has led to the use of a measuring technique, here called min-max-sampling, where only the maximum and minimum deformations for a time period that each lasts 1.5 seconds have been saved (together with the maximum time value for the same period), see Fig. 6. The maximum and the minimum values are mean values of the four COD-gauges respectively. This technique results in smaller data files and the possibility of measuring without saving to a file, for approximately 17 days. The disadvantage with the technique is that the precision becomes somewhat lower at the start and at the end of each fatigue test. This was partly solved by sampling the start of each fatigue test with 60 Hz and when it was assessed that phase 2 was reached, i.e. a constant deformation rate was obtained, the sampling was changed to min-max-sampling. The intentions were then, when phase 3 was reached i.e. the failure phase, to switch back to sampling with 60 Hz. This was not practically possible since the time period of this phase could be so short that there was not enough time to make the switch. So, min-max-sampling was kept until the test was finished. The technique is not a perfect solution but the accuracy was under the circumstances satisfactory.

The analysis of the data has been performed with the computer programme MATLAB™ (the MathWorks Inc.).

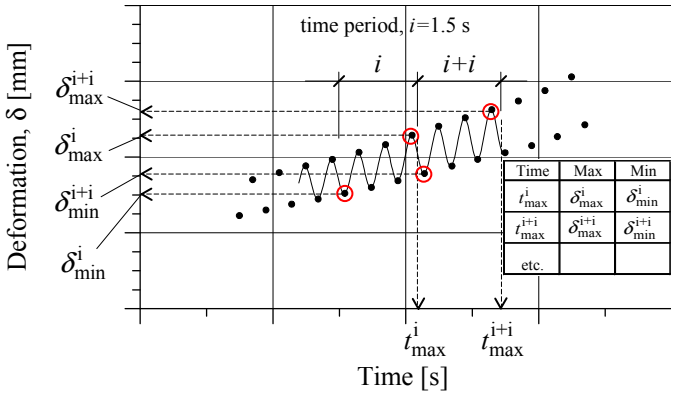

Fig. 6 - Description of the developed measuring technique where the maximum and minimum deformations for a time period of 1.5 seconds are stored together with the maximum time value during the same period.

3 RESULTS

The compressive concrete strength of the new concrete was tested on 150 mm cubes in October 2004 (6 months after casting). The mean concrete compressive strength was 72.2 MPa with a standard deviation of 1.9 MPa and a coefficient of variation of 3 %. The tensile splitting strength tested on similar cubes was 5.5 MPa with a standard deviation of 0.04 MPa and a coefficient of variation of 1 %. According to the Swedish concrete recommendations, BBK9418 (1994), the corresponding uniaxial tensile strength is set to 80% of the tensile splitting strength, i.e. 4.4 MPa.

The compressive and the splitting tensile concrete strengths of the old concrete are presented in Thun[23]. The mean concrete core compressive strength was 72.6 MPa, with a standard deviation of 4.2 MPa and a coefficient of variation of 6 %, and the tensile splitting concrete strength was 4.7 MPa, with a standard deviation of 0.6 MPa and a coefficient of variation of 14 %. The properties for the old concrete were tested in October 2000, approximately 32 years after the bridge was cast.

When the above-mentioned properties of the new and the old concrete are compared it can be seen that they are rather similar. What must be mentioned is that the newly cast concrete cubes have been stored in a water tank until the day before testing while the old test specimens have been stored in room temperature, in the same room as the test equipment, until the day for testing. This difference in storing conditions could according to Möller et al.[24] result in a 10-15 % lower strength for the new specimens stored in water.

3.1 Uniaxial tensile tests

In Fig. 7 it is shown how the fracture energy, G_F, and the crack width, w, have been defined and determined.

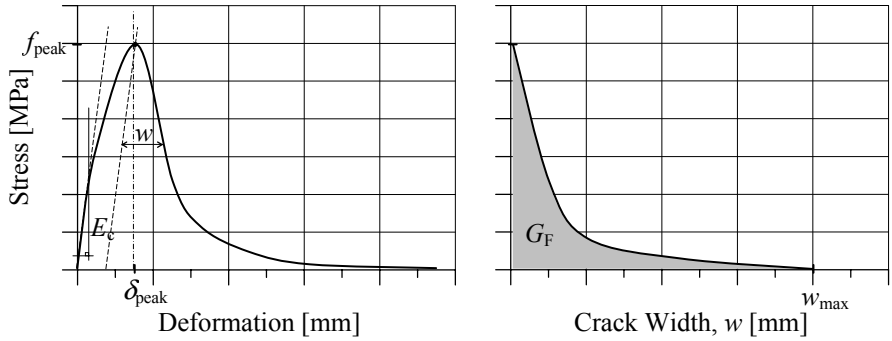

Fig. 7 - Determination of fracture energy, G_F. To the left: A schematic stress-deformation curve showing the definitions used for the peak stress, f_{peak}, the elastic modulus E_c, the deformation at peak load, δ_{peak}, and the crack width, w. To the right: The stress-crack-width-curve defining the fracture energy G_F and the maximum crack width obtained in a test, w_{max}.

In Fig. 8a, the mean uniaxial tensile strength curve is shown for new concrete. In the figure the lower and upper bounds of all tensile tests are also presented (i.e. these lines are a combination of all tests). In Fig. 8b the mean stress-crack-width curve is presented for the new concrete.

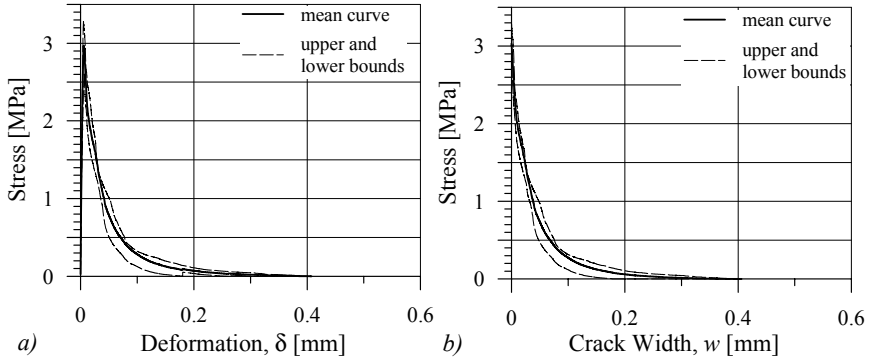

Fig. 8 - Mean uniaxial tensile tests on new concrete with lower and upper bounds. a) stress-deformation curves and b) stress-crack width curves. Mean curve based on 8 static tests.

In Fig. 9, the same information is given for the old concrete.

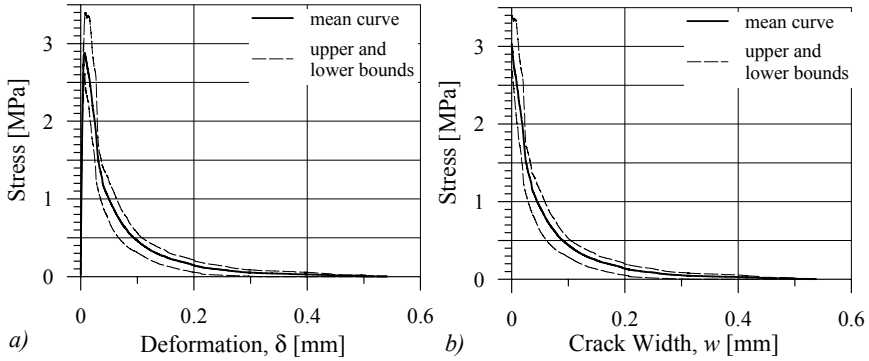

Fig. 9 - Mean uniaxial tensile tests on old concrete. a) stress-deformation curves and b) stress-crack width curves. Mean curve based on 3 static tests.

In Table 1 a summary is presented of the results. The mean uniaxial tensile strength for the eight tests performed on new concrete was 3.0 MPa (13.5 kN) with a standard deviation of 0.2

MPa (coefficient of variation 6.5%). For the old concrete the mean value of the uniaxial tensile strength was 3.0 MPa with a standard deviation of 0.3 MPa (coefficient of variation 36%).

Table 1 - Summary of properties from performed uniaxial tensile tests on new and old concrete. m is the mean value, s is the standard deviation and CoV is the coefficient of variation (CoV=s/m). Definitions see Fig. 7 and results in Appendix A in Thun[17].

New concrete							
Test no.	d [a)] [mm]	F_{peak} [kN]	f_{peak} [MPa]	δ_{peak} [mm]	w_{max} [mm]	E_c [GPa]	G_F [N/m]
HTS3	75	12.24	2.77	0.0084	0.26	27.7	104.2
HTS5	74.8	14.47	3.29	0.0053	0.26	34.5	124.7
HTS6	75.1	14.37	3.24	0.0058	0.18	35	85.5
HTS8	75.1	12.95	2.92	0.0055	0.34	32.4	117.9
HTS9	75	12.83	2.9	0.0056	0.15	34	116.5
HTS10	75	12.97	2.94	0.0055	0.37	33.7	138.4
HTS11	74.7	13.89	3.17	0.0052	0.34	34.8	128.5
m =	75.0	13.4	3.0	0.006	0.3	33.2	116.5
s =	0.2	0.9	0.2	0.001	0.1	2.6	17.3
V =	0.002	0.06	0.07	0.19	0.31	0.08	0.15
Old concrete							
LTS1	75.5	12.04	2.68	0.0081	0.32	33.1	104.5
LTS2	76	13.72	3.02	0.0049	0.5	33.9	171.8
LTS3	74.3	14.75	3.4	0.0079	0.54	31	203.4
m =	75.3	13.5	3.0	0.0070	0.5	32.7	159.9
s =	0.9	1.4	0.4	0.0018	0.1	1.5	50.5
V =	0.012	0.101	0.119	0.257	0.259	0.046	0.316

[a)] The diameter, d, of the core at the notch is a mean value of four measurements in different directions of the cross-section.

3.2 Fatigue tests

In Table 2 the results from the fatigue tests performed on new concrete are presented. Note that f_{max} is 90 % of f_{peak}, which is the mean uniaxial tensile strength of 8 tests, see Fig. 3 and Fig. 7. Test no. 20 was stopped at 5 million load cycles and a uniaxial tensile test was performed which first resulted in a failure at the adhesive layer. The specimen was then cut again to remove the old adhesive and a new uniaxial tensile test was preformed. This time the failure happened in the milled notch with a tensile strength of 2.37 MPa as a result.

Table 2 - Results from fatigue tests on new concrete. Plus-sign indicates high level (60%) and minus-sign indicates low level (40%), according to factorial design. A, B and MLL (Mean Load Level) see definitions in Fig. 3 and results in Appendix A in Thun[17].

Test	**Load levels % of f_{peak}**				**Factorial design**		**Actual loads [kN]**			**Run order**	**No. load Cycles**
no.	A	B	Amp.	MLL	Amp.	MLL	A	B	Amp.		N_{max}
2	30	90	60	60	+	+	4.0	12.1	8.1	8	96
12	40	80	40	60	-	+	5.4	10.7	5.3	3	227 283
16	20	60	40	40	-	-	2.7	8.0	5.3	6	623 683
17	20	60	40	40	-	-	2.7	8.0	5.3	1	1 350 166
20	20	60	40	40	-	-	2.7	8.0	5.3	7	5 000 000 [a)]
25	10	70	60	40	+	-	1.3	9.4	8.1	5	132 645
28	30	90	60	60	+	+	4.0	12.1	8.1	12	14
30	40	80	40	60	-	+	5.4	10.7	5.3	2	20
32	40	80	40	60	-	+	5.4	10.7	5.3	9	1659
33	10	70	60	40	+	-	1.3	9.4	8.1	11	2661
34	10	70	60	40	+	-	1.3	9.4	8.1	10	121 518
35	30	90	60	60	+	+	4.0	12.1	8.1	4	60

[a)] The test was stopped at 5 million load cycles and a uniaxial test was performed.

In Table 3 the results from the fatigue tests performed on old concrete are presented. Note that f_{max} is 90 % of f_{peak}, which is the mean uniaxial tensile strength of 3 tests, see Fig. 3 and Fig. 7. Tests no. L5, L7, L13, L15 and L16 were stopped since no indications were obtained during the tests of an imminent fatigue failure. After they were stopped static uniaxial tensile tests were performed in load control. The results from these tests are presented in Table 4.

Table 3 - Results from the fatigue tests performed on old concrete. Plus-sign indicates high level (60%) and minus-sign indicates low level (40%), according to factorial design. A, B and MLL (Mean Load Level) see definitions in Fig. 3 and results in Appendix A in Thun[17].

Test	**Load levels % of f_{peak}**				**Factorial design**		**Actual loads [kN]**			**Run order**	**No. load cycles**
no.	A	B	Amp.	MLL	Amp.	Level	A	B	MLL		N_{max}
L4	30	90	60	60	+	+	4.1	12.2	8.1	1	82
L5	10	70	60	40	+	-	1.4	9.5	8.1	2	1 000 000 [a)]
L6	30	90	60	60	+	+	4.1	12.2	8.1	3	2074
L7	10	70	60	40	+	-	1.4	9.5	8.1	4	2 050 001 [a)]
L8	10	70	60	40	+	-	1.4	9.5	8.1	5	11711
L10	30	90	60	60	+	+	4.1	12.2	8.1	6	4
L11	30	90	60	60	+	+	4.1	12.2	8.1	7	7
L12	30	90	60	60	+	+	4.1	12.2	8.1	8	55 964
L13	40	80	40	60	-	+	5.4	10.8	5.4	9	1 522 201 [a)]
L14	40	80	40	60	-	+	5.4	10.8	5.4	10	26
L15	40	80	40	60	-	+	5.4	10.8	5.4	11	1 166 000 [a)]
L16	40	80	40	60	-	+	5.4	10.8	5.4	12	7 077 000 [a)]

[a)] The test was stopped and a uniaxial test was performed.

In Table 4 the results from the static uniaxial tensile tests performed after the fatigue tests with the "run-outs" are presented. If the load levels that were used in the fatigue tests are recalculated with the new obtained tensile strength it is shown that the used load levels as well as the load amplitude were lower than intended in these fatigue tests.

Table 4 - Results from static uniaxial tensile strength after fatigue test on old concrete and results in Appendix A in Thun[17].

Test no.	d [a)]	F_{peak}	f_{peak}	δ_{peak}	Load levels used in fatigue tests – % of F_{peak}				Amplitude – % of F_{peak}	
					Intended		Actual		Intended	Actual
	[mm]	[kN]	[MPa]	[mm]	A	B	A	B		
LTS5	76.4	14.9	3.25	0.0084	10	70	9	64	60	55
LTS7	75.8	16.95	3.59	0.0091	10	70	8	56	60	48
LTS13	75.7	15.83	3.52	0.012	40	80	34	68	40	34
LTS15	75.5	18.24	4.07	0.0084	40	80	30	59	40	29
LTS16	75.6	15.68	3.49	0.009	40	80	34	69	40	35

[a)] *The diameter, d, of the core at the notch is a mean value of four measurements of the cross-section.*

3.2.1. Definitions used in fatigue curves

A number of parameters have been determined from the fatigue curves and they are visually shown in Fig. 10. n^{U}_{1-2} and δ^{U}_{1-2}, the number of load cycles and the deformation respectively, define the point on the upper fatigue curve where phase 1 ends and phase 2 starts. n^{L}_{1-2} and δ^{L}_{1-2} is the same point on the lower curve. n^{U}_{2-3} and δ^{U}_{2-3}, the number of load cycles and the deformation respectively, define the point on the upper fatigue curve where phase 2 ends and phase 3 starts. n^{L}_{2-3} and δ^{L}_{2-3} is the same point on the lower curve. δ^{U}_{α} and δ^{L}_{α} are the deformation rate for the upper and lower fatigue curve respectively during phase 2 [mm/cycle]. δ^{A}_{1-2} is the deformation amplitude at the point where phase 1 changes to phase 2 and δ^{A}_{2-3} is the deformation amplitude at the point where phase 2 changes to phase 3. δ^{A}_{max} is the maximum amplitude measured during the fatigue test, often at the very end of the test. δ_{ul} is defined as the highest deformation measured during the fatigue test for a complete cycle.

The inflection points, e.g. the point (n^{U}_{1-2}, δ^{U}_{1-2}), have been determined in the following way. With the help of the Matlab™, a linear equation has been fitted to the test data for phase 2 which gives the slope δ^{U}_{α}. This linear equation has in turn been compared to the measurement data and where the difference between the linear equation and the measurement data, is larger than the deformation rate, δ^{U}_{α}, multiplied with a load cycle increment, Δn (individual for each test), an inflection point has been found. For the tests which have lasted for a short time a load cycle increment, Δn, of 0.01 has been used. This low increment has not been possible to use for the longer fatigue tests where min-max sampling has been used, due to the fact that the data scatter more. This definition and method of determining the inflection points are not exact, however, the method gives an approximation that is satisfactory, since the increase in deformation is small for the tests that last for more than approximately 10000 cycles.

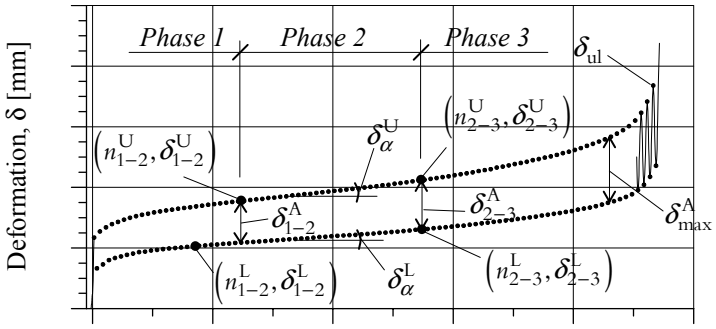

Fig. 10 – Graph showing, in principal, the definition of parameters from fatigue tests.

In Table 5 different parameters that are of interest from the fatigue curves are summarised for the new concrete. For tests no. 16, 17 and 20 none of the parameters defined in Fig. 10 (except N_{max}) has been possible to determine due to the fact that these tests have been very affected by a temperature variation during the tests. The definitions of the parameters are given in Fig. 10.

Table 5 - Selected parameters from fatigue tests on new concrete. Definitions are given in Fig. 10 and results in Appendix A in Thun[17].

Test no.	**Level**	**Amp.**	n^{U}_{1-2} [cycles]	δ^{U}_{1-2} [mm]	n^{U}_{2-3} [cycles]	δ^{U}_{2-3} [mm]	δ^{U}_{α} [$\cdot 10^{-3}$, mm/cycle]	δ_{ul} [mm]	δ^{A}_{max} [mm]	N_{max} [cycles]
30	+	-	7.33	0.0099	14.2	0.0137	0.5512	0.0204	0.0069	20
32	+	-	181.8	0.0055	428.8	0.0060	0.0017	0.0201	0.0063	1 659
12 [a)]	+	-	4175	0.0034	176090	0.0033	[b)]	0.0099	0.0038	227 283
35	+	+	13.38	0.0066	41.2	0.0092	0.0969	0.0156	0.0071	60
2	+	+	17.23	0.0084	49.8	0.0103	0.0560	0.0305	0.0101	96
28	+	+	1.67	0.0075	8	0.0105	0.4740	0.0162	0.0073	14
33	-	+	346.5	0.0073	1531	0.0090	0.0014	0.0215	0.0103	2 661
34 [a)]	-	+	29030	0.0040	85460	0.0044	$7.55 \cdot 10^{-6}$	0.0142	0.0096	121 518
25 [a)]	-	+	99060	0.0081	114330	0.0089	$5.47 \cdot 10^{-5}$	0.0209	0.0107	132 645
Test no.	**Level**	**Amp.**	n^{L}_{1-2} [cycles]	δ^{L}_{1-2} [mm]	n^{L}_{2-3} [cycles]	δ^{L}_{2-3} [mm]	δ^{L}_{α} [$\cdot 10^{-3}$, mm/cycle]	δ^{A}_{1-2} [mm]	δ^{A}_{2-3} [mm]	N_{max} [cycles]
30	+	-	7.63	0.0076	14.71	0.0107	0.4467	0.0019	0.0032	20
32	+	-	167.7	0.0036	461.8	0.0041	0.0016	0.0019	0.0019	1 659
12 [a)]	+	-	2490	0.0020	178620	0.0017	[b)]	0.0014	0.0016	227 283
35	+	+	13.71	0.0039	44.63	0.0059	0.0659	0.0027	0.0036	60
2	+	+	19.8	0.0053	49.14	0.0063	0.0348	0.0033	0.0039	96
28	+	+	4.97	0.0056	7.67	0.0065	3.2214	0.0032	0.0039	14
33	-	+	313.2	0.0037	1625.8	0.0050	0.0010	0.0035	0.0040	2 661
34 [a)]	-	+	85560	0.0015	3020	0.0015	$1.30 \cdot 10^{-6}$	0.0026	0.0030	121 518
25 [a)]	-	+	105970	0.0044	114540	0.0046	$2.58 \cdot 10^{-5}$	0.0041	0.0044	132 645

[a)] Min-max-sampling has been used to measure the deformation. [b)] The deformation rate has been almost zero. This test has partly been affected by the temperature/ moisture variation.

Table 6 - Selected parameters from fatigue tests on old concrete. Definitions are given in Fig. 10 and results in Appendix A in Thun[17].

Test no.	Level	Amp.	n_{1-2}^{U} [cycles]	δ_{1-2}^{U} [mm]	n_{2-3}^{U} [cycles]	δ_{2-3}^{U} [mm]	δ_{α}^{U} [$\cdot 10^{-3}$, mm/cycle]	δ_{ul} [mm]	δ_{max}^{A} [mm]	N_{max} [cycles]
L11	+	+	3.12	0.0086	5.1	0.0102	0.7707	0.0123	0.0062	7
L14	+	-	7.17	0.0061	16.28	0.0071	0.1025	0.0104	0.0031	26
L4	+	+	22.73	0.0092	62.64	0.0135	0.1061	0.0213	0.0096	82
L6 part 1	+	+	197.5	0.0050	515.5	0.0054	0.0011	0.0129	0.0052	2 074
L6 part 2	+	+	947	0.0064	1446	0.0072	0.0015	0.0129	0.0052	2 074
L8 part 1 [a)]	-	-	2358	0.0063	4896	0.0070	0.0003	0.0180	0.0093	11 711
L8 part 2 [a)]	-	-	6331	0.0074	8068	0.0077	$0.18 \cdot 10^{-4}$	0.0180	0.0093	11 711
L12 [a)]	+	+	12254	0.0072	41810	0.0086	$0.46 \cdot 10^{-5}$	0.0174	0.0075	55 964
L10	+	+	-	-	-	-	-	-	-	4

Test no.	Level	Amp.	n_{1-2}^{L} [cycles]	δ_{1-2}^{L} [mm]	n_{2-3}^{L} [cycles]	δ_{2-3}^{L} [mm]	δ_{α}^{L} [$\cdot 10^{-3}$, mm/cycle]	δ_{1-2}^{A} [mm]	δ_{2-3}^{A} [mm]	N_{max} [cycles]
L11	+	+	3.23	0.0051	5.27	0.0063	0.5581	0.0036	0.0040	7
L14	+	-	11.1	0.0046	14.99	0.0050	0.0780	0.0018	0.0020	26
L4	+	+	22.57	0.0056	66.79	0.0087	0.0683	0.0036	0.0052	82
L6 part 1	+	+	284.5	0.0026	514.5	0.0028	0.0008	0.0025	0.0026	2 074
L6 part 2	+	+	913.5	0.0035	1446.5	0.0041	0.0011	0.0029	0.0031	2 074
L8 part 1 [a)]	-	-	2372	0.0029	4958	0.0034	0.0002	0.0034	0.0042	11 711
L8 part 2 [a)]	-	-	6768	0.0037	7956	0.0038	$0.93 \cdot 10^{-4}$	0.0038	0.0039	11 711
L12 [a)]	+	+	10252	0.0041	43512	0.0052	$0.33 \cdot 10^{-4}$	0.0030	0.0035	55 964
L10	+	+	-	-	-	-	-	-	-	4

[a)] *Min-max-sampling has been used to measure the deformation.*

4 ANALYSIS

4.1 Uniaxial tensile tests

The mean tensile strength for the newly cast concrete is as mentioned earlier 3.0 MPa with a somewhat low standard deviation of 0.2 MPa. Therefore it is perhaps not surprising that the tests show a similar behaviour and stiffness up to the peak load - compare curves in Fig. 8 and values in Table 1. It is especially after the peak load on the descending branch of the stress-deformation curve that the different tests start to deviate from each other. This is reflected on the maximum crack width, w_{max}, and the fracture energy, G_F. The mean fracture energy, G_F, is 116.5 N/m with a standard deviation 17.3 N/m and a coefficient of variation of 15 %. In this case there is especially one test that deviates from the others, i.e. test no. HTS6.

When the uniaxial tensile tests for the old concrete are compared there are higher dispersions. Unfortunately it was only possible to perform three uniaxial tensile tests before the fatigue tests due to few test specimens. The mean tensile strength for the old concrete was the same as for the newly cast concrete i.e. 3.0 MPa with a standard deviation of 0.4 MPa (for the newly cast concrete the standard deviation is 0.2 MPa). The tests with the old concrete show a similar pattern as the newly cast concrete i.e. the curves start to deviate on the descending branch of the

stress-deformation curve. The most significant difference is the dispersion for the fracture energy, G_F. The mean fracture energy is 159.9 N/m but the standard deviation is as high as 50.5 N/m and the coefficient of variation is 31.6 %, see Table 1. If the curves in Fig. 9 are studied it is possible to see that for one of the tests, LTS3, the stress does not drop immediately when the peak stress is reached. Instead the specimen continues to resist for a while at this high level which results in a very high fracture energy, G_F, (203.4 N/m). The reason for this ductile behaviour is probably due to the fact that one larger aggregate is situated in the milled notch and that the cracks have to go around this aggregate.

If the static uniaxial tensile curves in Fig. 8 and Fig. 9 are studied – especially the lower and upper bounds - it is very evident that each specimen is what could be called "an individual", therefore it is important to show these upper and lower bounds since particularly the descending branch deviates.

As some of the fatigue tests were ended due to no obvious signs of an imminent fatigue failure, uniaxial tensile tests were performed on these specimens, see results in Table 4. A very surprising thing is that all but one test show a higher tensile strength after a fatigue test that lasted between 1 million and 7 million load cycles than the mean value of the static uniaxial tensile tests before the fatigue tests. What does this peculiarity depend on? Is it due to the fact that too few static tensile tests have been performed with old concrete and the ones that were performed do not represent the specimens which were participating in the fatigue tests? Another explanation could be that the static tests after the fatigue test was performed in load control, not in displacement control, but since these tests were done with a slower pace (approximately $3.5 \cdot 10^{-5}$ mm/s compared to $10\text{-}20 \cdot 10^{-5}$ mm/s) it would give lower values of the tensile strength.

4.2 Factorial design

From the result it cannot be seen which one of the two varied factors, i.e. the load level and the amplitude, that has the highest influence on the number of load cycles to failure, see Appendix A in Thun[17].

Why this result then? As mentioned earlier the analysis assumes that the levels are fixed which they are not entirely. The reason for this is the variation in the static uniaxial tensile strength, which is the basis for the load levels. For example, when it is assumed that the load level is 60% of F_{peak} it could as well be 50 % or 70 %. Another factor that could influence the result, even though the highest efforts have been made to reduce it, is the variation in temperature for the fatigue tests that lasted for a longer time (a few days or more). Since the specimens of newly cast concrete were not sealed during the fatigue tests, the moisture content has been changed which induces shrinkage. According to Möller et al. (1994) the tensile strength drops when the drying process starts and with time the moisture gradient is equalised and after 1 or 2 months the tensile strength has reached its full capacity again. Another phenomenon that is connected to the nature of a fatigue test is the time which introduces creep effects.

A reason for the somewhat unclear result is that the two chosen amplitudes and load levels are too close to each other. Perhaps a more distinct result would have been obtained if there had been a higher difference between the chosen levels.

Even though the method did not give an answer to the asked question, it is believed that a method like factorial design is a very useful tool when designing experiments, since a good structure of the tests is obtained.

Factorial design was not used in the fatigue tests of old concrete. The reason for this is that there was not enough time to perform the tests in this way. The risk was too high that the first tests were tests that could last for a long time which would end in the fact that only a few tests were going to be conducted. Therefore the tests that were estimated to last few load cycles were performed first and the ones that could last for very many load cycles were run last. Now it turned out that all the tests could be conducted. This way of designing an experiment could according to Montgomery be classified as a best-guess design.

4.3 Fatigue tests

The fatigue tests have been surrounded by some difficulties. The main problem was that the test equipment was moved from the location where the pilot tests had been performed and a stable electric current and temperature were difficult to obtain in the new location. To solve the problem with the unstable electric current new COD-gauges were purchased with more suitable sensitivity which partly solved the problem. However, these new COD-gauges had a very high "spring force" that could affect the tests in the way that they could contribute to the fracture of the test specimens. The solution of the problem with the temperature turned out to be more complicated than believed. The best solution seemed to be to move the equipment to a room where the temperature was as constant as possible and to use a "COD-dummy" that would only measure the temperature change during the fatigue tests and afterwards compensate the measurements with this curve. Unfortunately it was found that these steps were not enough. The equipment was then moved to a room in the basement. When tests were performed they showed that the old COD-gauges did not give the same feedback signal as the new ones which resulted in the fact that these could not be used at all as dummies. New tests were performed where two new COD-gauges were compared but it was shown that they did not give a similar feed back signal unless the dummy was placed next to the specimen that was mounted in the test equipment. If the "COD-dummy" was placed like this it would not be possible to perform the tests at all. The best solution was to seal the ventilation as much as possible and to measure a "trend curve" before each fatigue test. This would result in a temperature curve that could be used to compensate the tests for the temperature deviation. This curve could of course only be used if the tests did not last too long and there were no dramatic changes in the temperature during this period of time. Unfortunately, it turned out that it was only possible to use this method for one of the tests that lasted for a longer period. Test no. L5 has been temperature compensated, see appendix Thun (2006), but tests no. L7, L13, L15 and L16 were not possible to compensate due to big difference between the measured temperature-trend-curve a few hours before the tests started and the conditions during the actual tests. The other tests have not been compensated.

4.3.1. General findings

From the results in Table 5 several interesting findings are worth comments. If the slopes, i.e. δ_{α}^{U} and δ_{α}^{L}, for the upper and lower curves in the fatigue test are compared the upper curve is steeper (except for one test i.e. no. 32). In other words the two curves are separating which increases the deformation amplitude (compare δ_{1-2}^{A} and δ_{2-3}^{A}). This deformation amplitude reaches its maximum value at the end of each test (see δ_{max}^{A}). This should at first glance be more pronounced for the tests where the amplitude as well as the load level have been high since the specimen is more strained in these cases but the phenomenon could be found for all variations in load level and amplitude.

Another thing that could be found in Table 5 is that there is a big difference between the deformation rate (δ_{α}^{U}) for the tests that lasted below about 3000 load cycles and the ones that

lasted for more than 120000 load cycles. With this in mind one can suspect a sort of fatigue limit in the sense that below a certain load level there is a need for many load cycles before failure occurs. Where this limit is, is not possible to say from the results in this investigation only that there is a very low deformation rate for a mean load level and an amplitude less than 40% of f_{peak}.

The values for the ultimate deformation, δ_{ul}, and the maximum deformation amplitude, δ_{max}^{A}, are uncertain in the tests where min-max-sampling has been used to measure the deformation. This is due to the fact that, see Fig. 6, a sinus-shaped curve is not possible to obtain according to the definitions that could be found in Fig. 10. Therefore a range has been presented where the ultimate deformation and the maximum deformation amplitude is.

In Table 5 a very well-known problem when performing a tensile fatigue test is shown, i.e. the scatter in the result. If the number of load cycles to failure, N_{max}, for tests no. 30, 32 and 12 is compared, N_{max} varies between 20 and 227283 load cycles, even though the same amplitude and load level have been used.

4.3.2. Deformation criterion

The main objective with the performed fatigue tests was to verify or reject a deformation criterion, originally proposed by Balázs[1] for bond slip, for plain concrete exposed to cyclic tensile load.

The possible relationship between the deformations in a fatigue test and the static test, has been a subject for investigations by some researchers over the years. It has been stated by some researchers that the fatigue failure occurs when the fatigue curve meets the "imagined" static curve on the descending branch in the static stress-deformation curve (point A in Fig. 11) and that this corresponds to the failure deformation in a fatigue test (denoted δ_{ul} in these tests). The deformation criterion for fatigue failure proposed by Balázs[1] is that the deformation at peak load, point B in Fig. 11, during a static test corresponds to the deformation at the changeover between phases two and three during a fatigue test. There have also been efforts to identify the corresponding point on the fatigue curve to Point C on the static curve, see Fig. 11.

In Fig. 11 the fatigue curve and the normalized stress-deformation curve are presented for test no. L8. The load has been varied between the load levels 70 % and 10 % of F_{peak} (from the static tests). In Fig. 11 (to the right) the cyclic load curve in the normalized stress-deformation curve is only an illustration, not the real curve. No other correlation is found besides the correlation between the static peak deformation and the deformation where phase 3 starts in the fatigue curve (point B) – as stated by the criterion by Balázs[1]. If the fatigue curve instead is compared to the lower bound from the static test, the criterion is still valid but another suggested idea is also to some extent confirmed i.e. the ultimate failure deformation in a fatigue test corresponds to the deformation in the static curve, where the fatigue curve meets the static stress-deformation curve on the descending branch (point A). Unfortunately the measurements for test no. L8 have only been performed with min-max-sampling. This results in the fact that the definition for the ultimate deformation, δ_{ul}, the one used in Fig. 10, could not be used since the resolution is too bad. Instead a deformation range is used where the ultimate deformation, δ_{ul}, is situated. However, even if this deformation range is used the correlation between the point A in the static curve and the ultimate deformation in the fatigue curve, is surprisingly good. A correlation for point C in the static curve and a point in the fatigue curve is not as evident.

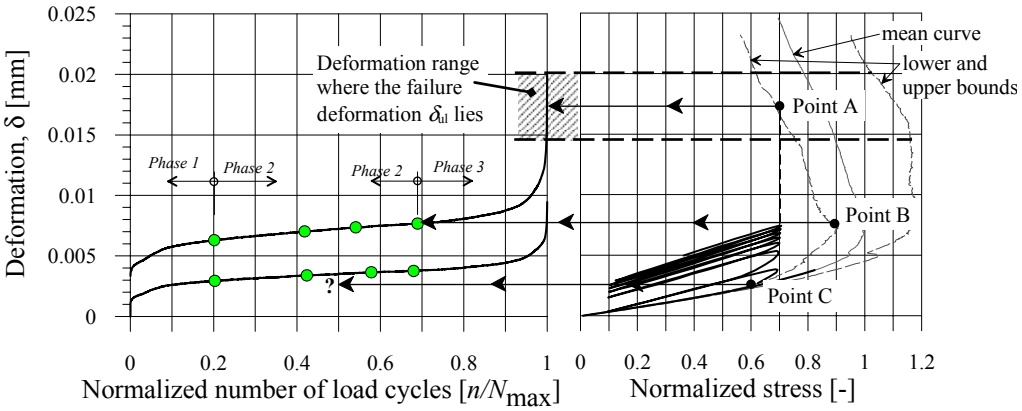

Fig. 11 - Result from the cyclic tensile fatigue test of specimen L8. The mean deformation development for the four COD-gauges is shown to the left. This curve is compared with the normalized mean static deformation-stress curve (to the right) obtained in the uniaxial tensile tests.

This phenomenon could also be found for test no. L6. In Fig. 12 the fatigue curve and the normalized stress-deformation curve are presented. The load has been varied between the load levels 90 % and 30 % of F_{peak} (from the static tests). In Fig. 12 (to the right) the cyclic load curve in the normalized stress-deformation curve is only an illustration, not the real curve. The above-mentioned correlation for point A and B is valid for the mean curve in this case – not the lower bound as for test no. L8. For the other fatigue tests the phenomenon is not as evident. This is probably due to the scatter in the uniaxial static tests.

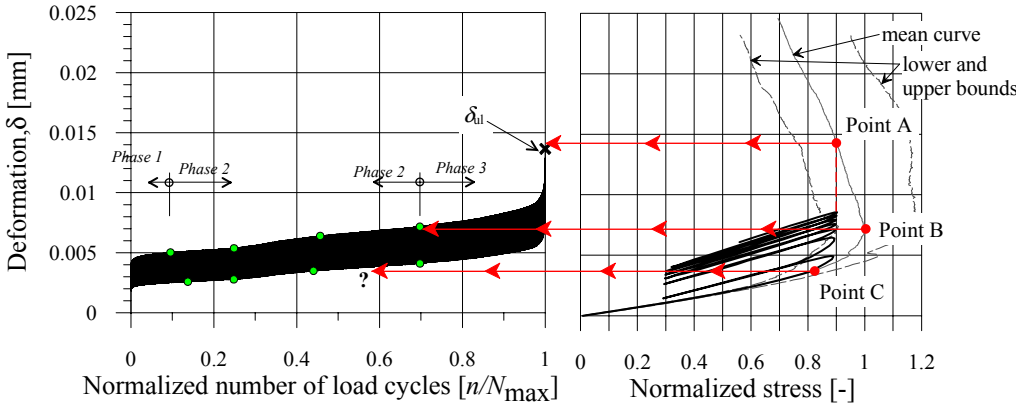

Fig. 12 - Result from the cyclic tensile fatigue test of specimen L6. The mean deformation development for the four COD-gauges is shown to the left. This curve is compared with the normalized mean static deformation-stress curve (to the right) obtained in the uniaxial tensile tests.

In Fig. 13 the deformations when phase 2 ends and phase 3 starts, δ_{2-3}^{U} i.e. where the failure phase starts, are presented for the fatigue test performed on new and old concrete. If the variation in the deformation at the peak load between the static tests is considered, it could be seen for the tests performed on new concrete that the criterion is fairly valid. For the tests with old concrete the correlation is even better than for the newly cast concrete if it is compared to the mean curve. A problem is that a specific behaviour, the fatigue test, is compared to a mean behaviour, the static test. It seems that the correlation depends on how well the mean static curve represents the specimen that is used in the fatigue test.

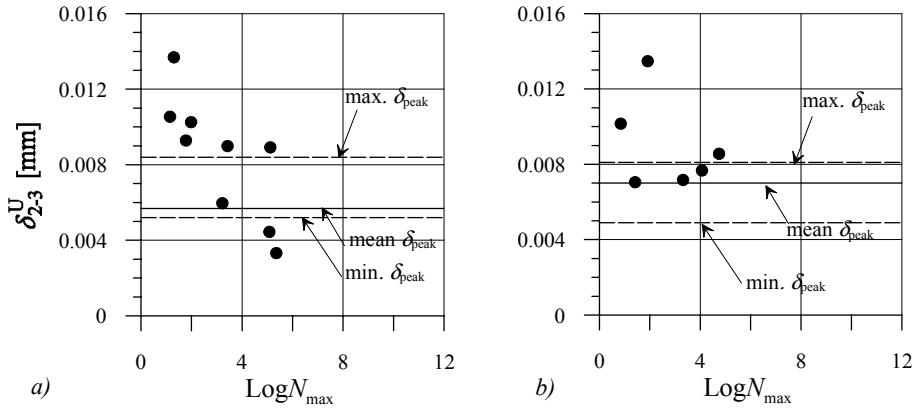

Fig. 13 - Deformation when phase 2 ends, i.e. $\delta^U_{2\text{-}3}$, on the y-axis and the logarithm of the number of load cycles to failure, N_{max}, on the x-axis. The horizontal lines represent the mean, maximum and the minimum deformation at peak load during static tensile tests, δ_{peak}. a) New concrete and b) Old concrete.

An interesting observation is that phase 2 is repeated as shown in Fig. 14 (test no. 32). This is also the case for another two of the tests. Since this second part of phase 2 in all the three cases, lasted a long part of the whole test, it has been decided that it is the second phase 2 that decides where phase 3 starts. One explanation for the intermediate part between the two phase 2:s could be difficulties for the crack to go around/through an aggregate that is situated in the milled notch. When it quite suddenly passes this difficulty it becomes first unstable and then after a while a stable crack propagation continues which leads to a new phase 2. Another explanation can be that this is something that is always present in a tensile fatigue test, but due to the high resolution of the measurements in these tests, it is easier to detect.

Fig. 14 also shows a typical pattern where the deformation, when the failure phase begins, does not correspond to the deformation at peak load in the static test. Instead it corresponds to a deformation in the descending branch of the stress-deformation curve - beyond the peak deformation. This is something that is common for the tests that have lasted for less than approximately 3000 load cycles. However, this is true if only the mean static curve is considered – if it is compared to the lower bound from all the tests the correspondence is fairly good.

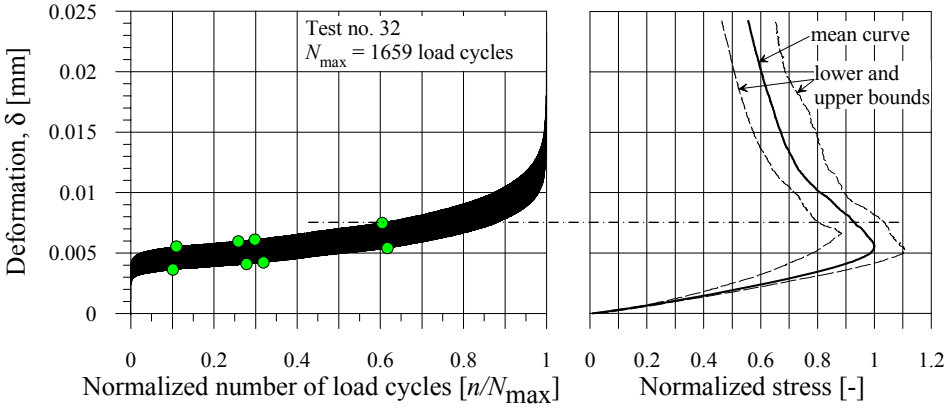

Fig. 14 - Result from the cyclic tensile fatigue test of specimen 32. The mean deformation development for the four COD-gauges is shown to the left. This curve is compared with the normalized mean static deformation-stress curve (to the right) obtained in the uniaxial tensile tests.

A typical result is shown in Fig. 15, for tests where the number of load cycles is higher than 3000. Here, the agreement between the fatigue curve and the static curve is quite satisfactory, especially for test no. 34.

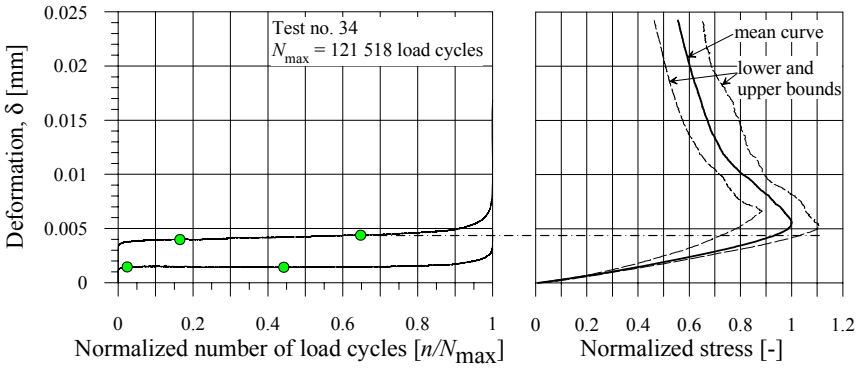

Fig. 15 - Result from the cyclic tensile fatigue test of specimen 34. The mean deformation development for the four COD-gauges is shown to the left. This curve is compared with the normalized mean static deformation-stress curve (to the right) obtained in the uniaxial tensile tests.

In Fig. 16 to Fig. 18 results from the fatigue tests of old concrete are presented for some typical cases. The same phenomenon as for the new concrete where phase 2 is repeated could also be found for the old concrete (2 of 12 tests).

The main difference between the tests with old and new concrete is that for the old concrete the deformation criterion is fulfilled for all cases where fatigue failure has been obtained, whereas for the new concrete this was the case only if the upper and lower bounds were considered. Another difference is that for the old concrete more fatigue tests were stopped before fatigue failure was obtained due to no imminent signs of failure. This is most probably connected to the fact that too few uniaxial tensile tests were performed before the fatigue tests. When uniaxial tensile tests later on were performed on the specimens that had not failed, it was shown that the load levels used in the fatigue tests were lower than intended.

In Fig. 16 the fatigue curve and the normalized stress-deformation curve are presented for test no. L8 (the amplitude and the load level was 60 % and 40 % of F_{peak}, respectively). The correlation between the two curves is very good.

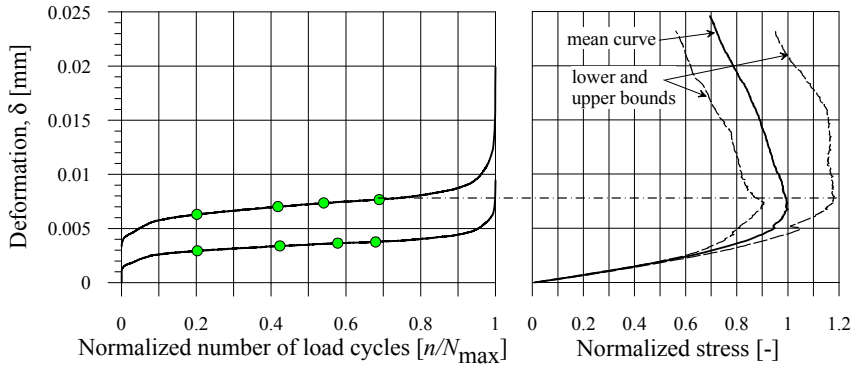

Fig. 16 - Result from the cyclic tensile fatigue test of specimen L8. The mean deformation development for the four COD-gauges is shown to the left. This curve is compared with the normalized mean static deformation-stress curve (to the right) obtained in the uniaxial tensile tests.

In Fig. 17 the fatigue curve and the normalized stress-deformation curve are presented for test no. L12 (the amplitude and the load level was 40 % and 60 % of F_{peak}, respectively). The correlation between the two curves is reasonably good, compare values in Table 3 and Table 6.

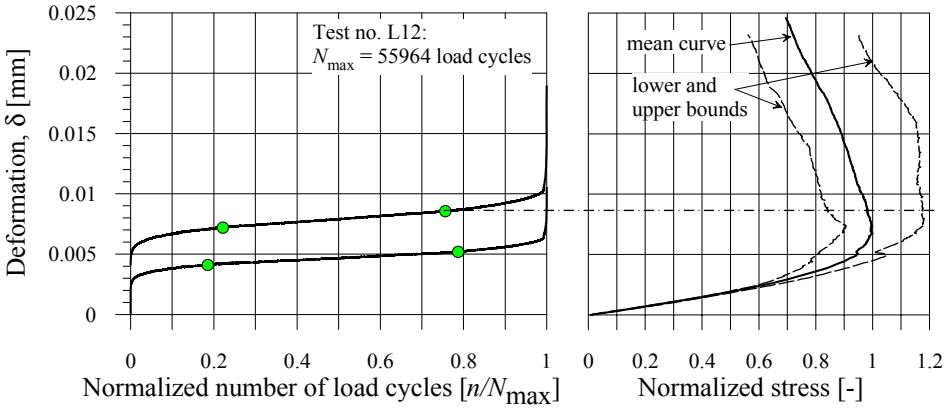

Fig. 17 - Result from the cyclic tensile fatigue test of specimen L12. The mean deformation development for the four COD-gauges is shown to the left. This curve is compared with the normalized mean static deformation-stress curve (to the right) obtained in the uniaxial tensile tests.

In Fig. 18 the fatigue curve and the normalized stress-deformation curve are presented for test no. L4 (the amplitude and the load level were both 60 % of F_{peak}). The correlation between the two curves is not as good as for the other tests presented above. However, if the fatigue curve is compared with the upper bound from the static test the correlation is acceptable. This shows how important it is to have in mind the dispersion of the uniaxial static tensile curve.

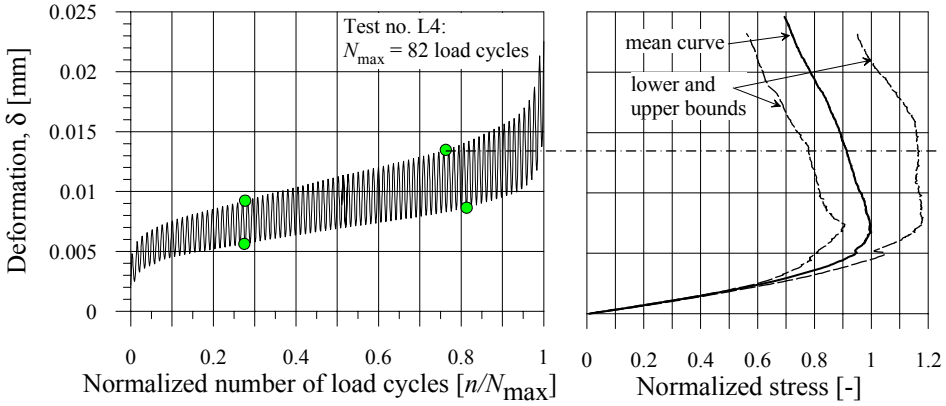

Fig. 18 - Result from the cyclic tensile fatigue test of specimen L4. The mean deformation development for the four COD-gauges is shown to the left. This curve is compared with the normalized mean static deformation-stress curve (to the right) obtained in the uniaxial tensile tests.

In Fig. 19 the load versus the deformation is shown for test no. 2 and test no. L10.

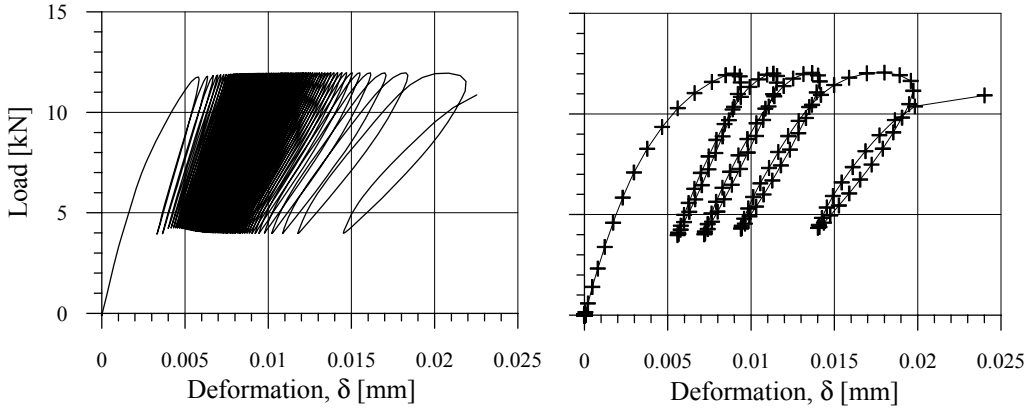

Fig. 19 – The load and deformation curve for test no. 2 to the left and test no. L10 to the right.

4.4 Equations for cyclic load in tension

The most common way to present results from fatigue tests is to use so-called Wöhler curves, Wöhler[25] (1858-70). Over the years several Wöhler curves have been proposed by researchers regarding cyclic loading in compression, but not so many that regard cyclic loading in tension. In Fig. 20 the results from the tests performed on new concrete are presented and a Wöhler curve has been determined, using linear regression analysis. The following equation has been derived:

$$S_{\max} = \frac{f_{\max}}{f_{\text{peak}}} = 0.945 - 0.0495 \cdot \log N = 0.945 - \frac{\log N}{20.2} \tag{1}$$

where $S_{\max}$ is equal to ($f_{\max}/f_{\text{peak}}$), $f_{\max}$ is the higher stress level used in the fatigue test and f_{peak} is the uniaxial static mean peak stress in the stress-deformation tests. All performed fatigue tests have been included, i.e. R ($\sigma_{\min}/\sigma_{\max}$) varies between 0.14 and 0.5, normally a Wöhler curve is plotted for R = constant.

However, Wöhler curves are normally defined to give $S_{\max} = 1$ for $\log N = 0$. If Eq. (1) is forced to pass the y-axis at 1.0 the equation becomes (the coefficient of correlation, r, then drops from 0.84 to 0.81):

$$S_{\max} = 1 - 0.0615 \log N = 1 - \frac{\log N}{16.3} \tag{2}$$

Eq.(1) can be compared to an equation for cyclic splitting tension load proposed by Tepfers[9] according to:

$$S_{\max} = \frac{f_{\text{r}}^{\max}}{f_{\text{r}}^{'}} = 1 - \frac{1}{C}(1-R)\log N = 1 - \frac{\log N}{16.7}(1-R) = 1 - 0.0597(1-R)\log N \tag{3}$$

Here N is the number of load cycles up to fatigue failure, $R = f_{\text{r}}^{\min} / f_{\text{r}}^{\max}$, $f_{\text{r}}^{\max}$ is the upper limit of fluctuating splitting stress in tension, $f_{\text{r}}^{\min}$ is the lower limit of fluctuating splitting stress in tension and $f_{\text{r}}^{'}$ is the static splitting strength in tension and C (=16.3) is the number of load cycles for $S = R = 0$.

If the Eqs. (2) and (3) are compared, Eq. (3) gives approximately the same curve as Eq. (2) for $R = 0$. Eq. (2) is also very similar to Wöhler curves for concrete in compression where C usually varies between 10 and 17. In Fig. 20 Eq. (1) and (2) are shown and in the figure test no. 20

is also plotted, a so-called run-out, a test which was stopped at 5 million load cycles, since there were no signs of an imminent fatigue failure.

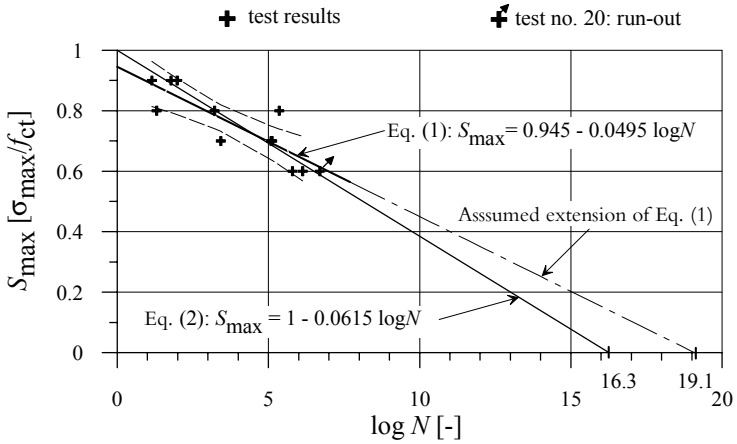

Fig. 20 - A Wöhler curve for cyclic load in tension based on the tests of new concrete. Regression analysis for Eq. (1) is based on y = kx + m. The correlation coefficient, r, is 0.84, the coefficient of determination, r-squared, is 0.71. The dashed lines are 95% confidence limits. Test no. 20 – a so-called run-out – is not included in the regression analysis.

No Wöhler curve has been possible to present for the tests on old concrete. Unfortunately there were only 7 tests of 12 that failed due to fatigue failure. The other 5 tests were stopped due to no signs of an imminent fatigue failure. These tests were afterwards exposed to a uniaxial static tensile test, see result in Table 4.

In Fig. 21 all the fatigue tests that have been performed are shown together with Eq. (3) for R = 0, 0.14, 0.33 and 0.5. As can be seen some of the fatigue tests ends after fewer cycles than predicted by Eq. (3). However, there are also several run-outs and the dispersion is considerable.

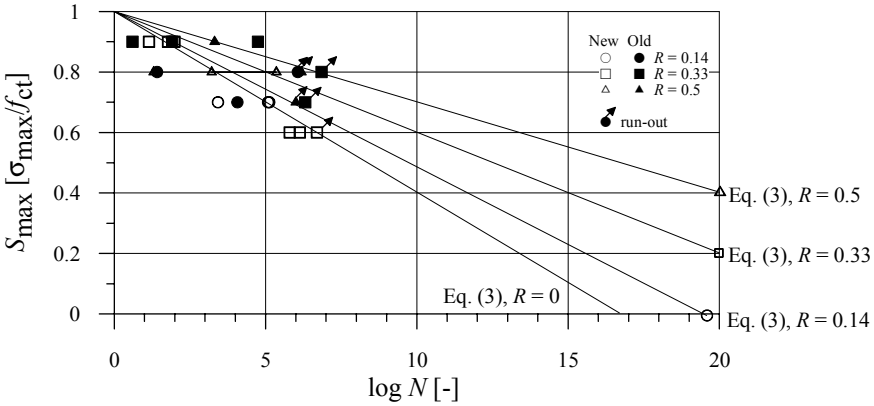

Fig. 21 – Figure showing results from all performed fatigue tests (new and old concrete). The result is compared with an equation proposed by Tepfers[9].

In Fig. 22 another interesting result is shown. In the figure the deformation rate for the upper fatigue curve for phase 2, δ_{α}^{U}, is shown on the y-axis and the logarithm of the number of load cycles where the failure phase begins, $log\, n_{2-3}^{U}$, in the fatigue tests is shown on the x-axis. The interesting thing is that there is a very distinct difference between the tests that have lasted for

more than approximately 300 load cycles (approximately log *n* equal to 2.5) compared to the others, if the deformation rate is compared. The test either breaks almost directly or it lasts for very many load cycles. A regression analysis has been performed and the equation becomes:

$$\delta_\alpha^{\mathrm{U}} = 0.0165 \cdot e^{\left(-2.83 \cdot \log n_{2\text{-}3}^{\mathrm{U}}\right)} \tag{4}$$

where $\delta_\alpha^{\mathrm{U}}$ is the deformation rate for the upper fatigue curve, [mm/load cycle].

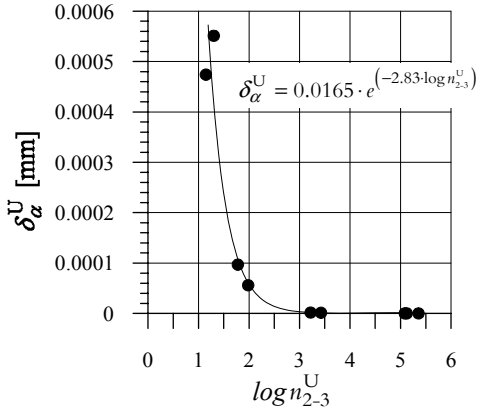

Fig. 22 - Deformation rate of phase 2, i.e. $\delta_\alpha^{\mathrm{U}}$, on the y-axis versus the logarithm of the number of load cycles where phase 3 begins, $\log n_{2\text{-}3}^{\mathrm{U}}$, on the x-axis. Regression analysis is based on y =exp(a+bx). The coefficient of determination, r-squared, is 0.96.

4.5 Assessment of remaining service life due to fatigue in tension

How can the remaining number of load cycles to failure be estimated for a concrete structure, e.g. for a railway bridge, exposed to cyclic loading in tension? From tests presented in this paper the following approach is possible:

The deformation criterion proposed by Balázs[1] is used together with the idea by Daerga & Pöntinen[2] to perform a static test on a bridge and to use the result to compare the peak deformation with measured deformations from fatigue tests for other similar bridges. (As an alternative, an analytical/numerical model can be used for a prediction of the static load deformation curve, instead of a static test).

How can the deformation criterion be applied on an existing structure? In Fig. 23 an illustration of a possible scenario is shown. It could start with the measurements of the deformation δ_1 and δ_2 over the period Δn to obtain the deformation rate δ_α, which then can be calculated according to:

$$\delta_\alpha = \frac{\left(\delta_2 - \delta_1\right)}{\Delta n} \tag{5}$$

The number of remaining load cycles to where the failure phase begins, i.e. the change over between phase 2 and 3, is equal to N or $N_{2\text{-}3}$ which can be calculated according to:

$$N = N_{2\text{-}3} = \frac{\left(\delta_{\mathrm{peak}} - \delta_1\right)}{\delta_\alpha} = \frac{\Delta n\left(\delta_{\mathrm{peak}} - \delta_1\right)}{\left(\delta_2 - \delta_1\right)} \tag{6}$$

where δ_{peak} is mean deformation at peak load from a static test of a similar structure or from an assessment of the actual structure. The mean deformation should be used in e.g. a Monte-Carlo

analysis so that the number of load cycles is obtained with a dispersion. This analysis will of course only give an estimate of the number of load cycles to where the failure phase begins. It is also assumed that, when the measurements are performed, it is performed during phase two in the fatigue investigation.

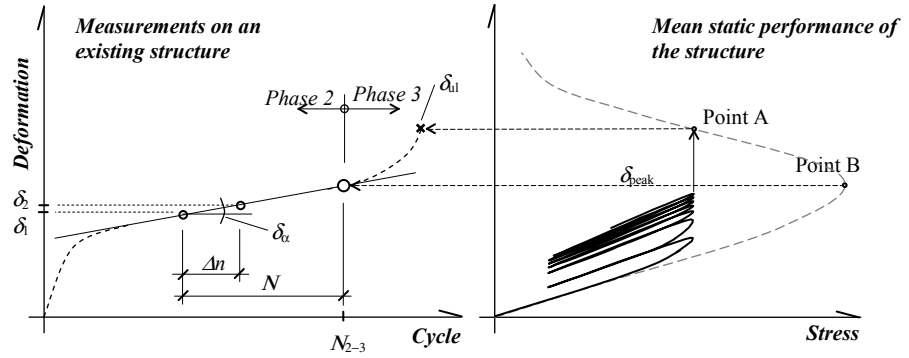

Fig. 23 - Proposal of how the deformation criterion could be used in an assessment of an existing structure loaded in tension.

In Fig. 24a, to the left, results from a fatigue test performed on a damaged *railway sleeper* is presented, see Thun et al.[26]. The damage was in form of more or less severe cracking which is believed to be caused by delayed ettringite formation. There is no shear reinforcement and failure usually occurs as a tensile, bending, shear or bond failure. In Fig. 24b and Fig. 24c, the load-deflection curves for similar railway sleepers are presented. The static tests in Fig. 24b were performed during the same period as the fatigue tests and the static tests in Fig. 24c were performed on similar sleepers but earlier. As can be seen, the correlation is good between the deflection at peak load in the static load-deflection curve and the deflection for the tests performed on similar sleepers but earlier (4 of the 6 static tests) and the correlation for the tests performed during the same period as the fatigue tests is very good for 2 of them. This indicates that the criterion could be used if the dispersion in the static tests is considered. In the fatigue tests the most common failure type was wire slip and in the static test it were wire slip, shear and bending failure.

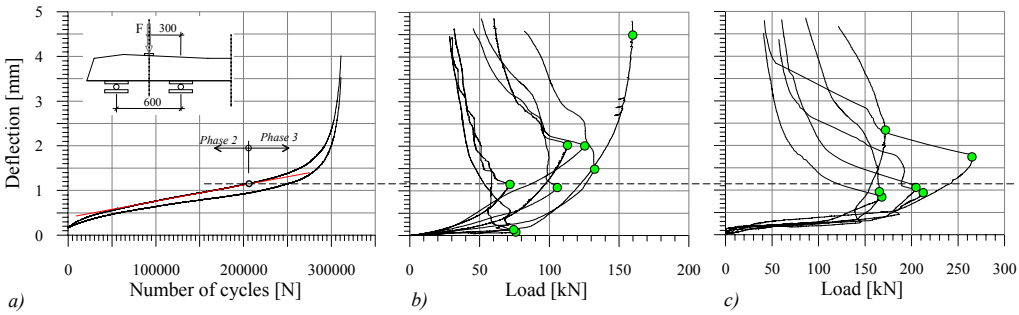

Fig. 24 – a) Result from fatigue test performed on a damaged railway sleeper to the left, b) Results from static tests performed on similar sleepers and during the same period and c) Results from six static tests performed on similar sleepers but earlier. The dots in the graphs to the right mark the deflection at peak load.

At Luleå University of Technology a *reinforced concrete trough bridge* was exposed to a fatigue test but the test was stopped after 6 million load cycles since there were no signs of an

imminent failure, see Paulsson et al.[27,28]. After the fatigue test the bridge was exposed to a static test but did not fail since not enough load could be applied on the bridge, see Fig. 25.

In Fig. 25b the deflection at the middle of the span from the fatigue test is shown on the y-axis and the number of load cycles on the x-axis. In Fig. 25a the static load-deflection curve is shown. The axle load was varied between 50 kN and 360 kN and the deflection was measured during the test. The upper curve in the graph in Fig. 25b,d corresponds to an axle load of 250 kN and the lower curve to an axle load of 0 kN. The measurements were performed in the way that the fatigue tests were stopped after a predetermined number of load cycles and the deflection was measured. Due to safety reasons the axle load 250 kN was used to measure the deflection instead of the 360 kN that was used as the upper load level in the fatigue test (cracks were also mapped at these stops on the bottom surface of the bridge deck). Since no failure curves are present, the following must be assumed. Firstly, the static load-deflection curve must be extended to failure and in Fig. 25a a possible extension of the load-deflection curve is shown with a dashed line resulting in a peak deflection of approximately 9.5 mm (note that this is not the total deformation, neither the dead load deformation nor the permanent creep deformation from the earlier fatigue test are included, which makes it a conservative value). Secondly it must be assumed that the bridge has reached phase 2, i.e. between the points that are marked in the right graph in Fig. 25. Since the deflection curve in Fig. 25a is for the load 250 kN these deflections must be recalculated to correspond to the load 360 kN, i.e. the load used in the fatigue test. A simplified way this can be done by assuming that the bridge is linear elastic which results in the following deflections:

$$\delta_1 = 4.409 \cdot \frac{360}{250} = 6.349 \text{ mm}$$

$$\delta_2 = 4.619 \cdot \frac{360}{250} = 6.651 \text{ mm}$$

The deformation rate can approximately be calculated as $\delta_\alpha = (6.65\text{-}6.35)/(5.558\text{-}3.829)\cdot 10^6 = 1.75\cdot 10^{-7}$ mm/cycle. If we also assume that the tension-shear deformations in the slab are proportional to the total deformations, we can with Eq. (5) calculate the number of load cycles N when the failure phase begins for tension-shear failure in the slab:

$$N = N_{2\text{-}3} = \frac{\left(\delta_{\text{peak}} - \delta_1\right)}{\delta_\alpha} = \frac{\left(9.5 - 6.349\right)}{1.7 \cdot 10^{-7}} \approx 18.5 \cdot 10^6 \text{ load cycles}$$

As no tensile-shear failure occurred in the bridge but rather yielding of the longitudinal reinforcement and a possible compression failure, these failure types have to be investigated too. With concrete compression following similar fatigue behaviour as in tension, the result above also holds for a compressive fatigue failure. For reinforcement fatigue, code calculations gave results of a capacity of less than 2 million cycles, Paulsson et al.[27].

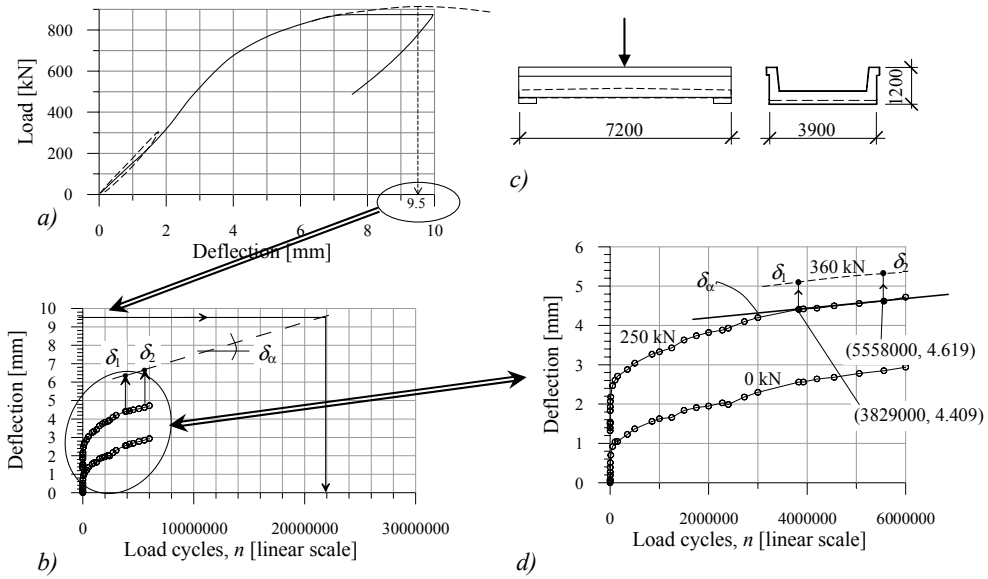

Fig. 25 – Estimation of the number of load cycles when the failure phase begins from deflections at midspan during fatigue loading of a railway trough bridge with a span of 7m. a) The continuous curve refers to static postloading while the dashed curve to the left refers to static preloading at the axle load 300kN. The axle load 875 kN was held constant for 70 minutes, from Paulsson et al.[27], b) The lower curve is measured at the axle load 0 kN and the one above at 250 kN and c) The critical section in concrete tensile fatigue is the connection between the slab and the beams as there is no shear reinforcement in the slab. d) A detail of b).

If the proposed method to use the deformation criterion by Balázs is studied, it is dependent on a correct deformation at peak load from the static test and that the bridge has reached phase 2 when the measurements of the deformation rate are performed. Both these conditions are questionable for the bridge. If the shape of the fatigue curve is studied it is not unlikely that the bridge is still in phase 1 and since the bridge did not fail in the static test there are uncertainties in the assumed static failure load and in the corresponding deformation. Nevertheless, if the bridge is still in phase 1 and 6 million load cycles have already been conducted so far, the bridge will probably manage a very high number of load cycles before failure – $18.5 \cdot 10^6$ load cycles are probably not such a bad estimation, see Fig. 25. The maximum load used in the fatigue test, i.e. 360 kN, is also not that high since the bridge manages at least 875 kN, approximately 40 % of the failure load. This will also contribute to the conclusion that the bridge would manage very many load cycles before fatigue failure occurs. The fact that the bridge is probably still in phase 1 is best visualised if the values on the axis are increased as in Fig. 25b. Not forgetting that the number of cycles to where the failure phase begins that is mentioned above is for fatigue failure in tension.

5 DISCUSSION AND CONCLUSIONS

The tests presented indicate that the deformation criterion proposed by Balázs[1] may also be applied to plain concrete exposed to cyclic tensile fatigue load if the dispersion of the static tests is taken into account. If the result in this investigation is added to the two other investigations where this criterion has been indicated, i.e. bond failure between reinforcing bars, Balázs[1], and concrete and small beams exposed to cyclic bending load, Daerga & Pöntinen[2], it seems reasonable to apply the failure criterion also to existing concrete structures.

How could this be done? The ultimate use of it would be when a bridge monitoring system calls the bridge manager and reports that it is 10 000 load cycles until fatigue failure! This science fiction scenario could be a reality if the deformation was continuously measured and if a modem was connected to the monitoring system and when some triggers were fulfilled the system calls a specific telephone number. A static failure test must also have been performed (or modelled) on a similar structure so that the deformation at peak load is known. With the help of the deformation rate and the peak deformation, and their dispersions, Eq. (6) would give an estimate of the number of load cycles when fatigue failure begins.

The next step could be to investigate why the deformation criterion seems to be valid for plain concrete exposed to cyclic load in tension.

The findings in this investigation could be summarised as follows:

- The fatigue tests indicate that the deformation criterion proposed by Balázs[1] is, if the dispersion in the static test is taken into account, plausible for plain concrete exposed to fatigue load in tension. The criterion has in this investigation to some extent been confirmed on reinforced railway sleepers.
- If the dispersion is considered the ultimate deformation in a fatigue test could correspond to the deformation in the static curve where the upper load level in the fatigue test "meets the static curve" on the descending branch.
- The method used to design the experiments performed in this investigation, i.e. factorial design, did not give any evident result which of the two factors varied in the fatigue test that had the highest influence on the number of load cycles to failure (the load amplitude and the mean load level). However, the method seems to be a suitable method to use in experiments since it can give additional bonus information. An example where the method has been used successfully is e.g. Utsi[29] where influencing factors on concrete mixtures' properties have been studied.
- Uniaxial tensile tests performed on specimens exposed to between 1 million and 7 million load cycles can give higher tensile strengths than tests performed on similar specimens before fatigue tests.
- Sources of error in the fatigue tests that have lasted for several days are the variation of temperature in the laboratory, shrinkage and the creep effect.

6 ACKNOWLEDGEMENTS

The study has been financially supported by Banverket (the Swedish National Rail Administration). Special thanks to all people that have been involved in the project, especially the staff at TESTLAB, the test laboratory at Luleå University of Technology, where all experimental work has been performed. Thanks also to MSc. Jörgen Andersson who performed the pilot tests during his work with his master thesis at LTU.

7 NOTATION AND ABBREVIATIONS

COD	Crack Opening Displacement
Level A	Lower limit of the load during the cyclic uniaxial fatigue test
Level B	Upper limit of the load during the cyclic uniaxial fatigue test
N_{max}	number of load cycles until failure
S_{min}	normalized lower stress level, $S_{min} = \sigma_{min} / f_{ct}$

S_{max} normalized higher stress level, $S_{max} = \sigma_{max} / f_{ct}$

R normalized stress amplitude, $R = \sigma_{min} / \sigma_{max}$

$\varepsilon(\sigma_u)$ strain at peak load during a static test, Balázs[1]

8 REFERENCES

1. Balázs G. L. (1991). Fatigue of bond. ACI Material Journal (Detroit), Vol 88, No 6. pp. 620-629.
2. Daerga, P-A. & Pöntinen, D. (1993). A fatigue failure criterion for concrete based on deformation. Nordic Concrete Research (Oslo), No 2/1993. pp. 6-20.
3. Andersson J. (2000). Utmattning av betong: en studie av deformationerna vid utmattande dragbelastning (Concrete fatigue: a study of deformation under tensile cyclic load. In Swedish.). Master's thesis 2000:293, Division of Structural Engineering, Luleå University of Technology, Luleå 1998.
4. Thun H. (2001). Evaluation of concrete structures. Strength development and fatigue capacity. Licentiate thesis 2001:25. Division of Structural Engineering, Luleå University of Technology, Luleå, Sweden, June 2001. pp. 164. ISBN 91-89580-08-2
5. Nilsson M., Ohlsson U. and Elfgren L. (1999). Partial Coefficients for Concrete Strength for Railway Bridges along the railway line "Malmbanan". (Partialkoefficienter för hållfasthet i betongbroar längs Malmbanan). Division of Structural Engineering, Luleå University of Technology. Technical Report 1999:03. pp. 67. In Swedish.
6. Hordijk D. A. (1989). Deformation-controlled uniaxial tensile tests on concrete. Report 25.5-89-15/VFA. Delft University of Technology. pp. 118.
7. Rüsch H. and Hilsdorf H. (1963). Verformungseigenschaften von Beton unter Zentrischen Zugspannungen. Bericht Nr. 44. Materialprüfungsamt für das Bauwesen der Technischen Hochschule München.
8. Cornelissen H. A. W. (1986a). State-of-the-art report on fatigue of plain concrete. Delft, The Netherlands:Delft University of Technology. Report 5-86-3. pp. 62.
9. Tepfers R. (1979). Tensile fatigue strength of plain concrete. ACI Journal Vol 76, No 8: pp. 919-933.
10. Gylltoft K. (1983). Fracture Mechanics Models for Fatigue in Concrete Structures. Doctoral Thesis 1983:25D. Luleå University of Technology. Division of Structural Engineering. pp. 210.
11. Rots J. G., Nauta P., Kusters G. M. A. and Blaauwendraad J. (1985). Smeared Crack Approach and Fracture Localization in Concrete. Heron, Vol. 30, No. 1, 1985.
12. Reinhardt H.-W., Cornelissen H. A. W. and Hordijk D. A. (1986). Tensile Tests and Failure Analysis of Concrete. ASCE Journal of Structural Engineering, Vol. 112, No. 11. pp. 2462-2477.
13. Yankelevsky D. Z. and Reinhardt H. W. (1989). Uniaxial Behavior of Concrete in Cyclic Tension. Journal of Structural Engineering, ASCE, Vol. 115, No. 1, January 1989. pp. 166-182.
14. Hordijk D.A. (1991). Loacal Approch to fatigue of concrete. Dissertation. Delft University of Technology, Delft, The Netherlands.

15. Duda H. and König G. (1991). Rheological Material Model for the Stress-Crack-Width Relation of Concrete Under Monotonic and Cyclic Tension. ACI Materials Journal, V 88, Issue:3. pp. 278-287.

16. Kessler-Kramer C. (2002). Zugtragverhalten von Beton unter Ermüdungs-beanspruchung. Institut für Massivbau und Baustofftechnologie. Universität Karlsruhe. Dissertation. Karlsruhe 2002. pp. 286.

17. Thun H. (2006). Assessment of Fatigue Resistance and Strength in Existing Concrete Structures. Doctoral Thesis 2006:65. Division of Structural Engineering, Department of Civil and Environmental Engineering, Luleå University of Technology, Luleå, Sweden. December 2006. ISBN 978-91-85685-03-5

18. BBK 94 (1994, 1996). Swedish Recommendations for Concrete Structures. Volume 1 – Design, Volume 2 – Materials, Construction, Control. Svensk Byggtjänst, Stockholm 1994, 185 + 116 pp. ISBN 91-7332-686-0, 91-7332-687-9. Supplement 1996. pp. 57. ISBN 91-7147-274-6. In Swedish.

19. Daerga P-A. (1992). Some experimental fracture mechanics studies in mode I of concrete and wood. Licentiate Thesis 1992:12L, 1st ed April 1992, 2nd ed June 1992. Division of Structural Engineering, Luleå University of Technology. pp. 81.

20. Noghabai K. (1998). Effect of Tension Softening on the Performance of Concrete Structures. Experimental, Analytical and Computational Studies. Doctoral thesis 1998:21, Div of Structural Engineering, Luleå University of Technology, Luleå, Sweden, 1998. pp.147.

21. Hedlund H. (2000). Hardening concrete. Measurements and evaluation of non-elastic deformation and associated restraint stresses. Doctoral Thesis 2000:25, December 2000. pp. 394. ISBN 91-89580-00-1

22. Groth P. (2000). Fibre Reinforced Concrete - Fracture Mechanics Methods Applied on Self-Compacting Concrete and Energetically Modified Binders. Doctoral Thesis 2000:04, January 2000. pp. 214.

23. Thun H. (2006a). Paper A. Concrete Strength in old Swedish Concrete Bridges. Assessment of Fatigue Resistance and Strength in Existing Concrete Structures. Doctoral Thesis 2006:65. Division of Structural Engineering, Department of Civil and Environmental Engineering, Luleå University of Technology, Luleå, Sweden. December 2006. ISBN 978-91-85685-03-5

24. Möller G., Petersons N. and Elfgren L. (1994). Strength (Hållfasthet). Betonghandbok – Material utgåva 2. Avsnitt 11. Stockholm: Svensk Byggtjänst. ISBN:91-7332-709-3. pp. 132. In Swedish.

25. Wöhler A. (1858 -70). Tests to determine forces and deformations of railway carriage axles. (In German). Zeitschrift fur Bauwesen (Berlin), Vol 8, 1858, pp 641-652; Vol 10, 1860, pp 583-616, Vol 13, 1863, pp 233-258; Vol 16, 1866, pp 67-84; Vol 20, 1870. pp. 73-106.

26. Thun H. (2006f). Paper F. Load Carrying Capacity of Cracked Concrete Railway Sleepers. Assessment of Fatigue Resistance and Strength in Existing Concrete Structures. Doctoral Thesis 2006:65. Division of Structural Engineering, Department of Civil and Environmental Engineering, Luleå University of Technology, Luleå, Sweden. December 2006. ISBN 978-91-85685-03-5

27. Paulsson B., Töyrä B., Elfgren L., Ohlsson U. and Danielsson G. (1996). Load Bearing Capacity of Concrete Bridges. Research and development project. (Forsknings- och utvecklingsprojekt avseende betongbroars bärighet. “30 ton på Malmbanan“). Rapport 3.3 Infrastruktur, Banverket, Borlänge 1996. pp. 51 + appendix. In Swedish.

28. Paulsson B., Töyrä B., Elfgren L., Ohlsson U. and Danielsson G. (1997). Increased Loads on Railway Bridges of Concrete. “Advanced Design of Concrete Structures“ (Ed. by K. Gylltoft et al.), Cimne, Barcelona, 1997. pp. 201-206. ISBN 84-87867-94-4.

29. Utsi S. (2003). Self-Compacting Concrete - Properties of Fresh and Hardening Concrete for Civil Engineering Applications. Licentiate Thesis 2003:19. Division of Structural Engineering, Luleå University of Technology, Luleå, Sweden, June 2003. pp. 198.

Paper E

Load Carrying Capacity of Cracked Concrete Railway Sleepers

by Håkan Thun, Ulf Ohlsson and Lennart Elfgren

Submitted for publication in
Structural Concrete, Journal of the fib

Load Carrying Capacity of Cracked Concrete Railway Sleepers

by Håkan Thun, Sofia Utsi and Lennart Elfgren

Synopsis

The load carrying capacity of damaged prestressed concrete railway sleepers has been investigated. The sleepers had an age of five to ten years and the damage, in form of more or less severe cracking, is believed to be caused by delayed ettringite formation. The following tests have been performed: bending capacity of a) the midsection, b) the rail section, c) horizontal load capacity of the fastener, d) control of the concrete properties and e) fatigue capacity in bending of the rail section. A visual inspection and classification of the damages are also presented.

The purpose of the tests has been to get information about how the cracking influences the remaining load carrying capacity compared to an un-cracked sleeper. The test results have been compared with calculations according to the Swedish railway code for sleepers.

The test results show that railway sleepers are quite robust. Small cracks do not seem to influence the load carrying capacity and it is first when the cracking is very severe that the load carrying capacity is reduced significantly.

Introduction

Railway sleepers made of prestressed concrete have been used extensively during the last few decades in Sweden. Sleepers made of pine were substituted in the 1950s when prestressed concrete became available for sleepers, see Andersson & Berg[1]. The advantages with concrete sleepers compared to pine sleepers are e.g. long service life, high bearing capacity and no use of environmental hazardous chemicals such as creosote (used to increase the service life of timber).

A railway sleeper has several functions such as: being an elastic foundation for the rails, keeping the right distance between the rails and cooperating with the rail so the railway track is resistant to flexuous movement in the horizontal direction. It is easily understood that a sleeper must withstand various types of loads, weather conditions etc., without losing its properties during its service life. Normally, concrete sleepers sustain their properties for more than 50 years. However, in Sweden some sleepers made between 1992 and 1996 have started to deteriorate. They have obtained cracking of a more or less severe kind and some of them have even lost most of their bearing capacity. The cracking is believed to be caused by so-called delayed ettringite formation, which leads to an internal expansion and, gradually, cracks. In combination with moisture and/or cyclic frost erosion the deterioration may accelerate.

What is then delayed ettringite formation (DEF)? During the last few years the mechanism behind DEF has been discussed in the concrete society, see e.g. Scrivener & Skalny[2]. Especially what part it has - does it act alone or together with other mechanisms in creating the expansion and the cracking? Besides, the ettringite ($Ca_6[Al(OH)_6]_2(SO_4)_3 \cdot 26H_2O$) is formed during the hardening process of concrete but it is normally transformed into monosulphate with less water content ($3Ca_4[Al(OH)_6]_2(SO_4) \cdot 6H_2O$) after a few hours. Some researchers mean that if heat curing (steam-curing) and/or cement with high sulphate content are used, ettringite might form a long

time after the hardening is complete, see e.g. Scrivener & Skalny[2] causing delayed expansion and cracking.

Ettringite damages have been reported from many countries over the years and it is often sleepers that have started to deteriorate, see e.g. Tepponen & Eriksson[3], Collepardi[4], Hime[5] or Metha[6]. A summary of recent work in the research field of DEF could be found in Scrivener & Skalny[2]. Due to the many problems connected to DEF, recommendations have now been established in many countries, in particular regarding the use of heat curing which seems to be an important factor, e.g. in the German recommendations regarding heat curing, see DAfStb[7], the rules were revised due to the reported damages. In the new recommendations the following is stipulated for the curing of concrete that is often exposed to moisture or during longer time:

- maximum concrete temperature is 60 ºC (single values may be 5 ºC higher).
- temperature rise must be ≤ 20 ºC/h.
- pre-storage during at least 3 hours at maximum 30 ºC or during at least 4 hours at maximum 40 ºC.

The delayed ettringite process has in the case studied here reduced the service life to as few as five years. The origin of the delayed ettringite formation in this case is believed to be the production methods. In order to increase the production speed, the cement quantity was increased from ordinarily 420 kg/m^3 to 500 kg/m^3 and steam-curing was used during the hardening process in some of the production plants, see CBI[8]. The sleepers were made of prestressed concrete with the concrete class K60 (the Swedish concrete class K60 corresponds approximately to the concrete strength class C45/55 in Eurocode, e.g. EC2-draft (2003)[9]).The sleepers are prestressed with 8 strands (each strand consists of 4 wires with the diameter of 3 mm).

The mechanism behind DEF is not analysed in this paper. Instead, the remaining load carrying capacity of the damaged sleepers has been investigated and test results are presented. The purpose of the tests has been to get an idea of how the cracking influences the load carrying capacity and to determine how many and at what rate the damaged sleepers must be replaced from the track. In turn this also decides how much it will cost to replace the damaged sleepers. In 2001 the estimated cost of replacing them was more than 1000 million SEK (107 million euro or 140 million US dollars, press release 2001-11).

Load carrying capacity of sleepers and concrete fatigue capacity have earlier been studied at Luleå University of Technology (LTU), see Gylltoft & Elfgren[10], Gylltoft[11, 12], Emborg[13], Paulsson[14] and Ohlsson[15]. This paper is a summary of test reports by Elfgren[16] and Thun et al.[17, 18].

Visual Inspection and Classification

Visual Inspection

When Banverket (the Swedish National Rail Administration) in the late 1990s became aware of the problem with the cracked sleepers, several investigations were initiated. These showed, among other things, that the damaged sleepers could be found all over Sweden. About 3 million sleepers were inspected and approximately 500 000 sleepers were cracked. The visual inspections were performed with two inspectors walking on opposite sides along a railway track, which is a difficult and a time-consuming work.

The area on the sleeper where the first visible cracks appear when they lie in the track, seems to be on the upper side at the end, near the edge, see Figure 1. This leads to a problem since some sleepers have no cracks on the upper side but have cracks on the side towards the lower edge, see Figure 2. These cracks are not possible to detect at a visual inspection along the railway line as long as the macadam is not removed which might lead to missing some cracked sleepers at the inspection.

Figure 1 Picture showing how much of a sleeper that is visible when it is placed in the railway track and where the first visible cracks appear.

Classification

The first inspections led to a categorisation of the sleepers depending on the cracking. They were divided into three classes and the typical damages for each class are:

Class Green / OK: No visible cracks. No visible tendencies to develop major faults. No change in colour. The load carrying capacity is intact.

Class Yellow / Initial degradation: Some cracks. The cracking is of the kind that the load carrying capacity is almost intact. There might be cracks with a crackled pattern at the end of the sleepers. The sleepers might have a crack from the fastener and downwards. Yellow spots could be found. Typical crack patterns are given in Figure 2.

Class Red / Acute: The cracking is so severe that there is a considerable reduction of the load carrying capacity. There are typical longitudinal cracks in the middle of the sleeper. There are also cracks at the end of the sleepers with a crackled pattern. The sleepers might have a crack from the fastener and downwards. For a typical crack pattern see Figure 2. The concrete surface is discoloured by yellow spots.

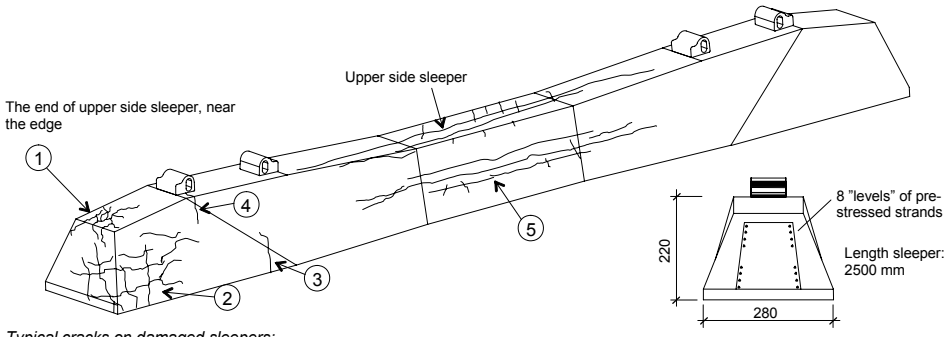

Typical cracks on damaged sleepers:
Green sleepers: No cracks.

Yellow sleepers: Area 1&2 - cracks in the range from one single crack to a quite developed crack pattern.

Red sleepers: Area 1&2 - fully developed crack pattern.

Red sleepers: Area 3 - bending crack in rail section (at the bottom edge).

Red sleepers: Area 4 - crack from fastener and down the side (some yellow sleepers had this crack also).

Red sleepers: Area 5 – crack pattern often in combination with long horizontal cracks.

Figure 2 Drawing of a typical damaged concrete sleeper with characteristic crack pattern classified as green (no cracks), yellow or red.

There were many yellow sleepers and the crack pattern varied among them so it was decided to divide them into subcategories, see Figure 3. The aim of these subgroups was to investigate if any variation of load capacity existed among them. The criterion used as a basis takes into account what kind of cracks an inspector has a chance to discover when he/she walks along the railway track. The sleepers are covered with macadam so it is only possible to notice damages on the upper side of the sleepers and also 10-20 mm along the top part of the sides, see Figure 1. The cracks that have been used as target have a width larger than 0.05 mm. These cracks are possible to see with the naked eye and can be discovered without the need of getting down on one's knees. These cracks are in this paper called *visible cracks*.

The subdividing of the yellow sleepers is thus only based on visible cracks on the upper side of the sleeper, at the ends, see Figure 3. Worth pointing out is that not all sleepers have two ends with the same type of damages. Some sleepers have several cracks at one end but no cracks at the other.

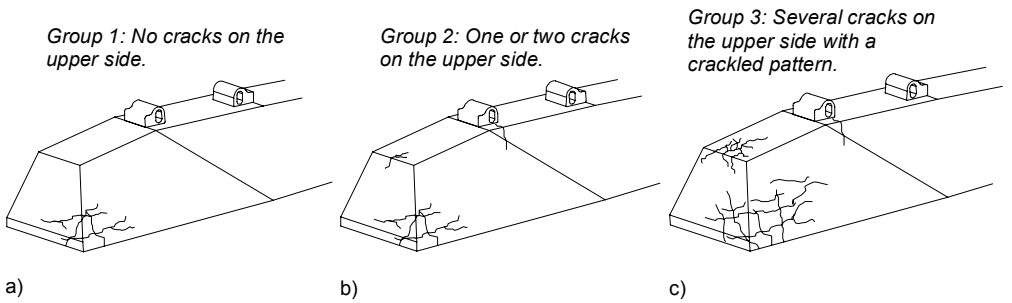

Figure 3 Typical cracks for sleepers of class yellow/initial degradation. a) *Sleepers in group 1 have no visible cracks on the upper side but there might be cracks on the side at the lower edge.* b) *Sleepers in group 2 have only 1 or 2 visible cracks on the upper side. They have fewer cracks on the side towards the lower edge than the sleepers in group 3 (the crackled pattern is not yet as "developed" as for group 3 sleepers).* c) *Sleepers in group 3 have cracks in a crackled pattern on the side as well as on the upper side.*

Required Capacity

Bending Capacity of Midsection and of Rail Section

According to the Swedish Rail Code, BVF 522.32[19], the moment capacity in the midsection must be M_{max} = 11 kNm and the safety factor against failure must be at least 1.75.

This leads to a moment capacity in the midsection of:

$$M_{f,mid} = 1.75 \cdot 11 = 19.25 \text{ kNm} \quad (1)$$

The moment capacity of the section where the rail is placed must be 15 kNm. With a safety factor against failure of 1.75 this results in a moment capacity of:

$$M_{f,rail} = 1.75 \cdot 15 = 26.25 \text{ kNm} \quad (2)$$

Horizontal Load Capacity of the Fastener

In the Swedish Rail Code there is no specification of how the horizontal load capacity could be tested or calculated. An estimation of the horizontal forces acting on a fastener has therefore been performed. An evaluation of the forces caused by the centrifugal acceleration and the wheel-rail interaction forces showed that the highest lateral force acting on each sleeper was about 33 kN (see evaluation in Thun et al.[16]).

Fatigue Capacity

Red sleepers were tested in the rail section, since previous tests had shown that this was the "weakest" part of the cracked sleepers[17]. The initial hypothesis was that the long horizontal cracks, see Figure 2, could be the main factor reducing the fatigue capacity.

All fatigue tests were performed under load control with a sinusoidal load cycle with a load frequency of 2.0 Hz. The two load levels, A and B in Figure 4, were kept constant during the test. In order to get a "soft" start of the fatigue test the load was increased with a rate of 0.5 kN/s until it reached a level that was higher than level A, see Figure 4, in order to secure that the hydraulic system did not break the specimen at the beginning of the test.

The maximum load level used in the fatigue tests (level B in Figure 4) i.e. 62.5 kN corresponds to the maximum load one sleeper is exposed to from a wagon wheel (a wagon wheel with the maximum axle load of 25 tons gives the total wagon weight of 100 tons and this load is distributed over 8 wheels which gives the wheel load of 12.5 tons distributed on two sleepers i.e. 62.5 kN on each sleeper), Bv Bärighet[20]. The load 80 kN corresponds to, with the same reasoning, an axle load of 32 tons. As load level A 20 kN was chosen.

It was decided to stop the fatigue tests after 2 million load cycles. These two million load cycles correspond to approximately 7 years of traffic for a railway line that is exposed to 10 trains a day with 20 wagons and 4 axles.

Worth mentioning is that a fatigue test according to the Swedish Rail Code for an un-cracked sleeper, should be performed in the way that the sleeper is loaded until the first bending crack is received on the bottom surface of the sleeper. Then the sleeper is loaded with a sinusoidal load with the frequency of 5 Hz between the loads 30 and 140 kN. The sleeper must manage at least 3 million load cycles at these load levels without failure. It is also only necessary to perform a fatigue test in the rail section.

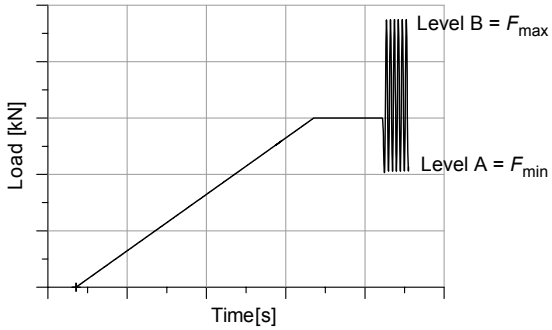

Figure 4 Graph showing, in principle, how the fatigue tests were started. In order to get a "soft" start of the test the load was increased with a rate of 0.5 kN/s until it reached a level that was higher than level A.

Results and Discussion

Before the tests started every sleeper was visually inspected and photographed. The condition of the sleepers varied from undamaged to very damaged. To be able to see the cracks more easily the sleepers were washed and especially interesting parts were moistened during inspection.

Concrete Strength Tests

The material properties of the concrete have been determined from uniaxial tensile and compressive strength tests on drilled cores with a diameter of 68 mm. The cores were obtained from the middle of the sleepers (the sleepers were first cut in two halves).

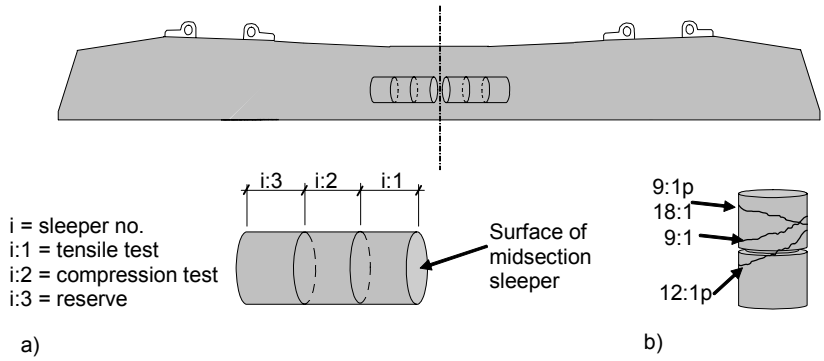

Figure 5 Test of material properties. a) *Location of cores and* b) *Crack planes for the test specimens 9:1p, 9:1, 18:1 and 12:1p.*

The mean concrete compressive strength for 22 tests was 100.4 MPa with a standard deviation of 6.6 MPa and a coefficient of variation of 0.07 (the lowest value was 85 MPa).

The mean concrete tensile strength for 18 tests was 3.8 MPa with a standard deviation of 0.4 MPa and a coefficient of variation of 0.11. The cores were glued to the load plates in the testing machine and a notch was formed by milling, see cracks according to Figure 5b. Four test specimens did not fail in the milled notch and have therefore not been included in the mean value. The tensile strength for these four tests was 0.90, 0.99, 0.38 and 2.44 MPa. If these tests are included in the calculation of the mean value the result is 3.3 MPa with a standard deviation of 1.1 MPa and a coefficient of variation of 0.33. For individual values see Thun et al.[16]

The concrete was specified to have a compressive strength of approximately 67 MPa (the Swedish concrete class K60 corresponds approximately to the concrete strength class C45/55 in Eurocode, e.g. EC2-draft (2003)[9]).

The compression strength is high. It varies between 85-109.3 MPa with a mean value of 100.4 MPa and a standard deviation of 6.6 MPa.

It is very revealing if cracks and/or crack planes are present in a tensile test. This would probably have been the case for the sleepers with the tensile strength of 0.90, 0.99, 0.38 and 2.44 MPa that did not fail in the milled notch. The results from these tests are nevertheless of less interest. One can say that the tensile strength derived from these tests represents the tensile strength that could be expected at the ends of the sleepers where a crack system has started to develop to where a crack system is very developed. This leads to the fact that a tensile strength of 0.4-2.44 MPa could be expected in these regions. In the tests where the crack came in the intended milled notch the tensile strength represents the tensile strength for an un-cracked sleeper or as in the case of the yellow sleepers in a region without cracks. The tensile strength is high no matter group/class. It varies between 2.97 – 4.44 MPa and a pattern between the classes has not been established.

Bending Capacity of Midsection

The sleepers were placed upside down on bearings at each rail section (distance between bearings: 1500 mm), Figure 6. Each bearing consisted of a steel cylinder (diameter 60 mm) and two steel plates (width 100 mm) and a rubber pad was placed between the bearings and the sleeper.

At the middle of the sleeper two bearings were mounted on the upper side at a distance of 150 mm from the symmetry line. Each bearing consisted of a steel cylinder (diameter 15 mm) and two steel plates (width 50 mm and a thickness of 15 mm). Between the bearings and the sleeper a rubber pad was mounted. A steel girder was placed on the bearings so the load could be applied symmetrically in proportion to the rail sections, see Figure 6. The displacement was measured by four LVDT-gauges, one on each side of the midsection to compensate for a possible rotation during the test. An LVDT-gauge was also mounted at each rail section to compensate

for the possible settlement of the supports. The test was run in displacement control and the load was applied with a rate of 0.02 mm/s. The sleepers were loaded until failure.

The test results are shown in Figure 6 and failure was caused by shear cracking, wire slip or wire failure. The maximum moment in Figure 6 is calculated as:

$$M(0.6) = M_{max} = \left(\frac{F}{2} \cdot 0.6\right) \text{kNm} \qquad (3)$$

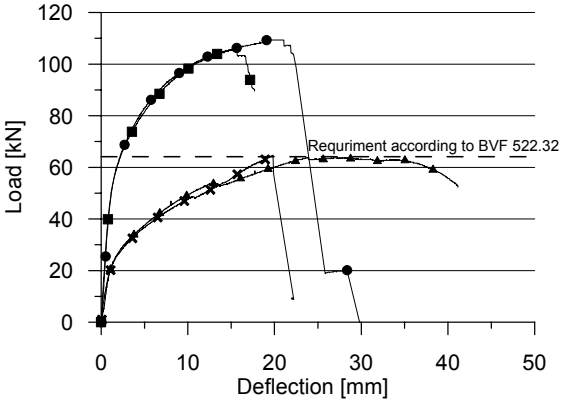

Sleeper no.	Class	F_{max} [kN]	M_{max} [kNm]	Failure type
× 2	red	65	19.5	shear
● 4	green	109	32.7	wire fracture
■ 5	green	106	31.8	wire fracture
▲ 6	red	64	19.2	wire slip

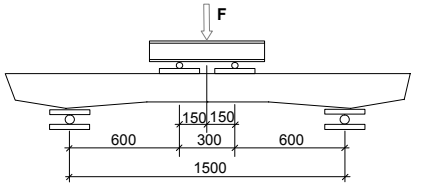

Figure 6 Test set-up for test of the bending capacity of midsection (unit: millimeters) and results from the tests.

The moment capacities are approximately 19 kNm for the red sleepers and 32 kNm for the green sleepers. This can be compared to 19.25 kNm which is the required moment capacity according to BVF 522.32[19] (including a safety factor of 1.75 against failure).

Thus, the bending capacity of the midsection of the tested sleepers is satisfactory even for the worst damaged sleepers, i.e. red sleepers. Worth mentioning is that these red sleepers were in a very bad condition, big pieces of concrete were missing and some wires were visible.

The bending capacity of the midsection does not seem to decrease significantly until the typical longitudinal cracks in the middle of the sleeper appear, see Figure 2.

Bending Capacity of Rail Section

The sleepers were placed on two bearings, the same as for the tests in midsection, at a distance of 300 mm on each side of the symmetry line of the rail section, see Figure 7.

In the middle of the rail section a steel plate, thickness 15 mm and width 50 mm, was placed with a rubber pad between the concrete and the steel. The test was run in displacement control and the load was applied via a hinged edge at a rate of 0.02 mm/s. The sleepers were loaded until failure. The displacement was measured by four LVDT-gauges; one at each side of the midsection of the rail section and by one LVDT-gauge at each support as in the test of the moment capacity in midsection.

Test results are shown in Figure 7. The failure was caused by wire slip or wire failure, shear cracking or bending moment cracking followed by concrete crushing or a combination of bending and shear cracking. The maximum moment in Figure 7 is calculated from:

$$M(0.3) = M_{max} = \left(\frac{F}{2} \cdot 0.3\right) \text{kNm} \qquad (4)$$

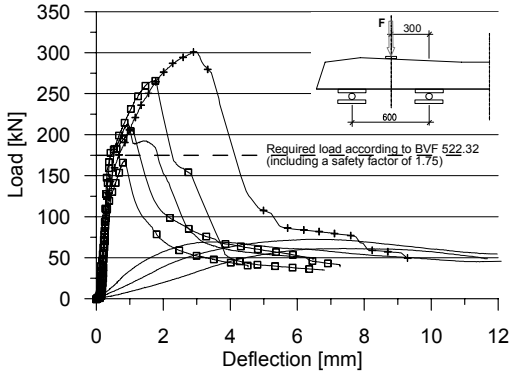

Sleeper no.	Class	F_{max} [kN]	M_{max} [kNm]	Failure type
1	Red	60	9	wire slip
3	Red	72	10.8	wire slip
6	Red	69	10.4	wire slip
22	Red	74	11.1	bending & shear
23	Red	171	25.7	bending & shear
24	Red	213	32	bending & shear
25	Red	165	24.8	bending & shear
□ 19	Yellow, group 3	168	25.2	bending & shear
□ 20	Yellow, group 3	205	30.8	bending
□ 21	Yellow, group 3	266	39.9	bending
+ 4	Green	301	45.2	wire fracture

Figure 7 Test set-up for test of the bending capacity of rail section and results from the tests.

The red sleepers have a moment capacity between 9 and 11 kNm while the green sleepers manage approximately 45 kNm. According to BVF 522.32[19], the sleepers must manage 26.25 kNm.

For the red sleepers the maximum load capacity varies between 60-213 kN (9–31.95 kNm). The result shows that when the sleepers are very damaged (no. 1, 3 and 6) the failure phase starts almost immediately after loading due to wire slip. For sleepers without a fully developed crack pattern and where the long horizontal cracks are limited to the midsection (if there are any at all), they have in most cases failed in shear. When the peak load is reached the wires start to slip which leads to a ductile fracture, see sleeper no. 22, 23, 24 and 25.

When the yellow and red sleepers are compared, some red sleepers (no. 23 - 25) reached the same load levels as the yellow sleepers, approximately 170 kN, which is probably due to a similar crack system in the area around the fastener. These two sleepers could have been classified as yellow sleepers, group 1, if they did not have short horizontal cracks on the side at midsection.

Red sleeper no. 22 deviates most from the other sleepers, when it only reached 74 kN (11.1 kNm). This is probably due to larger crack widths for the cracks at the end (and a longer crack along the “upper” wire) in combination with the fact that pieces of concrete are missing.

According to BVF 522.32[19] the sleepers must have a moment capacity of 26.25 kNm (including a safety factor of 1.75). There is only one sleeper of the tested red sleepers that manages the requirements, i.e. no.24 (32 kNm). Sleepers no. 23 and 25 nearly reach the requirements with 25.7 and 24.8 kNm. The rest of the red sleepers do not meet the requirements. All yellow sleepers manage the requirement except for one, no 19, that reaches 25.2 kNm.

Horizontal Load Capacity of the Fastener

The test arrangement is shown in Figure 8. The outer of the two fasteners has been tested. The sleeper was placed on a steel girder and tightened to prevent movement. A hydraulic jack and a load cell were mounted on a bar. The tests have been run in load control with a load velocity of 0.4 kN/s. To measure the displacement, an LVDT-gauge was placed horizontally against the fastener.

The test results are given in Figure 8. Failure is caused by the development of vertical cracks from the fastener and a horizontal crack along the wires. According to the analysis mentioned earlier the sleepers must manage 33 kN.

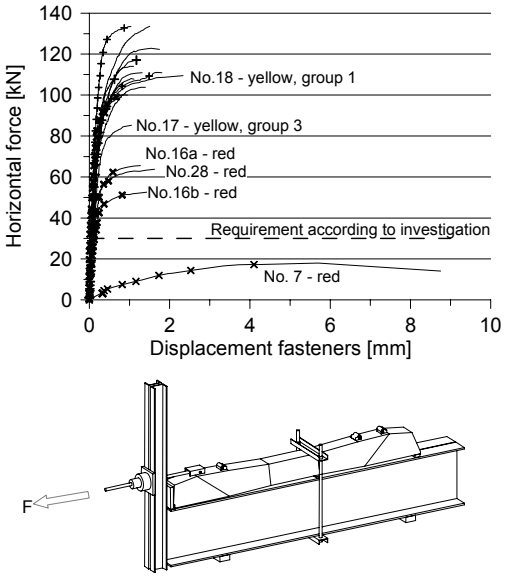

Sleeper no.	Class	Max horizontal force F_{max}, [kN]
× 7	Red	18
× 16a	Red	65.5
× 16b	Red	52.5
× 26	Red	100.2
× 27	Red	99
× 28	Red	63.7
+ 5	Green	117.1
+ 8	Green	133.5
+ 9	Green	111
10	Yellow, group 1	108.1
11	Yellow, group 1	103.8
17	Yellow, group 1	85.2
12 [a)]	Yellow, group 2	110.9
13	Yellow, group 2	114.1
14 [a]	Yellow, group 3	133.5
15	Yellow, group 3	122.9
18	Yellow, group 3	109.5

a) sleeper had a vertical crack from the fastener and downwards

Figure 8 Test set-up and results from the tests of the capacity of fasteners for horizontal load.

The horizontal load capacities of the fasteners for the green and yellow sleepers were 100-130 kN, which is several times higher than the load caused by the trains. Even the red sleeper with the lowest maximum capacity of 18 kN for a deformation of 5 mm may function if it is surrounded by green and yellow sleepers.

Small cracks, typical for yellow sleepers, do not seem to influence the horizontal load carrying capacity of the tested fasteners significantly. It is first when the cracking is very severe (i.e. red sleepers, where both longitudinal and vertical cracks appear) that the load carrying capacity is reduced significantly.

Red sleeper no. 7 managed the lowest load of all red sleepers, i.e. 18 kN. The rest of the sleepers managed over 52.5 kN. Worth mentioning is that sleeper No. 7 was in a much worse condition than the other red sleepers (the outer fastener and the concrete surrounding it had fallen off at one end). The risk that a sleeper in this bad condition could be missed at an inspection is probably very small.

The main reason why sleeper No. 7 managed a much lower load than sleepers No. 16 and No. 17 is probably because it has a vertical crack from the fastener and downwards. This was also combined with a very developed crack system. The vertical crack at the fastener and downwards probably comes from track forces, i.e. the presence of this crack depends on where it has been lying in the track, e.g. in curves, where it has been exposed to high forces. Sleepers No. 16 and 17 manage approximately the same load, but sleeper No. 17 looks more like a yellow sleeper because only the ends had a lot of cracks. Sleeper No. 16 looks more like sleeper No. 7 due to the fact that it has long horizontal cracks. As mentioned above it does not have the vertical crack at the fastener.

Fatigue Tests

The test set-up for the fatigue tests was the same as in the static tests in rail section, except that the distance between the supports was increased from 600 mm to 800 mm in order to reduce the strain of the hydraulic system, see Figure 7.

In Figure 9 results from the fatigue tests for sleeper s35 and sleeper s41 are presented. Sleeper s35 reached 320 017 load cycles and sleeper s41 reached 136 670 load cycles before failure.

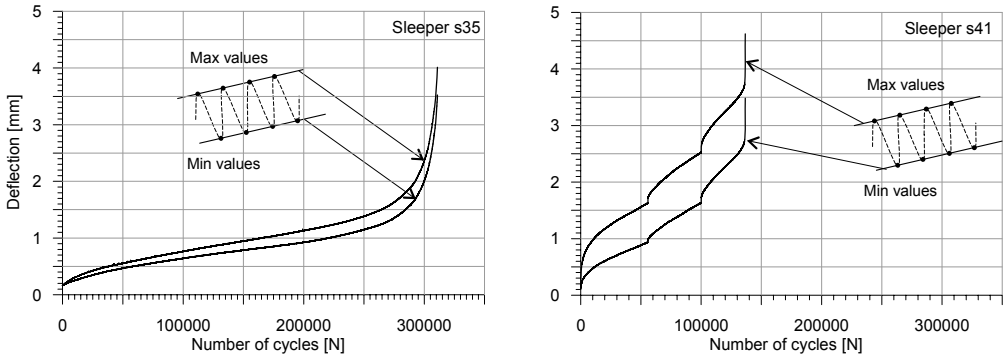

Figure 9 Deflections at rail section during fatigue test of sleeper no. s35 and s41 to the right.

The fatigue tests in the rest of the test series behaved in a similar manner, only the number of load cycles to failure differs. A summary is presented in Table 1.

Table 1 Summary of results from fatigue test.

Sleeper No	Class	Load levels fatigue test A-B [kN]	Load frequency [Hz]	Static failure load [b] [kN]	Moment capacity [kNm]	No. of cycles at failure
s29a	red	---	2	71.7	14.3	---
s29b	red	20-80	2	125.4	25.1	45 000 [a]
s30a	red	---	2	113	22.4	---
s30b	red	20-80	2	---	---	11554
s31a	red	---	2	75.9	15.2	---
s31b	red	20-80	2	---	---	223
s32a	red	---	2	74.4	14.9	---
s32b	red	20-80	2	152.6	30.5	>2 M cycles
s33	red	20-62.5	5	124.3	24.8	>2 M cycles
s34	red	20-62.5	5	177.9	35.5	>2 M cycles
s35	red	20-62.5	5	---	---	320071
s36	red	20-62.5	5	---	---	1827
s38	red	20-62.5	4	105.7	21.1	>2 M cycles
s39	red	20-62.5	4	132.5	26.5	>2 M cycles
s40	red	20-62.5	4	---	---	87042
s41	red	20-62.5	4	---	---	136670
s42	red	20-62.5	4	159.8	32	>2 M cycles

[a] *The test was stopped at 45 000 cycles and the sleeper was subjected to static load until failure.*

[b] *For the sleepers that managed 2 million load cycles.*

In the preliminary fatigue tests the sleepers were divided into two halves. The idea was to use one half in a static test (index: a) and the other half in a fatigue test (index: b). This method has been used in earlier projects at LTU regarding sleepers, see Gylltoft[11]. With this method an indication would be received if the plan of using 80 kN, as the upper load level in the fatigue test, would be possible. 80 kN is the wheel load that corresponds to the highest axle load used in Sweden. Furthermore, If the static failure load was close to 80 kN it would also be possible to see how a damaged sleeper behaved regarding fatigue load close to its maximum static capacity. This method was rejected after a few tests since the initial test result showed that two sleeper halves could have very different bearing capacity in the rail section even though they were “the

same" sleeper. Sleeper s32a is a good example of this. It had a static failure load of 74.4 kN. When the fatigue test for the other half was stopped after 2 million load cycles and a static test was performed the failure load became 152.6 kN which is almost twice the load 74.4 kN. This shows that even though a sleeper seems to have the same type of visible crack system at both ends it is the internal crack system that is crucial for the load capacity. The upper load level 80 kN was changed to 62.5 kN since this load corresponds to the maximum axle load that is used where the damaged sleepers could be found in Sweden at that time.

All of the tested red sleepers show a varying fatigue capacity. Seven of them failed in the fatigue test and six reached the settled limit of 2 million load cycles. All of them had the typical crack pattern and some of them also had long horizontal cracks along the sides (and in some cases even bending cracks in the rail section, at the lower edge, were present). The initial hypothesis that the long horizontal cracks would be the main reason that decided the fatigue capacity has not been confirmed by these tests. But, if the tested sleeper has had both the bending cracks in the rail section (on both sides) and the long horizontal cracks it has failed in the fatigue test.

The failure process due to cyclic loading in these tests is similar to a model presented by Balázs[21], see Figure 10. The model has successfully been used to describe bond failure between rebars and concrete. It could be described as, according to Balázs[21]; initially (from point A to point B, phase 1, in Figure 10) the slip rate decreases and then remains constant, phase 2, until point C. When point C (slip at τ_{bu}) is reached (phase 3), there is a rapid increase up to pull-out failure. Since exceeding the slip at maximum load in the static test, $s(\tau_{bu})$, failure is reached in some additional repetitions, $s(\tau_{bu})$ provides a safe fatigue failure criterion. The failure criterion may be called safe due to the difference between the number of load cycles up to $s(\tau_{bu})$ and failure.

In the fatigue tests three typical cases, i.e. deflection-versus-number of load cycle curves, have been identified: The first typical case is when the sleepers have failed after a few numbers of cycles (<2000). Here, no second phase according to Figure 10 exists, probably because of an almost non-existent bond between the concrete and the wires due to a highly developed internal crack system. The second typical case is almost identical to the deformation-versus-number of load cycle curves shown in Figure 10 - all three phases exist (see the result for sleeper s35 in Figure 9). The internal crack system is in this case probably evenly distributed over the sleeper which leads to the fact that all wires are working intact until the concrete is so cracked that the bond is zero. The third typical case is similar to case 2 with the exception that the first phase and the second phase are repeated a number of times until phase three is reached and the failure phase begins, see sleeper s41 in Figure 9. For the sleepers, this behavior is probably due to better bond at the beginning and that the bond gradually reduces accordingly as the bottom levels of strands lose their bond, see Figure 2.

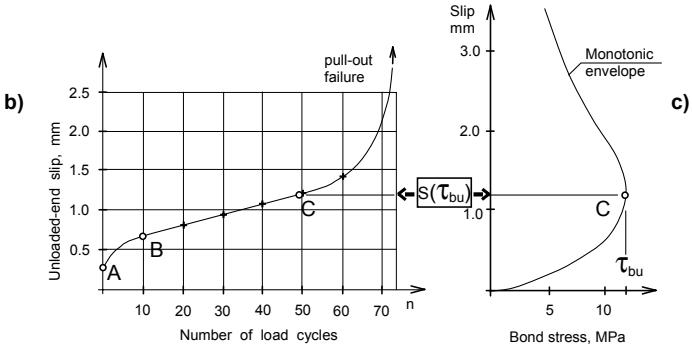

Figure 10 Bond fatigue process under repeated loading: b) *slip-versus-number of load cycles diagram and* c) *monotonic bond stress-slip diagram. From Balázs[21].*

The fatigue tests in this paper can be compared to fatigue tests made on prestressed concrete sleepers in Gylltoft[11] (similar dimensions, concrete strength etc.). In all tests the sleepers were

first cut in halves and one part was used for the static test and the other part for the fatigue test. The mean failure moment in the static tests was 46.7 kNm, which is almost twice the mean failure moment the cracked (red) sleeper managed in these tests. The fatigue tests were performed in the way that the sleepers were loaded up to the load level where the first visible crack (bending crack) appeared, and then a sinusoidal load cycling was initiated between approximately 10% and 50% of the static mean failure load.

In Gylltoft[11] all fatigue tested sleepers failed due to wire fracture and not due to wire slip as in this investigation. This is not surprising since there were no cracks that reduced the bond between the concrete and the wires or the anchorage length for the wires.

Another interesting detail in Gylltoft[11] is the result from the static tests for the run-outs in the fatigue tests. Three specimens did not fail in the fatigue test. If the static failure load for these "fatigue specimens" is compared to the failure load from their "other halves" that was used for the static test the difference is only about 5%. As mentioned earlier the difference for the cracked sleepers could be up to approximately 50%. This shows how important the bond between the concrete and wires is and how difficult it is to predict a capacity for the cracked sleepers.

Conclusions

Based on the investigation, the following conclusions can be drawn:

- High cement content (>500kg/m3) and high curing temperatures (> 60 ºC) may lead to delayed ettringite formation (DEF) causing extended cracking and early deterioration of concrete structures, see CBI8.
- The concrete strengths for the tested sleepers were high. The mean value for 22 compression tests was 100.4 MPa and the mean value for 18 tensile tests was 3.8 MPa.
- All tested sleepers have discolorations here and there. The colour is brown-yellow. Some of the sleepers had no visible cracks on the upper side but they had cracks on the sides towards the lower edge, see Figure 2.
- Despite extended cracking, railway sleepers may retain a high load carrying capacity. However, when longitudinal cracks destroy reinforcement bond and anchorage, the capacity is reduced. The concrete becomes fragile and pieces have a tendency to break off.
- If a sleeper has only one or two cracks on the upper side at the end of the sleeper, it has also fewer cracks on the side compared with a sleeper that has a lot of cracks on the upper side (at the end).
- The bending capacity of the midsection of the tested sleepers is enough to prevent failure with a safety factor of 1.75 against failure even for the worst damaged sleepers, i.e. red sleepers. The bending capacity of the midsection does not seem to decrease significantly until the typical longitudinal cracks in the middle of the sleeper appear, see Figure 2.
- The bending capacity of the rail section of the tested sleepers is not high enough for all tested sleepers. The bending capacity of the rail section seems to depend on the presence of longitudinal cracks at the end of the sleepers and between the fasteners. The tested sleepers with load capacities far below the requirement were in such a bad condition that they could probably not be missed in a visual inspection along the railway track.
- All sleepers but one had a horizontal load capacity of the fastener higher than the required load. The sleeper that did not manage the required load had so severe damages that even wires were visible and pieces of concrete had fallen off. An estimation is that the risk is very small that a sleeper with this kind of damages should not be found at an inspection.
- In the fatigue test 6 out of 13 tested sleepers failed after 223 to 136 670 load cycles. Seven out of 13 sleepers managed to carry more than 2 million load cycles, which is equivalent to train traffic for about 7 years.
- The two ends of a sleeper can have very different bearing capacity even though they are from the "same sleeper".

- No relation between the visible crack pattern and the fatigue capacity for the red sleepers has been established.
- Three typical deflection-versus-number of load cycle curves have been found even though the sleepers have had similar visible crack pattern.
- For the studied type of cracked railway sleepers the fatigue capacity varies a lot. In the worst case a cracked sleeper could last only a few hundred load cycles (i.e. a few number of trains) before failure and loses its bearing capacity.

Further Investigations

The sleepers are now inspected annually. An important question is how fast a green or yellow sleeper turns into a red one, i.e. how fast is the formation of ettringite? Weather conditions probably play an important role. An indication of this has been discovered on one sleeper. The midsection of this sleeper had been covered with equipment for the signalling system, a so-called “Balis”, and this part seemed to be in better condition (no visible cracks) in comparison with the ends where the crack system had developed quite a bit. If a sleeper will also be exposed to e.g. cyclic frost erosion the process ought to accelerate considerably.

Acknowledgements

The investigation was carried out on behalf of Banverket (the Swedish National Rail Administration). Mr Björn Paulsson and Mr Paul Nilsson together with their staff have provided information and help. TESTLAB (the test laboratory at Luleå University of Technology) has performed the tests in collaboration with the first two authors.

Notation

F_u ultimate force at failure.

$M_{f,\ mid}$ moment carrying capacity at the midsection of the sleeper including 1.75 safety factor against failure.

$M_{f,rail}$ moment carrying capacity at the rail section of the sleeper including 1.75 safety factor against failure.

References

1. Andersson, Evert and Berg, Mats (1999). Järnvägssystem och spårfordon. Del 1: järnvägssystem (Rail system and rail vehicles. Part 1: Rail systems. In Swedish). The Railway Group KTH, Centre for Research and Education in Railway Engineering. Royal Institute of Technology, KTH. 1999.
2. Scrivener K. and Skalny J. P. (2005). Conclusions of the International RILEM TC 186-ISA Workshop on Internal Sulphate Attack and Delayed Ettringite Formation. 4-6 Septem-ber 2002, Villars, Switzerland. Rilem, Materials and Structures, Issue: Volume 38, N° 280. pp. 659 – 663.
3. Tepponen Pirjo and Eriksson Bo.-Erik. (1987). Damages in concrete railway sleepers in Finland. Nordic Concrete Research, Oslo, V.6. 1987. pp. 199-209.
4. Collepardi Mario (1999). Damage by delayed ettringite formation. Concrete International, American Concrete Institute, Farmington Hills, MI, USA, V.21, No. 1. 1999. pp. 69-74.
5. Hime William (1996). Delayed ettringite formation - A concern for precast concrete? PCI Journal, Precast/Prestressed Concrete Institute, Chicago, IL, USA, V.41, No. 4. 1996. pp. 26-30.
6. Mehta, P. Kumar (2000). Sulphate Attack on Concrete: Separating Myths From Reality. Concrete International, Farmington Hills, MI, Vol 22, No. 8, August 2000. pp. 57-61.

Discussion by William G. Hime, Gunnar M. Idorn, and author in Vol 23, No. 2, February 2001. pp. 10-13.

7. DAfStb (1989). Richtlinie zur Nachbehandlung von Beton. (Rules for curing of concrete. In German) Deutscher Ausschuss fur Stahlbeton, Beuth Verlag GmbH, Vertriebsnummer 65013, Berlin, September 1989. pp. 6.
8. CBI (2000). Uppdragsrapport nr 2000-91. Mikrostruktur och kemisk analys av värmehärdade betongslipers med inre sprickbildning och massiv ettringitbildning. (Research report No. 2000-91. Micro structure and chemical analysis of heat cured concrete sleepers with inner cracks and massive ettringite formation. In Swedish). The Swedish Cement and Concrete Research Institute, CBI, Stockholm. pp. 61.
9. EC2-draft (2003). Final Draft prEN 1992-1-1, Eurocode 2: Design of concrete structures - Part 1-1: General rules and rules for buildings. prEN 1992-1-1:2003. December 2003. pp. 224.
10. Gylltoft, Kent and Elfgren, Lennart (1977). Utmattningshållfasthet för anläggningskonstruktioner (Fatigue of Civil Engineering Structures. In Swedish). Byggforskningen, Rap-port R68:1977, Stockholm 1987. pp.160. ISBN 91-540-2750-0
11. Gylltoft, Kent (1978). Utmattningsprov av betongsliprar - Utveckling av provnings- och mätmetodik vid experimentell utmattningsforskning (Fatigue of concrete sleepers. Test methods. In Swedish). Byggforskningen, Rapport R103:1978, Stockholm 1978. pp. 92. ISBN 91-540-2939-2.
12. Gylltoft, Kent (1983). Fracture Mechanics Models for Fatigue in concrete Structures. Doctoral Thesis 1983:25D. Division of Structural Engineering, Luleå University pf Technology, Luleå 1983. pp. 210.
13. Emborg Mats, Cederwall Krister and Elfgren Lennart (1982). Cable Couplers, Nordic Concrete Research, Oslo, 1982. pp. 5.1-5.14.
14. Paulsson Björn, Töyrä Björn, Elfgren Lennart, Ohlsson Ulf and Danielsson Georg (1997). Increased Loads on Railway Bridges of Concrete. Advanced Design of Concrete Structures (Ed. by K. Gylltoft, B. Engström, L.-O.Nilsson, N.-E. Wiberg and P. Åhman). CIMNE, Barcelona 1997. pp. 201-206. ISBN 84-87867-94-4
15. Ohlsson Ulf, Darega Per-Anders and Elfgren Lennart (1990). Fracture energy and fa-tigue strength of unreinforced concrete beams at normal and low temperatures. Engineer-ing Fracture Mechanics, Vol 35, No 1/2/3, Pergamon Press. pp. 195-203.
16. Elfgren, Lennart (2001). Värmehärdning av betong (Heat-curing of concrete. In Swe-dish). Division of Structural Engineering , Luleå University of Technology. Skrift, Luleå 2001. pp. 9.
17. Thun Håkan, Utsi Sofia and Elfgren Lennart (2001). Spruckna betongsliprars bärförmå-ga: provning av böjmomentkapacitet, dragkapacitet hos befästningar samt betonghållfast-het. (Bearing Capacity of Cracked Concrete Railway Sleepers. In Swedish). Division of Structural Engineering, Luleå University of Technology. Technical Report 2001:11. pp. 63.
18. Thun Håkan, Utsi Sofia and Elfgren Lennart (2003). Spruckna betongsliprars bärförmå-ga vid utmattande last. (Fatigue Capacity of Cracked Concrete Railway Sleepers. In Swed-ish). Division of Structural Engineering, Luleå University of Technology. Technical Report 2003:04. pp. 23.
19. BVF 522.32 (1995). Tekniska bestämmelser, sliprar av betong (Technical Regulations, Concrete Sleepers. In Swedish). Banverket, Borlänge. pp. 6+2.
20. BV Bärighet (2000). Bärighetsberäkning av järnvägsbroar. (Assessment of Railway Bridges. In Swedish). Handbok BVH 583.11. Banverket, CB, Borlänge 2000-03-01. pp. 108 + 6 bilagor.
21. Balázs, L. György (1991). Fatigue of bond. ACI Material Journal (Detroit), Vol 88, No 6. pp. 620-629.

Appendix A

Result from Tensile Fatigue Tests

A Result from Tensile Fatigue Tests

Table of Contents

A.1 Factorial Design

There are several experimental strategies that can be used. In Montgomery (2001) factorial design is described as a strategy where the involved factors are varied together instead of e.g. one at a time. One big advantage with it is that it considers interactions between the factors. Factorial design is in other words said to be a suitable method to examine if a factor has an influence on a specific variable or not. Montgomery (2001) writes that factorial design means that in each complete replication of the experiment all possible combinations of the studied levels of the examined factors are investigated. Montgomery exemplifies it as: if there are a levels of factor A and b levels of factor B, each replicate contains all ab treatment combinations. When factors are arranged in factorial design they are often said to be crossed. Montgomery further writes that the effect of a factor is defined to be a change in the response produced by a change in the level of the factor. Since this refers to the primary factors of interest in the experiment, it is often called a main effect. In a two-factor factorial experiment the levels are denoted with low (-) and high (+), this could also be written as a "2^2-factorial design" and in a more general form "2^k-factorial design", where the "2" is the number of levels and the "k" represents the number of factors. In an analysis it is also assumed that the factors are fixed, the design is randomised and the factors are normally distributed. Often statistic software is used to set-up and analyse 2^k-factorial designs. In this analysis the computer software Statgraphics (by Statistical Graphics Corp.) has been used.

In Figure A.1 the method is explained with an example and for a more thorough explanation of the theory of factorial design see Montgomery (2001). In Figure A.1a the test matrix is shown.

The example is a 2^2 factorial design that consists of two factors, 1 and 2, varied at two levels, high and low. The tests are replicated twice and the response is called *Y*. In Figure A.1b to Figure A.1d the results are presented from an analysis with the help of the software Statgraphics. In Figure A.1b a so-called Pareto chart, a bar chart, is presented where each factor is represented with a horizontal bar. There is also a vertical line that is used to test the significance of the effect, here the significance level, α, equal to 5% has been chosen. If any bar stretches beyond this line the factor has a significant influence on the result. In this case both factor 1 and 2 separately have a significant influence on the result but they are independent of each other (no interaction). In a main effects plot, see Figure A.1c, the effect on the response *Y* from each tested factor is shown. It can be seen from the example that a lower value of factor 1 gives a lower value of *Y* than keeping it at a high level. In Figure A.1d the interaction plot, where the response variable for each combination of factor 1 and 2 is shown. From the example it is shown that there is no interaction between the factors (the two lines would then cross each other). The example gives that if factor 1 is high and factor 2 is low it results in a *Y* equal to 35. If factor 1 is kept at a high level and factor 2 is also high it results in a *Y* equal to 30.

Run	Factor		Treatment	Response
	One	Two	combination	
1	+	-	1 high, 2 low	37
2	-	+	1 low, 2 high	19
3	+	+	1 high, 2 high	32
4	-	-	1 low, 2 low	27
5	+	+	1 high, 2 high	29
6	-	-	1 low, 2 low	26
7	+	-	1 high, 2 low	33
8	-	+	1 low, 2 high	18

a)

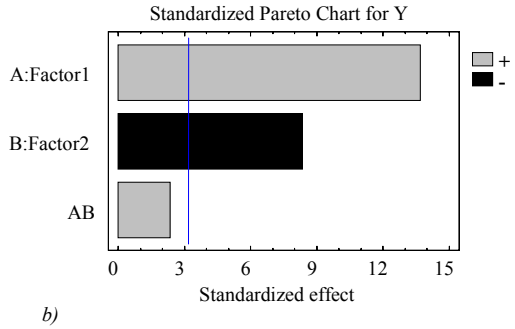

b)

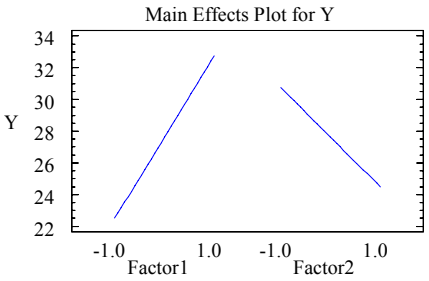

c)

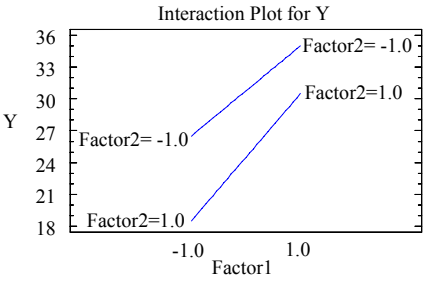

d)

Figure A.1 Factorial design according to Montgomery (2001). a) Example matrix, b) Results from analysis in Statgraphics – Pareto chart, c) Results from analysis in Statgraphics – Main effects plot and d) Results from analysis in Statgraphics – interaction plot.

Which of the two varied factors, i.e. the load level or the amplitude, has the highest influence on the number of load cycles to failure for newly cast concrete? In Figure A.2 the result from the analysis performed with factorial design is presented. The Pareto chart in Figure A.2a shows that none of the two factors, neither the amplitude nor the load level, has a significant influence on the number of load cycles to failure – none of them reaches beyond the blue vertical line that represents a statistical significance at the 95 % confidence level. Nor is there any interaction for the two that have a significant influence on the result, see *AB*. One could say that they both have somewhat equal influence on the number of load cycles. In Figure A.2b, the main effects

plot, it is shown that if the load level is low it results in a high number of load cycles which is not surprising. The same could be said for the amplitude, i.e. a low amplitude results in a high number of load cycles. In this context it must be remembered that if the amplitude is too low the test becomes a test with sustained load. In the interaction plot, Figure A.2c, it is shown that no interaction is shown for the two. A high load level and a high amplitude give the lowest number of cycles to failure. It is also shown that a low load level and a high amplitude give approximately the same number of load cycles as if the load level is high and the amplitude is low.

With the help of the results from this analysis it is not possible to say which one of the two factors that has the highest influence on the number of load cycles to failure.

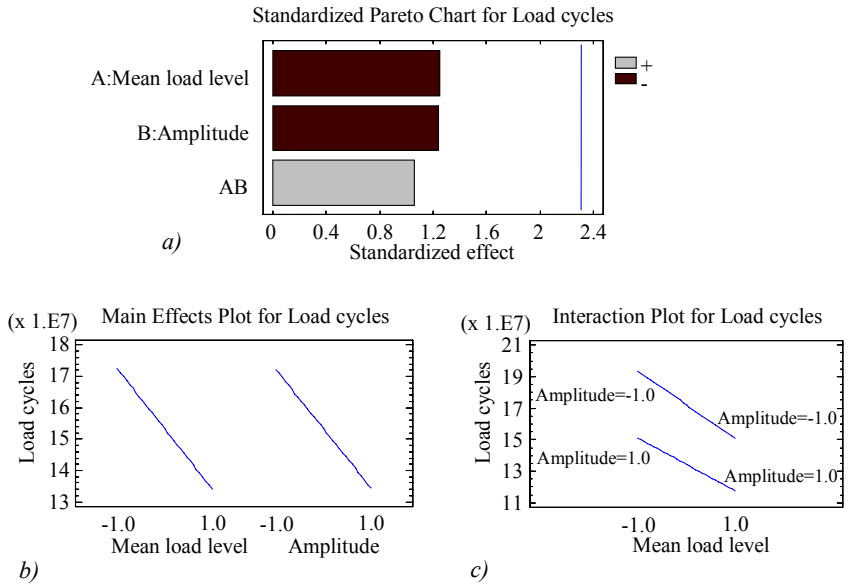

Figure A.2 Results from analysis with factorial design in Statgraphics. a) A Pareto chart, b) the Main effects plot and c) the Interaction plot.

A.2 Results from Tensile Fatigue Tests and Uniaxial Tests

In this section results from the fatigue tests are presented. The normalized mean deformation development from the fatigue test for the four COD-gauges is shown to the left in each figure. This curve is compared with the normalized mean static deformation-stress curve (to the right) obtained in the uniaxial tensile tests.

For specimens no. L13 and L15 fatigue failure did not occur. They were stopped at 1 522 201 and 1 166 000 load cycles and their fatigue curves are presented in Figure A.21 and Figure A.23. In these figures it is shown that these tests have been very influenced by, most likely, a temperature change during the tests. The same occurred for test no. L5 but in this case it was possible to temperature compensate it, see Thun (2006e), since the difference between the measured temperature-trend-curve a few hours before the tests started and the conditions during the actual tests were not too big. For specimens no. 20, L7 and L16 fatigue failure did not occur. They were stopped at 5 000 000, 2 050 001 and 7 077 000 load cycles and due to very large file size no fatigue curves have been possible to present. They would probably look like e.g. L5.

A.2.1 New Concrete

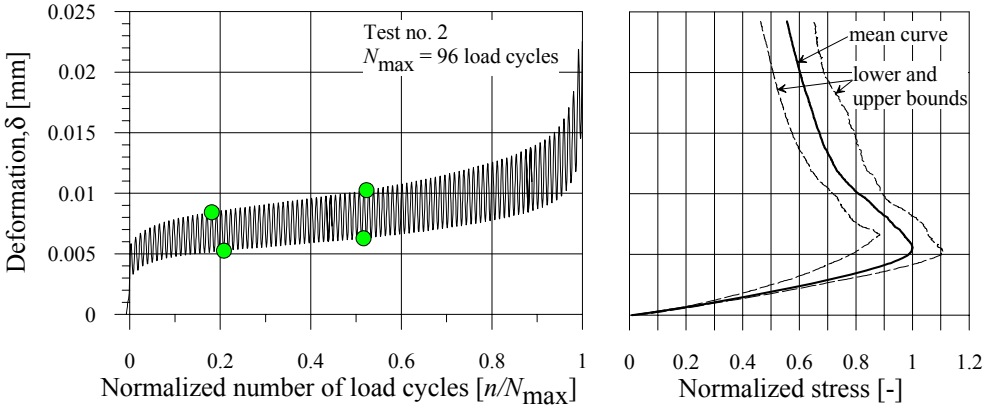

Figure A.3 Result from the cyclic tensile fatigue test of specimen 2.

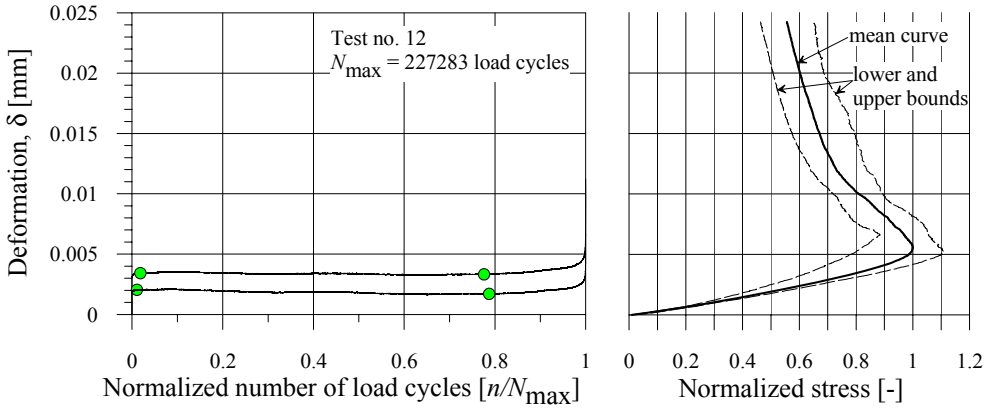

Figure A.4 Result from the cyclic tensile fatigue test of specimen 12.

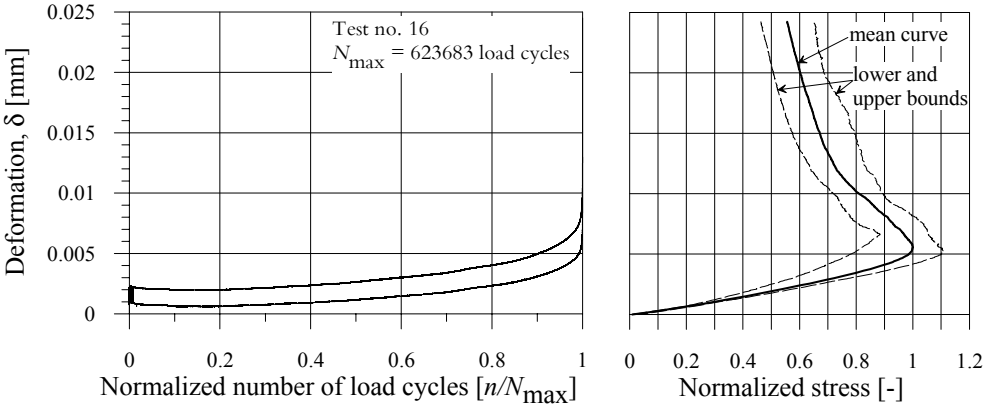

Figure A.5 Result from the cyclic tensile fatigue test of specimen 16.

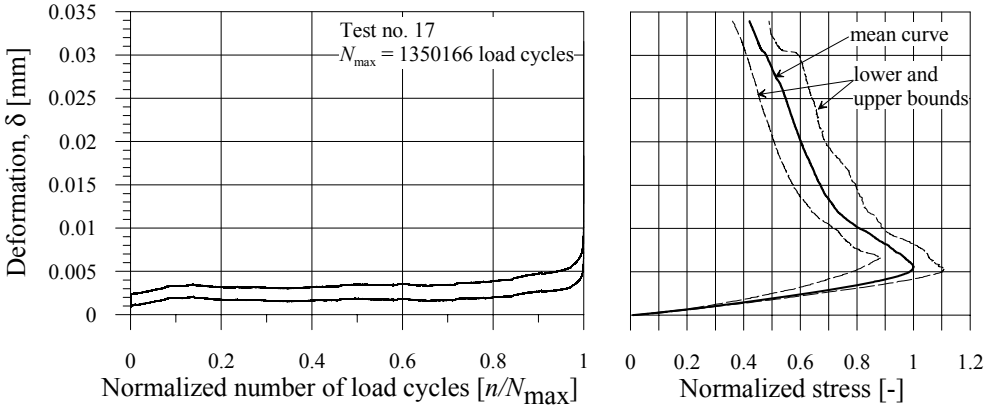

Figure A.6 Result from the cyclic tensile fatigue test of specimen 17.

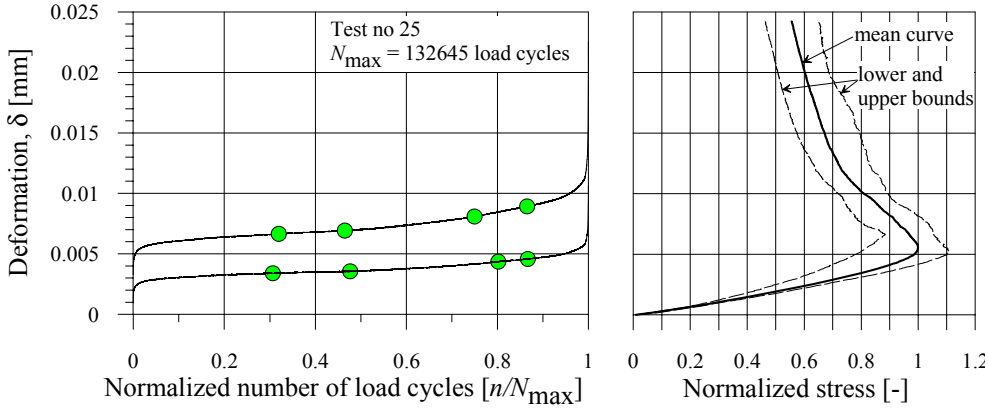

Figure A.7 Result from the cyclic tensile fatigue test of specimen 25.

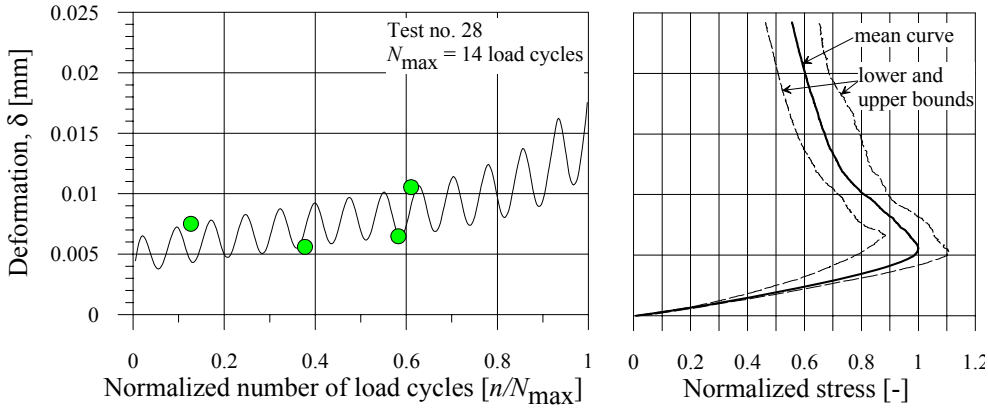

Figure A.8 Result from the cyclic tensile fatigue test of specimen 28.

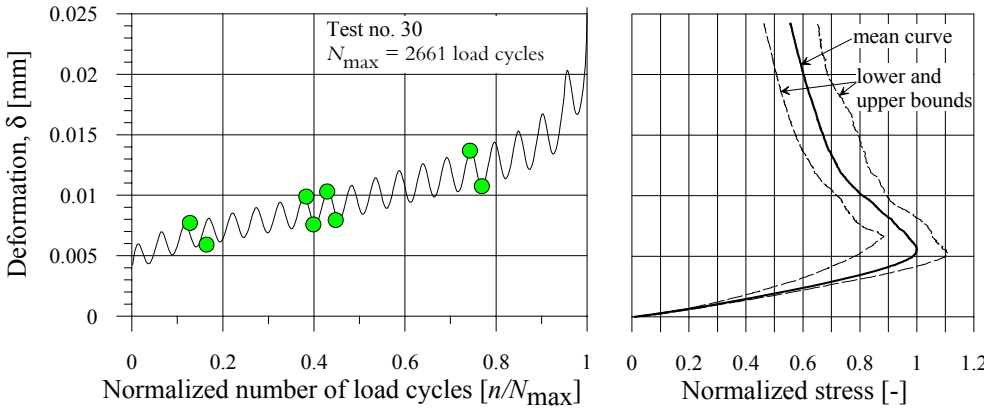

Figure A.9 Result from the cyclic tensile fatigue test of specimen 30.

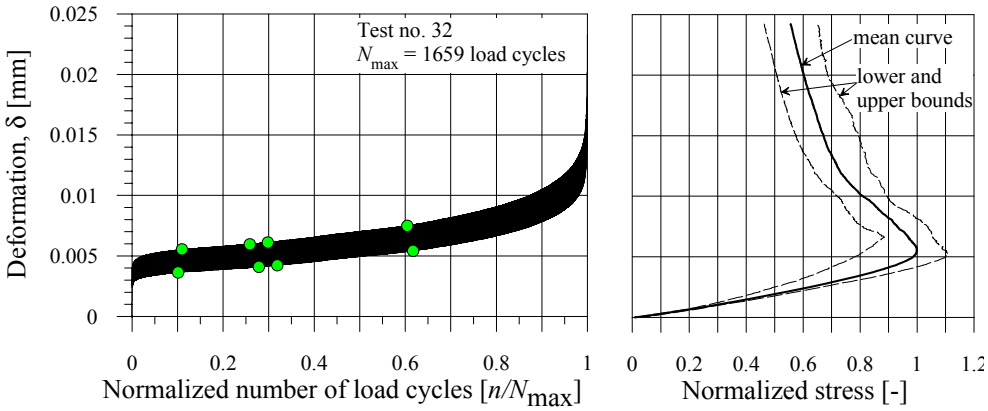

Figure A.10 Result from the cyclic tensile fatigue test of specimen 32.

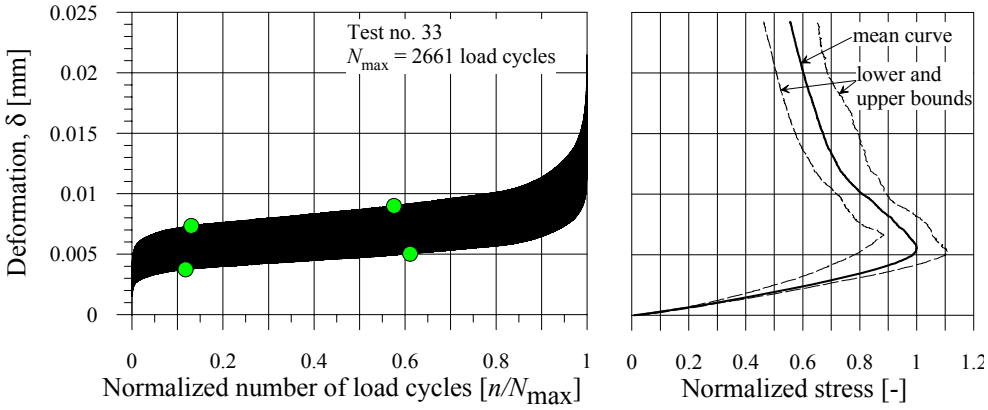

Figure A.11 Result from the cyclic tensile fatigue test of specimen 33.

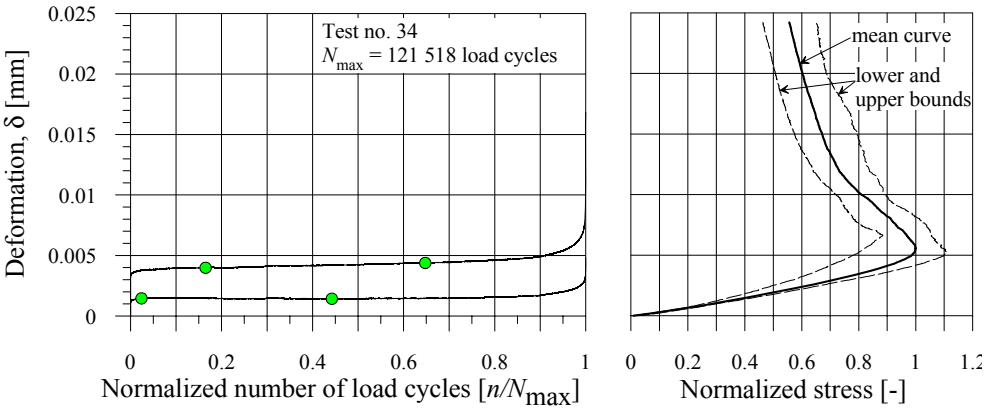

Figure A.12 Result from the cyclic tensile fatigue test of specimen 34.

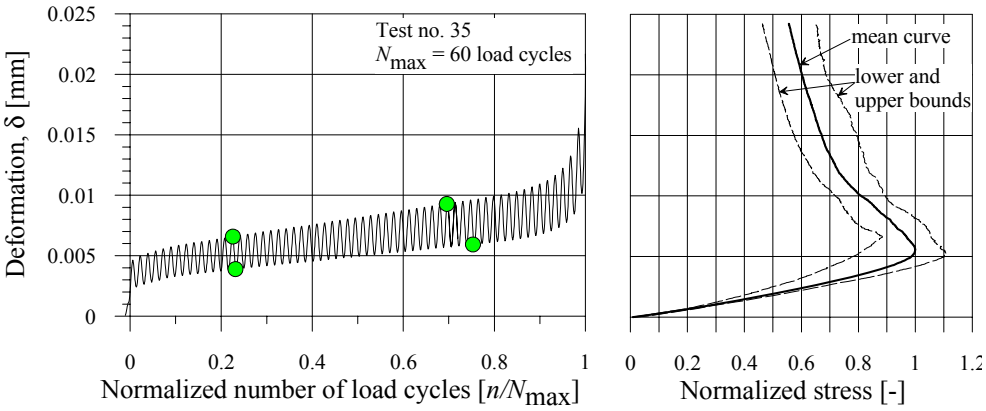

Figure A.13 Result from the cyclic tensile fatigue test of specimen 35.

A.2.2 Old Concrete

The concrete specimens are drilled from an old railway bridge - the Lautajokki Bridge.

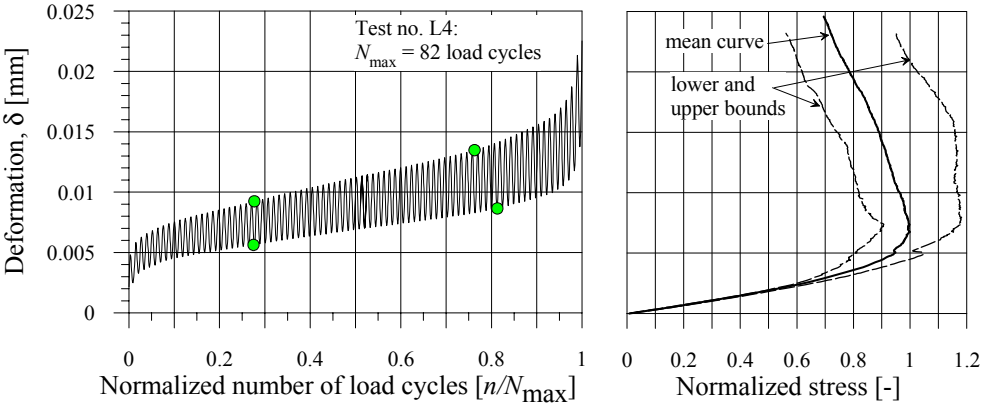

Figure A.14 Result from the cyclic tensile fatigue test of specimen L4.

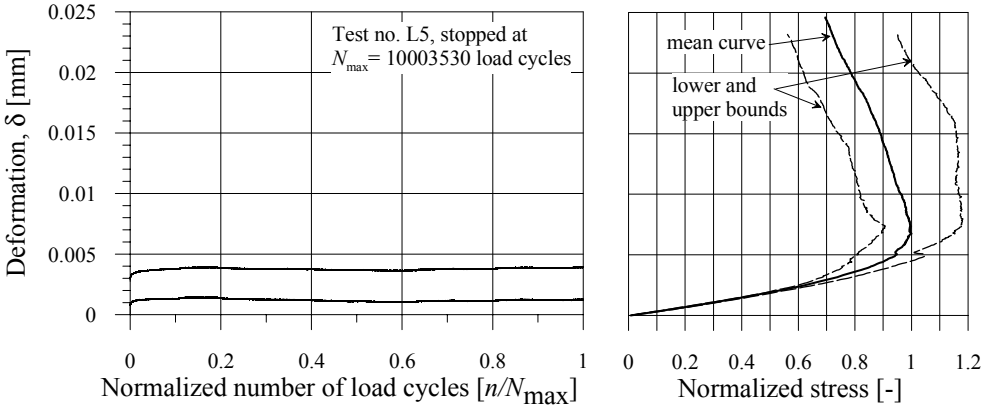

Figure A.15 Result from the cyclic tensile fatigue test of specimen L5.

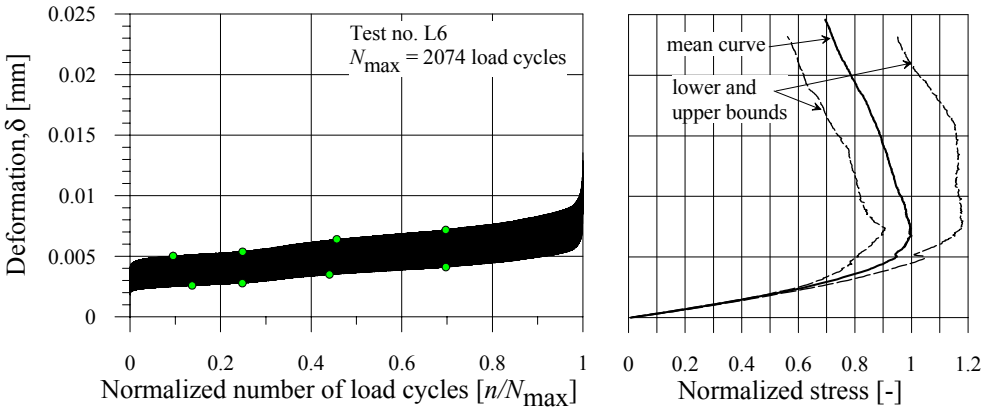

Figure A.16 Result from the cyclic tensile fatigue test of specimen L6.

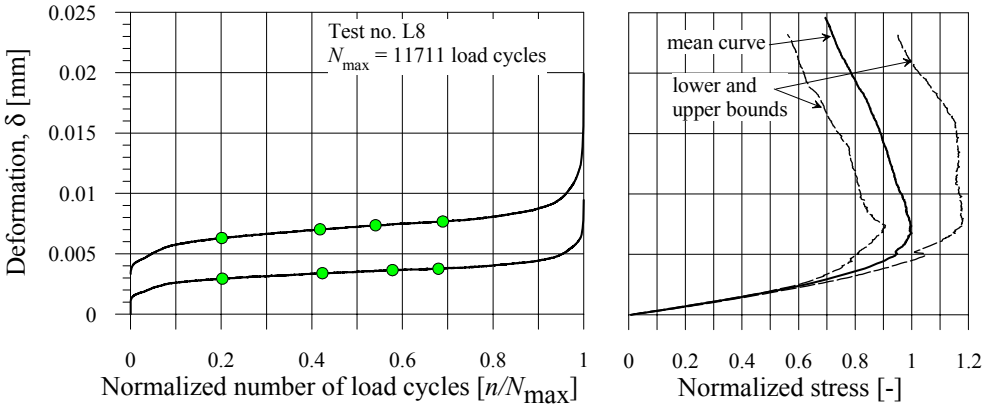

Figure A.17 Result from the cyclic tensile fatigue test of specimen L 8.

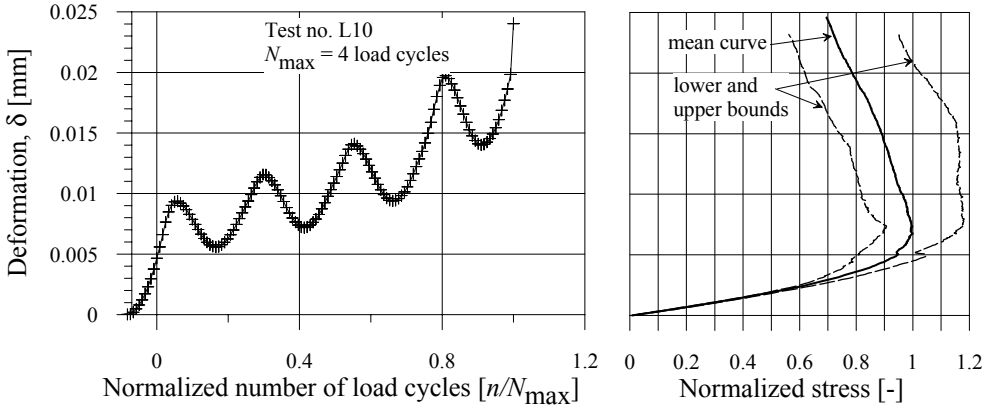

Figure A.18 Result from the cyclic tensile fatigue test of specimen L10.

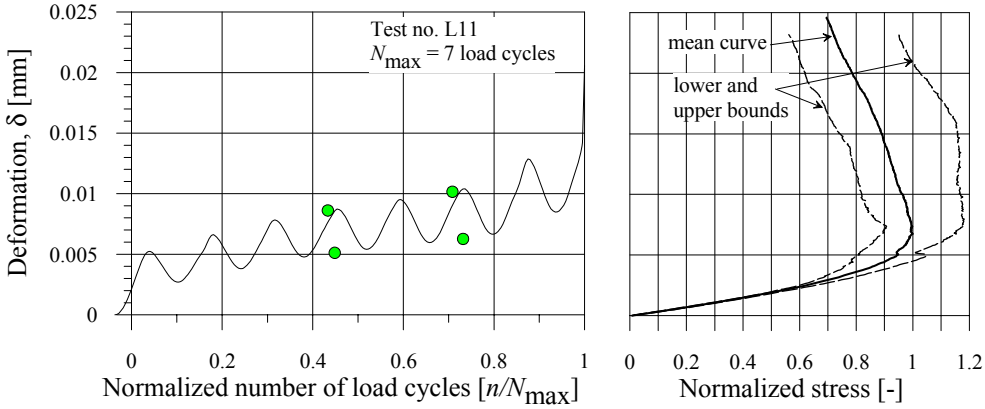

Figure A.19 Result from the cyclic tensile fatigue test of specimen L11.

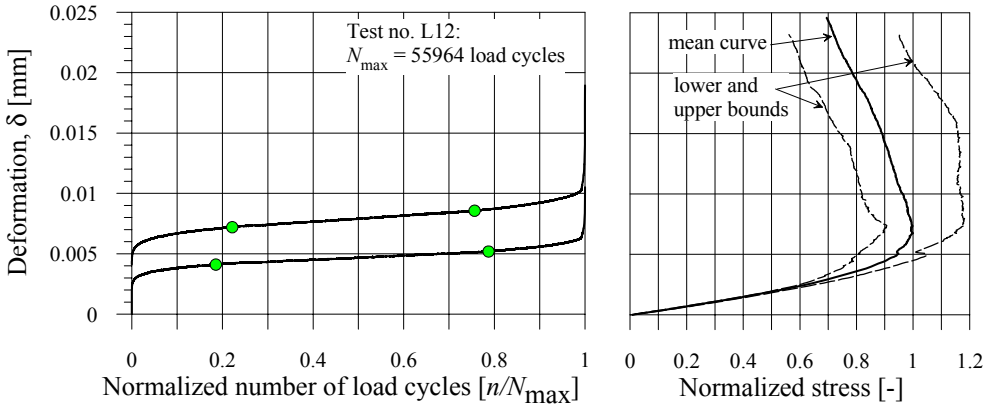

Figure A.20 Result from the cyclic tensile fatigue test of specimen L12.

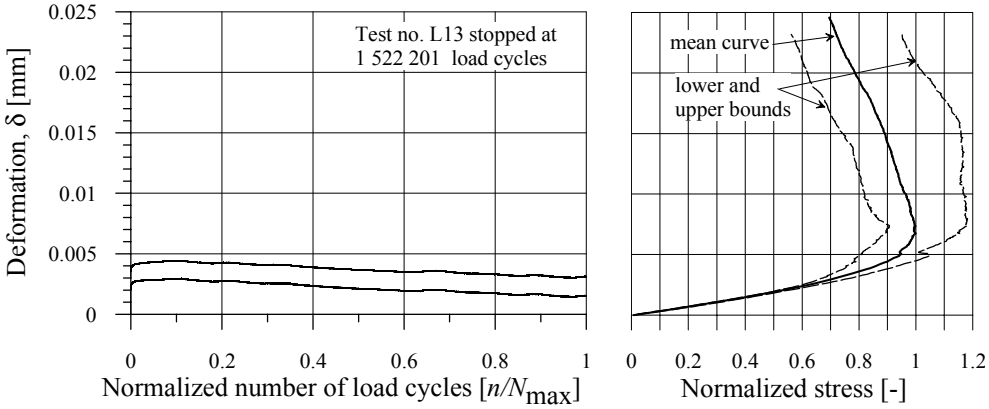

Figure A.21 Result from the cyclic tensile fatigue test of specimen L13.

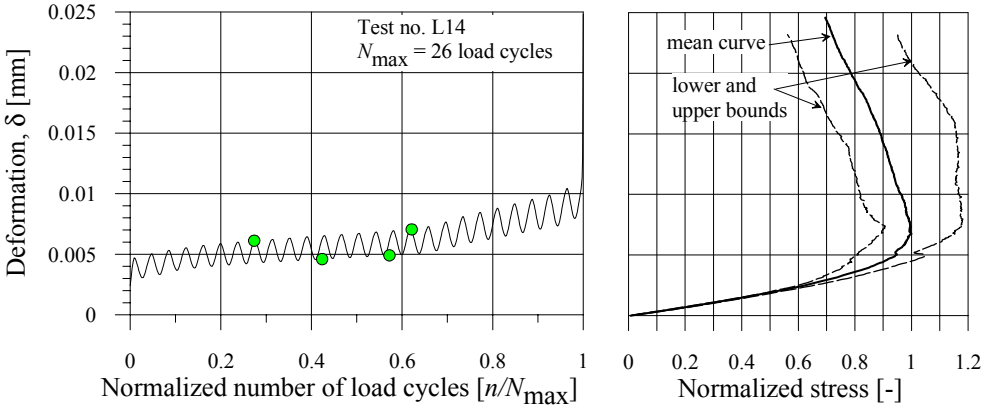

Figure A.22 Result from the cyclic tensile fatigue test of specimen L14.

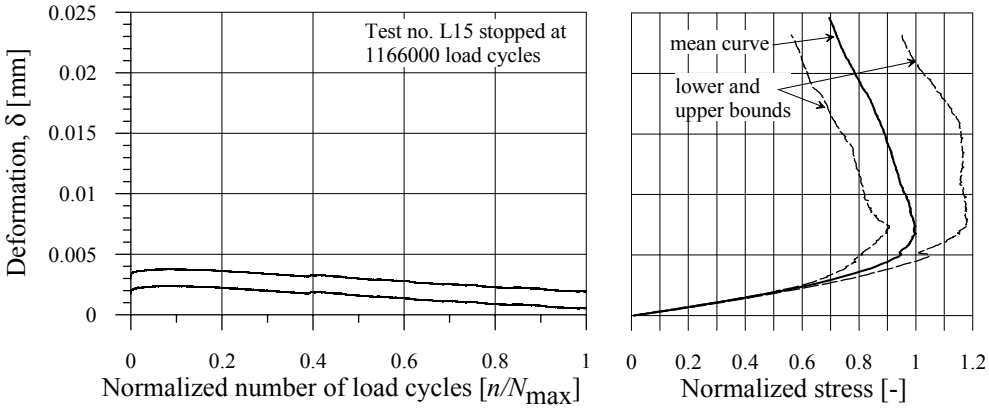

Figure A.23 Result from the cyclic tensile fatigue test of specimen L15.

A.2.3 References

Montgomery D.C. (2001). Design and Analysis of Experiments. 5th Ed. John Wiley & Sons, Inc. pp. 684. ISBN 0-471-31649-0

Möller G., Petersons N. and Elfgren L. (1994). Strength (Hållfasthet). Betonghandbok – Material utgåva 2. Avsnitt 11. Stockholm: Svensk Byggtjänst. ISBN:91-7332-709-3. pp. 132. In Swedish.

Thun (2006e). Paper E. Concrete Fatigue Capacity in Tension – a Study of Deformations. Assessment of Fatigue Resistance and Strength in Existing Concrete Structures. Doctoral Thesis 2006:65. Division of Structural Engineering, Department of Civil and Environmental Engineering, Luleå University of Technology, Luleå, Sweden. December 2006. ISBN 978-91-85685-03-5

A.3 Photographs of the Failure Surface of the Tested Specimens

In this section photographs of the failure surfaces of all specimens that have been tested are presented, except for test no. HTS1.

A.3.1 New Concrete

In general the failure surface of these specimens consists of some larger stones (~1×1 cm) which have loosened, some larger stones where the crack has passed through and a few visible air bubbles. This is considered to be "a normal failure surface". If the failure surface of the specimen deviates from this it is commented in the figure text.

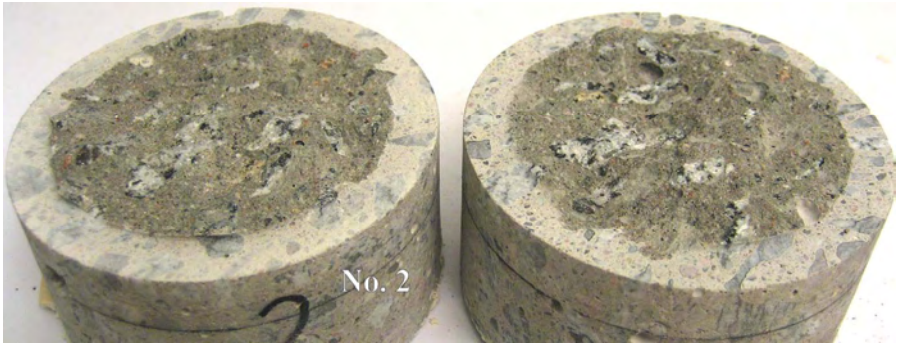

Figure A.24 Photograph showing the failure surface for test No. 2 after fatigue test.

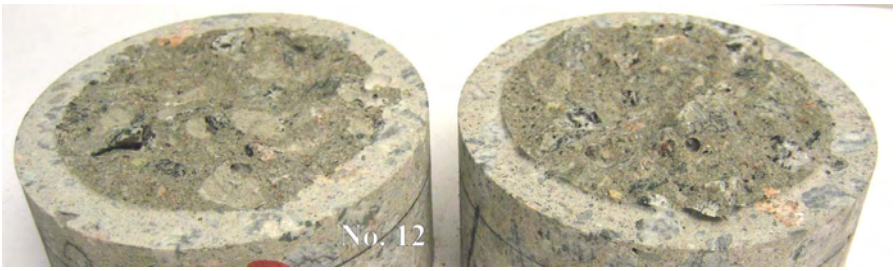

Figure A.25 Photograph showing the failure surface for test No. 12 after fatigue test.

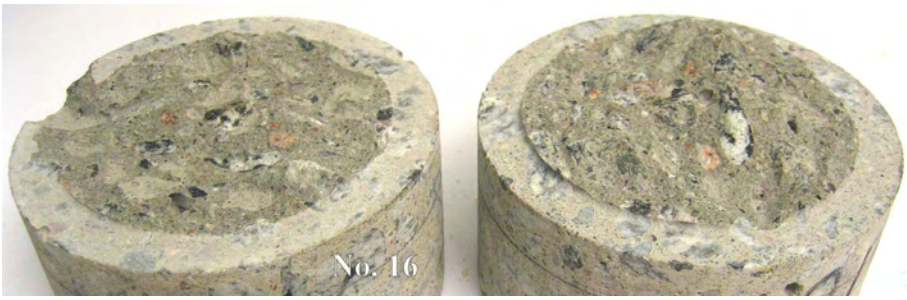

Figure A.26 Photograph showing the failure surface for test No. 16 after fatigue test. One larger stone has loosened from the notch.

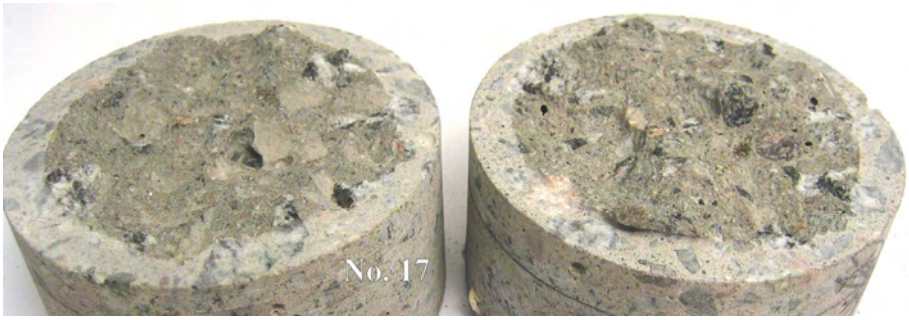

Figure A.27 Photograph showing the failure surface for test No. 17 after fatigue test.

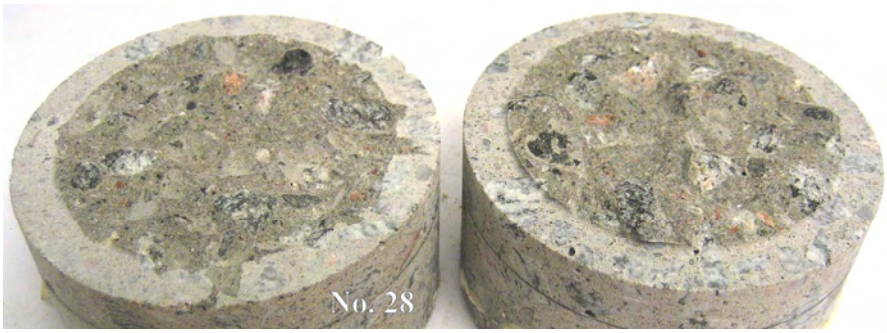

Figure A.28 Photograph showing the failure surface for test No. 28 after fatigue test.

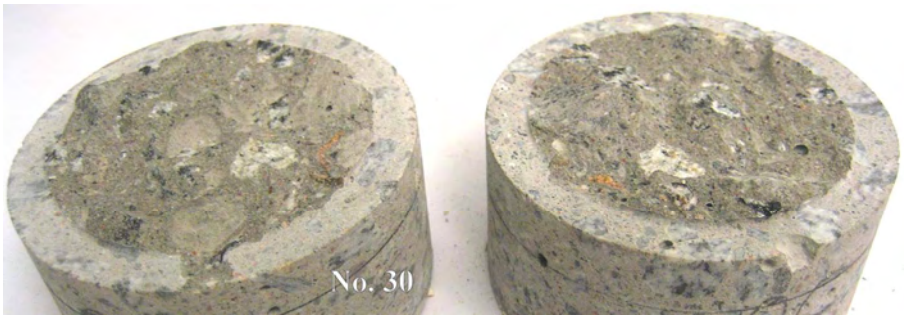

Figure A.29 Photograph showing the failure surface for test No. 30 after fatigue test.

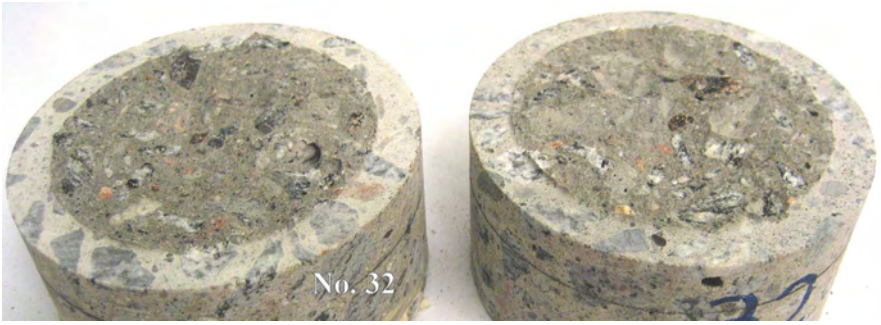

Figure A.30 Photograph showing the failure surface for test No. 32 after fatigue test.

Figure A.31 Photograph showing the failure surface for test No. 33 after fatigue test.

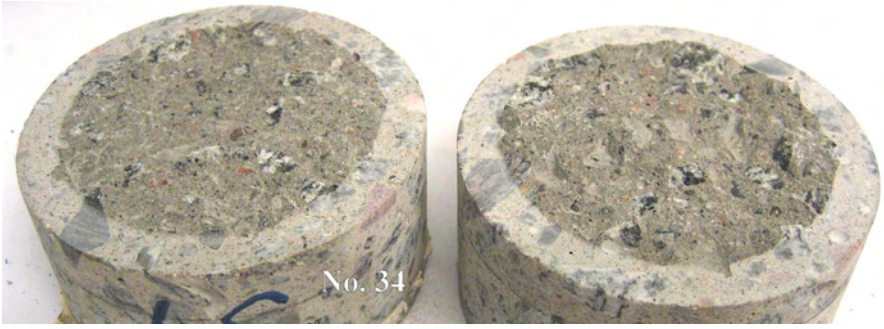

Figure A.32 Photograph showing the failure surface for test No. 34 after fatigue test.

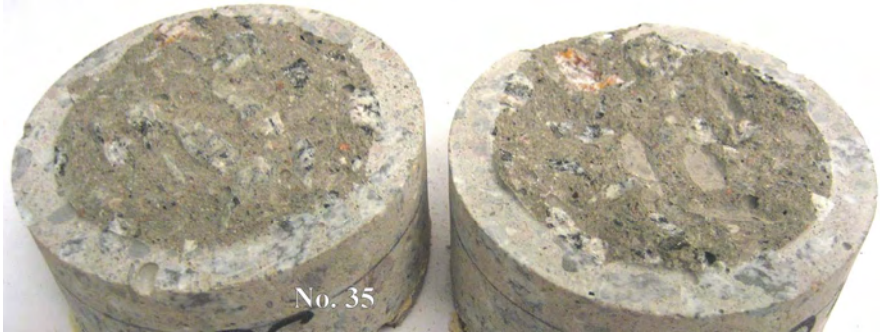

Figure A.33 Photograph showing the failure surface for test No. 35 after fatigue test.

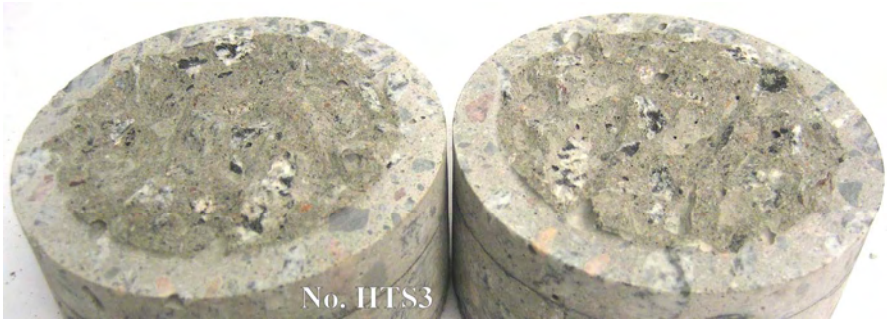

Figure A.34 Photograph showing the failure surface for test No. HTS3 after tensile test.

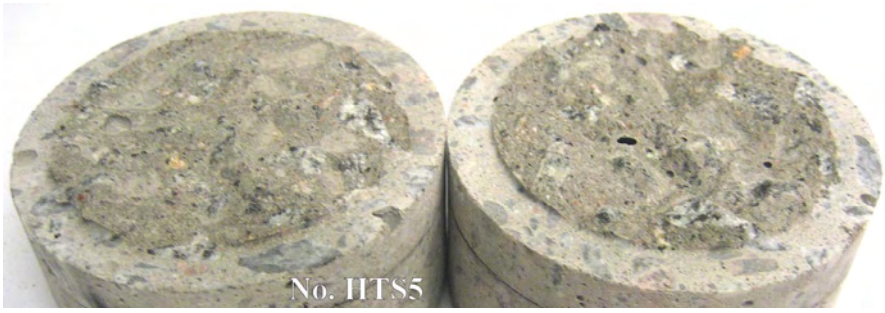

Figure A.35 Photograph showing the failure surface for test No. HTS5 after tensile test.

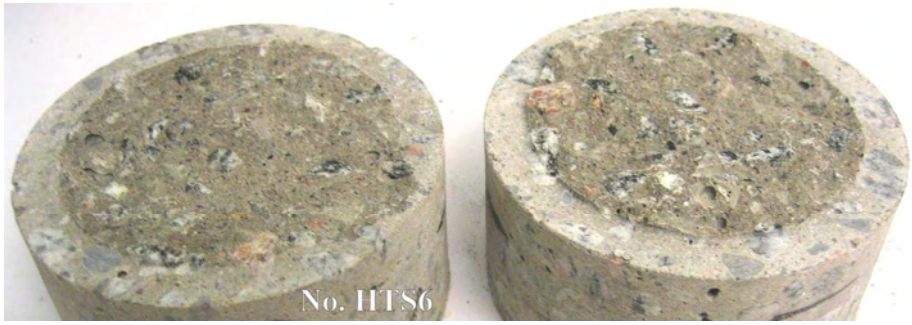

Figure A.36 Photograph showing the failure surface for test No. HTS6 after tensile test.

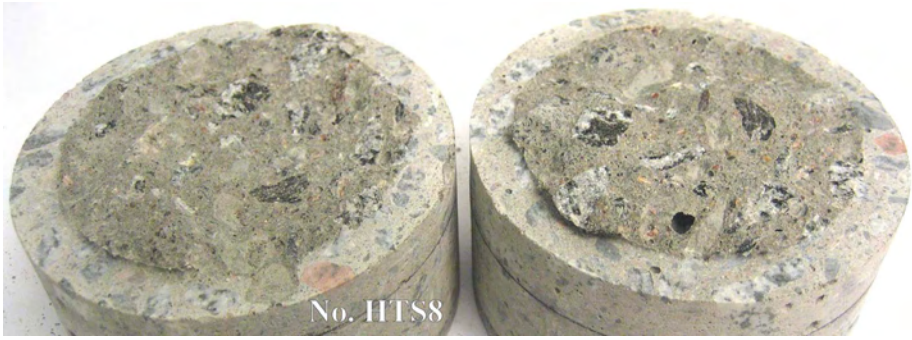

Figure A.37 Photograph showing the failure surface for test No. HTS8 after tensile test.

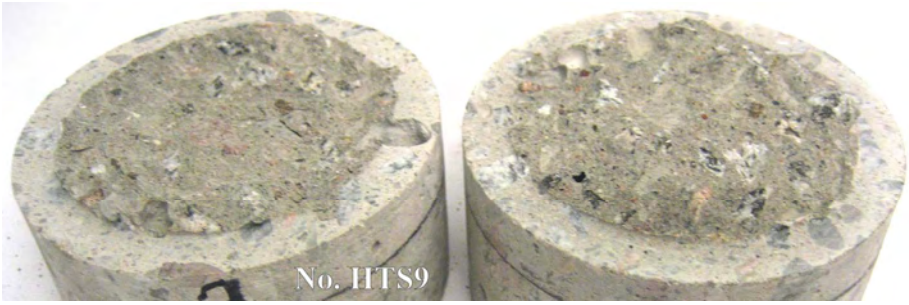

Figure A.38 Photograph showing the failure surface for test No. HTS9 after tensile test.

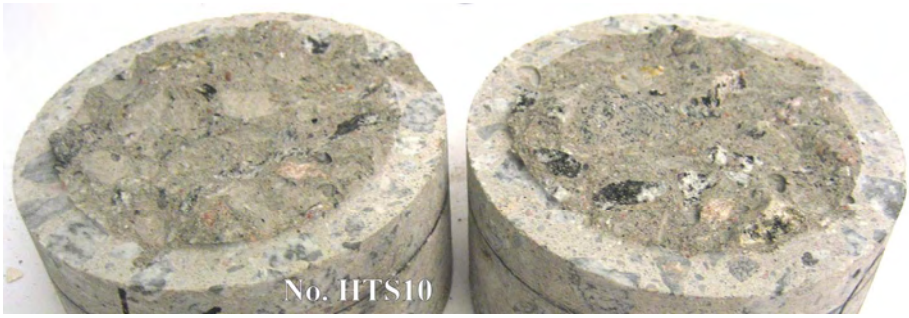

Figure A.39 Photograph showing the failure surface for test No. HTS10 after tensile test.

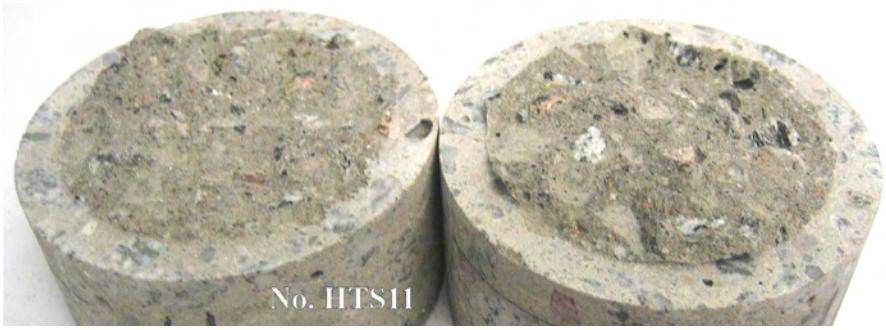

Figure A.40 Photograph showing the failure surface for test No. HTS11 after tensile test.

A.3.2 Old Concrete

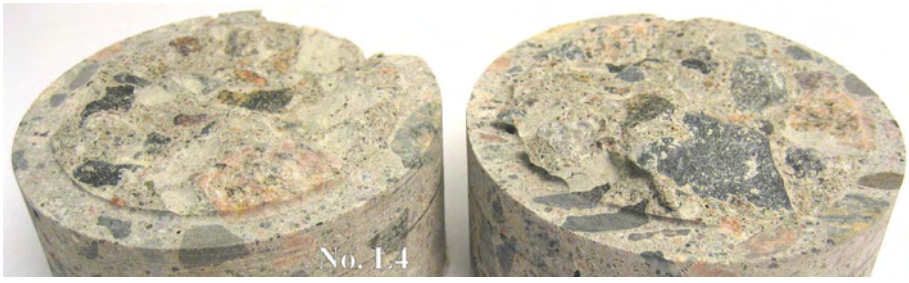

Figure A.41 Photograph showing the failure surface for test No. L4 after fatigue test. A part of the notch has loosened.

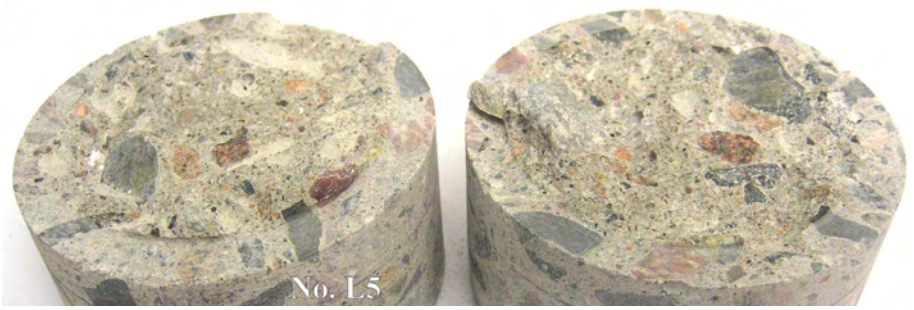

Figure A.42 Photograph showing the failure surface for test No. L5 after fatigue test.

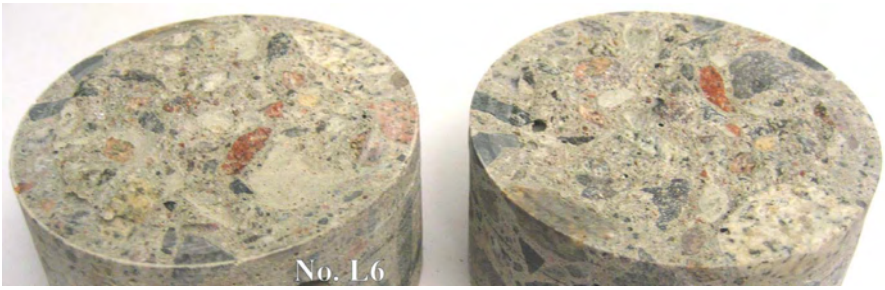

Figure A.43 Photograph showing the failure surface for test No. L6 after fatigue test.

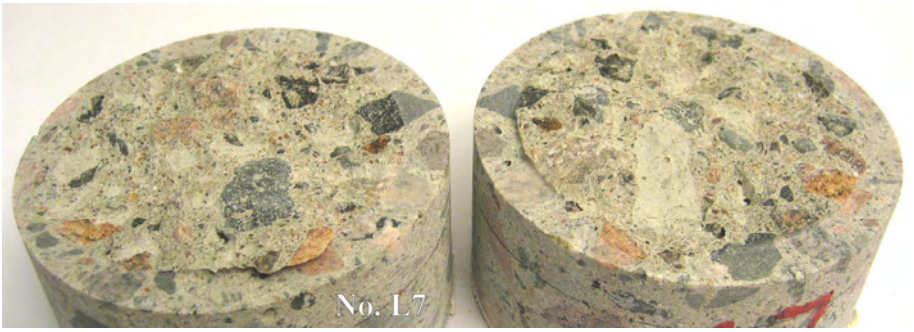

Figure A.44 Photograph showing the failure surface for test No. L7 after fatigue test.

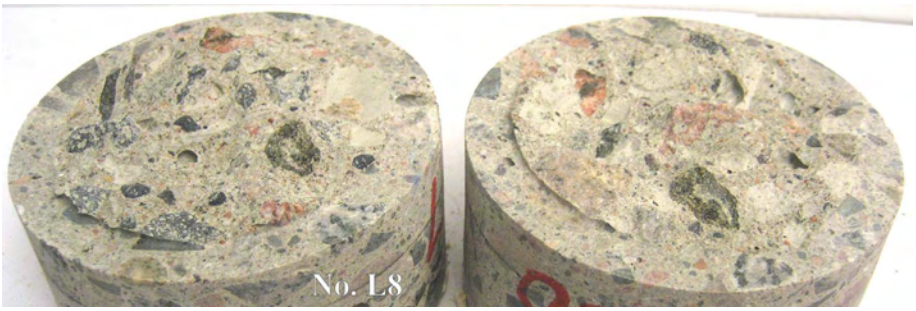

Figure A.45 Photograph showing the failure surface for test No. L8 after fatigue test.

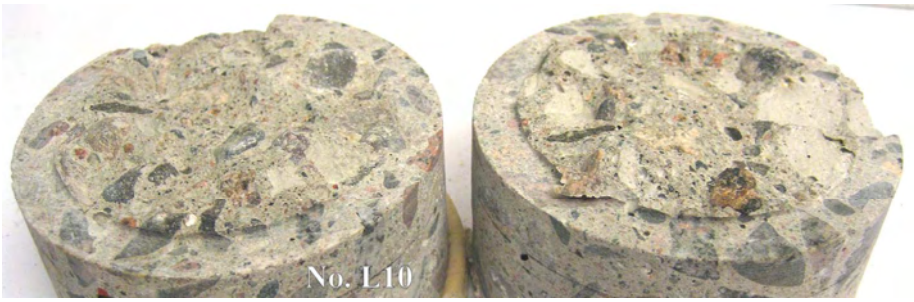

Figure A.46 Photograph showing the failure surface for test No. L10 after fatigue test. A part (1/7) of the notch has loosened.

Figure A.47 Photograph showing the failure surface for test No. L11 after fatigue test.

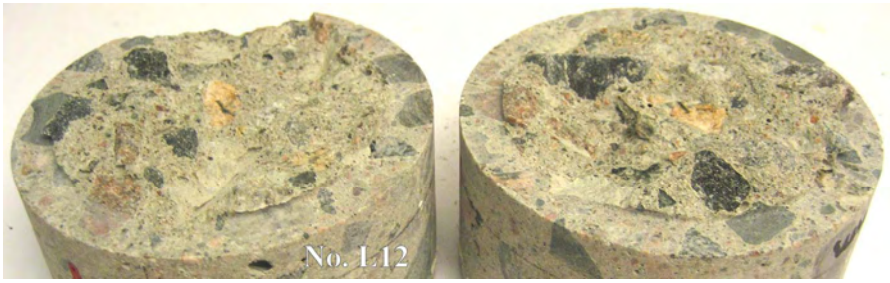

Figure A.48 Photograph showing the failure surface for test No. L12 after fatigue test. A part (1/5) of the notch has loosened.

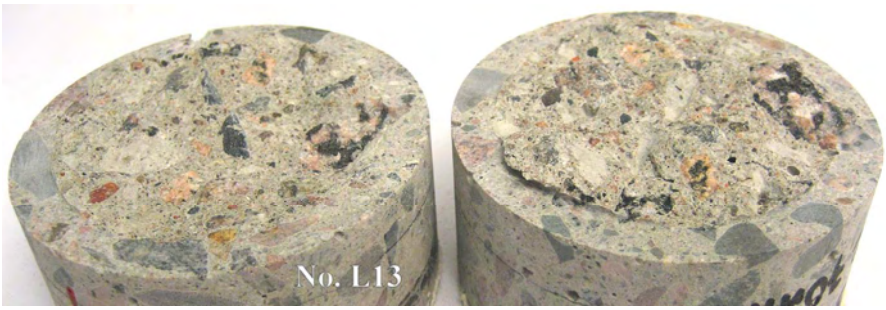

Figure A.49 Photograph showing the failure surface for test No. L13 after fatigue test.

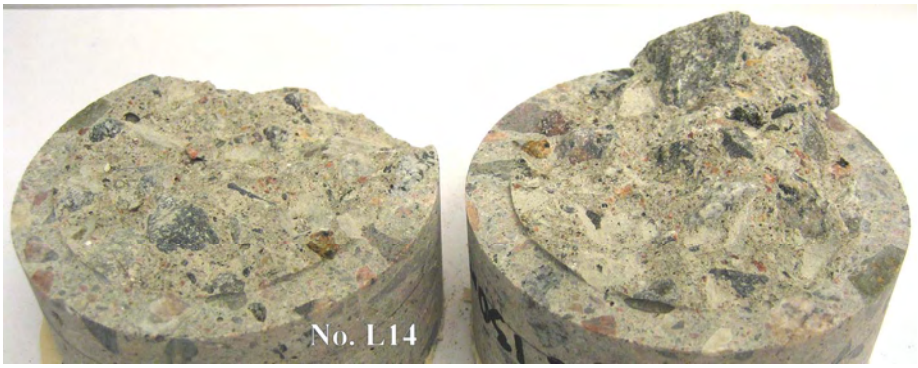

Figure A.50 Photograph showing the failure surface for test No. L14 after fatigue test. Very large stone in the notch. 1/3 of the notch has loosened.

Figure A.51 Photograph showing the failure surface for test No. L15 after fatigue test.

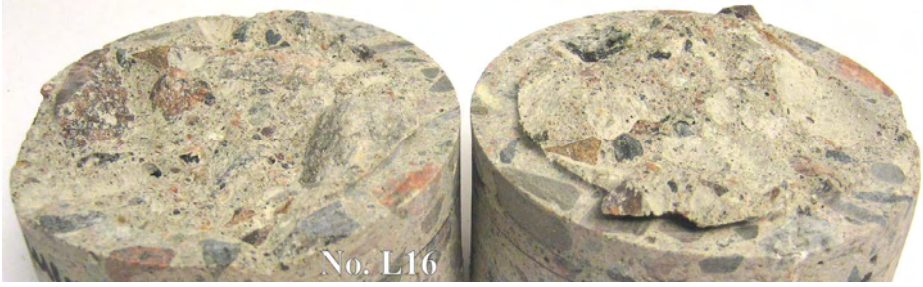

Figure A.52 Photograph showing the failure surface for test No. L16 after fatigue test.

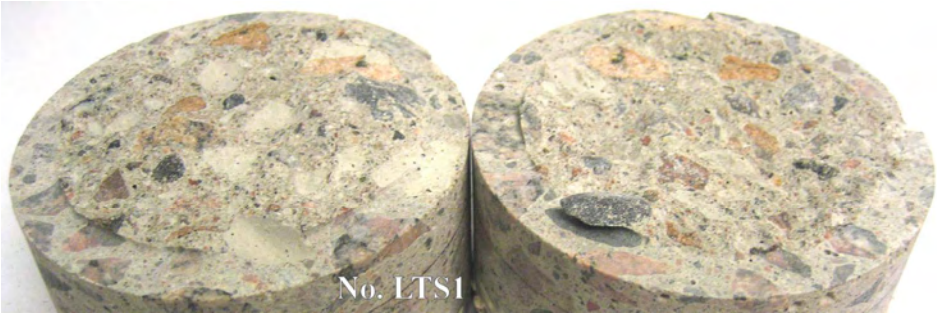

Figure A.53 Photograph showing the failure surface for test No. LTS1 after tensile test.

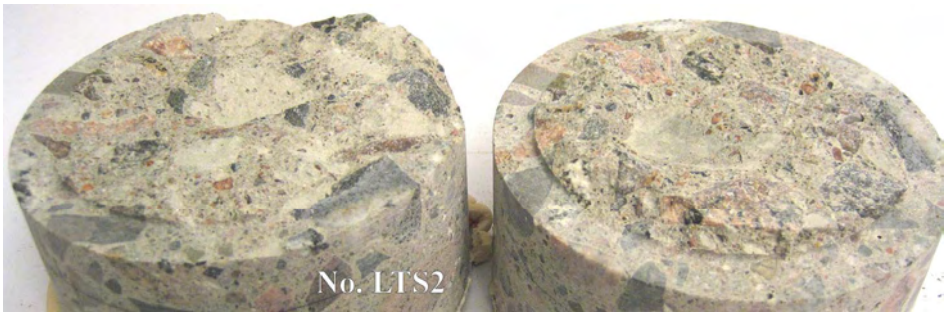

Figure A.54 Photograph showing the failure surface for test No. LTS3 after tensile test.

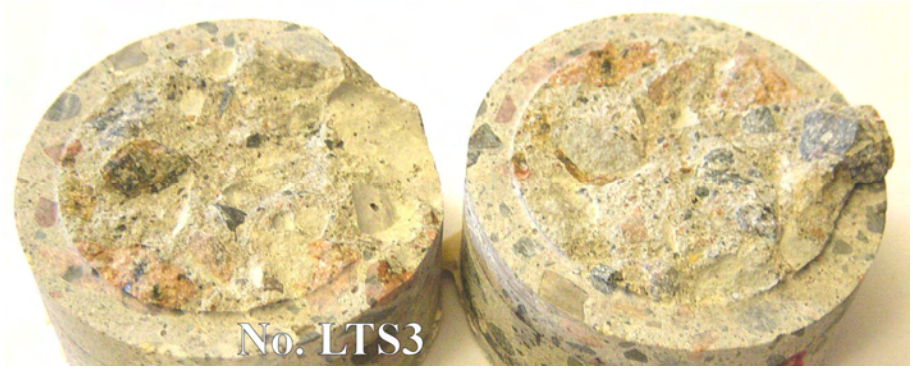

Figure A.55 Photograph showing the failure surface for test No. LTS3 after tensile test. Large stone in the notch. 1/4 of the notch loosened.

DOCTORAL AND LICENTIATE THESES

Division of Structural Engineering, Luleå University of Technology

Doctoral Theses

Ulf Arne Girhammar (1980). Dynamic Fail-Safe Behaviour of Steel Structures. Doctoral Thesis 1980:060D. 309 pp.

Kent Gylltoft (1983). Fracture Mechanics Models for Fatigue in concrete Structures. Doctoral Thesis 1983:25D. 210 pp.

Thomas Olofsson (1985). Mathematical Modelling of Jointed Rock Masses. In collaboration with the Division of Rock Mechanics. Doctoral Thesis 1985:42D, 143 pp.

Lennart Fransson (1988). Thermal ice pressure on structures in ice covers. Doctoral Thesis 1988:67D. 161 pp.

Mats Emborg (1989). Thermal stresses in concrete structures at early ages. Doctoral Thesis 1989:73D. 285 pp.

Lars Stehn (1993). Tensile fracture of ice. Test methods and fracture mechanics analysis. Doctoral Thesis 1993:129D, September 1993, 136 pp.

Björn Täljsten (1994). Plate Bonding. Strengthening of existing concrete structures with epoxy bonded plates of steel or fibre reinforced plastics. Doctoral Thesis 1994:152D, August 1994, 283 pp.

Jan-Erik Jonasson (1994). Modelling of temperature, moisture and stresses in young concrete. Doctoral Thesis 1994:153D, August 1994, 227 pp.

Ulf Ohlsson (1995). Fracture Mechanics Analysis of Concrete Structures. Doctoral Thesis 1995:179D, December 1995, 98 pp.

Keivan Noghabai (1998). Effect of Tension Softening on the Performance of Concrete Structures. Doctoral Thesis 1998:21, August 1998, 150 pp.

Gustaf Westman (1999). Concrete Creep and Thermal Stresses. New creep models and their effects on stress development. Doctoral Thesis 1999:10, May 1999, 301 pp.

Henrik Gabrielsson (1999). Ductility in High Performance Concrete Structures. An experimental investigation and a theoretical study of prestressed hollow core slabs and prestressed cylindrical pole elements. Doctoral Thesis 1999:15, May 1999, 283 pp.

Groth, Patrik (2000). Fibre Reinforced Concrete – Fracture Mechanics Methods Applied on Self-Compacting Concrete and Energetically Modified Binders. Doctoral Thesis 2000:04, January 2000, 214 pp. ISBN 978-91-85685-00-4.

Hans Hedlund (2000). Hardening concrete. Measurements and evaluation of non-elastic deformation and associated restraint stresses. Doctoral Thesis 2000:25, December 2000, 394 pp ISBN 91-89580-00-1.

Anders Carolin (2003). Carbon Fibre Reinforced Polymers for Strengthening of Structural Members. Doctoral Thesis 2003:18, June 2003, ISBN 91-89580-04-4. 190 pp.

Martin Nilsson (2003). Restraint Factors and Partial Coefficients for Crack Risk Analyses of Early Age Concrete Structures. Doctoral Thesis 2003:19, June 2003, ISBN: 91-89580-05-2, 170 pp.

Mårten Larson (2003). Thermal Crack Estimation in Early Age Concrete – Models and Methods for Practical Application. Doctoral Thesis 2003:20, June 2003, ISBN 91-86580-06-0. 190 pp.

Erik Nordström (2005). Durability of Sprayed Concrete. Steel fibre corrosion in cracks. Doctoral Thesis 2005:02, January 2005, ISSN 1402-1544. 151 pp. ISBN 978-91-85685-01-1.

Rogier Jongeling (2006). A Process Model for Work-Flow Management in Construction. Combined use of Location-Based Scheduling and 4D CAD. Doctoral Thesis 2006:47, October 2006, ISSN 1402-1544. 191 pp. ISBN 978-91-85685-02-8

Carlswärd J (2006). Shrinkage cracking of steel fibre reinforced self compacting concrete overlays – Test methods and theoretical modelling. Doctoral Thesis 2006:55. Division of Structural Engineering, Department of Civil and Environmental Engineering, Luleå University of Technology, Luleå, Sweden. December 2006. pp. 250. ISBN 978-91-85685-04-2

Licentiate Theses

Lennart Fransson (1984). Bärförmåga hos ett flytande istäcke. Beräkningsmodeller och experimentella studier av naturlig is och av is förstärkt med armering. Licentiate Thesis 1984:012L.

Mats Emborg (1985). Temperature stresses in massive concrete structures. Viscoelastic models and laboratory tests. Licentiate Thesis 1985:011L, May 1985, rev November 1985, 163 pp.

Christer Hjalmarsson (1987). Effektbehov i bostadshus. Experimentell bestämning av effektbehov i små- och flerbostadshus. Licentiate Thesis 1987:009L, October 1987, 72 p.

Björn Täljsten (1990). Förstärkning av betongkonstruktioner genom pålimning av stålplåtar. Licentiate Thesis 1990:06L, May 1990.

Ulf Ohlsson (1990). Fracture Mechanics Studies of Concrete Structures. Licentiate Thesis 1990:07L, May 1990, 8+12+18+7+21 pp.

Lars Stehn (1991). Fracture Toughness of sea ice. Development of a test system based on chevron notched specimens. Licentiate Thesis 1991:11L, September 1990, 88 pp.

Per Anders Daerga (1992). Some experimental fracture mechanics studies in mode I of concrete and wood. Licentiate Thesis 1992:12L, 1ed April 1992, 2ed June 1992, 81 pp.

Henrik Gabrielsson (1993). Shear capacity of beams of reinforced high performance concrete. Licentiate Thesis 1993:21L, May 1993, 109 pp. 18 June.

Keivan Noghabai (1995). Splitting of concrete in the anchoring zone of deformed bars. A fracture mechanics approach to bond. Licentiate Thesis 1995:26L, May 1995, 123 pp.

Gustaf Westman (1995). Thermal cracking in high performance concrete. Viscoelastic models and laboratory tests. Licentiate Thesis 1995:27L, May 1995, 125 pp.

Katarina Ekerfors (1995). Mognadsutveckling i ung betong. Temperaturkänslighet, hållfasthet och värmeutveckling. Licentiate Thesis 1995:34L, October 1995, 137 pp.

Patrik Groth (1996). Cracking in concrete. Crack prevention with air-cooling and crack distribution with steel fibre reinforcement. Licentiate Thesis 1996:37L, October 1996, 128 pp.

Hans Hedlund (1996). Stresses in High Performance Concrete due to Temperature and Moisture Variations at Early Ages. Licentiate Thesis 1996:38L, October 1996, 240 pp.

Mårten Larson (2000). Estimation of Crack Risk in Early Age Concrete. Simplified methods for practical use. Licentiate Thesis 2000:10, April 2000, 170 pp.

Bernander, Stig (2000). Progressive Landslides in Long Natural Slopes. Formation, potential extension and configuration of finished slides in strain-softening soils. Licentiate Thesis 2000:16, May 2000, 137 pp.

Martin Nilsson (2000). Thermal Cracking of young concrete. Partial coefficients, restraint effects and influences of casting joints. Licentiate Thesis 2000:27, October 2000, ISSN 1402-1757, 267 pp.

Erik Nordström (2000). Steel Fibre Corrosion in Cracks. Durability of sprayed concrete. Licentiate Thesis 2000:49, December 2000, 103 pp.

Anders Carolin (2001). Strengthening of concrete structures with CFRP – Shear strengthening and full-scale applications. Licentiate thesis, June 2001, ISBN 91-89580-01-X 2001:01 120 pp

Håkan Thun (2001). Evaluation of concrete structures. Strength development and fatigue capacity. Licentiate thesis 2001:25. June 2001, ISBN 91-89580-08-2, 164 pp

Patrice Godonue (2002). Preliminary Design and Analysis of Pedestrian FRP Bridge Deck. Licentiate thesis 2002:18, 203 pp

Jonas Carlswärd (2002). Steel fibre reinforced concrete toppings exposed to shrinkage and temperature deformations. Licentiate thesis 2002:33, August 2002, 46 + 66 pp.

Sofia Utsi (2003). Self-Compacting Concrete - Properties of fresh and hardening concrete for civil engineering applications Licentiate thesis 2003:19, June 2003, 36 +149 pp

Anders Rönneblad (2003). Product Models for Concrete Structures - Standards, Applications and Implementations. Licentiate thesis 2003:22, June 2003, 29 + 75 pp.

Håkan Nordin (2003). Strengthening of Concrete Structures with Pre-Stressed CFRP. Licentiate Thesis 2003:25, June 2003, 57 +68 pp.

Arto Puurula (2004). Assessment of Prestressed Concrete Bridges Loaded in Combined Shear, Torsion and Bending, Licentiate Thesis 2004:43, November 2004, 102 + 110 pp.

Arvid Hejll (2004). Structural Health Monitoring of Bridges. Monitor, Assess and Retrofit. Licentiate Thesis 2004:46, November 2004, 43 + 85 pp.

Ola Enochsson (2005). CFRP Strengthening of Concrete Slabs, with and without Openings. Experiment, Analysis, Design and Field Application. Licentiate Thesis 2005:87, November 2005, 154 pp.

Markus Bergström (2006). Life Cycle Behaviour of Concrete Structures – Laboratory test and probabilistic evaluation". Licentiate Thesis 2006:59, December 2006. 173 pp. ISBN 978-91-85685-05-9